To my Family

09051

CHARACTERIZATION OF THE MURINE N-FORMYL PEPTIDE CHEMOTACTIC RECEPTOR

KYRIACOS ANDREOU MITROPHANOUS

Thesis submitted in fulfilment of the conditions
for the degree of Doctor of Philosophy
of the University of London

Department of Biochemistry and Molecular Biology
Royal Free Hospital School of Medicine

December 1995/6

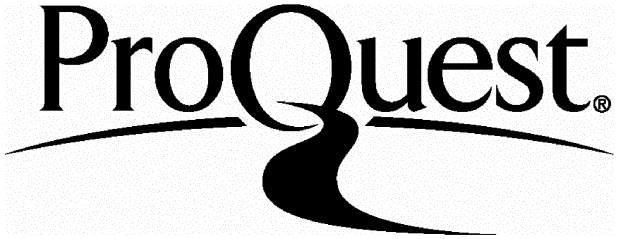

NW432

ABSTRACT

The N-formyl peptide receptor (FPR) present on neutrophils is of importance in providing the host with a detection mechanism of broad specificity for invading microorganisms and damaged tissue. The aim of this project was to develop an accurate physiological model for the study of FPR.

Since neutrophils isolated from blood leukocytes are heterogenous, short lived and terminally differentiated they do not make good models for the study of FPR. Hence, the need for *in vitro* model systems. The current model used, the human leukaemic cell line (HL-60), does not produce fully mature neutrophils. In contrast, the murine pluripotent stem cell line (FDCP), can be fully differentiated to mature neutrophils. This cell line was therefore chosen for the characterization and development of a model system for the FPR.

A detailed study of cytokine-mediated differentiation was undertaken. Differentiated FDCP cells, expressed FPR and showed cell adhesion and degranulation in response to N-formyl peptides. The kinetics of the expressed murine FPR and the efficacy of a number of synthetic N-formyl peptides was established. The peptide formyl-Norleu-Leu-Phe-Norleu-Tyr-Lys bound with high and low affinity dissociation constants of 3.7 and 22.6 nM, respectively. The number of receptors was estimated to be 79 000 per cell with 25% being of high affinity. The differentiated FDCP cells, neutrophils had low affinity binding for the peptide fMet-Leu-Phe as compared to human and rabbit neutrophils. Attempts were first made to clone the human and then the murine FPR gene. However, the putative genes were cloned by another group before completion of this work. The *muFPR* gene, which was transcribed and expressed in murine FDCP cells differentiated to neutrophils, was identified from six putative genes by reverse transcriptase PCR. The time course of transcription was consistent with the appearance of functional FPR during differentiation.

ACKNOWLEDGEMENTS

My greatest thanks go to my supervisor, Dr. Bambos Charalambous, for his guidance and support throughout my doctorate work.

I am grateful to Dr. Murphy for his gift of the huFPR clone and to Lyn Healy for her kind gift of the FDCP and WEHI cell lines.

I am grateful to everyone in the department for making my time spent there enjoyable. I would particularly like to thank Zac, Helen, Alex, Stuart, Chris, Alithea and Richard (indeed here's to the next chapter!). My special thanks to Mounir for all his help, friendship and stubborn assistance.

Finally I would like to thank my mother, father, Eleni and Imelda for their, support, patience and understanding. I dedicate the thesis to them.

TABLE OF CONTENTS

LIST OF FIGURES

LIST OF TABLES

ABBREVIATIONS

aa	amino acid
AA	arachidonic acid
ADP	adenosine diphosphate
Ala	Alanine
ATP	adenosine triphosphate
B_{max}	Maximum number of receptors per cell
bp	Base pairs
BSA	Bovine serum albumin
C-terminal	Carboxy-terminal
cAMP	Cyclic adenosine-3',5'-monophosphate
cDNA	Complementary DNA
Ci	Curie (3.7×10^{10} Bq)
CIP	Calf intestinal phosphatase
CsCl	Caesium chloride
DAG	Diacylglycerol
dATP	Deoxyadenosine triphospate
dbcAMP	N^6 0^2 - dibutyryl adenosine 3' 5'-cyclic monophosphate
dCTP	Deoxycytidine triphospate
dGTP	Deoxyguanidine triphospate
DMSO	Dimethyl sulphoxide
DNA	Deoxyribonucleic acid
DNase	Deoxyribonuclease
dNTP	Deoxyribonucleoside triphosphates
dTTP	Deoxythymidine triphospate
E. coli	*Escherichia coli*
EC_{50}	50% effective concentration
EDTA	Ethylenediamine tetra-acetic acid
fMLF	fMet-Leu-Phe
[^{3}H]-fMLF	fMet-Leu-Phe-[phenylalanine-ring-3,4,5,-^{3}H(N)]
fMLFF	fMet-Leu-Phe-Phe
fMLFK	fMet-Leu-Phe-Lys
fnLLFnLYK	formyl-Norleu-Leu-Phe-Norleu-Tyr-Lys
[^{125}I]-fnLLFNLYK	formyl-Norleu-Leu-Phe-Norleu-^{125}I-Tyr-Lys

G protein	Guanine nucleotide regulatory protein
G-CSF	Granulocyte colony stimulating factor
GDP	Guanosine diphosphate
GET	Glucose, EDTA and Tris-HCl
GIT	Guanidinium thiocyanate and β-mercaptoethanol
Glu	Glutamate
GM-CSF	Granulocyte-macrophage colony stimulating factor
GPCR	G-protein coupled receptors
GTP	Guanosine triphosphate
H_2O_2	Hydrogen peroxide
HCl	Hydrochloric acid
IL-3	Interleukin 3
IL-8	Interleukin 8
IP_3	Inositol-1,4,5-trisphosphate
kb	Kilobases
K_d	Dissociation constant
L	Ligand
LB	Luria-Bertaini broth
Leu	Leucine
LR	Ligand/receptor complex
LRG	LR plus G-protein
LRX	Desensitised ligand/receptor complex
LTB_4	Leukotriene B_4
mRNA	messenger RNA
N-terminal	Amino-terminal
NAD^+	Nicotinamide adenine dinucleotide (oxidized form)
NADH	Nicotinamide adenine dinucleotide (reduced form)
NADPH	Nicotinamide adenine dinucleotide phosphate (reduced form)
NBT	2,2'Di-p-nitrophenyl-5,5'-diphenyl-3,3'-[3,3'-dimethoxy 4,4'diphenylene]-ditetrazolium chloride
NE	Sodium acetate and EDTA
NSB	Non-specific binding
O_2^-	Superoxide anion

OCl^-	Hypochlorite
OD_{260}	Absorbance at 260nm
OD_{280}	Absorbance at 280 nm
ORF	Open reading frame
PAF	1-O-alkyl-2-acetyl-sn-glyceryl-3-phosphorylcholine
PAGE	Polyacrylamide gel electrophoresis
PBS	Phosphate buffered saline
PCR	Polymerase chain reaction
PI	Phosphatidylinositol
PI-PLC	Phophoinositide-specific phospholipase C
PI-PLD	Phophoinositide-specific phospholipase D
PKC	Protein kinase C
PLA_2	Phospholipase A_2
PLC	Phospholipase C
PML	Polymorphonuclear leukocytes (granulocytes, neutrohphils, basophils, and eosinophils.
R	Receptor
RNA	Ribonucleic acid
RNase A	Ribonuclease A
rpm	Revolutions per minute
RT-PCR	Reverse transcription polymerase chain reaction
S.E.M.	Standard error of the mean
SDS	Sodium dodecyl sulphate
SSC	Sodium citrate and sodium choloride buffer
STR	Seven hydrophobic putative transmembrane domains
TBE	Tris-borate EDTA buffer
TE	Tris-EDTA buffer
TEMED	N,N,N',N'-tetramethylethylenediamine
TFN buffer	Tris-$CaCl_2$ buffer
TMD	Seven α-helical transmembrane-domains
Tris	Tris(hydroxymethyl)-aminomethane
UTR	Untranslated region
UV	Ultraviolet
v/v	Volume per volume

Val	Valine
w/w	Weight per weight
w/v	Weight per volume
x g	Centrifugal force (x unit gravitational field)

CHAPTER 1

GENERAL INTRODUCTION

1.1 Introduction

Neutrophils constitute the primary defense mechanism of the immune system. They contain specific cell surface receptors for chemoattractants such as N-formyl peptides (Williams *et al.*, 1977). When these receptors are stimulated, a biological response is induced via a G protein coupled mechanism. This includes chemotaxis, lysosomal enzyme release, and superoxide anion production (Perez *et al.*, 1992).

Chemoattractant receptors, of which the N-formyl peptide receptor (FPR) is one, provide a means for the immune system to detect damaged tissue and microbial infections. Neutrophils have chemoattractant receptors for a variety of ligands including lipid derivatives, polypeptides and peptides. There are two classes of chemoattractants: the classical chemoattractants and the chemoattractant cytokines (chemokines). The classical chemoattractants are C5a, LTB_4 and PAF, as well as FPR (Probst *et al.*, 1992). The chemokines include interleukin-8 (IL-8), 'regulated on activation, normal T-cell expressed and secreted' (RANTES) and monocyte chemotactic proteins 1, 2 and 3 (MCP-1, -2, and 3).

Following tissue damage, FPR binds N-formyl peptides derived from either invading microorganisms or from mitochondrial debris resulting from tissue damage. FPR is a 350 amino acids glycosylated membrane protein expressed by cells of myeloid origin such as neutrophils, monocytes, macrophages and eosinophils (Boulay *et al.*, 1990a; Owen, Jr. *et al.*, 1991; Koo *et al.*, 1982). It is coupled to intracellular effectors through guanine nucleotide regulatory proteins (G proteins) (Jacobs *et al.*, 1995). These G protein coupled receptors (GPCR) are modelled topologically to consist of seven putative transmembrane spanning helices. This modelling is based not only

on their hydropathy profiles, but also on their similarity to bacteriorhodopsin. Bacteriorhodopsin was the first GPCR to be crystallized and its tertiary structure elucidated (Engelman *et al.*, 1980). The mammalian chemoattractant receptors belong to a subgroup within the GPCR family. Chemoattractant receptors have low overall amino acid homologies (25-35%) but mediate similar responses within leukocytes namely chemotaxis, release of lysosomal enzymes, and oxidant production.

During the course of this work the FPR gene has been cloned from human (Boulay *et al.*, 1990a), rabbit (Ye *et al.*, 1993) and murine (Gao and Murphy, 1993) cells. Using the prototype N-formyl peptide fMLF as ligand, a comparison of FPR affinities revealed two classes of receptors: high and low affinity (Gao and Murphy, 1993). The human and rabbit FPRs belong to the high affinity class while the murine FPR and human FPRL1 (a homologue of human FPR) belong to the low affinity class.

Neutrophils are primarily responsible for defense against invading microorganisms. They are also the main cellular elements in acute inflammation, especially during the early stages. When a chemoattractant receptor binds its ligand, it causes the cell to migrate along the chemotactic gradient until it reaches the point of highest chemoattractant concentration. The neutrophil produces and releases oxidant and cytotoxic compounds (defensins) from intracellular granules (Lehrer *et al.*, 1993). Neutrophils also release digestive enzymes which can remove tissue debris as well as kill microorganisms. Defensins are peptides of 29-35 amino acid residues that include six invariant cysteines which cyclize via their intramolecular bonds to form a stable triple-stranded β-sheet configuration (Lehrer *et al.*, 1993). Defensins constitute 5% of total cellular protein in human and rabbit neutrophils but are not

found in murine neutrophils (Matsuoka *et al.*, 1993). They have a wide spectrum of antimicrobial activity.

Neutrophils remain in the bone marrow for five days after fully maturing. From there they circulate through out the body for approximately ten hours before entering the tissues at sites of inflammation. This means that any neutrophils isolated from blood are terminally differentiated and short lived. Circulating neutrophils are also heterogenous in density, cell surface antigens, and functional properties (surface adherence, response to chemoattractants, aggregation and phagocytosis). This heterogeneity may originate from distinct stem cells or reflect functional maturational differences from a common stem cell line. Thus, blood neutrophils are not a good model for the study of neutrophils or FPR. Therefore, this points to the need for *in vitro* model systems (Polakis *et al.*, 1988).

The human promyelocytic leukaemia cell line (HL-60) has been used as a model for the study of FPR and other chemoattractant receptors (Perez *et al.*, 1992; Boulay *et al.*, 1990a; Sham *et al.*, 1995). HL-60 cells can be differentiated to neutrophils by a variety of non-physiological agents (Polakis *et al.*, 1988; Lubbert *et al.*, 1991; Collins, 1987) such as DMSO and dibutyryl cAMP (dbcAMP). This induces production of neutrophil-like cells expressing FPR as well as other chemotactic receptors (Chaplinski and Niedel, 1982; Perez *et al.*, 1992). These neutrophil-like cells have impaired functional characteristics, such as a deficient myeloperoxidase/peroxide/halide system (Pullen and Hosking, 1985; Sham *et al.*, 1995).

A murine pluripotent stem cell line (FDCP) has been established (Spooncer *et al.*, 1986) and shown to be capable of differentiation into different leukocytes. In contrast to HL-60 cells, FDCP cells have a normal karyotype, are nonleukaemic, and grow continuously in the presence of interleukin-3 (IL-3) (Crompton, 1991). IL-3 also supports the development of lineage restricted myeloid progenitor cells such as megakaryocytic, neutrophil/macrophage, erythroid, eosinophil and mast cells. Granulocyte macrophage colony-stimulating factor (GM-CSF) and granulocyte-CSF (G-CSF) support the further development of these cells into neutrophils, which is analogous to the differentiation and development of neutrophils *in vivo* (Heyworth *et al.*, 1990a; Heyworth *et al.*,1990b).

Towards the understanding of the role of FPRs in neutrophil action, I will give a description of chemoattractants and their receptors, the kinetics of ligand binding, signal transduction, leukocyte migration, anti-microbial activity of neutrophils, and the HL-60 and the FDCP cell lines.

1.2 Chemoattractants

A variety of chemotactic peptides and their receptors orchestrate the directed migration of leukocytes to sites of inflammation. All chemoattractants are potent stimuli for chemotaxis, induction of inflammation, activation of microbicidal degranulation, and oxidant production of neutrophils (Oppenheim *et al.*, 1991; Hwang, 1990).

Leukocyte accumulation is vital for wound healing and other immunologically mediated functions. The analysis of the migration of leukocytes was not quantifiable *in vitro* until the development of the Boyden chamber (Boyden, Jr., 1962). This is a chemical gradient established across a microporous filter through which leukocytes can migrate. The Boyden chamber also enabled the *in vitro* characterization of a number of chemoattractants. Factors that act as chemoattractants include lipid derivatives (Leukotreine B_4, LTB_4 and Platelet activating factor, PAF), polypeptides (activated fifth component of complement, C5a and interleukin-8, IL-8), and peptides (N-formyl peptides). The activation of a chemoattractant receptor by its ligand leads to cell accumulation at the site of injury and production of cytotoxic products and chemoattractants such as IL-8 (Cassatella *et al.*, 1992).

Chemoattractants are divided into the classical chemoattractants and the chemoattractant cytokines (chemokines).

1.2.1 Classical Chemoattractants

Classical chemoattractants include the N-formyl peptides, C5a, LTB_4, and PAF.

1.2.1.1 N-formyl Peptides

In 1967 leukocytes were shown to chemotax towards products derived form bacteria (Keller and Sorkin, 1967). Synthesised N-formyl peptides were also shown to have this effect (Schiffmann *et al.*, 1975). This led to the identification of a number of peptides which were active at concentrations of approximately 0.1nM (Showell *et al.*, 1976). The formyl group was shown to be essential to the activity of N-formyl

peptides. In addition, the presence of methionine in the first position resulted in the most potent peptides. This is thought to be due to its effect on peptide conformation and to specific receptor interactions (Prossnitz *et al.*, 1995).

Prokaryotic proteins contain formylmethionine at their N-terminus. Eukaryotic organisms have N-formylmethionine proteins only in their mitochondria which are thought to have evolved from prokaryotic symbionts. The N-formyl group provides a ready marker for the immune system to recognise prokaryotic infections or the trauma-induced lysis of its own cells. Either event will release N-formyl peptides which cause the chemotaxis of neutrophils and the activation of the immune response.

The receptor on human polymorphonuclear phagocytes shows dissociation constants of 0.53 and 24.4 nM (Koo *et al.*, 1982). For other cell types and species, differing values were obtained (see Table 1.1).

1.2.1.2 Activated fifth component of complement-C5a

The activated fifth component of complement (C5a) is a 74 amino acid glycoprotein cleaved from the fifth component of complement (C5) during complement activation (Quehenberger *et al.*, 1992; Gerard and Gerard, 1994). The receptor was first demonstrated on neutrophil cells by Chenoweth and co-workers (Chenoweth and Hugli, 1978). Neutrophils were shown to have approximately 3 x 10^5 receptors per cell with a dissociation constant of 2nM (Huey and Hugli, 1985).

1.2.1.3 Platelet-Activating Factor

Platelets produce a group of acetyl-alkylglycerol ether analogs of phosphotidylcholine (1-O-alkyl-2-acetyl-sn-glyceryl-3-phosphorylcholine) called PAF. This is a phospholipid chemoattractant and anaphylatoxin (Hwang, 1990).

1.2.1.4 Leukotriene B_4

LTB_4 is a chemotactic lipid similar to PAF, and mainly acts on neutrophils. It is produced by activated mast cells via the lipoxygenase pathway of arachidonic acid metabolism. The receptor kinetics of LTB_4 resemble those of PAFR (Schepers *et al.*, 1992). Its receptor has yet to be cloned.

1.2.2 Chemoattractant Cytokines (Chemokines)

Since 1986 a superfamily of closely related and conserved cytokines have been identified, cloned and sequenced. The chemokine superfamily consists of small (8-10kDa), inducible, proinflammatory proteins that have a 20 - 50% homology at the amino acid level (Oppenheim *et al.*, 1991). They are divided into two groups: the α-chemokines and the β-chemokines (Kelvin *et al.*, 1993; Baggiolini *et al.*, 1994). This division is based on the conserved cysteine residues, with the α-chemokines having an intervening amino acid between the first and second of the four conserved cysteines (C-X-C) and the β-chemokines having no intervening amino acid (C-C). Fourteen distinct α-chemokines and twelve β-chemokines have been identified at either the protein or at the cDNA level. Members of the α-chemokine subfamily include interleukin 8 (IL-8), γ-interferon-induced peptide (Ip-10), epithelium-derived neutrophil attractant 78 (ENA-78), macrophage inflammatory protein αβ (MIP-2αβ). The β-chemokine subfamily includes macrophage inflammatory protein 1α (MIP-1α), macrophage inflammatory protein 1β (MIP-1β), 'regulated on activation, normal

T-cell **e**xpressed and **s**ecreted' (RANTES) and monocyte chemotactic proteins 1, 2, 3 (MCP-1, -2, -3) (Murphy, 1994).

1.3 Chemoattractant Receptors

The analysis of leukocyte chemoattractant receptors began with the use of radiolabelled N-formyl peptides which were shown to bind specifically to cell surface receptors (Williams *et al.*, 1977). The sequences of the chemoattractant receptors were established through the use of cloning strategies employing expression and homology hybridization. Many receptor sequences have been established in this way (Boulay *et al.*, 1990b; Honda *et al.*, 1991; Gerard and Gerard, 1991; Boulay *et al.*, 1991; Holmes *et al.*, 1991; Murphy and Tiffany, 1991; Gao *et al.*, 1993; Ye *et al.*, 1992).

Chemoattractant receptor genes have an unusual structural organization. They lack introns within the open reading frame (ORF) but have at least one large intron between the points of transcription and translation (Gao *et al.*, 1993; Murphy *et al.*, 1993; Gerard *et al.*, 1993; Mutoh *et al.*, 1993). The IL-8 and C5a receptor genes are on human chromosome 2 (Ahuja *et al.*, 1992; Gerard *et al.*, 1993), while the N-formyl peptide receptor genes are on chromosome 19 (Gerard *et al.*, 1993).

1.3.1 Predicted Structure of Chemoattractant Receptors

Hydropathy analysis of chemoattractant receptors shows that they contain seven putative hydrophobic transmembrane domains (STR). These are conserved among most members of this superfamily (Probst *et al.*, 1992; Savarese and Fraser, 1992; Baggiolini *et al.*, 1994). A structural model of STRs has been proposed from

statistical analyses of sequences in the hydrophobic domains and the known structure of bacteriorhodopsin and rhodopsin (Savarese and Fraser, 1992; Baldwin, 1993). These include an extracellular amino-terminus (N-terminus); an intracellular carboxy terminus (C-terminus); seven α-helical transmembrane-domains (TMD) perpendicular to the plasma membrane and kinked in TMD II, IV, V, VI and VII by intrahelical prolines; three intracellular and extracellular connecting loops composed of hydrophilic amino acids; and a disulphide bond linking cysteine residues in the extracellular loops 1 and 2. Figure 1.1 shows the predicted structure of FPR.

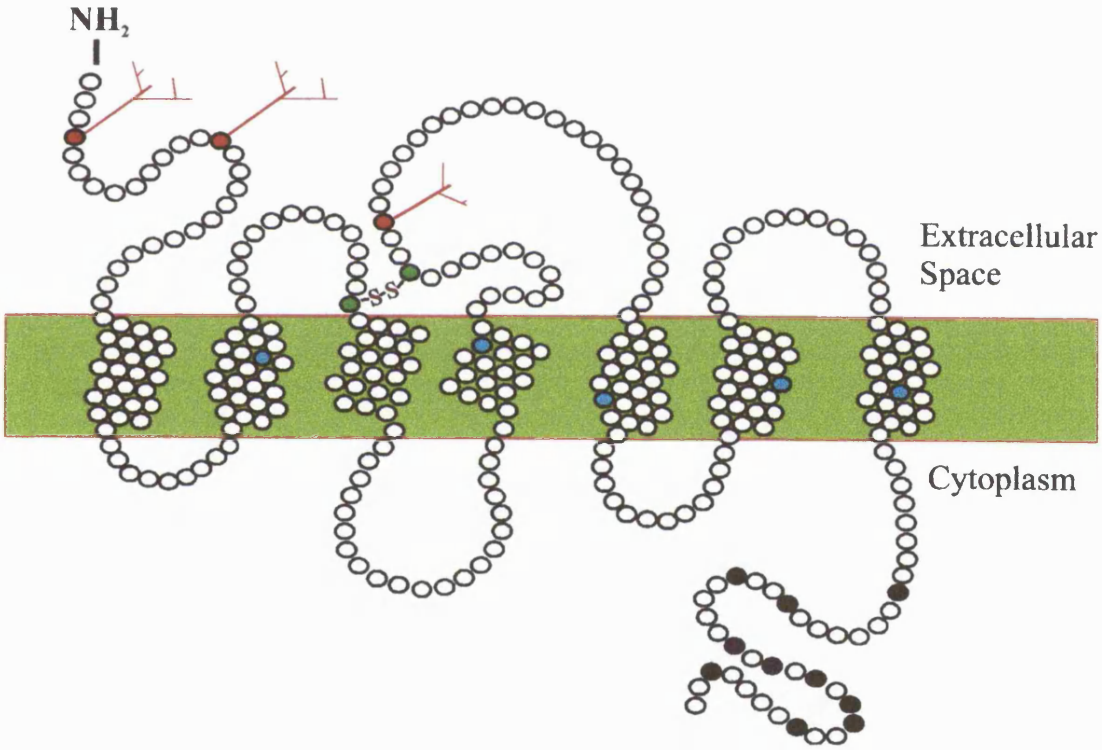

Figure 1.1 Structural model of the human formyl peptide receptor (huFPR). Black circles represent sites of multiple serine and threonine residues for potential phosphorylation. Blue and green circles represent conserved prolines and cysteines, respectively. Red circles with branched structures represent potential N-linked glycosylation sites.

1.3.2 Features of Chemoattractant Receptors

There are no common motifs or residues that can be used to distinguish chemoattractant receptors from other types of STRs. However, five consensus features have been identified. These are as follows: the receptors are all approximately 350 amino acids in length, which is among the shortest of the STRs; they have approximately 20% overall amino acid identity to each other; their intracellular loops are rich in basic amino acids and can be modelled to form cationic α-helices (Savarese and Fraser, 1992; Murphy *et al.*, 1992); their N-termini are unusually acidic (Probst *et al.*, 1992; Ahuja and Murphy, 1993) and their RNAs are expressed in leukocytes. As in other members of the STR family, the N-terminus contains sites for asparagine-linked glycosylation. The C-terminus contains many serine and threonine residues which could be phosphorylated (Savarese and Fraser, 1992).

1.3.3 The N-Formyl Peptide Receptor Subfamily (FPR)

Over the period of this work three human, one rabbit and six murine FPRs have been cloned and sequenced. They have an overall homology, at the amino acid level, of 50-75% (see Appendix 1).

1.3.3.1 Human FPR

In 1990 two cDNA clones (fMLP-R98 and fMLP-R26) were isolated from a cDNA library. This was constructed from mRNA isolated from neutrophil-like cells (Boulay *et al.*, 1990a). The latter were obtained by differentiating a human cell line (HL-60). COS cells were conferred with high affinity binding of N-formyl peptides when transformed with these clones. The binding of ligand to the receptor caused cytoskeletal reorganization and degranulation in heterologous cell types (Didsbury

et al., 1992; Murphy and McDermott, 1991; Ali *et al.*, 1993). This proved that these cDNAs encoded a receptor which mediates the migration and cytotoxic responses in neutrophils in response to N-formyl peptides. In 1993 another cDNA clone of huFPR was isolated from the human leukemic cell line, U937 cells, differentiated to neutrophils. This was designated UF1 (Haviland *et al.*, 1993).

fMLP-R26 differs from fMLP-R98 in the following respects: the 5' untranslated region (UTR) of fMLP-R98 showed a 16bp deletion at position -1 to -17 as compared to fMLP-R26; the sequence also diverged in the 3' UTR, at position 1175 and 1219-1220 (see Appendix 2); 3' UTR of fMLP-R98 was extended by 661bp as compared to fMLP-R26. In the coding region there were two base substitutions C to G at position 301, and C to A at position 1037, resulting in the replacement of Val^{101} and Glu^{346} in fMLP-R26 by Leu^{101} and Ala^{346} in fMLP-R98.

UF1 had a combination of the variations found in fMLP-R98 and fMLP-R26. As compared to fMLP-R98 and fMLP-R26, UF1 had an extra 16bp on the 5' UTR. UF1 was identical to fMLP-R26 in the 5' UTR, the nucleotide 301 (non-silent variation), and was polyadenylated at the same nucleotide position. UF1 was identical to fMLP-R98 at the nucleotide position 1037 (non-silent variation) and at position 1175 (base pair deletion).

All the cDNAs encoded for a 350 amino acid polypeptide. The differences between fMLP-R26, fMLP-R98 and UF1 were attributed to allelic variations, differing polyadenylation of the primary transcript (the additional 3' UTR of fMLP-R98), and the alternative splicing of exon 2. This is because genomic and Southern mapping data demonstrate a single-copy gene with no evidence for multiple coding exons.

In 1992 De Nardin *et al* showed that there are no introns within the coding region of the FPR gene (De Nardin *et al.*, 1992). The variable splicing resulted in two mRNAs species of 1.33 and 1.38 kb in HL-60 neutrophil-like cells and human monocytes (Haviland *et al.*, 1993; Murphy *et al.*, 1993).

The gene symbol for FPR was designated *FPR1* (Murphy *et al.*, 1992) and the gene product, huFPR. Figure 1.2 show the structural organization of the *FPR1* gene. This was found to be a single copy gene with no introns in the ORF. The structural organization of the *FPR1* gene was found to be approximately 6kb in length (Murphy *et al.*, 1993). The 5' UTR resides on three exons. The start sites for transcription and translation are separated by approximately 5kb. *FPR1* contains three *Alu* repeats, one in each intron and a third in the 3' UTR. The promoter contains a non-consensus TATA box and an inverted CCAAT element. Dibutyryl cAMP can induce the differentiation of HL-60 cells to neutrophil-like cells. These differentiated cells express huFPR. This means that *FPR1* is transcribed. However, there is no cyclic AMP response element within 450bp of the transcription start point. The presence of exon 2 imparts the potential for the formation of stem-loop structures which could effect mRNA stability.

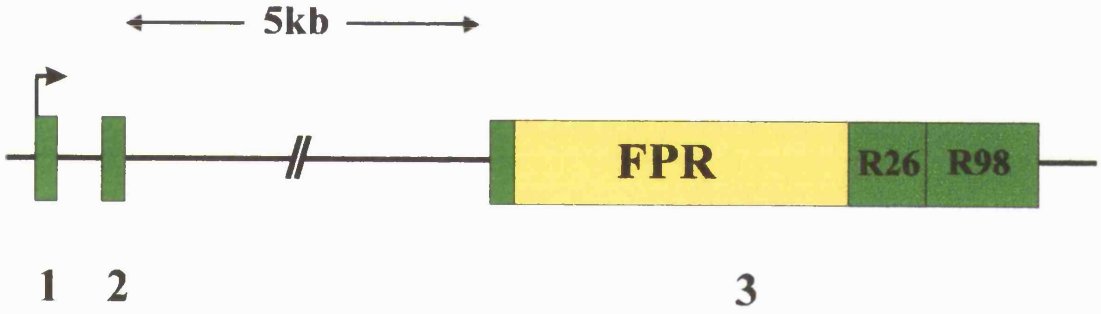

Figure 1.2 Structural organization of the human formyl peptide receptor gene (*FPR1*). The transcription start point is 4902bp from the start codon. The arrow represents the start point of transcription. The numbers represent exons. The boxes labelled R26 and R98 represent the 3' UTR of fMLP-R26 and 3' UTR of fMLP-R98, respectively. The green boxes represent untranslated regions of the gene. The yellow box represents the open reading frame.

1.3.3.2 Human FPR Homologues

In 1992, two research groups identified a homologue to huFPR, from cDNA libraries constructed from HL-60 neutrophil mRNA. Ye and co-workers isolated a 1.65kb cDNA having a 69% homology, at the amino acid level, to huFPR and encoding a polypeptide of 351 amino acids (Ye *et al.*, 1992). Murphy and co-workers isolated a 2.6kb cDNA having a 69% homology, at the amino acid level, to huFPR and encoding a polypeptide of 351 amino acids (Murphy *et al.*, 1992). There are two differences between the clones, an extra 733bp in the 5' UTR and 256bp in the 3' UTR. The ORFs were identical. These two differences were attributed to allelic variations and different polyadenylation of the primary transcript. This homologue was designated FPRL1 and its gene *FPRL1* (FPRL1 - human formyl peptide receptor like-1). Two FPRL1 transcripts were detected in HL-60 differentiated to neutrophil-like cells (2.6 and 3.5 kb) (Murphy *et al.*, 1992; Durstin *et al.*, 1994).

Through the screening of human genomic DNA with huFPR and FPRL1 probes another putative gene, designated *FPRL2*, was identified. FPRL1 is expressed both in neutrophils and monocytes, while FPRL2 transcripts have only been identified in monocytes (Durstin *et al.*, 1994). In the same year Bao and co-workers isolated three human FPR clones from a human genomic library (Bao *et al.*, 1992). They sequenced these clones and designated them huFPR, FPRH1 and FPRH2; these are in fact huFPR, FPRL1 and FPRL2, respectively. FPRL1 and FPRL2 have 69% and 56% homology to huFPR, respectively. Gerard and co-workers showed that the FPR genes cluster at chromosome 19q13.3 (Gerard *et al.*, 1993).

huFPR binds the N-formyl peptide, fMLF, with a high affinity (K_d ~ 0.53 and 24.4 nM (Koo *et al.*, 1982). The FPRL1 receptor FPRL1R has a low affinity for fMLF (K_d ~ 430nM) (Ye *et al.*, 1992). FPRL2 receptor FPRL2R does not bind fMLF.

1.3.3.3 Species variants of FPR

Table 1.1 gives a summary of the dissociation constants of FPR from different species and cell types. Because of the different methodologies used to obtain kinetic data, a direct comparison, of dissociation constants and receptor numbers, cannot be made.

Species and Cell Type	Assay	Dissociation Constant (k_d) nM	Receptors per Cell (10^{-3})	Reference
Human (PMNs)	fMLF [^{3}H]	10.0-22.3	55	(Williams *et al.*, 1977)
Human (M)	fMLF [^{3}H]	30.2	84	(Benyunes and Snyderman, 1984)
Human (M)	fnLLFnLYK [^{125}I]	1.7-2.7	10-18	(Weinberg *et al.*, 1981)
Human (PMNs)	fnLLFnLYK [^{125}I]	1.0	120	(Niedel *et al.*, 1979)
Human (FPRL2)	Transfected cells	430	-	(Ye *et al.*, 1992)
Human (huFPR)	Ca^{2+} (fMLF)	0.5	-	(Gao and Murphy, 1993)
Murine (PMNs)	Chemotaxis (fMLF)	1000	-	(Sasagawa *et al.*, 1992)
Murine (muFPR)	Ca^{2+} (fMLF)	100	-	(Gao and Murphy, 1993)
Rabbit (PMNs)	fMLF [^{3}H]	0.5-4.3	94	(Kermode *et al.*, 1991)
Rabbit (PMNs)	fnLLF	1.5	100	(Aswanikumar *et al.*, 1977)

Table 1.1 Comparison of N-formyl peptide receptor kinetic data.
M represents monocytes. PMN represents polymorphonuclear neutrophils. fMLF represents fMet-Leu-Phe. fnLLF represents fNle-Leu-Phe. fnLLFnLYK represents fNle-Leu-Phe-Nle-Tyr-Lys.

1.3.3.4 Rabbit

Rabbit FPR (rabFPR) has 78% homology, in the ORF to huFPR (Ye *et al.*, 1993). Two transcripts of 1.5 and 3 kb can be detected in rabbit neutrophils. rabFPR has a high affinity for fMLF (K_d ~ 4.3nM) (Kermode *et al.*, 1991).

1.3.3.5 Murine

Six genes have been isolated from a murine genomic library. These have been designated muFPR and muFPRL1-5. They have a 54-76% homology to huFPR (Gao and Murphy, 1993; Murphy, 1994). muFPRL3 is a pseudogene. muFPRL1, 2, 4 and 5 have approximately 55% homology to huFPR. muFPR has 76% identity to huFPR. All these lack introns within their ORFs. MuFPR has a low affinity for fMLF (Gao and Murphy, 1993; Sasagawa *et al.*, 1992).

1.3.4. FPR Structure/Function Analysis

Although the three-dimensional structure of FPR is not known, the use of sequence comparisons (with other members of the GPCR family), biochemical, biophysical and genetic analyses, have provided insights into the structure and function of FPR.

1.3.4.1 Ligand-binding Site

Receptor chimera studies (where individual domains of huFPR were exchanged with those of human C5aR and of huFPRL1R) suggest that formation of the high affinity binding site for fMLF involves the coordinated participation of all the extracellular loops and adjacent portions of the TMDs of FPR (Gao and Murphy, 1993; Perez *et al.*, 1993; Quehenberger *et al.*, 1993). Although the N-terminus was shown to be unimportant in ligand binding as substitution with either the huC5aR or huFPRL1R N-terminus had no great effect (Quehenberger *et al.*, 1993), later experiments

demonstrated that once the ligand had bound it caused a conformational change in the receptor (Perez *et al.*, 1994). This resulted in the N-terminus moving over the ligand to form a lid over the binding pocket. Although the N-terminus appears to be glycosylated (Malech *et al.*, 1985), deglycosylation has no affect on ligand binding.

Using fluorescein-labelled N-formyl peptides, in conjunction with quenching and antibody studies, Sklar and co-workers showed that the binding pocket is only big enough to accommodate five amino acids (Fay *et al.*, 1993). Once the fluorescein labelled peptide has bound, it becomes quenched. This is thought to be through protonation. The binding pocket is thought to be a hydrophobic subdomain involving the TMDs, with the protonation being carried out by His90 located in the first extracellular loop.

The principal sequence differences between the species and subtypes of FPR are on the extracellular domains. This suggests that the receptors are coupled to the same G proteins but bind to different ligands (Gao and Murphy, 1993). The availability of the FPR variants provides a useful tool for refining the binding pocket model using site-directed mutagenesis.

1.3.4.2 G protein-coupling Domain

The intracellular loops 2 and 3 are known to be important for G protein coupling for many of the G Protein coupled receptors (Savarese and Fraser, 1992). Peptides were synthesised to specific sites and used to probe the formation of physical complexes between solubilized FPR and bovine brain $G_i\alpha$ (Bommakanti *et al.*, 1993). These studies showed that the proximal portion of the C-terminus segment of FPR binds $G_i\alpha$. Peptides corresponding to intracellular loops 2 and 3 and

extracellular loop 2 were inactive. An anti-$G_i\alpha$ antibody was prevented from binding to $G_i\alpha$ by peptides derived from the second intracellular loop and by a fusion protein derived from the C-terminus of huFPR (Schreiber *et al.*, 1994). A peptide derived from the third intracellular loop did not block binding. When the basic amino acids or the serines and threonines of the third intracellular loop were mutated, neither the binding affinity nor signal transduction were significantly affected (Prossnitz *et al.*, 1993). It seems therefore, that unlike other STRs, the third intracellular loop is not involved in the coupling of FPR to G proteins. Rather, it is the second intracellular loop and the C-terminus that are involved in coupling.

1.3.5 The Genetic Organization of other Chemotactic Receptors

1.3.5.1 The C5a Receptor (C5aR)

The cDNA for the human C5a receptor (huC5aR) was cloned in 1991 (Gerard and Gerard, 1991; Boulay *et al.*, 1991), and that for the murine in 1992 (muC5aR) (Gerard *et al.*, 1992). MuC5aR has 65% homology to huC5aR. HuC5aR and huFPR are approximately 34% identical and their mRNA distribution is very similar, indicating that the genes may be coordinately regulated. There is only one huC5aR gene but it has an unusual organization. As mentioned earlier, with a few exceptions such as the tachykinin receptors which have multiple introns (Gerard *et al.*, 1991b; Gerard *et al.*, 1991a), the majority of the STR superfamily are intronless within the ORF (Libert *et al.*, 1989). In the C5aR gene the initiating methionine codon is separated from the single exon (exon 2) containing the rest of the coding region, by an intron approximately 9kb in length (Gerard *et al.*, 1993).

1.3.5.2 The Platelet-Activating Receptor (PAFR)

Platelets produce a group of acetyl-alkylglycerol ether analogs of phosphotidylcholine (1-O-alkyl-2-acetyl-sn-glyceryl-3-phosphorylcholine) called PAF. This is a phospholipid chemoattractant and anaphylatoxin (Hwang, 1990). The PAF receptor cDNA was first cloned from a cDNA guinea pig lung library by expression cloning (Honda *et al.*, 1991). Guinea pig leukocytes contain three PAFR transcripts of 2, 3, and 4 kb. These are also expressed in the spleen, lung, brain, liver, kidney and heart. The human homologue is 83% identical to the guinea pig (Kunz *et al.*, 1992; Nakamura *et al.*, 1991).

The gene structure of huPAFR matches that of the other chemoattractant receptors. It is a single copy gene found on chromosome 1. It has an intronless ORF and two differentially expressed 5' non-coding exons that have distinct initiation sites. The gene is approximately 6kb in length (Mutoh *et al.*, 1993; Chase *et al.*, 1993).

1.3.5.3 The Leukotriene B_4 Receptor (LTB_4)

LTB_4 is a chemotactic lipid similar to PAF. Its main effects are on neutrophils. It is produced by activated mast cells via the lipoxygenase pathway of arachidonic acid metabolism. There are approximately 2.7×10^5 receptors per cell for LTB_4 with dissociation constants of 0.39nM (Goldman and Goetzl, 1982). The receptor kinetics of LTB_4 resembles those of PAFR (Schepers *et al.*, 1992) and the gene encoding fot the receptor has yet to be cloned.

1.4 Kinetics

With the development of complementary spectrofluorometric and flow cytometric techniques, real-time analysis of the receptor in membrane preparations and whole cells can be carried out. These approaches have been used to study ligand-receptor and receptor-processing events in neutrophil membranes, permeabilized neutrophils, and intact neutrophils. Kinetic studies show that ligand (L) binds to the receptor at a diffusion limited rate and that the receptor (R) undergoes rapid transitions involving three states. These are, ligand/receptor (LR), LR plus G-protein (LRG), and a desensitised state (LRX) which forms in seconds. The spectroscopic data suggest that the binding pocket can accommodate only up to five amino acids and that the peptide becomes protonated upon binding. Protonation is thought to be through His-90, putatively located in the first extracellular loop (Fay *et al.*, 1993).

Pertussis toxin treatment of neutrophils disrupts the coupling between the chemotactic receptor and the G proteins (Bokoch and Gilman, 1984). Ligand-receptor interactions have a time-dependent heterogeneity. Within seconds of the ligand binding to the receptor, the latter rapidly dissociates from the G protein (Sklar *et al.*, 1985a). To achieve a maximal respiratory burst, all the receptors have to be activated (Sklar *et al.*, 1985a), but only 15 receptors per cell need to be occupied to achieve actin polymerization (Sklar *et al.*, 1985b) and phosphatidylinositol triphosphate production (Eberle *et al.*, 1990). Cytoskeletal activation is maintained at an occupancy of less then 1% while the respiratory burst begins to desensitise at below 10% (Omann and Sklar, 1988). Thus, the cells are able to chemotax at low chemoattractant concentrations and will only begin their respiratory burst when they

reach the site of inflammation where the chemoattractants are at their highest concentration.

1.4.1 Kinetics on Permeabilized Cells

For neutrophil activation, a ternary complex involving peptide ligands (L), receptors (R), and G proteins (G) must assemble. If guanine nucleotide is present or G protein is treated with pertussis toxin, there is rapid dissociation of the ligand/receptor complex (LR) in approximately 5 seconds (Sklar *et al.*, 1987). In the absence of G protein and in the presence of ligand a slowly dissociating complex, in approximately 500 seconds, is detected. This is thought to be the ternary complex (LRG). Further analysis of this ternary complex indicated that the dissociation occurs within 100 milliseconds. This is because the cell contains GTP levels of several hundred micromolar (Posner *et al.*, 1994). Therefore, once the ternary complex has formed, the G protein is activated.

Equilibrium binding studies performed by cytometry showed that RG has two orders of magnitude higher affinity than R for L. This is due to the difference in dissociation rate constants as the association constants of RG and R are the same, approximately $3 \times 10^7\ M^{-1}\ sec^{-1}$. Once L has bound, LRG has a dissociation constant of $1 \times 10^{-3}\ sec^{-1}$ as compared to LR's $1 \times 10^{-1} sec^{-1}$ (Fay *et al.*, 1991; Neubig and Sklar, 1993). Analyses of the receptors indicated that approximately 50% are coupled to G protein. The rest are slowly associating, to form LRG, with a half-time of minutes (Posner *et al.*, 1994).

1.4.2 Kinetics on Intact Cells

The measurement of receptor dynamics in intact cells is far more difficult to interpret because of receptor processing. Receptor processing includes desensitization of membrane bound receptors, internalization, and up-regulation of receptors from secretory granule stores. When the cell is stimulated with ligand, degranulation increases receptor numbers by 30 000 per minute (Norgauer *et al.*, 1991). This creates a biphasic binding response. First, the receptors in the plasma membrane bind ligand (30-60 seconds). Secondly, the newly up-regulated receptors bind ligand (3-4 minutes). In the intact cell there are thought to be three different receptor forms (Sklar *et al.*, 1989), one of which is quickly dissociating (LR) and two of which are slowly dissociating (LRX and LRG).

The slowly dissociating receptor form, found after activation at 37°C but prior to internalization, is thought to be the desensitized receptor (LRX). LRX formation is energy dependent, probably through ATP-dependent phosphorylation. It is probable that LRX forms spontaneously. However, if energy metabolism is poisoned (adenine and guanine nucleotide levels fall) LRG is trapped and so cannot convert to LRX.

The second slowly dissociating receptor form is the LRG. Conversion of LRG to LR and G is mediated by guanine nucleotide.

By uncoupling the G protein from the receptor (pertussis toxin treatment) and depleting energy levels (adenine and guanine nucleotide levels fall) rapidly dissociating LR is formed.

1.4.3 Whole Cell Model of Ligand-Receptor Interactions

Using the information provided by ternary complex behaviour in permeabilized cells and the identification of three distinct receptor forms from the intact cell studies, a whole cell model of ligand-receptor interactions has been proposed by Sklar and co-workers.

Receptor forms are interconverted rapidly, in the whole cell, giving rise very quickly, to the desensitized receptor (LRX) (Sklar *et al.*, 1989). In the early phase of ligand binding a rapidly dissociating complex, similar to LR, forms. The formation of the slowly desensitizing receptor LRX then follows and within only one minute, LRX can be detected. Following a lag time of 30 seconds, LRX is internalized with a half-time of 3 minutes. The receptors are either precoupled to G protein or are uncoupled may couple slowly. The quaternary complex LRG▪GTP forms at a rate of 10 per second. The uncoupled receptor desensitizes (LRX) at a rate of 0.1 per second. This is slowly dissociating and is subsequently internalized with the ligand still bound. When the ligand binds to the receptor it causes a rapid increase in the amount of active LRG. This reaches a maximum within tens of seconds and then decreases. This is because the receptors become saturated over minutes. This is mirrored in the stimulation of the cell. That is, cell responses are initiated within seconds, reaching maximal levels within tens of seconds and then decreasing over several minutes (Sklar *et al.*, 1985a). This decrease is thought to be due to the loss of the active form of the receptor. Figure 1.3 gives a summary of the kinetic data.

Studies with α- and β-adrenergic receptors (Cotecchia *et al.*, 1990; Samama *et al.*, 1993) indicate that the model described above is not accurate with respect to the question of receptor precoupling. It is thought that the unligated form of the receptor

exists in an inactive state which has a low affinity for G protein. When the receptor binds ligand it is activated through a conformational change creating a receptor with high affinity for G protein (Perez *et al.*, 1994). Only the active receptor can mediate signal transduction events. Thus, the receptors may not be precoupled to G protein but rapidly couple once ligand has bound to them. It has been proposed that the βγ subunits of the G protein may act to keep the G protein close to the receptor and that the Gα subunit will only interact with the receptor once the ligand has bound to the receptor and converted it into the high affinity state (Prossnitz *et al.*, 1995).

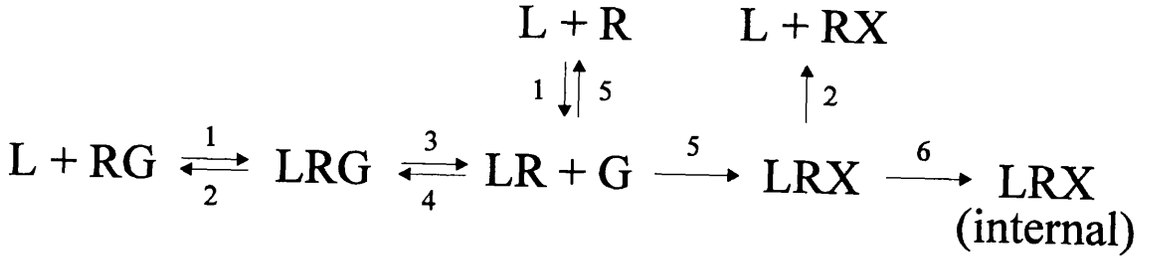

1=3.0 x 10^{7} M^{-1} Sec^{-1}
2=1.0 x 10^{-3} Sec^{-1}
3=1.0 x 10^{1} Sec^{-1}

4=1.0 x 10^{-2} Sec^{-1}
5=1.0 x 10^{-1} Sec^{-1}
6=3.0 x 10^{-3} Sec^{-1}

Figure 1.3 Kinetics of N-formyl peptide binding to FPR.
L, ligand; G, G-protein; LR, ligand/receptor complex; LRG, LR plus G-protein, LRX, desensitised ligand/receptor complex.

1.5 Signal Transduction

Signal transduction is a multiple step process, where the primary signal is received on the external surface of the cell and has to be converted into a cellular response. The fact that, guanosine 5'-3-O-(thio)triphosphate (GTPγS) decreased the affinity of N-formyl peptide for FPR (Snyderman *et al.*, 1984) and that *B. pertussis* toxin (ADP-ribosylates $G_i\alpha$ subunits (Kaziro *et al.*, 1991)) prevented cell activation by ligand indicated that G protein was involved in the signal transduction of chemoattractant receptors. In 1993 liganded huFPR was shown to couple to G_i protein (Schreiber *et al.*, 1993; Goetzl *et al.*, 1994). The receptor can send a signal either through multiple G proteins which can activate multiple effectors or from a single G protein which can also activate multiple effectors.

N-formyl peptide binding to FPR on neutrophils causes a number of effects including cytoskeletal remodelling, shedding of selectin, and upregulation of adhesion molecules, chemotaxis, granule secretion, and activation of NADPH oxidase. These effects occur as the concentration of ligand increases. The model for signal transduction in neutrophils is as follows. The receptor's affinity is increased by conformational changes due to the binding of heterotrimeric G protein containing bound GDP. In neutrophils the main G protein involved in signal transduction is thought to be $G_i\alpha 2$ and $G_i\alpha 3$ (Murphy *et al.*, 1987). When the receptor binds ligand the GDP is exchanged for GTP, by the G protein α subunit, causing the dissociation of α from the βγ subunits.

Three types of phospholipases are activated by chemoattractants, phospholipase C (PLC), phospholipase A_2 (PLA_2), and phospholipase D (PLD).

Phosphatidylinositol-specific phospholipase C (PLC) is activated after G protein activation, resulting in the accumulation of inositol 1,4,5,-trisphophate (IP_3) and diacylglycerol (DAG) (Kupper *et al.*, 1992). IP_3 induces the release of Ca^{2+} from intracellular stores (Pittet *et al.*, 1992). DAG remains in the membrane activating protein kinase C (Farago and Nishizuka, 1990). DAG is also produced by phosphatidic acid produced when phosphatidylcholine is hydrolysed by phospholipase D. The activation of PLC is believed to precede that of PLD. The βγ subunits activate a phophoinositide-specific phospholipase C (PI-PLC) called phospholipase $C_{\beta 2}$ (Dickenson *et al.*, 1995).

1.5.1 Amplification

Studies using pulse stimulation and real-time analysis have shown that a single receptor leads to 100 000 actin monomers polymerising and the production of 100 000 superoxide radicals (Sklar, 1986). These processes involve two distinct pathways, although both use the pertussis toxin sensitive G protein. There appears to be no amplification at this level, that is, one receptor activates only one Gα subunit. In the presence of saturating ligand, β-adrenergic receptor stimulation leads to the release of phosphate from GTP at the rate of 100 per minute per β-adrenergic receptor while in the case of FPR this is 1 per minute per FPR (Mueller *et al.*, 1991).

Amplification in the superoxide radical pathway is thought to arise when an activated G protein activates a single phospholipase C to produce hundreds to thousands of hydrolysed phosphatidyinositols (Sklar, 1986). This in turn leads to the release of tens of thousands of free calcium ions, which activates large numbers of protein kinase C and leads to the assembly of oxidative complexes giving the oxidative burst. For the full activation of the respiratory burst calcium influx must be triggered

by the ligand (Truett *et al.*, 1988). There is enough signalling capacity to respond if all the receptors are occupied. In the case of actin polymerization when a hundred receptors are occupied the net capacity of the cells has been used up; that is ten million actins. This pathway does not involve intracellular calcium but probably phosphatidylinositol 3-kinase through the activated G-protein directly or indirectly (Eberle *et al.*, 1990). Figure 1.4 gives a schematic summary of the signalling pathway.

This differential amplification reflects the physiological response of the neutrophil to various concentrations of N-formyl peptides. That is, at low concentrations of N-formyl peptide, and therefore low receptor occupancy, the actin response, thought to mediate cell movement, is maximal. Where there is a high concentration of N-formyl peptide, and therefore high receptor occupancy (near or at the site of chemoattractant release), the respiratory burst and release of cytotoxic material is maximal.

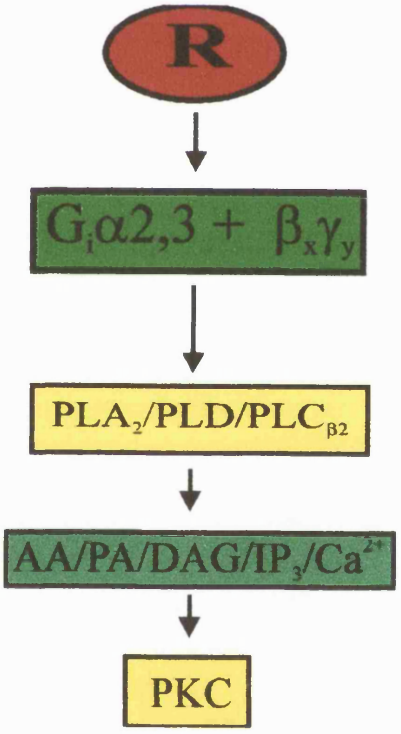

Figure 1.4 Signalling by chemotactic receptors.
R represents the receptor. PKC represents protein kinase C. PLA_2, PLD and $PLC_{\beta 2}$ represent the various phospholipases. AA represents arachidonic acid. PA represents phosphatidic acid. DAG represents diacylglycerol. IP_3 represents inositol 1,4,5,-trisphophate.

1.6 Leukocyte Migration

Leukocytes are the primary agents in the body's defence system acting against invading microorganisms (Weissman and Cooper, 1993). This system is divided into the non-specific (granulocytes and macrophages) and the specific (lymphocytes).

In the non-specific system, granulocytes (neutrophils, eosinophils, and basophils) destroy microorganisms by releasing cytotoxic compounds from their intracellular granules and by phagocytosing them (Lehrer *et al.*, 1993). Macrophages also destroy microorganisms in this way.

The specific lymphoid system involves the antigen-specific cellular immune defense. B lymphocytes produce antibodies which bind to foreign organisms. Antibodies act to destroy foreign organisms by the activation of either the complement system (which perforates the membrane of the microorganism) or phagocytosis. Phagocytosis is carried out by macrophages which have receptors for the antibodies coating the microorganism (opsonization).

T lymphocytes act primarily by cell to cell contact. There are two main populations of T lymphocytes. The first set destroys the cells (killer cells) which have foreign antigens. The second coordinates the haemopoietic cells in the immune response (helper cells) and causes the effector cells to multiply.

Leukocytes continuously circulate through the blood and lymphatic system. When there is tissue damage and inflammation, leukocytes are recruited to the site. This is highly specific (Butcher, 1991). This means that neutrophils selectively enter sites

of acute inflammation or tissue damage, while eosinophils enter sites of allergic reactions and parasitic infections.

To effectively survey and respond to infections, the cells of the immune system must circulate. They do this in a non-adherent state (in the blood and lymph). When activated they rapidly become adherent. Leukocyte migration and homing is a multi-step process involving tethering/rolling, triggering, strong adhesion, and migration. It also involves the interaction of leukocytes with the endothelium (Butcher, 1991; Springer, 1994).

Leukocytes have the lowest blood flow rates when in the postcapillary venules. The flow rate in these areas is reduced during inflammation because of vessel dilation. Tethering is a loose and transient adhesion mediated by the selectin family of adhesion molecules. (Carlos and Harlan, 1994; Kishimoto and Rothlein, 1994; Lawrence *et al.*, 1994). This tethering is not strong enough to hold the cells permanently because of the shear forces generated by the blood flow. This gives rise to rolling.

There are three selectins, named because of their lectin-like affinity for carbohydrate bearing ligands. L-selectin is located on leukocytes, P-selectin and E-selectin on stimulated endothelium. Histamine and thrombin up-regulate P-selectin from intracellular stores. On the other hand, E-selectin upregulation requires *de novo* protein synthesis. This is stimulated by interleukin 1 (IL-1) and tumour necrosis factor-α (TNF-α). More than one selectin can be expressed by cells, thus fine tuning the process.

The tethering leads to cell-cell interactions (leukocytes and endothelium). These interactions are a way of triggering the leukocytes.

Leukocytes respond to ligands on the endothelial cell surface activating strong adhesion (activating integrins) in less than a second. The integrins are present on circulating leukocytes but are not active. Chemokines and other chemotactic molecules can trigger integrin activation. Chemokines are heparin-binding molecules which can become associated with proteoglycans of endothelial cells. CD44 is a prominent proteoglycan and is known to bind β-chemokine MIP-1β (Tanaka *et al.*, 1993). Thus, a rolling T lymphocyte will encounter it and respond by activating the integrin α4β1 causing tight adhesion. Rolling leukocytes can be triggered by the immunoglobulin superfamily adhesion molecule CD31. CD31 is found on endothelia, monocytes, neutrophils and some T lymphocyte populations. Occupancy of CD31 by ligand leads to signal transduction followed by integrin activation (Shimizu *et al.*, 1992).

Once integrins have been activated they bind to members of the immunoglobulin superfamily on the endothelial cells. The main integrins involved in this phase are the β_2 CD11a/CD18, CD11b/CD18 and β_1 integrin very late antigen-4 (VLA-4) (Carlos and Harlan, 1994; Kishimoto and Rothlein, 1994; Alon *et al.*, 1995). CD11a/CD18 and CD11b/CD18 interact with the intercellular adhesion molecule-1 (ICAM-1) and other endothelium ligands. VLA-4 binds to vascular cell adhesion molecule-1 (VCAM-1) and to the matrix component fibronectin. There is an increase in the numbers of ICAM-1 and VCAM-1 due to IL-1 and TNF-α induction.

Once they have bound to the luminal side of the endothelium, leukocytes migrate through the endothelium within minutes. When they have reached the subendothelial basal membrane they are trapped by the extracellular matrix of the basal membrane (Hourihan *et al.*, 1993). Transmigration begins with the locomotion of the adherent leukocyte to the endothelial cell-cell junction which it traverses by a mechanism that involves homotypic binding between CD31 on leukocytes and on endothelium (Muller *et al.*, 1993; Berman and Muller, 1995; Bogen *et al.*, 1994). The leukocyte is thought to be guided across the endothelium and through the tissues to its target by gradients of chemoattractants which are produced at the site of injury (such as N-formyl peptides, LTB_4, and PAF). At the inflammatory lesion the leukocyte becomes activated to carry out its functions in host defence.

For the cell to be mobile it must form new adhesion contacts at the 'front' while at the 'back' these must be reduced. At least two mechanisms are thought to be involved. First, the transient integrin activation. This is probably due to the rapid decrease in the CD31 and other chemokine signals (Muller *et al.*, 1993). Secondly, shedding occurs. That is, L-selectin is shed from the cell surface of leukocyte after they are activated (Kishimoto *et al.*, 1989). In addition, it is thought that large numbers of soluble adhesion molecules in the blood may reduce adhesion by blocking adhesion ligands and modulating migration (Schleiffenbaum *et al.*, 1992; Gearing and Newman, 1993).

1.7 Antimicrobial Activity of Neutrophils

To fulfil its role in host defence against invading microorganisms, the neutrophil contains many cytotoxic substances such as proteases and bactericidal substances,

and it has the ability to assemble an electron transport chain (NADPH oxidase) that is capable of generating large amounts of reactive oxygen species. This process must be tightly controlled as the neutrophil is mobile and present in the entire vascular bed. At sites of inflammation the cell adheres to the endothelium, and migrates into tissue to phagocytose and kill invading microorganisms.

The neutrophil is equipped with many discrete granule subsets and vesicles. These are mobilized in a strictly ordered process (Sengelov *et al.*, 1993; Kjeldsen *et al.*, 1994a) which convert the neutrophil from a quiescent state into a highly active and destructive state.

Secretory vesicles are scattered throughout the cytoplasm (Borregaard *et al.*, 1987; Borregaard *et al.*, 1990) and are formed in the late stages of neutrophil development in the bone marrow (Borregaard *et al.*, 1993). They contain plasma proteins that are exocytosed when the membrane of secretory vesicles fuses with the plasma membrane (Borregaard *et al.*, 1992). They are exocytosed by very low (nanomolar range) concentrations of chemoattractants which do not mobilize granules (Sengelov *et al.*, 1993; Borregaard *et al.*, 1994). These include N-formyl peptides, PAF, IL-8 and LTB_4. The vesicles also contain the N-formyl peptide receptor (Sengelov *et al.*, 1994) and CD11b/CD18 (Pizcueta and Luscinskas, 1994).

The secretory vesicles are the first to be mobilized in response to very low concentration of chemoattractants. This results in mobilization of secretory vesicles changing the neutrophil from a rolling, L-selectin presenting cell to a CD11b/CD18 presenting cell capable of adhering to ICAM-1 which is present on endothelium.

Thus secretory vesicles are of importance in determining the interaction of circulating neutrophils with endothelium.

There are two types of granules in neutrophils, the peroxidase positive granules, also known as azurophil granules or primary granules, and the peroxidase-negative granules, known as specific granules.

The peroxidase-negative granules are heterologous in their size and matrix content varying from granules high in lactoferrin (specific granules) but lacking gelatinase to granules containing both and to granules low in lactoferrin but high in gelatinase (gelatinase granules) (Kjeldsen *et al.*, 1993). In contrast the membranes are similar, sharing CD11b/CD18, FPR and components of the NADPH oxidase system, cytochrome b_{558} (Plesner *et al.*, 1994; Kjeldsen *et al.*, 1994b). The heterogeneity of the granule contents is probably due to controlled timing of biosynthesis of granule proteins (Borregaard *et al.*, 1995). Stimulation of neutrophils with N-formyl peptide mobilizes these granules in a preferential way with the gelatinase granules mobilized first, then the granules containing both, and finally the specific granules (Sengelov *et al.*, 1993; Kjeldsen *et al.*, 1994a). This means that nanomolar concentrations of N-formyl peptide may lead to the mobilization of 25% of total cell gelatinase but only 2-5% of total lactoferrin (Dewald *et al.*, 1982). The gelatinase is probably important in the migration of neutrophils through tissue as its preferred substrate, type IV collagen, is the main constituent of basement membranes (Murphy *et al.*, 1982). Collagenase, which degrades interstitial type I-III collagens is located in specific granules which are mobilized after gelatinase granules.

When the neutrophil arrives at the site of inflammation it will have exocytosed 38% of its gelatinase and 21% of its lactoferrin. In contrast, only 7% of its myeloperoxidase will have been exocytosed. This is found in the peroxidase positive granules.

Therefore, at the site of inflammation the neutrophils, the receptors for phagocytosis, and NADPH oxidase components will be on the cell surface but the azurophil granules containing bactericidal and proteolytic enzymes will be inside the cell ready for fusion with phagocytic vacuoles containing ingested microorganisms.

1.7.1 Respiratory Burst

Neutrophils are able to deploy a group of highly reactive oxidizing agents, including oxidized halogens, oxidizing radicals, and singlet oxygen. The precursor of these oxidants is superoxide anion ($O_2^{\cdot}$) which is produced during the respiratory burst and is catalysed by the enzyme NADPH oxidase (Borregaard *et al.*, 1984; Borregaard, 1988). The NADPH oxidase is a membrane -associated electron transport chain which catalyses the one-electron reduction of oxygen to $O_2^{\cdot}$ at the expense of NADPH (see Figure 1.5).

The oxidase has the following components. The two membrane-bound proteins $gp91^{phox}$ and $p22^{phox}$ make up the cytochrome b_{558}. and two cytosolic components $p67^{phox}$ and $p47^{phox}$. These have been identified by the use of patients with chronic granulomatous disease (CGD) (Chanock *et al.*, 1994).

1. Electron Transfer by NADPH oxidase

$$NADPH + 2O_2 \longrightarrow NADP^+ + H^+ + 2O_2^{\cdot-}$$

2. Spontaneous Reaction

$$2O_2^{\cdot-} + 2H^+ \longrightarrow H_2O_2 + {}^1O_2$$

$$O_2^{\cdot-} + H_2O_2 \longrightarrow \cdot OH + OH^- + {}^1O_2$$

3. Myeloperoxidase Reactions

$$H_2O_2 + Cl^- \longrightarrow H_2O + OCl^-$$

$$2OCl^- + H_2O \longrightarrow 2Cl^- + {}^1O_2 + H_2O$$

4. Cell Protective Reactions

$$O_2^{\cdot-} + O_2^{\cdot-} + 2H^+ \xrightarrow{\text{Superoxide dismutase}} H_2O_2 + O_2$$

$$2H_2O_2 \xrightarrow{\text{Catalase}} 2H_2O + O_2$$

Figure 1.5 Generation of toxic radicals by the respiratory burst.
The toxic products which kill microorganisms are shown in red. $O_2^{\cdot-}$, superoxide anion; OCl^-, hypochlorous anion; ${}^1O_2$, singlet oxygen;•OH, hydroxyl free radical. The enzymes superoxide dismutase and catalase act to protect the neutrophil.

1.8 Human Leukaemic (HL-60) Cells and Murine Pluripotent Stem Cells (FDCP)

Two cell lines were used for the study of FPR; HL-60 and FDCP.

1.8.1 Human Leukaemic (HL-60) Cells

HL-60 is a factor-independent cell line which can be induced to differentiate *in vitro* to a number of different cell types (Collins *et al.*, 1977; Gallagher *et al.*, 1979). In suspension culture, these cells have an unusually quick doubling time (36 to 48 hours). Most myeloid leukaemia cells, when cultured in suspension, proliferate for a few cell divisions, then go into growth arrest and undergo cell death. It appears that the surface expression of transferrin and insulin receptors is critical for the proliferative capacity of HL-60. This is because these cells will proliferate in serum-free nutrient containing transferrin and insulin (Breitman *et al.*, 1980). Transferrin and insulin receptor expression decreases as these cells are induced to differentiate (Sutherland *et al.*, 1981; Chaplinski *et al.*, 1986). HL-60 cells are also thought to produce colony-stimulating factors which act as autostimulators (Dittmann and Petrides, 1991). HL-60 cells can be induced to differentiate into four general cell types: granulocytes; monocytes; macrophage-like cells and eosinophils.

1.8.2 Pluripotent Stem Cells differentiation by cytokines

Cytokines are a family of glycosylated extracellular proteins which modulate immunological, inflammatory and reparative host responses to injury. Many of these cytokines are secreted during immunologic and inflammatory responses. They are cellular signals that regulate local, and at times systemic, inflammatory responses. They are not usually present in serum. They generally act on nearby cells or directly on themselves. They modulate reactions of the host to foreign antigens or injurious

agents by regulating the growth, mobility, and differentiation of leukocytes and other cells.

Haematopoietic colony stimulating factors are cytokines that stimulate a limited number of pluripotent stem cells. These are mainly found in the bone marrow and can stimulate the production of large numbers of platelets, erythrocytes, neutrophils, monocytes, macrophages, eosinophils, basophil/mast cells, and lymphocytes. Most of these cells are short-lived in the blood. *In vitro*, the formation of mature cells from pluripotent stem cells is supported by a number of cytokines.

Three growth factors are known to control the production of neutrophils. First, interleukin 3 (IL-3), a multilineage stimulating factor which facilitates the survival and stimulates the proliferation of stem cells, as well as the proliferation and development of committed progenitor cells (neutrophil/macrophage, eosinophil, erythroid, mast cell and megakaryotype lineages). Secondly, granulocyte-macrophage colony stimulating factor (GM-CSF), a multilineage stimulating factor. Unlike IL-3 it has a limited range (neutrophil/macrophage, eosinophil, and megakaryotype lineages). Thirdly, granulocyte colony stimulating factor (G-CSF), stimulates progenitor cell development to yield mature neutrophils.

1.8.3 Murine Pluripotent Stem Cells (FDCP)

FDCP cells are derived from long term marrow cultures. They have a normal karyotype, are nonleukaemic, and grow continuously in the presence of interleukin-3 (IL-3) (Crompton, 1991). All stem cells from regenerating tissue are characterised by their ability to undergo differentiation and by their potential for self renewal. In the

haematopoietic system, the regulation of self renewal and differentiation of stem cells is controlled by soluble growth factors leading to a variety of lineage restricted progenitor cells. The production of haematopoietic growth factors occurs at multiple sites in the body and by a variety of cell types. Their production is elevated by immunological reactions and products of infectious agents which call for the recruitment of white blood cells involved in host defense.

The optimum concentrations of cytokines for the differentiation of FDCP cells to neutrophils is IL-3 (1 $U.ml^{-1}$), GM-CSF (50$U.ml^{-1}$) and G-CSF (1000$U.ml^{-1}$) (Spooncer *et al.*, 1986). The cells produced with these cytokines show a mature polymorphonuclear cell morphology as compared to the blast-cell like morphology of the undifferentiated FDCP. Spooncer and co-workers using the oxidative burst process normally seen in mature neutrophils, demonstrated that FDCP cells exhibit a similar response (Spooncer *et al.*, 1986). This indicated that neutrophils, produced from differentiating FDCP cells, were functionally mature. In this study I confirm these findings and expand them into other neutrophil characteristics and the study of the FPR.

1.9 Aims of the Study

Neutrophils isolated from blood, are short lived and terminally differentiated. They therefore do not make good models for the study of their function and FPR. This is especially problematic with respect to gene expression. There is therefore a need for *in vitro* model systems which mimic normal differentiation and lead to the development of mature cells.

The overall objective of the project is to develop a better model than the currently used human promyelocytic leukaemia cell line (HL-60). When HL-60 cells are differentiated to neutrophils they exhibit impaired cellular responses to N-formyl peptides. The pluripotent murine cell line FDCP was chosen for the development of an alternative and more accurate model of neutrophil function and in particular N-formyl peptide mediated events.

The aims are therefore first to study the cytokine mediated differentiation process in order to determine and optimise the conditions for producing mature neutrophils which respond physiologically and reproducibly to N-formyl peptide stimulation. Since this is a murine cell system the second objective is to study the kinetics and specificity of murine FPR to different N-formyl peptides, and compare these to the human and rabbit FPRs.

Another aim of this work is to extend the detailed characterisation of murine FPR to the DNA level. To determine the sequence and the structural organisation of the gene, PCR cloning and genomic library screening is to be carried out.

Given that FDCP cells may provide not only a model of mature neutrophils, but also an *in vitro* system for studying cell differentiation in response to cytokines, a further aim is to study the tissue-specific expression of FPR in order to determine the identity of the major gene isoform and the time course of transcription during differentiation. The genetic data could then be compared to the phenotypic expression of FPR mediated functions.

The data from this work will provide the basis for the rational design of experiments to elucidate structural and functional relationships of FPR.

CHAPTER 2

MATERIALS AND METHODS

2.1. Materials and suppliers

Analytical grade chemicals were used in this study, and all solutions were prepared using deionised water. Materials were obtained from the following suppliers:-

General laboratory reagents and equipment

BDH:	BDH Laboratory Supplies Merck Ltd., Lutterworth, Leicestershire.
SIGMA:	Sigma Chemical Co. Ltd., Poole, Dorset.
WHATMAN:	Whatman Scientific Ltd., Maidstone, Kent.
BRAIDWOOD LABORATORIES	Braidwood laboratories,Becenham,Kent BR3 1JJ.

Culture Media

GIBCO-BRL:	Life Technologies Ltd., Renfrew Road, Paisley.
FLOW:	ICN Biochemicals Ltd., High Wycombe, Buckinghamshire.
	OXOID; Oxoid Ltd., Basingstoke, Hampshire.

Radiolabelled Compounds

AMERSHAM:	Amersham International plc., Aylesbury, Buckinghamshire.
NEN:	New England Nuclear Ltd., New Road, Southampton.

Molecular Biology Products

BOEHRINGER-MANNHEIM	Bell Lane, Lewis, East Sussex.
INVITROGEN:	British Bio-technology Ltd., Abingdon, Oxon, OX14 3YS.
PHARMACIA:	Pharmacia Biotech, Knowlhill, Milton Keynes.

PROMEGA: Promega Ltd., Epsilon House, Southampton.

QIAGEN: Hybaid Ltd., Teddington, Middlesex.

NBL: Northumbria Biologicals Ltd., Cramlington, Northumberland.

2.2. Tissue culture

The HL-60 cell line was donated by Dr. J. Cunningham, Department of Surgery, Royal Free Hospital. The FDCP and WEHI-3b cell lines were donated by Lyn Healy, Chester Beatty laboratories, ICRF.

2.2.1. Thawing and storing cells

2.2.1.1. Thawing cells

A vial was removed from liquid nitrogen and thawed rapidly with gentle agitation in a 37°C waterbath. The outside of the vial was quickly decontaminated with 70% ethanol. Cells were placed into a 25 cm^2 flask containing 10ml of fresh complete medium. After 24 hours incubation, the old medium was discarded and replaced with fresh complete medium. All cells were maintained at 37° C, 5% CO_2, 95% humidity. After a maximum of 20 passages fresh cells were thawed from frozen stocks.

2.2.1.2. Storing cells

Cells used for freezing were healthy log-phase cultures (>97% viability). They were pelleted by centrifugation at 1,000 x g for 10 minutes and resuspended in fresh complete medium at a density of 5 x 10^6 cells/ml. The cell suspension was diluted

with an equal volume of fresh freezing medium 20% v/v dimethyl sulphoxide (DMSO) in medium (horse serum; FDCP cells, complete medium; HL-60 and WEHI-3b) to yield a final DMSO concentration of 10% v/v and maintained at 4°C. The diluted cell suspension was then dispensed into 2ml aliquots. The cells were frozen slowly by placing freezing vials in an insulated container at -20°C for one hour and then at -70°C overnight. Finally, the cells were stored in liquid nitrogen.

2.2.1.3. HL-60

HL-60 cells were grown in suspension culture in RPMI 1640, supplemented with 2mM L-Glutamine, 1mM sodium pyruvate, penicillin (100U/ml), streptomycin (100µg/ml), and 15% v/v heat inactivated foetal bovine serum. Density was maintained between 5 x 10^5 and 10 x 10^6 cells/ml by subculturing every 2-3 days.

2.2.1.4. FDCP

FDCP-A4 cells were grown in suspension culture in Fishers medium, supplemented with 10% v/v WEHI-3b conditioned medium as a source of IL-3, penicillin (100U/ml), streptomycin (100µg/ml), and 20% v/v horse serum. Cells were subcultured every 2-3 days. The cells were maintained at a density of 5 - 50 x 10^4 cells/ml.

2.2.1.5. WEHI-3b

WEHI-3b cells were grown in McCoys medium, supplemented with penicillin (100U/ml), streptomycin (100µg/ml), and 10% v/v foetal bovine serum. Cells were subcultured every 2-3 days to a density of 5 x 10^4 cells/ml (Heyworth *et al.*,1990b).

2.2.1.6. Conditioned Medium

The supernatant medium of 6-7 day cultures WEHI-3b cells was collected. This was then filter sterilized by passage through a 0.22µm filter. The supernatant was aliquoted and stored at -20° C.

2.2.2.1. Differentiation of HL-60

HL-60 cells were differentiated with N^6 0^2 - dibutyryl adenosine 3' 5'-cyclic monophosphate (0.6mM). 2 x 10^6 cells/ml were differentiated under the same conditions used in culturing.

2.2.2.2. Differentiation of FDCP

The FDCP cells were differentiated in Iscoves medium supplemented with 20% v/v foetal bovine serum, penicillin (100u/ml), and streptomycin (100µg/ml). 5 x 10^4 cells/ml were differentiated with interleukin-3 (IL-3) (1U/ml), granulocyte macrophage colony-stimulating factor (GM-CSF) (50U/ml), and granulocyte colony-stimulating factor (1000U/ml). The control cells were grown in IL-3 (~1000U/ml).

2.2.2.3. Assay for cell type

Estimation of number of neutrophils was carried out by examination of Prodiff-stained (Braidwood laboratories) preparations of cells by pelleting onto a glass slide (cytospins). The proportion of neutrophils to total leukocytes was calculated by reading the slide under transmitted bright field (x 50). Three slides were counted of two hundred cells per slide. 80% of the cells were found to be neutrophils.

The percentage of functional neutrophils was estimated by determining the presence of stained azurophilic granules and the formation of pseudopods in the

presence of the N-formyl pepdied, fMet-Leu-Phe-Lys (fMLFK). The cells were incubated in PBS, contaning fMLFK 50µM, for 15 minutes at 37°C, pelleted onto a glass slide, and the percentage of cells containing black azurophilic granules was counted.

Cell samples were taken at regular intervals, washed in PBS in 10ml tubes centrifuged at 100 x g for 10 minutes, pelleted, and kept at -70°C to be used for RNA isolation. Cells to be used in the binding experiments and the NBT assay were washed in phosphate-buffered saline and then in binding assay buffer.

2.3.1 Physiological assay for differentiated cells - NBT Assay

Cells were incubated in an NBT (2,2'Di-p-nitrophenyl-5,5'-diphenyl-3,3'-[3,3'-dimethoxy-4,4'diphenylene]-ditetrazolium chloride) mixture (pre-equilibrated at 37°C). The mixture contained NBT (0.01% w/v), fMet-Leu-Phe-Lys (fMLFK) 70µM in binding assay buffer (400µl) to which 200µl of cells were added (2-4 x 10^6 cells/ml). The control had no fMLFK. This was then incubated at 37°C for 15 minutes The cells were then placed at 4°C for 5 minutes and pelleted at 2000 rpm for 10 minutes at 4°C. The cells were then incubated with 750µl methanol (70% v/v) in order to disrupt the cell membrane. The lysed cells were centrifuged to pellet the cell granules. The pellet was resuspended in 300µl of potassium hydroxide (2M) and left for 14 hours at room temperature to lyse the granules. The mixture was then processed by the addition of 375µl Dimethylsulphoxide. The absorbance was then measured at 620nm and 450nm. The measure of NBT reduction was calculated by subtracting the 450nm value from the 620nm value. The value obtained from the NBT assay with fMLFK was subtracted from the NBT assay without fMLFK to obtain

the absorbance change due to the fMLFK. The absorbance values were calculated for 1 x 10^6 cells.

2.4. Radioligand binding assays

2.4.1. Tritiated fMLF-[^{3}H]-fMLF

The binding study was carried out using [^{3}H]-fMLF (formylmethioine-leucine-phenylalanine) (NEN). Cells were incubated for 90 minutes on ice with varying concentrations of the radioligand. These were then pelleted and washed in Hanks Balanced Salt solution. Scintillant was added and the radioactivity measured. Non-specific binding was determined in the presence of a 1000 times excess of unlabelled fMLF.

2.4.2. Radioiodination of a chemotactic peptide

Formyl-Nle-Leu-Phe-Nle-Tyr-Lys was iodinated with [^{125}I] to formyl-Nle-Leu-Phe-Nle-^{125}I-Tyr-Lys ([^{125}I]-fnLLFnLYK) by a modification of Niedel (Niedel *et al.*, 1979). Formyl-Nle-Leu-Phe-Nle-Tyr-Lys (fnLLFnLYK) was dissolved in dry dimethylformamide:triethylamine (99:1) to a final concentration of 1.0mM. This was then diluted with methanol to 0.1mM. 10µl of the 0.1mM fnLLFnLYK (1nmol) was added to 100µl of 250mM sodium phosphate, pH7.6, and to 2 to 3 mCi of carrier-free [^{125}I], and to 10µl of 1.0mM chloramine-T (10nmol) in water and the reaction was left for 10 minutes at room temperature. The reaction was terminated by the addition of 100µl of 20% v/v glycerol in water. The mixture fractionated on a 15ml Bio-Gel P-2 column equilibrated with 25mM NaOH. 70.4% of the peptide was iodinated giving a specific activity of 1500-1700Ci.mmol^{-1}.

2.4.3. Thin layer chromatography

The [^{125}I]-fnLLFnLYK produced a single radioactive spot after thin layer chromatography, with *the following* R_F values in the follwing solutions: in chloroform:methanol:acetic acid (3:1:1) R_F= 0.7, chloroform:methanol:triethylamine (5:2:1) R_F= 0.18, and 1-butanol:acetic acid:water (4:1:1:) R_F= 0.65. The iodinated peptide was neutralized with Na_2PO_4 and diluted to 60nM with binding assay buffer plus 0.1% w/v bovine serum albumin. The sample was then divided into aliquots and stored at -20°C.

2.4.4. Binding assay

The standard binding assay was carried out as follows: 2 x 10^5 cells were incubated with 400fmol [^{125}I]-fnLLFnLYK for 60 minutes at 4°C in 1ml of binding assay buffer (15mM sodium phosphate, 123mM NaCl, 1mM $CaCl_2$, 0.1% w/v bovine serum albumin, pH 6.75) in a 4ml plastic tube. The binding was terminated by the addition of 2ml of binding assay buffer at 4°C then whirly mixed and filtered through a 1.0µm pore size filter (Millipore). The filtered cells were washed in 10ml of binding assay buffer at 4°C and counted directly for [^{125}I]. Nonsaturable binding was defined as the amount of [^{125}I]-fnLLFnLYK bound in the presence of an excess of unlabelled fnLLFnLYK (400pmol). In this study binding will always refer to total binding minus nonsaturable binding. Experiments were carried out at least three times and in triplicate and the standard error of the mean was consistently less than ±5%.

2.4.5. Calculations

The binding of [^{125}I]-fnLLFnLYK was used as a functional assay for FPR and was measured essentially according to the methods described by Niedel (Niedel *et al.*,

1979). The binding of [^{125}I]-fnLLFnLYK to FPR can be expressed by the following equations:-

$$R + L \rightleftharpoons RL \quad (1)$$

$$K_d = [R][L] / [RL] \quad (2)$$

$$[R]_T = [RL] + [R] \quad (3)$$

where R = Free FPR

L = Free [^{125}I]-FP

RL = Bound [^{125}I]-FP

K_d = Dissociation constant

$[R]_T$ = Total FPR concentration

Substituting [R] in equation (2) for $[R]_T$ - [RL] gives:

$$K_d = [L][R]_T / [RL] - [L][RL] / [RL] \quad (4)$$

Rearranging equation (4) gives:

$$[RL] / [L] = [R]_T / K_d - [RL] / K_d \quad (5)$$

At equilibrium [RL] / [L] can be measured experimentally as a ratio of bound to free [^{125}I]-fnLLFnLYK (B/F). Thus equation (5) simplifies to:

$$B/F = [R]_T / K_d - B / K_d \quad (6)$$

The most common graphical analysis method is the *Scatchard plot* of B/F against F. For a single binding site model, the plot is a straight line with an intercept on the B/F axis (when B = 0) of B / K_d, a slope of $-1 / K_d$, and an intercept on the F-axis of $[R]_T$.

A curvilinear *Scatchard plot* indicates that there is more than one type of binding site. By repeated substitution of estimated values on a trial and error basis the theoretical curve which fits the experimental curve can be found. This is called the iterative procedure and is usually carried out by computer.

2.5. Molecular biology techniques

The methods used in DNA work were essentially as described by Maniatis and co-workers (Maniatis *et al.*, 1982) with some modifications. Plasticware, glassware, and media were routinely sterilized by autoclaving for 15-20 minutes at 121°C (15 pounds/inch^2). Chemicals were either autoclaved or filter sterilized and the highest grades available were used.

2.5.1. Genomic DNA extraction

Cells were pelleted, washed in phosphate buffered saline (PBS), and added to 50mM Tris.HCl pH 7.5, 10mM ethylenediamine tetra-acetic acid (EDTA) pH 8.0, 50mM NaCl and 2% v/v sodium dodecyl sulphate (SDS). Proteinase K was added to the buffer to a final concentration of 150µg/ml and the specimens were incubated at 37°C for 2-16 hours. The DNA was purified with half volumes of phenol:chloroform mix (75% v/v phenol, 15% v/v chloroform, 0.05% v/v 8-hydroquinoline and equilibrated with 0.5M Tris.HCl pH 8.0) vortexed and centrifuged

at 13,000 rpm for 5 minutes and the supernatant retained. The supernatant was added to an equal volume of a 25:24:1 (v:v:v) mixture of phenol:chloroform:isoamylalcohol and centrifuged as before. Phenol:chloroform extraction was repeated until no white proteinaceous material could be seen at the interface. The DNA was precipitated by the addition of 0.2 volume of 3M sodium acetate and 3 volumes 100% ethanol. The DNA precipitate was collected by spooling with a pasteur pipette whose end had been sealed and shaped into a U. The DNA was then washed twice with 70% v/v ethanol and resuspended in TE (10mM Tris.HCl pH 8.0 and 1mM EDTA) and stored at 4°C. The concentration was estimated and the solution diluted to 1mg/ml.

2.5.2. RNA isolation

Cells were washed in PBS pelleted and resuspended in GIT (4M guanidinium thiocyanate, 0.1M Tris.HCl pH7.5 and 1% v/v β-mercaptoethanol). The cells were lysed by sequetial passage through a 19, 23 and 25 gauge needle. Cells were then layered on 0.8ml of 5.7M Caesium Chloride in Beckman centrifuge tubes. The tubes were centrifuged for 3 hours at 55 000rpm at 20°C. The pellet of RNA was then washed in ethanol (80% v/v), air dried and resuspended in water. The RNA was then aliquoted and stored at -70°C.

2.5.3. Quantitation of Nucleic Acids (DNA/RNA)

DNA concentrations were accurately measured by spectrophotometric absorbance readings of diluted DNA and RNA solutions at 260nm and 280nm. An absorbance of 1.0 at 260nm was taken to be equivalent to a concentration of 50µg/ml for double-stranded DNA, and 40µg/ml for single-stranded DNA and RNA. For oligonucleotides (amplimers) an OD of 1 corresponds to ~20µg/ml. The purity of the preparations

was estimated by the ratio of the absorbances at 260nm and 280nm. Pure DNA and RNA preparations have an OD_{260}/OD_{280} ratio of ≥ 1.8 and 2.0, respectively.

Ethidium bromide fluorescence upon UV illumination (302nm) is directly proportional to the amount of DNA in which it has intercalated. Therefore, a rapid and very accurate method of double stranded DNA measurement is the visual comparison of the intensity of DNA bands to the intensity of λ molecular weight marker bands containing a known amount of DNA.

2.5.4. Restriction of DNA

Restriction endonucleases type II are DNases that recognize specific nucleotide sequences. These enzymes cleave double-stranded DNAs and produce unique, equal molar fragments of a DNA. The restriction reaction was typically composed of the substrate DNA, and the desired restriction enzyme in its appropriate buffer. This was incubated at the enxyme's optimal temperature for one hour. Enzymes were used at a concentration of 2 to 5 units per microgram of DNA. The enzyme reactions were monitored by agarose gel electrophoresis. For genomic DNA 15µg was digested and run on 0.7% w/v agarose gel. For plasmid DNA 1µg was usually digested.

2.5.5. Agarose gel electrophoresis

Separation of DNA fragments, generated after restriction digestion, was achieved by agarose gel electrophoresis, using a horizontal submarine gel apparatus (Bio-Rad). Gel concentrations used were dependent on the size of the DNA fragments to be analyzed and the degree of separation required. Most of the DNA fragments used in this study for further manipulations were of such a size that they were

usually resolved in agarose gels with concentrations between 0.7 and 1.0% w/v. Gels were prepared by microwaving the required amount of agarose in 0.5 x TBE (45mM Tris-borate buffer, 1mM EDTA, pH 8.0). Ethidium bromide was added to the melted agarose (cooled to 45°C) to a final concentration of 0.5 µg/ml. The agarose was then poured into a gel former and allowed to set for approximately one hour at room temperature. Prior to loading onto the gel, DNA samples were mixed with 0.1 volume of 10 x loading buffer (0.4% w/v bromophenol blue and 67% w/v glycerol in 0.5 x TBE buffer). Electrophoresis was typically carried out in 0.5 x TBE buffer at a constant voltage of 60 to 100V for 20 to 60 minutes. Molecular weight markers were provided by λ DNA restricted with *Hind* III, or *Eco* RI, *Bgl* II or (0.5 to 23 kb). DNA bands were visualized using a LKB UV transilluminator (2011 Macrovue) and photographed using a Polaroid hand camera and Polaroid type 667 film.

2.5.6. Southern transfer

A Southern Blot technique was used in order to transfer, by capillary action, the DNA onto a Hybond N+ filter. After the DNA fragments were run on a standard agarose gel (usually 0.7% w/v), the gel was transferred to a glass baking dish and unused areas trimmed away. The bottom left hand corner was also removed to orientate the gel. The DNA in the gel was depurinated by constant agitation for 15 minutes in 250mM HCl. The DNA was then denatured over a period of 45 minutes by constant agitation on a rotary platform while the gel was soaked with several volumes of 1.5M sodium chloride and 0.5M sodium hydroxide. After this 45 minute period, the gel was rinsed gently in deionised water and neutralised by soaking in several volumes of a 1M Tris.HCl pH 7.4, 1.5M NaCl solution for 30 minutes on a rotary platform. A support for the gel was then made by wrapping a piece of glass in a piece of Whatman 3MM paper. The support was placed in a baking dish filled with transfer

buffer (10 x SSC: Sodium citrate, 0.15M; soidum chloride, 1.5M; pH7.0). The filter was presoaked in 2 x SSC for 5 minutes. A corner was then cut from to orientate it in relation to the gel. The gel was inverted onto the 3MM papers on the support. Two pieces of 3MM paper cut to the size of the gel were wetted in 2 x SSC and placed on top of the filter. Paper towels were then placed on top of the 3MM papers and weighed down to establish capillary flow from the reservoir, through the gel and onto the filter. The transfer was left for 16 hours. The filter was then removed from the apparatus and baked for 1 hour at 80°C to fix the DNA to the filter.

2.5.7. Radiolabelling of the probe

The probe used in the DNA hybridization experiments (Section 2.5.3) was prepared according to the protocol supplied with the Random Primed DNA labelling Kit (Boehringer Mannheim). A sample (50ng) of the coding region of the FPR cDNA, was first denatured by heating for 10 minutes at 100°C and then chilled at 4°C immediately. To a 0.5 ml eppendorf tube on ice, the following reagents were added: 25ng of the denatured DNA, 3µl of dNTP mixture (dATP:dGTP:dTTP = 1:1:1), 2µl of random hexanucleotides in 10 x reaction mixture (2 M N-[2-hydroxyethyl]piperazine-N'-[2-ethanesulfonic acid (HEPES), pH 6.6, 2mM Tris-HCl pH 7.0, 0.1mM EDTA, 4mg/ml BSA), 5µl of [α-^{32}P] dCTP (50µCi, 3,000 Ci/mmol), sterile distilled water to yield a total volume of 19µl, and finally, 1µl of Klenow enzyme (2 units). The mixture was incubated for 30 minutes at 37°C. The reaction was terminated by heating at 65°C for 10 minutes. Non-incorporated [α-^{32}P] dCTP was removed by chromatography on Sephadex G-50. A 2ml syringe was filled with sephadex G-50 and glass wool added to prevent leakage of the sephadex. The resin was pre-equilibrated with 10mM TE (pH8.0). The syringe was centrifuged at 3000rpm for 5 minutes or until the sepharose had dried. The labelled probe was

then loaded on the resin and an eppendorf used to collect the eluent which was produced upon centrifugation at 3000rpm for 5 minutes.

2.5.8. Hybridization

The pre-hybridization buffer consisted of 0.5% w/v blocking agent (Amersham), 0.1% w/v SDS, 5% w/v dextran sulphate and 100µg/ml of denatured sheared heterologous DNA (Salmon sperm). 0.25-0.125 ml/cm^3 pre-hybridization buffer was used.

The pre-hybridization was carried out at 65°C for two hours. The probe was added and hybridization continued for a further 4 to 16 hours. The incubation was continually rotated in a Hybaid oven.

2.5.9. Washing

Two washes of 15 minutes each with 5 x SSC (0.1% w/v SDS) followed by two washes of 0.1 - 5 x SSC (0.1% w/v SDS), depending on the stringency required were carried out. All washes were done at 65°C.

2.5.10. Detection

The filter was wrapped in cling film to prevent drying, placed in a film cassette containing film, and left for varying time lengths depending on the signal strength of the probe.

2.6. Polymerase Chain Reaction

2.6.1. cDNA synethsis by reverse transcritptase

200ng of total RNA was reverse transcribed using an antisense amplimer. The mixture consisted of: 1 x reaction buffer (25mM KCl, 4mM Tris-HCl pH8.4, 0.16mM $MgCl_2$, 2µg/ml BSA; 200µM dNTPs; 1µM antisense primer; 40 units of Rnasein; 3mM Dithiothreitol; 200ng total RNA; 800 units of AMV reverse transcriptase, in a total volume of 50µl. The mixture was heated to 65°C for 20 minutes, then placed at 4°C for 3 minutes, the enzyme added and, the mixture incubated at 42°C for 45 minutes.

2.6.2. Amplification of DNA by PCR

PCR was carried out on a hybaid thermal reactor using 25% of the reverse transcribed material or approximately 100ng of genomic DNA. The following reaction was set up in a mini-eppendorf to a final volume of 100µl: 1 x salt buffer (10mM Tris-HCl pH 8.8, 50mM KCl, 1.5mM $MgCl_2$, 0.1% v/v Triton X-100); 200µM dNTPs; 1µM sense and 1µM antisense primer; DNA of varying concentration; 2.5U Taq polymerase. Mineral oil was used to limit evaporation from the reaction mixture (100µl). Thermal cycling consisted of 95°C for 4 minutes followed by thirty cycles of 90 seconds at 95°C, 90 seconds at 50°C, and 180 seconds at 72°C and a final extension of 72°C for 7 minutes.

2.6.3. Optimization of PCR - $MgCl_2$

The optimal concentration of magnesium ions required for the PCR system was determined with a series of buffers containing increasing concentrations of $MgCl_2$: 1.0mM, 1.5mM, 2.0mM, 2.5mM, 3.0mM, 3.5mM, 4.0mM, 4.5mM and 5.0 mM. The

PCR was performed with murine genomic DNA (100ng) and was then analysed on a 1.0% w/v agarose gel. The optimal $MgCl_2$ concentration for the set of primers was established by visual inspection of the ethidium bromide stained gel.

2.6.4. Optimization of PCR - Amplimers

The primers were titrated to the following concentrations; 0.2µM, 0.4µM, 0.6µM, 0.8µM, 1.0µM, 1.2µM, 1.4µM, 1.6µM, 1.8µM and 2.0µM. The PCR was performed using the above primer concentrations and the same conditions as before. The optimal primer concentration was determined by inspection of the PCR products on a 1.0% w/v agarose ethidium bromide stained gel.

2.6.5. Optimization of PCR - Cycling

The cycling conditions of the PCR were varied to achieve optimal amplification of the target DNA. The hybaid thermal cycler was programmed varying the denaturing, annealing and extension times. The optimal PCR cycling conditions were determined by inspection of the amplification patterns on a 1.0% w/v agarose ethidium bromide stained gel.

2.6.6. Optimization of PCR - Sensitivity

The sensitivity of the PCR was determined using the titration of genomic or plasmid DNA containing: 10^{10}, 10^8, 10^6, 10^4, 10^2 and 10 copies. The PCR was performed under the conditions described above. The sensitivity was estimated by visual inspection of a 1.0% w/v agarose gel stained with ethidium bromide.

2.6.7 'Hot Start' PCR

'Hot start' PCR prevents the extension of any primer/DNA complexes which form at low temperatures, and are thus non-specific, (D'Aquila *et al.*, 1991). 'Hot start' PCR involves setting up a standard PCR reaction and omitting only the polymerase. The reaction mixture is then heated to 95°C, for 5 minutes, and then cooled to 85°C and the DNA polymerase added. The PCR then proceeds as normal. 'Hot start' PCR was used as a standard procedure.

2.7. Molecular cloning

2.7.1. DNA agarose gel purification

DNA was electrophoresed through 1% w/v low melting point gels at 50 Volts, so as not to melt the gel. The DNA was visualized by UV light and the fragment of amplified DNA excised from the gel using a scalpel. The gel slice was placed in a 1.5 ml microcentrifuge tube and 4 volumes of elution buffer (20mM Tris.HCl pH 8.0 and 1mM EDTA) were added. It was then heated to 65°C for 10 minutes. To remove the agarose and other impurities 0.5 volume of phenol was added and the temperature was kept at 65°C for a further minute, or until the agarose had melted completely. The DNA was then purified as before by phenol extraction and once with phenol:chloroform. The DNA was finally precipitated using 0.2 volumes of 4M ammonium acetate with 2 volumes of 100% ethanol, washed in 70% v/v ethanol, vacuum dried, and resuspended in 20µl of water.

2.7.2. Blunt ending DNA fragments

The 3' recessed termini created by digestion of DNA with restriction enzymes were blunted by using the Klenow fragment of *E. coli* DNA polymerase I. The enzyme

works quite well in most restriction enzyme buffers but, if necessary, DNA samples can be resuspended in Klenow enzyme buffer (50mM Tris-HCl, pH 7.2, 10mM $MgSO_4$, 0.1mM DTT). The Klenow polymerase (1 unit) was added to 20µl of DNA fragment samples (0.1 to 0.5µg) containing all four deoxyribonucleoside triphosphates (dNTPs) at 300µM and then incubated at 30°C for 30 minutes The enzyme reaction was terminated by the addition of 2µl of 0.5M EDTA, followed by either phenol:chloroform extraction or heat inactivation at 65°C for 10 minutes.

2.7.3.Dephosphorylation of vector 5' DNA ends

Removal of the 5' phosphate groups leaves a hydroxy terminus, preventing the unwanted recircularisation of the linearised vector. The vector was dephosphorylated to prevent the linearised vector from re-ligating: 28µl vector pUC19 (linearised with *sma* 1), 4µl 10x calf intestinal phosphatase buffer, 3µl calf alkaline phosphatase (CIP), (5U/µl), and 5µl water. The reaction was carried out at 37°C for 60 minutes An additional 2µl of the CIP (5U/µl) was then added and the reaction continued for another 60 minutes at 55°C. The vector DNA was then purified as described in Section 2.7.5.

2.7.4. Phosphorylation of 5' DNA fragments

The fragment to be inserted must be phosphorylated to allow it to ligate with the dephosphorylated vector. The phosphorylation reaction was as follows:28µl of DNA, 4µl 10x kinase buffer, 1µl 50mM ATP, 2µl T4 kinase (5U/ml), 5µl water. The reaction mix was left at 37°C for 45 minutes. The vector DNA was then purified as described in Section 2.7.5.

2.7.5. Purification of DNA

Phenol extraction is a rapid method for purification of nucleic acids. The removal of proteins was achieved by extracting aqueous solutions of nucleic acids with phenol:chloroform and then with chloroform. This procedure also inactivates and removes enzymes. Stocks of phenol equilibrated with Tris-HCl (pH8.0) contained 0.1% w/v 8-hydroxyquinoline as an antioxidant. Stocks of chloroform contained 4% v/v isoamylalcohol. While the phenol and chloroform extracted lipids and denatured proteins, the isoamylalcohol reduced foaming during the extraction and facilitated the separation of the aqueous and organic phases. An equal volume of phenol:chloroform (1:1) was added to a DNA preparation and mixed thoroughly by vortexing. The mixture was then centrifuged to separate the phases at 12,000 x g in a microfuge for 2 minutes. The top (aqueous) layer containing DNA was carefully removed and re-extracted with chloroform as before. The recovery of nucleic acids was then achieved by ethanol precipitation.

The ethanol precipitation was carried out by the addition of 0.1 volume of 3M sodium acetate (pH 4.8) and 2 volumes of ethanol 100% v/v at -20°C. The mixture was routinely held at -20°C for 30 minutes to 16 hours or -70°C for 15 to 20 minutes. The precipitate was collected by centrifugation at 12,000 x g for 10 minutes in a microfuge. The pellet was then washed with 70% v/v ethanol and dried either by inversion for 20 minutes at room temperature or under vacuum for a few minutes. Finally, the nucleic acids were dissolved in either TE or sterile distilled water.

2.7.6. Ligation

The PCR amplified DNA was ligated into the dephosphorylated vector pUC19 *Sma* I/CIP (50µg) in 1 x ligation buffer (50mM Tris.HCl pH 7.6, 10mM dithiothreitol and

500µg/ml bovine serum albumin), 1µl of 6mM ATP, and 2U of T4 DNA ligase, in a final volume of 15µl. It was then incubated at 15°C for 24-48 hours. A control ligation was also performed with no insert DNA.

2.7.7. Competent cell production

In order to introduce DNA into cells, competence was artificially induced in *E. coli* cells (JM105) by treating them with calcium chloride prior to adding DNA. This was performed as described by Maniatis and co-workers (Maniatis *et al.*, 1982) with some modifications. A single colony of *E.coli* (JM105) from a fresh plate was inoculated into 10ml of LB and incubated at 37°C for 16-20 hours on a shaker. A 500µl aliquot was inoculated into 400ml of LB and incubated as above until the absorbance of the solution at 550nm reached 0.2 OD units. The cells were pelleted by centrifugation at 1700 x g for 15 minutes. The cells were then resuspended in ice cold TFN buffer (10mM Tris.HCl pH8.0 and 50mM $CaCl_2$) to a volume of 200ml and incubated on ice for 20 minutes. The cells were pelleted as before then resuspended in 20ml of TFN buffer and kept on ice. The competent JM105 cells were dispensed in 400µl aliquots and snap frozen on dry ice before being stored at -70°C.

2.7.8. Transformation

For transformation, up to 100ng of DNA in a volume of less than 10µl was added to a 200µl aliquot of competent cells. After incubating on ice for 45 minutes with occasional mixing every 15 minutes, the cells were heat-shocked at 42°C in a circulating water bath for exactly 90 seconds and then immediately returned to an ice bath and held for 60 seconds. A small volume (0.8 ml) of LB medium prewarmed at 37°C was added to each tube and then incubated at 37°C, for 30 to 45 minutes

to allow the expression of the antibiotic resistance gene. Following incubation, 100µl of the transformed cells were plated out onto prewarmed LB agar plates containing ampicillin (100µg/ml) and grown overnight at 37°C. An aliquot of 100µl was plated onto agar plates containing 100µg/ml ampicillin and incubated at 37°C for 18-20 hours. The agar plates included 40µg/ml isopropyl-β-D-thiogalactopyranoside and 40µg/ml indolyl-β-D-galactosidase which enable the selection of *E.coli* colonies containing a plasmid with insert DNA. This was done by visual inspection of the plate as colonies containing the recombinant plasmid are white and wild-type plasmid are blue. A control of pUC19 plasmid without insert was included in the transformation. White colonies were inoculated in 10ml of LB containing 50µg ampicillin for mini-preparation of plasmid DNA.

2.7.9. Plasmid DNA preparation by the alkaline lysis methods (Minipreps)

A tube containing 5 ml of LB (1% w/v bacto-tryptone (Oxoid), 0.5% w/v bacto-yeast extract (Oxoid), 1.0% w/v NaCl, pH 7.0) medium was inoculated with a single bacterial colony from a freshly streaked LB plate and grown overnight at 37°C with constant shaking. Appropriate antibiotics were present in the media and plates, depending on the plasmids being prepared (e.g. 50-100 µg/ml of ampicillin). Samples (1.5ml) of each overnight culture were then transferred to 1.5ml eppendorf tubes and centrifuged at 6,000 x g in a microfuge for 30 seconds. The pellets were each resuspended in 250µl of GET buffer (50mM glucose, 10mM EDTA, 25mM Tris-HCl, pH 8.0) and incubated for 5 minutes on ice. The cells were then lysed by the addition of 250µl of a solution of 0.2M NaOH, 1% w/v SDS and incubated for 5 minutes on ice. Neutralization was achieved by adding 200 µl of 3 M sodium acetate (pH 4.8) and incubating on ice for 10 to 60 minutes. The precipitate of cellular DNA and debris was removed by centrifugation at 12,000 x g for 10 minutes

in a microfuge. The supernatants containing plasmid DNA were transferred to fresh 1.5ml eppendorf tubes. To each supernatant was then added 0.9ml of cold ethanol, followed by incubation at -20°C for 30 minutes or 15 minutes at -70°C to precipitate nucleic acids. The precipitate was collected by centrifugation at 12,000 x g for 10 minutes and resuspended in 200µl of NE (0.3M sodium acetate, pH 7.0, 1mM EDTA). After 15 minutes at room temperature, the suspension was vortexed and extracted with a 1:1 phenol:chloroform mix. The sample was then re-precipitated by the addition of 2 volumes of cold ethanol (100%). After incubation at -20°C or -70°C as before, the plasmid DNA was pelleted by centrifugation at 12,000 x g for 10 minutes, washed with 70% v/v ethanol, dried and resuspended in 20 to 50 µl of TE or sterile water, depending on the plasmid copy number. The plasmid DNA was stored at -20°C.

DNA obtained by the alkaline lysis method also contained a large amount of RNA. To remove this, the DNA was treated with the enzyme RNase A (Sigma) which had been heated for 10 minutes at 100°C to inactivate any DNase activity. The RNase A was added to a DNA preparation at a concentration of 50µg/ml and incubated for 30 to 60 minutes at 37°C. The reaction was terminated by phenol/chloroform extraction and the DNA was recovered by ethanol precipitation. If the DNA was used for monitoring restriction digestions, the RNase was simply added to the restriction reactions and no further steps were required.

The recovery of plasmid DNA was verified by restriction enzyme digestion of approximately 1µg of DNA, with 2U of *Eco* RI endonuclease, 2U of *Hind* III endonuclease and visualization after electrophoresis and ethidium bromide staining on a 0.7% w/v agarose gel.

2.7.10. Dideoxy Sequencing

The plasmid DNA (3-5 µg) was denatured by the addition of 5µl of 1M NaOH, 0.5M EDTA in a final volume of 25µl and incubated at room temperature for 15 minutes. The denatured template was purified by centrifugation through a sepharose CL-6B column. The column was prepared by perforating a 0.5ml microcentrifuge tube with a needle and adding glass beads (450-600 µm) to the bottom of the micocentrifuge tube which was then filled with sepharose CL-6B equilibrated in TE. The column was placed into a 1.5ml microcentrifuge tube, also perforated with a needle, for support. The microcentrifuge tubes were then placed in a 15ml centrifuge tube then the whole column assembly centrifuged at 1,700 g for 4 minutes. The perforated 1.5ml microcentrifuge was removed, and replaced with an intact one, and the plasmid DNA was added to the column and centrifuged as before.

After purification, 8.5µl of denatured plasmid DNA was added to 1µl of 10 x TM buffer (100mM $MgCl_2$ and 100mM Tris.HCl pH 8.4), 0.5pmol of forward and reverse sequencing primers and then incubated at room temperature for 15 minutes. The plasmid with the annealed primers was sequenced using the Sequenase Version 2.0 (USB, USA.) according to the manufacturer's instructions. Briefly, 10µl of annealed template (plasmid DNA)-primer was added to 1µl of 10mM DTT, 2µl of labelling nucleotide mix (1.5µM dGTP, 1.5µM dCTP, 1.5µM dTTP) at a 1:5 dilution, 0.5µl (5µCi) [α-^{35}S] dATP, and 3 units of Sequenase enzyme (T7 DNA polymerase). It was then incubated at room temperature for 4-5 minutes. The reactions were terminated by adding 3.5µl of labelling reaction into each of 4 microcentrifuge tubes containing 2.5µl of the appropriate dideoxy/deoxynucleotide mixes (each mix contains 80µM dATP, 80µM dTTP, 80µM dCTP, 80µM dGTP and 50mM NaCl), then

replacing the relevant dNTP with: G mix 8µM ddGTP; A mix 8µM ddATP; T mix 8µM ddTTP and the C mix 8µM ddCTP. Then these were incubated at 37°C for a further 5 minutes. The reaction was stopped by the addition of 4µl of formamide stop mix (98% v/v deionized formamide, 10mM EDTA, 0.01% w/v bromophenol blue, 0.001% w/v xylene cyanol). The sequencing reactions were heated to 95°C for 5-10 minutes before being loaded onto a sequencing gel.

A 6% v/v polyacrylamide sequencing gel (10 x filtered TBE buffer, 50% w/v urea, 1/7 v/v volume of acrylamide mix (38% v/v acrylamide, 2% v/v N,N'-methylene bisacrylamide)) was set with the addition of 1/100 volume of 10% w/v ammonium persulphate and 1/500 volume of N,N,N',N'-tetramethylethylenediamine (TEMED). The sequencing reactions were electrophoresed through the sequencing gel at 38-40 Watts for a 50ml gel in 1 x TBE buffer for 2 hours. The gel was then fixed in 10% v/v acetic acid for 30 minutes with occasional agitation, blotted dry onto 3MM filter paper. The blotted gel and supporting filter-paper were transferred to a slab drier, with vacuum pump, for 2-3 hours at 80°C. The dried gel was then exposed to X-ray film for 18-48 hours and the sequence of the DNA read manually from the developed autoradiograph with the aid of a light-box.

2.8 Colony screening

Bacteria were plated out on agar plates in the standard way. The plates were incubated at 37°C for approximately 8 hours so that the colonies were visible (0.5mm). Hybond-N+ disc membranes were marked (for orientation) and placed on to the surface of the agar touching the colonies. The disc was then lifted and placed on a fresh agar plate and incubated at 37°C. This was then repeated with a fresh

disc. The colonies were grown to a diameter of 0.5mm and then one disc was screened and the other kept at 4°C as a reference.

The DNA was fixed to the membrane by lifting it from the plate and placing it for 1 minute on two sheets of Whatman 3MM paper which had been saturated in 0.5M NaOH. The disc was then transferred to a hybridization bottle contaning 5 x SSC. This was then vigorously shaken to remove bacterial debri. The wash was repeated a total of three times. The disc was then dried on 3MM paper and stored under vacuum prior to hyridization (see Section 2.5.8).

CHAPTER 3

THE POTENTIAL OF FDCP TO DIFFERENTIATE INTO NEUTROPHILS USING CYTOKINES

3.1 Introduction

Neutrophils, isolated from blood, are short lived and terminally differentiated. This makes them unsuitable for the study of differentiation and gene expression, hence the need for *in vitro* model cell systems.

Human leukaemic cells (HL-60) are currently used for the study of differentiation and in particular the study of neutrophil chemotactic receptors such as FPR, PAFR, IL-8R and C5aR (Perez *et al.*, 1992; Boulay *et al.*, 1990a; Moser *et al.*, 1993; Boulay *et al.*, 1991). This cell line is not an ideal system because of incomplete differentiation to neutrophils. The objective of this particular study was to determine whether murine pluripotent stem cells (FDCP) (Spooncer *et al.*, 1986) could be developed into a model system for the characterization of the neutrophil formyl peptide receptor (FPR). Because the FDCP cell line is derived from stem cells it has the potential to be fully differentiated in response to natural cytokines.

The HL-60 cell line was derived from a patient with acute promyelocytic leukaemia. These cells grow continuously as myeloblasts and promyelocytes. In most cultures approximately 5% of HL-60 cells exhibit spontaneous differentiation to morphologically mature cells including myelocytes, metamyelocytes, and neutrophils (Collins *et al.*, 1977). By the addition of specific inducing agents, including polar-planar compounds such as dimethyl sulphoxide (DMSO) and N^6 0^2 - dibutyryl adenosine 3' 5'-cyclic monophosphate (dbcAMP), this spontaneous differentiation can be greatly increased so that most of the cells acquire morphological, functional, enzymatic and surface membrane antigen characteristics of mature granulocytes (Polakis *et al.*, 1988; Lubbert *et al.*, 1991; Collins, 1987). However, this

differentiation is defective and incomplete. HL-60 cells exhibit a reduced nuclear-cytoplasmic ratio, loss of nuclei, decreased azurophilic granules and morphologically become metamyelocytes and banded neutrophils rather than fully differentiated neutrophils. The differentiated cells also lack lactoferrin indicating that they are deficient in secondary granules. Lactate dehydrogenase measurements indicate that the differences between HL-60 and normal granulocytes are consistent with incomplete differentiation (Pantazis *et al.*, 1981). Differences are also present within the myeloperoxidase/peroxide/halide killing system in HL-60 neutrophils (Pullen and Hosking, 1985). Dibutyryl cAMP (dbcAMP) induces production of neutrophil-like cells expressing FPR (Chaplinski and Niedel, 1982; Perez *et al.*, 1992) as well as other chemotactic receptors. HL-60 cells, when terminally differentiated to granulocytes with retinoic acid and presumably other differentiating agents, die via programmed cell death, apoptosis (Martin *et al.*, 1990).

In contrast, FDCP cells are derived from long term marrow cultures. They have a normal karyotype, are nonleukaemic, and grow continuously in the presence of interleukin-3 (IL-3). All stem cells of regenerating tissue are characterised by their ability to undergo differentiation and by their potential for self renewal. In the haematopoietic system, the regulation of stem cell renewal and differentiation is controlled by soluble growth factors leading to a variety of lineage restricted progenitor cells.

The growth factors specifically involved in the differentiation of FDCP cells are granulocyte macrophage colony-stimulating factor (GM-CSF) and granulocyte colony-stimulating factor (G-CSF). FDCP grow continuously *in vitro* in the presence of interleukin-3 (IL-3). Without IL-3 the cells apoptose (Crompton, 1991). In high

concentrations of IL-3 the cells continue to grow but do not react to the presence of other growth factors such as G-CSF and GM-CSF. This suggests that IL-3 modulates the receptors for other growth factors. Therefore IL-3, when used alone, is a potent stimulus for the proliferation of stem cells but is a poor stimulus for their differentiation. IL-3, at low concentrations, supports the development of lineage restricted myeloid progenitor cells such as megakaryocytic, neutrophil/macrophage, erythroid, eosinophil and mast cell. GM-CSF is a potent differentiation stimulus but when acting alone, is a poor proliferation stimulus. Therefore, in order to obtain self-renewal and differentiation, a low concentration of IL-3 with intermediate levels of GM-CSF is required. G-CSF is neither a proliferation nor a differentiation stimulus of any potency, but it can synergize with IL-3 and GM-CSF in these processes. The optimum concentrations of growth factors for the differentiation of FDCP cells to neutrophils is 1 $U.ml^{-1}$ of IL-3, 50$U.ml^{-1}$ of GM-CSF and 1000$U.ml^{-1}$ of G-CSF (Spooncer *et al.*, 1986). The cells produced with these cytokines show an apparently normal mature polymorphonuclear cell morphology compared to the promyelocyte like morphology of the undifferentiated FDCP. Spooncer and co-workers using the respiratory burst process normally seen in mature neutrophils demonstrated that FDCP cells exhibit a similar response indicating the phenotype of differentiated neutrophils (Spooncer *et al.*, 1986). This study confirms these findings and extends them into other neutrophil characteristics, in particular the FPR.

To justify the use of FDCP cells for the detailed characterization of FPR they must be shown to be a better model system than the HL-60 cell line currently in use. This is because FDCP cells are much harder to grow and maintain than HL-60 cells it is important to establish whether enough differentiated cells can be obtained and whether these cells exhibit the morphology and physiology of mature neutrophils.

Further, these cells should be reproducibly differentiated into neutrophils. Therefore a comparison between differentiated HL-60 and FDCP differentiated neutrophils was undertaken.

The respiratory burst in neutrophils is triggered by opsonized microorganisms and high concentrations of chemotactic factors such as N-formyl peptides. These agents act on specific receptors which transduce the signal across the cell membrane and ultimately cause degranulation and the respiratory burst. The respiratory burst involves the one-electron reduction of oxygen to superoxide anion ($O_2^{\cdot}$). This reaction is catalysed by NADPH oxidase. These superoxideanions lead to the production of reducing agents such as hydrogen peroxide, oxidized halogens and superoxide and hydroxyl radicals (see Section 1.7.1, Figure 1.5).

Nitro blue tetrazolium (NBT) is a clear, yellow, water-soluble compound but when reduced it precipitates to a deep blue dye called diformazan a (Collins *et al.*, 1979) (Figure 3.1). The reduction of NBT can be used to assay the respiratory burst in response to biological factors in order to determine the maturation state of the neutrophils.

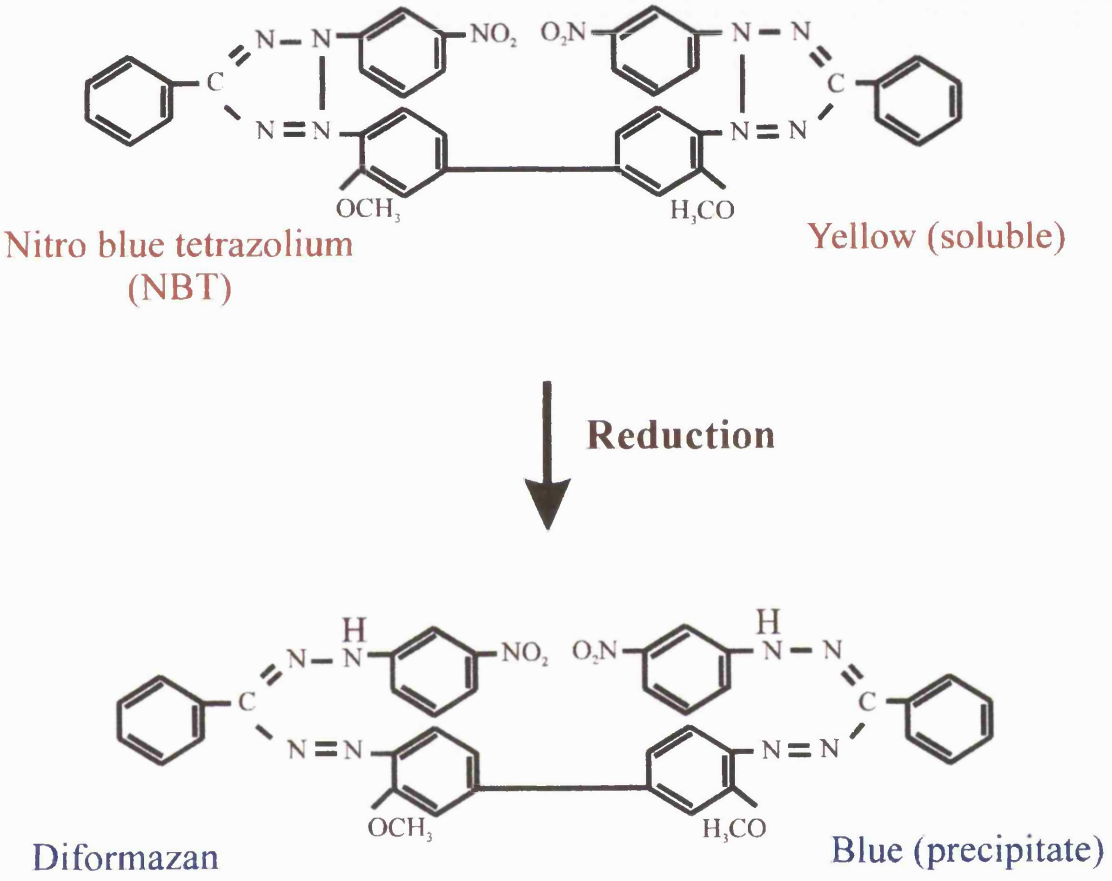

Figure 3.1 NBT reduction.
Nitro blue tetrazolium (clear, yellow, water-soluble) is reduced to diformazan (a blue precipitate).

3.2 Culturing of FDCP and HL-60 cells

Growth studies were performed on HL-60 and FDCP cells to determine the seeding density and frequency of subculturing for the optimal culturing conditions. This was calculated by seeding flasks containing 20 ml of medium with various cell concentrations (from 2 to 12 x 10^4 cells.ml^{-1} for FDCP and 1 to 10 x 10^4 cells.ml^{-1} for HL-60 cells). As shown in Figure 3.2 the optimum seeding density for FDCP cells was 12 x 10^4 cells.ml^{-1}, having a doubling time of 48-72 hours. All seeding densities reach approximately the same density of 67 x 10^4 cells.ml^{-1} except for cells seeded at a density of 2 x 10^4 cells.ml^{-1} which fail to grow. Therefore FDCP cultures were regularly seeded at 12 x 10^4 cells.ml^{-1} and after 72-96 hours of growth were subcultured. As Figure 3.3 shows, the doubling time of HL-60 cells was 24-36 hours. All the cultures reached a similar density of approximately 40 x 10^5 cells.ml^{-1}. The culture with the lowest seeding density (2 x 10^4 cells.ml^{-1}) failed to reach the same cell density as that of the highest seeded culture (2 x 10^5 cells.ml^{-1}). HL-60 cell cultures were therefore regularly seeded at 1 x 10^5 cells.ml^{-1} and subcultured every 48-72 hours.

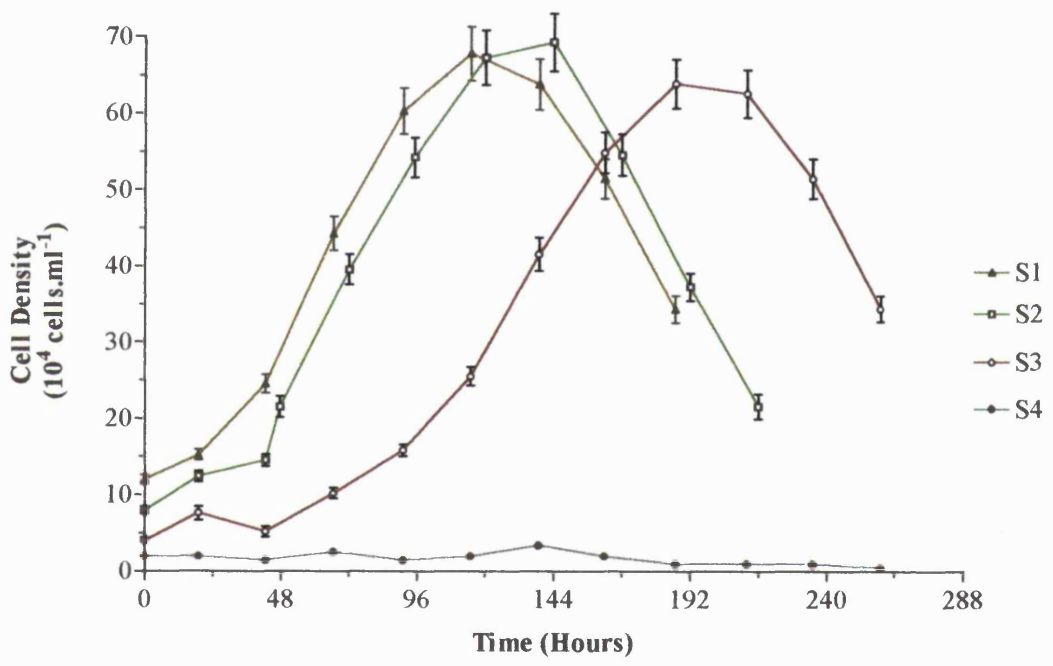

Figure 3.2 FDCP cell proliferation.
Cells were seeded at various densities in identical media and their cell numbers were then estimated every 24 hours to obtain growth curves. S1 = 12 x 10^4 cells.ml^{-1}, S2 = 8 x 10^4 cells.ml^{-1}, S3 = 4 x 10^4 cells.ml^{-1}, S4 = 2 x 10^4 cells.ml^{-1}. Each data point on the graph represents the mean $\pm$ S.E.M. of at least three experiments carried out in triplicate.

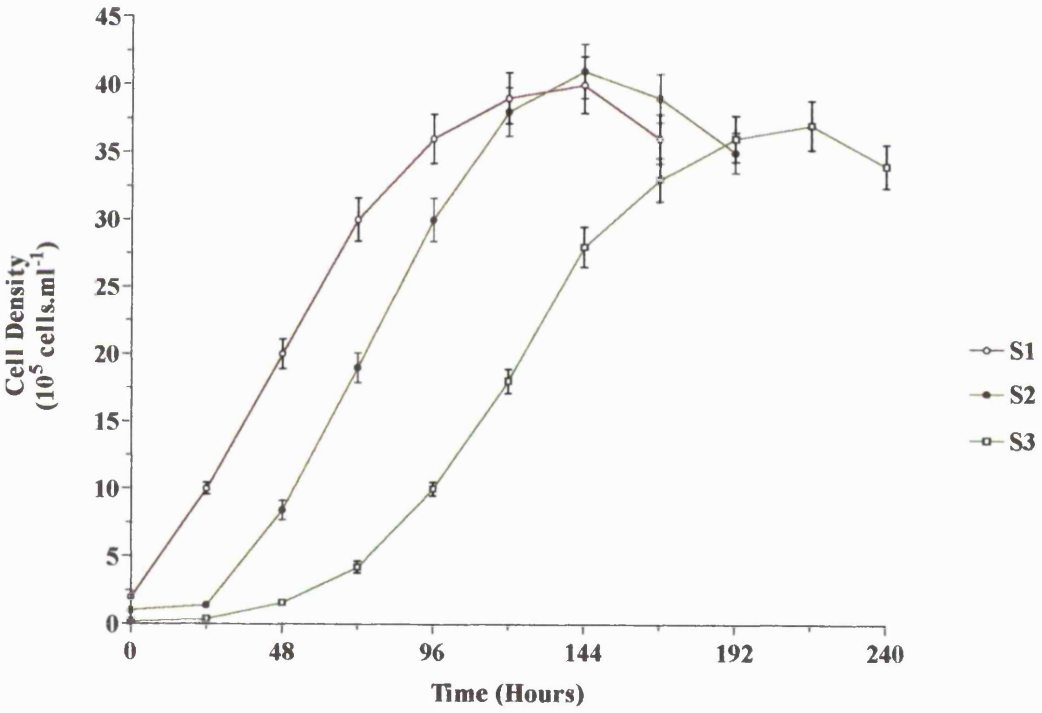

Figure 3.3 HL-60 cell proliferation.
Cells were seeded at various densities in identical media and their cell numbers were then estimated every 24 hours to obtain growth curves. S1 = 2 x 10^5 cells.ml^{-1}, S2 = 1 x 10^5 cells.ml^{-1}, S3 = 0.2 x 10^5 cells.ml^{-1}. Each data point on the graph represents the mean $\pm$ S.E.M. of at least three experiments carried out in triplicate.

3.3 Differentiation and proliferation of FDCP and HL-60 cells

To determine the optimum seeding densities of cells grown under differentiating conditions, several flasks were seeded at densities from 2.5-7.5 x 10^4 cells.ml^{-1} in the presence of 1U.ml^{-1} of IL-3, 50U.ml^{-1} of GM-CSF and 1000U.ml^{-1} of G-CSF. These cytokine concentrations had previously been reported to produce the maximum number of mature neutrophils (Spooncer *et al.*, 1986). Figure 3.4 shows the effect of differentiating agents on FDCP cell growth. All seeding densities reached a similar cell density of approximately 35 x 10^4 cells.ml^{-1} except for cells seeded at a density of 2.5 x 10^4 cells.ml^{-1} which failed to proliferate. As the stationary phase was reached after 6-7 days in culture, it was decided that the seeding density of 7.5 x 10^4 cells.ml^{-1} was optimal. HL-60 cells have been studied extensively in the past and the optimum concentration of dbcAMP is 0.5mM with a cell density of 0.5 - 1.0 x 10^6 cells.ml^{-1} (Chaplinski and Niedel, 1982).

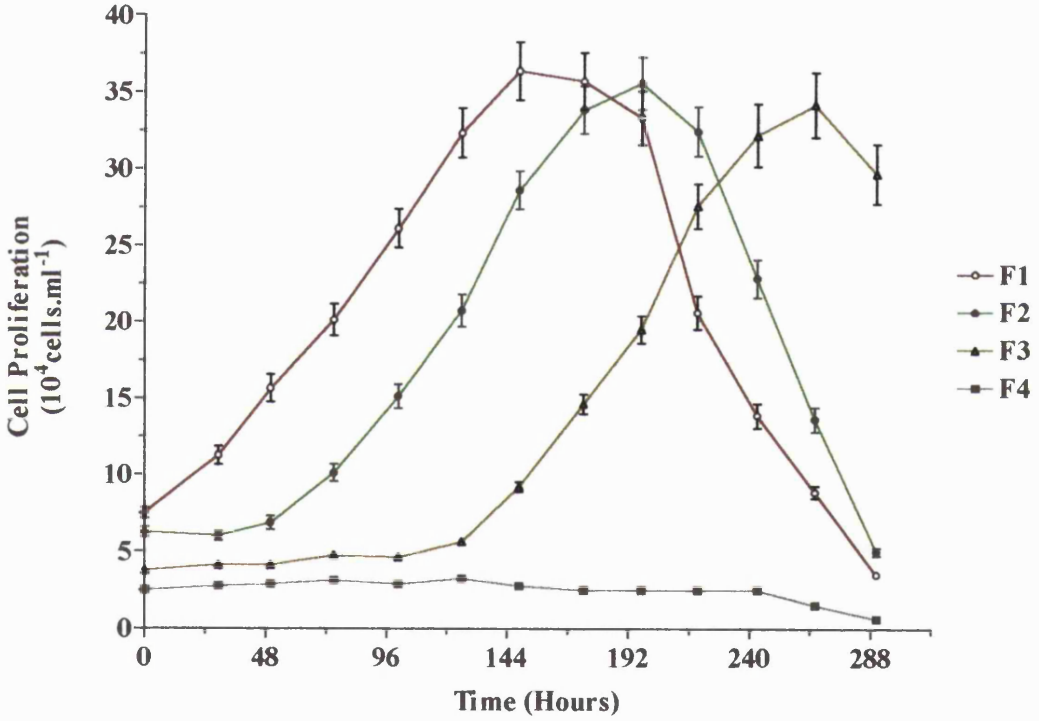

Figure 3.4 Proliferation of differentiating FDCP cells.
FDCP cells were seeded at different densities in the same media containing identical cytokines (1U.ml^{-1} of IL-3, 50U.ml^{-1} of GM-CSF and 1000U.ml^{-1} of G-CSF). Seeding density are: F1 = 7.5 x 10^4 Cells.ml^{-1}; F2 = 6.25 x 10^4 Cells.ml^{-1}; F3 = 3.75 x 10^4 Cells.ml^{-1}; F4 = 2.5 x 10^4 Cells.ml^{-1}. Each data point on the graph represents the mean $\pm$ S.E.M. of at least three experiments carried out in

3.4.1 Functional characterization of differentiated FDCP and HL-60 cells

The morphology of the differentiated cells can be established by carrying out glass adherence and enzyme assays which are present only in neutrophils.

3.4.2 Functional assays - the respiratory burst

An estimate of the number of neutrophils was made by staining differentiated cells with Prodiff. By measuring the number of black azurophilic granules in the neutrophils, in response to N-formyl peptide stimulation of NBT reduction, the number of neutrophils that were functionally active could be estimated. As Figures 3.5 and 3.6 show the proportion of cells which were neutrophils and promyelocytes in differentiating FDCP and HL-60 cultures, respectively. The values are represented as a percentage of the maximum reached. After six days 79.4% of FDCP cells were functioning as neutrophils. On day seven this rose to 84.5%, but the overall number of cells had dropped. Figure 3.6 shows that 74% of HL-60 cells were functioning as neutrophils and this rose to 78.4% after five days. But again the total number of cells fell.

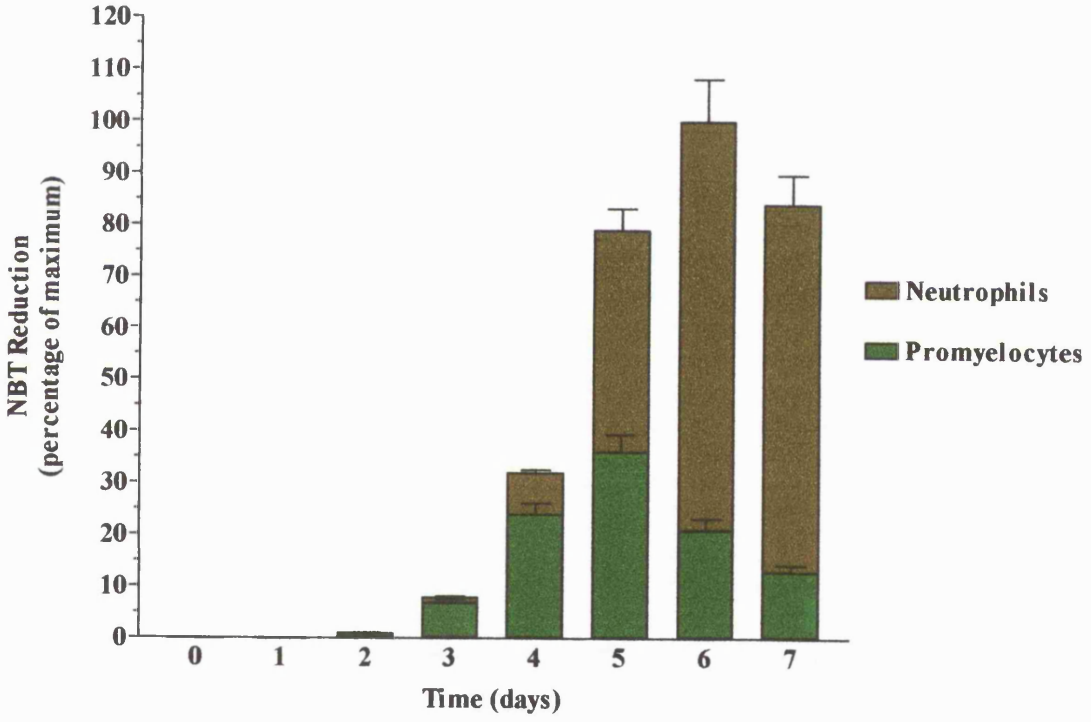

Figure 3.5 Identity of differentiating FDCP cells.
FDCP cells were seeded at a density of 7.5 x 10^4 Cells.ml^{-1}. The number of neutrophils was estimated by staining and the number of functional cells with the NBT assay. The values are expressed as a percentage of the maximum value reached and each data point on the graph represents the mean $\pm$ S.E.M. of at least three experiments carried out in triplicate.

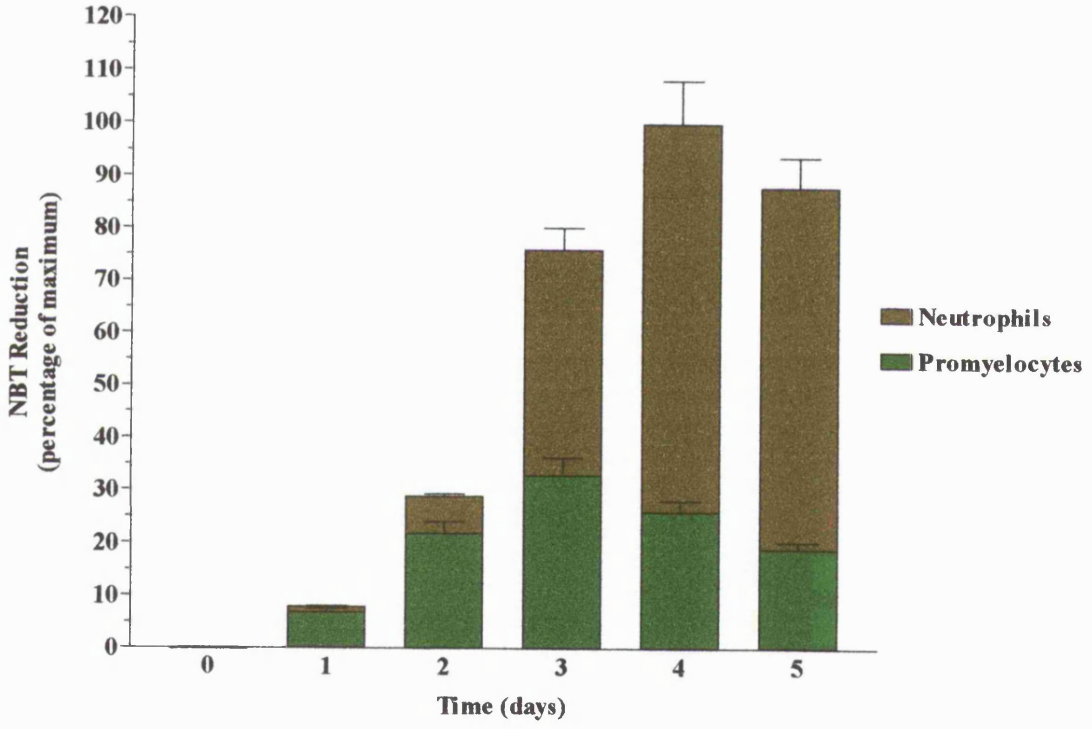

Figure 3.6 Identity of differentiating HL-60 cells.
HL-60 cells were seeded at a density of 2.0 x 10^5 Cells.ml^{-1}. The number of neutrophils was estimated by staining and the number of functional cells with the NBT assay. The values are expressed as a percentage of the maximum value reached. Each data point on the graph represents the mean $\pm$ S.E.M. of at least three experiments carried out in triplicate.

3.4.3 Proliferation assay

It was important to know the effect of cytokines on the proliferation of the cells as there is a direct relationship between proliferation and differentiation, proliferation stops when differentiation begins. As Figure 3.7 shows the effect of cytokines on the growth of FDCP cultures. In the absence of any cytokines (A) or in the presence of 1000U.ml^{-1} G-CSF (E) the cells did not proliferate and after seven days there was only cellular debris.50U.ml^{-1} of GM-CSF (D) alone gave a 1.7 fold increase in cell number. 1U.ml^{-1} of IL-3 (C) gave a 1.3 fold increase in cell numbers. 50U.ml^{-1} of GM-CSF and 1U.ml^{-1} IL-3 (F) caused a three fold increase in cell number. 1U.ml^{-1} of IL-3, 50U.ml^{-1} of GM-CSF and 1000U.ml^{-1} of G-CSF (G) acting together, gave an almost five fold increase in cell number. 100U.ml^{-1} of IL-3 (B) alone gave a nine fold increase in cell number. Figure 3.8 shows the percentage of FDCP cells which were functioning as neutrophils in response to various cytokine concentrations and combinations. As can be seen from this figure, in the absence of cytokines and the presence of G-CSF alone no cells were present after seven days. Only cellular debris were present. IL-3. at concentrations of both 1U.ml^{-1} and 100U.ml^{-1}, gave rise to a population of undifferentiated cells. GM-CSF alone produced 83% neutrophil cells but when acting with 1U.ml^{-1} of IL-3 this dropped to 52%. 1U.ml^{-1} of IL-3, 50U.ml^{-1} of GM-CSF and 1000U.ml^{-1} of G-CSF together gave 85% neutrophils.

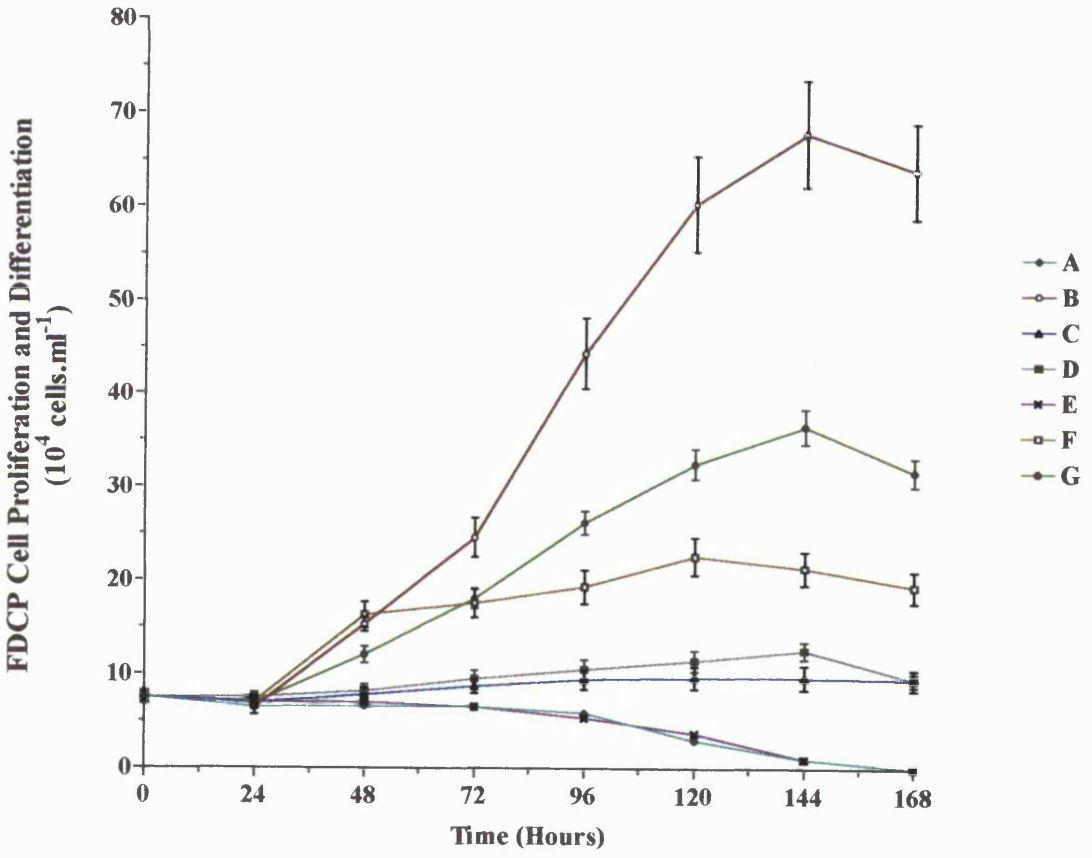

Figure 3.7 The proliferation and differentiation of FDCP cells.
FDCP cells were seeded at a density of 7.5 x 10^4 Cells.ml^{-1}. The number of cells was estimated every 24 hours. The cytokines concentrations used were: A = No cytokines, B = 100U.ml^{-1} IL-3, C = 1U.ml^{-1} IL-3, D = 50U.ml^{-1} GM-CSF, E = 1000U.ml^{-1} G-CSF, F = 1U.ml^{-1} IL-3 and 50U.ml^{-1} GM-CSF, G = 1U.ml^{-1} IL-3, 50U.ml^{-1} GM-CSF and 1000U.ml^{-1} G-CSF. Each data point on the graph represents the mean $\pm$ S.E.M. of at least three experiments carried out in triplicate.

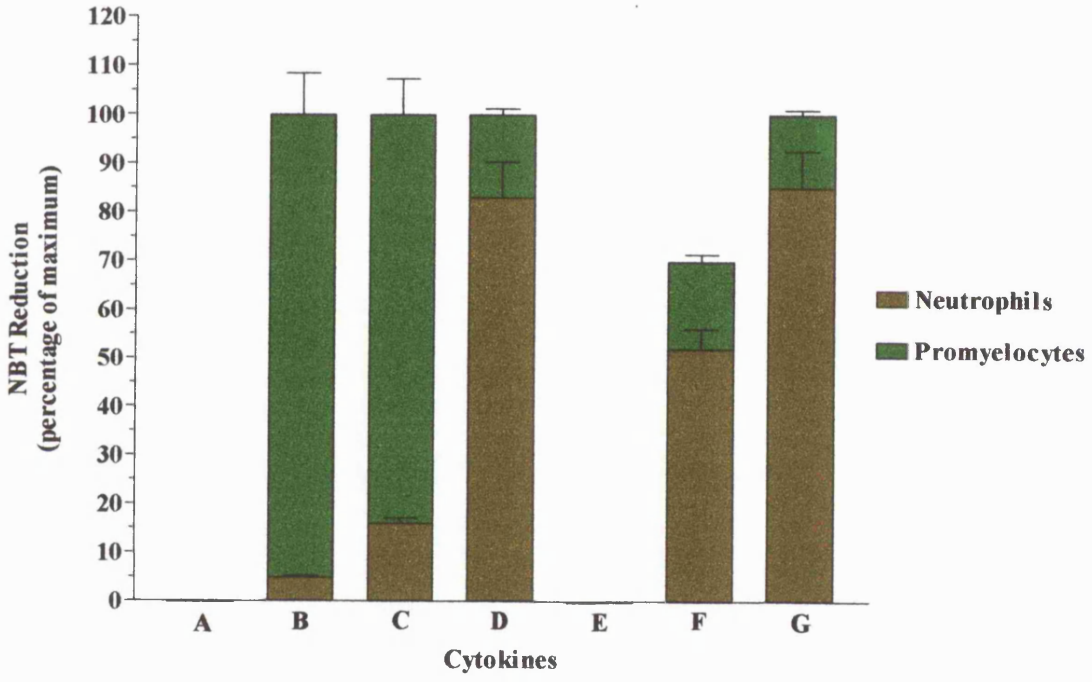

Figure 3.8 Differentiation of FDCP cells with various cytokines.
Assay of FDCP cells incubated for seven days with various cytokines. FDCP cells were seeded at a density of 7.5 x 10^4 Cells.ml^{-1}. The cytokines concentrations used were: A = No cytokines, B = 100U.ml^{-1} IL-3, C = 1U.ml^{-1} IL-3, D = 50U.ml^{-1} GM-CSF, E = 1000U.ml^{-1} G-CSF, F = 1U.ml^{-1} IL-3 and 50U.ml^{-1} GM-CSF, G = 1U.ml^{-1} IL-3, 50U.ml^{-1} GM-CSF and 1000U.ml^{-1} G-CSF. Each data point on the graph represents the mean $\pm$ S.E.M. of at least three experiments carried out in triplicate.

3.4.4 Adherence assay

To further characterise differentiation, the presence of adhesion molecules and actin polymerization were studied indirectly. A glass adherence assay is a quick and simple way to establish whether a cell has adhesion and chemotactic properties (Figure 3.9). A number of cells incubated on a cover slip for 15 minutes at 37°C, with N-formyl peptide (fMLFK), and their ability to spread was measured. A maximum number of HL-60 and FDCP cells spread on the cover slip after four and six days differentiation, respectively.

3.4.5 Quantitation of respiratory burst

As a measure of the functional activity of the respiratory system in neutrophils the reduction of NBT was only qualitative. This gave no information on the strength of the respiratory burst. Therefore, a quantitative assay was developed which involved the extraction and measurement of blue formazan. The NBT reduction assay was quantified for four day differentiated HL-60 and six day differentiated FDCP cells. It was found that the differentiated FDCP(D) and HL-60(D) cells produced a 323% and 267% stimulation, respectively. These numbers were obtained by comparing the amount of NBT reduction in the presence and absence of the N-formyl peptide (fMLFK). The non-differentiated FDCP(ND) and HL-60 (ND) show a 75% and 97% stimulation, respectively with fMLFK as compared to cells without fMLFK (Figure 3.10). Figure 3.11 shows that FDCP cells had a 100 fold greater respiratory burst response than HL-60 cells.

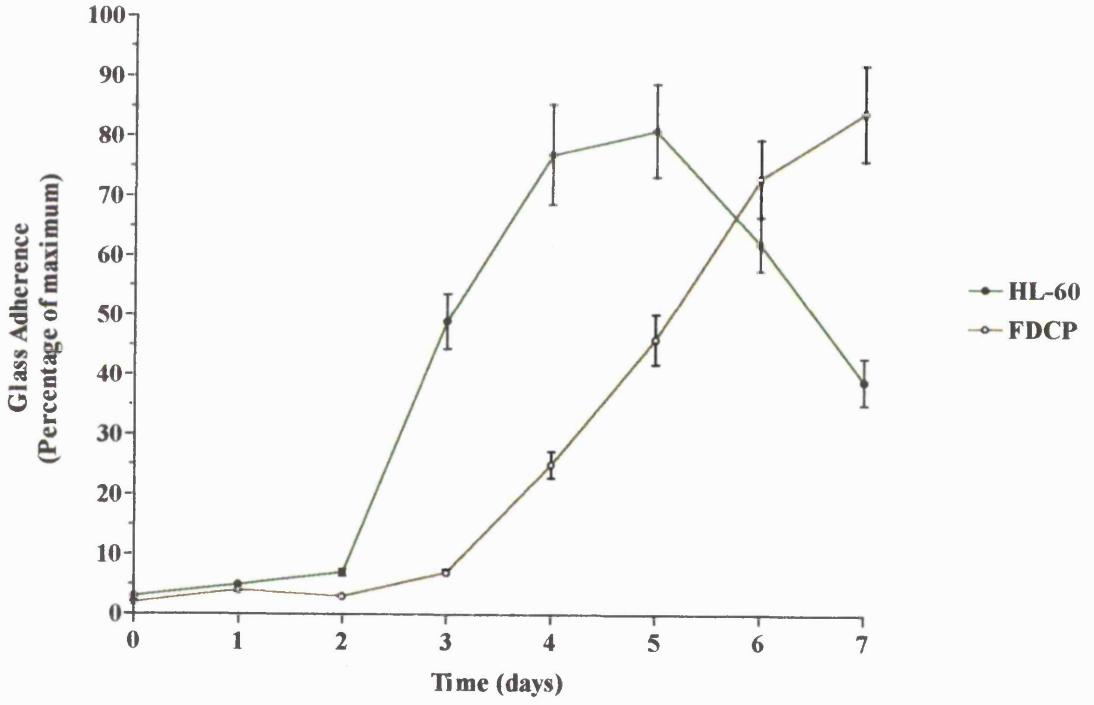

Figure 3.9 Glass adherence Assay.
Cells were placed onto a cover slip and incubated at 37°C for 15 minutes with fMLFK. The number of cells which had spread out was calculated and is expressed as a percentage of the total number of cells counted. Each data point on the graph represents the mean ± S.E.M. of at least three experiments carried out in triplicate.

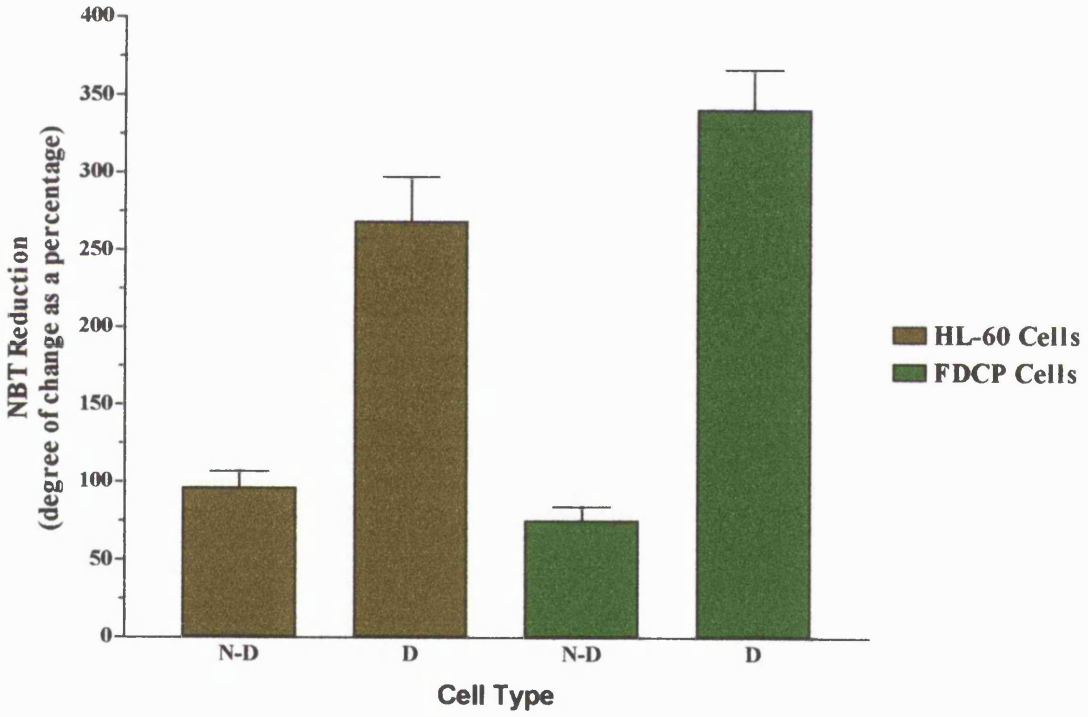

Figure 3.10 Comparison of respiratory burst in differentiated HL-60 and FDCP cells. Under standard conditions cells were assayed for NBT reduction after four and six days differentiation respectively. N-D; non-differentiated cells, D; differentiated cells. Each data point on the graph represents the mean ± S.E.M. of at least three experiments carried out in triplicate.

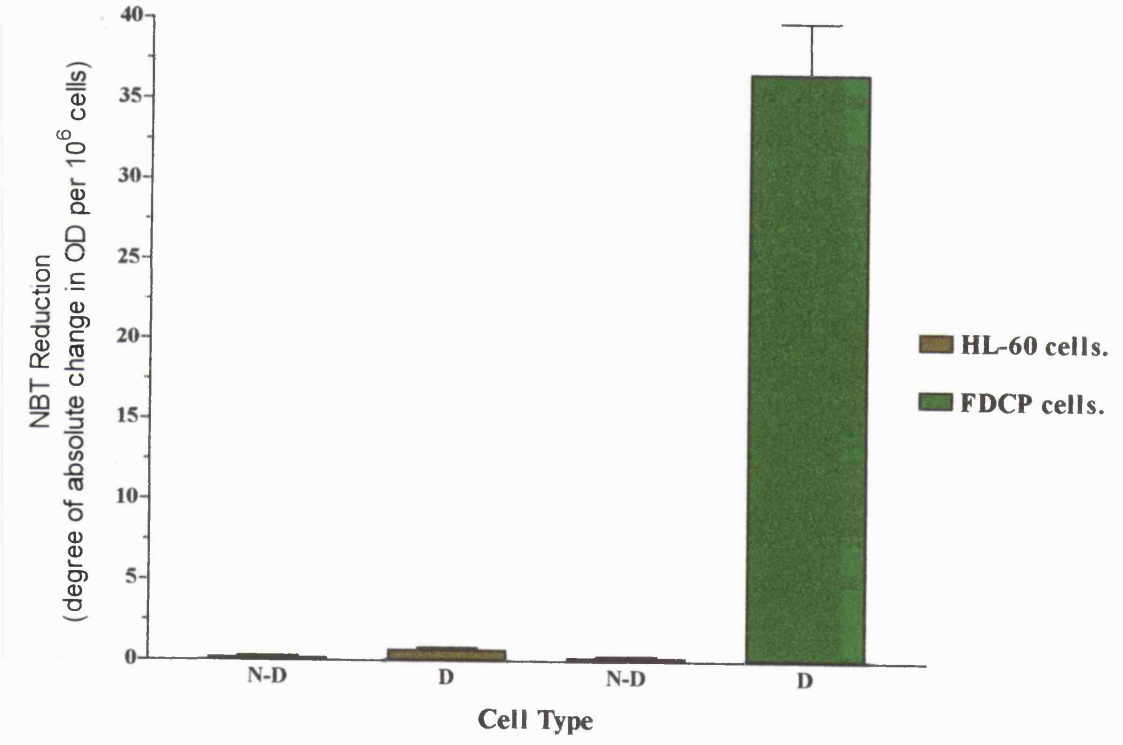

Figure 3.11 Comparison of the absolute levels in the respiratory burst in differentiated HL-60 and FDCP cells.
Four day differentiated HL-60 cells and six day differentiated FDCP cells were assayed under standard conditions. N-D; non-differentiated cells, D; differentiated cells. Each data point on the graph represents the mean $\pm$ S.E.M. of at least three experiments carried out in triplicate.

3.4.6 Dose-response assay

To determine whether the chemotactic peptide produces a true biological respiratory burst response via a cell receptor mediated pathway, the peptide must act in a specific and saturable manner. Figure 3.12 shows that fMLFK caused a concentration dependent and saturable stimulation response in both FDCP and HL-60 differentiated cells, with 50% effective concentrations (EC_{50}) of 56.0nM and 700.0nM, respectively.

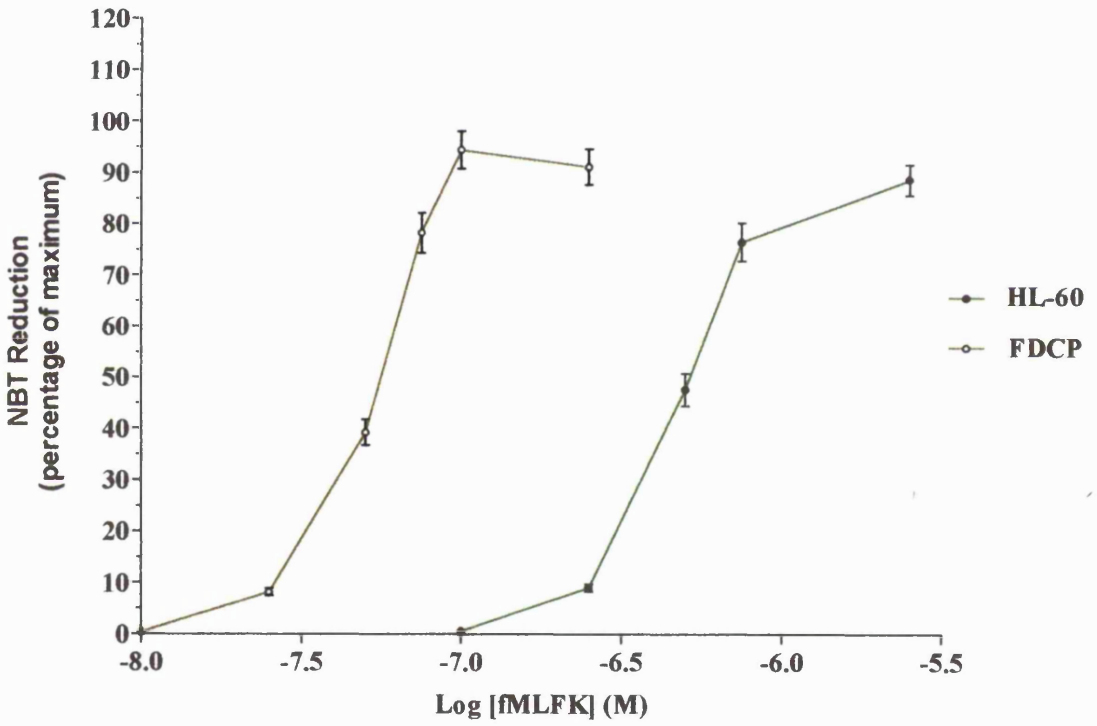

Figure 3.12 The respiratory burst in differentiated HL-60 and FDCP cells in response to fMLFK.
An NBT reduction assay was used to assay the respiratory burst. Using standard conditions cells were assayed for NBT reduction after four and six days differentiation to neutrophils for HL-60 and FDCP cells, respectively. The cells were incubated with various concentrations of fMLFK and the level of NBT reduction plotted as a percentage of maximum. Each data point on the graph represents the mean ± S.E.M. of at least three experiments carried out in triplicate.

3.5 Discussion

The seeding densities chosen for FDCP (12×10^4 cells.ml^{-1}) and HL-60 (1×10^5 cells.ml^{-1}) cells allowed the culture to proliferate before the nutrients were denatured and waste products accumulated. In addition, subculturing every 48-72 hours prevented the irreversible differentiation of the cells.

Below seeding densities of 2×10^{-4} cells.ml^{-1} of FDCP cells, proliferation failed to occur. This may have been due lack of cell-cell interactions. It may also be due to too few pluripotential cells so that the cytokines denature before logarithmic growth could occur. In the case of HL-60, there is evidence for the production of autostimulators (Brennan *et al.*, 1981) thought to be transferrin like molecules (Dittmann and Petrides, 1991).

The effect of cytokines on cell proliferation was entirely consistent with previously published observations (Spooncer *et al.*, 1986). In the absence of any cytokines. the cells fail to proliferate and hence apoptose. With only G-CSF the cells show no response acting as if cytokine is not present. With 1U.ml^{-1} of IL-3 there was very little proliferation, but there was a doubling in the percentage of neutrophils, as compared to 100U.ml^{-1} of IL-3. 100U.ml^{-1} of IL-3 showed the greatest proliferation and the lowest spontaneous differentiation. 50U.ml^{-1} of GM-CSF gave the highest percentage of neutrophils but virtually no increase in cell numbers. A combination of low IL-3 and GM-CSF gave a lower percentage of neutrophils but there was proliferation of cells. The combination of 1U.ml^{-1} of IL-3, 50U.ml^{-1} of GM-CSF and 1000U.ml^{-1} of G-CSF, gave a large percentage of neutrophils and a large increase

in cell numbers. Therefore, overall this cytokine mixture produced a high proportion of neutrophils and the largest total number of cells.

The glass adherence and the quantitative NBT assays indicated that the FDCP cells were very similar to HL-60 derived neutrophils. Their responses relative to their undifferentiated forms, were comparable. But the overall NBT reduction by FDCP cells was a hundred fold greater than HL-60 cells indicating that physiologically these cells were further differentiated than HL-60 cells. HL-60 cells have been shown to have a deficient myeloperoxidase/peroxide/halide system (Pullen and Hosking, 1985) which would account for the lower NBT reduction. This indicates that FDCP cells are a more accurate model system for the study of the FPR receptor expressed by neutrophils.

The response to fMLFK, as measured by NBT reduction, indicated that there is an N-formyl peptide receptor on differentiated FDCP cells and that it is dose-dependent and saturable. Also, this receptor has ten times the affinity (56nM as opposed to 700nM) of that found on differentiated HL-60 cells.

In conclusion the FDCP system can produce differentiated cells in response to physiological cytokines of which a large percentage function as neutrophils. These cells also respond to fMLFK in a dose-dependent and saturable manner, indicating the presence of FPR. FDCP cells are probably further if not totally differentiated (as indicated by the high NBT reduction) as compared to HL-60. The HL-60 cells are myeloid leukaemic, not pluripotential, and do not have normal growth factor requirements. In contrast FDCP cells are derived from long term marrow cultures.

They have a normal karyotype, are nonleukaemic, and can differentiate in response to natural cytokines.

CHAPTER 4

INVESTIGATION OF THE KINETIC PROPERTIES OF MURINE FPR IN DIFFERENTIATED MURINE PLURIPOTENT STEM CELLS (FDCP)

4.1 Introduction

This section describes the characterization of the murine FPR. In section 3 the optimum cytokine concentrations for the differentiation of FDCP cells to neutrophils were established and the expression of a functional N-formyl peptide receptor was demonstrated. The FDCP model was found to be physiologically more accurate than the HL-60 system. In addition to being more accurate, the FDCP cells provided an opportunity to characterize the murine FPR and compare its kinetics and structure to the human and rabbit FPRs. The study of ligand kinetics was undertaken by using labelled peptides to determine the dissociation constants of FPR, its receptor numbers per cell, and the specificity and relative potency of a number of formyl peptides.

Initially, an attempt was made to conjugate fMLF to a fluorescent label (FLOUS) but because of the similarity of the molecular weights of the peptide and label the unbound could not be separated from the bound. Therefore, the characterization of murine FPR with a fluorescently labelled peptide was abandoned in favour of [^{3}H]-fMLF.

The labelled ligand [^{3}H]-fMLF has been the commonly used label for the study of FPR (Koo *et al.*, 1982; Kermode *et al.*, 1991). This has provided information about the dissociation constants of the FPRs from human and rabbit cells. However, because of its low radiation level it requires a high number of cells to be used in binding assays and if a high concentration of the label is used it can lead to artefactual results created by ligand proteolysis and cell agglutination.

The peptide fnLLFnLYK has approximately ten-fold greater binding affinity for human FPR than does fMLF. This means that lower ligand concentrations can be used in the binding assay. This reduces the nonsaturable binding from 25 to 30% to 5 to 10%. In addition, this hexapeptide can be iodinated which results in specific activities 1 to 2 orders of magnitude greater than tritiated peptides. This allows less cells to be used in assays, which also results in decreased ligand proteolysis and cell agglutination (Niedel *et al.*, 1979).

In binding studies involving labelled peptides equilibrium is allowed to be reached with a specific number of cells usually, at 4°C to prevent internalization of the receptor ligand complex. However, at this temperature the membrane fluidity is also affected and influencing the dissociation constants. The only alternative is to use either chemical agents to prevent internalization, or membrane preparations, but these would also be non-physiological conditions.

As well as undifferentiated FDCP cells, WEHI-3b, were used in these experiments as negative controls. WEHI-3b cells are a monocyte derived cell line (Kajigaya *et al.*, 1990) which is routinely used to produce IL-3 conditioned media (see Section 2.2.1.5).

4.2 Binding studies with [^{3}H]-fMLF

As shown in section 3 FDCP cells were differentiated to neutrophils, which expressed FPR and which mediated N-formyl peptide cellular stimulation. A comparison with HL-60 cells showed that FDCP are probably further differentiated and hence closer physiologically to mature neutrophils. It was therefore decided that

the FDCP cells would make an ideal system for the study of the structure and function of FPR.

Cells were incubated with various concentrations of [^{3}H]-fMLF at 4°C for 90 minutes, washed, and the bound peptide estimated on a scintillation counter. Non-specific binding was determined in the presence of a 1000-fold excess of unlabelled fMLF. [^{3}H]-fMLF ligand bound to differentiated FDCP cells in a dose-dependent and saturable manner (Figure 4.1). The highest concentration of [^{3}H]-fMLF gave values which were inconsistent with the rest of the graph. It was therefore not used in the Scatchard transformation of the binding data. This analysis indicates that the specific binding data could be best fitted into a two-site model ($p<0.01$) with K_ds values for high and low affinity states of 7.1×10^{-7} and 2.0×10^{-6} M, respectively (Figure 4.2). By taking into account the number of cells used in the assay (2×10^6), the number of receptors (B_{max}) per cell can be calculated. This was in the order of 31 000 for the high, and 74 000 for the low affinity receptor. As approximately 80% of the cells were found to be neutrophils the actual number of receptors per cell would be 132 000 (see Section 3.4.2, Figure 3.5).

The non-specific binding was calculated to be approximately 25 to 28% of total binding (Figure 4.1). Because of the low specific activity of tritium and the low affinity of fMLF, a high number of cells had to be used (2×10^6) and a high concentration of ligand. This gave spurious results when high concentrations of ligand were used. To eliminate these problems the labelled ligand was changed to [^{125}I]-fnLLFnLYK.

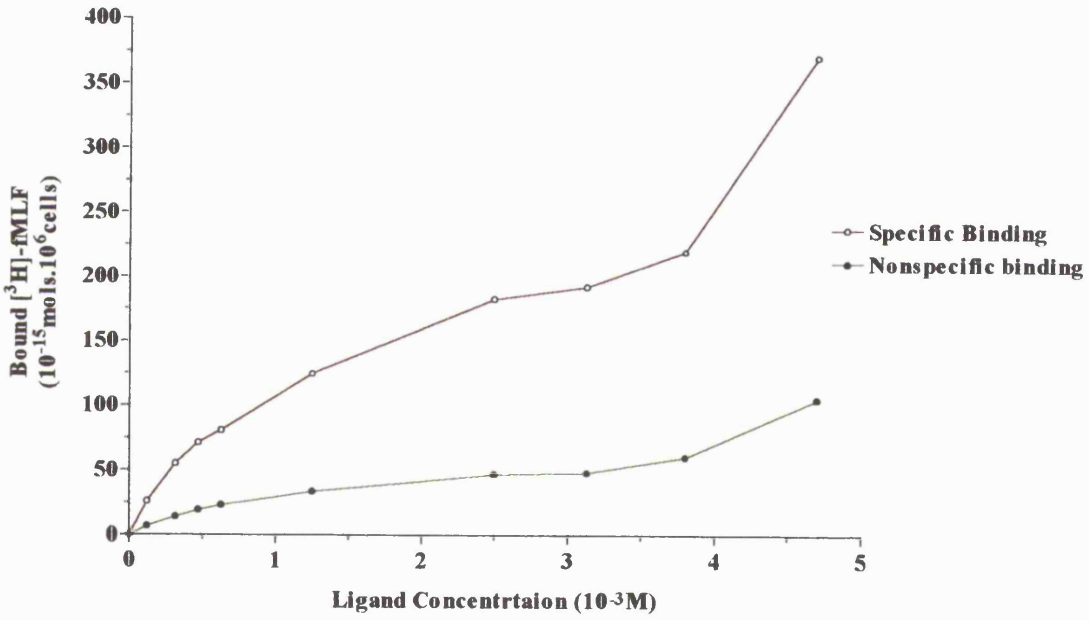

Figure 4.1 Specific binding of [^{3}H]-fMLP to differentiated FDCP cells. Nonspecific binding was determined in the presence of a 1000-fold excess of unlabelled fMLP. At least three experiments were carried out in triplicate and the S.E.M. was never greater than $\pm$ 5%.

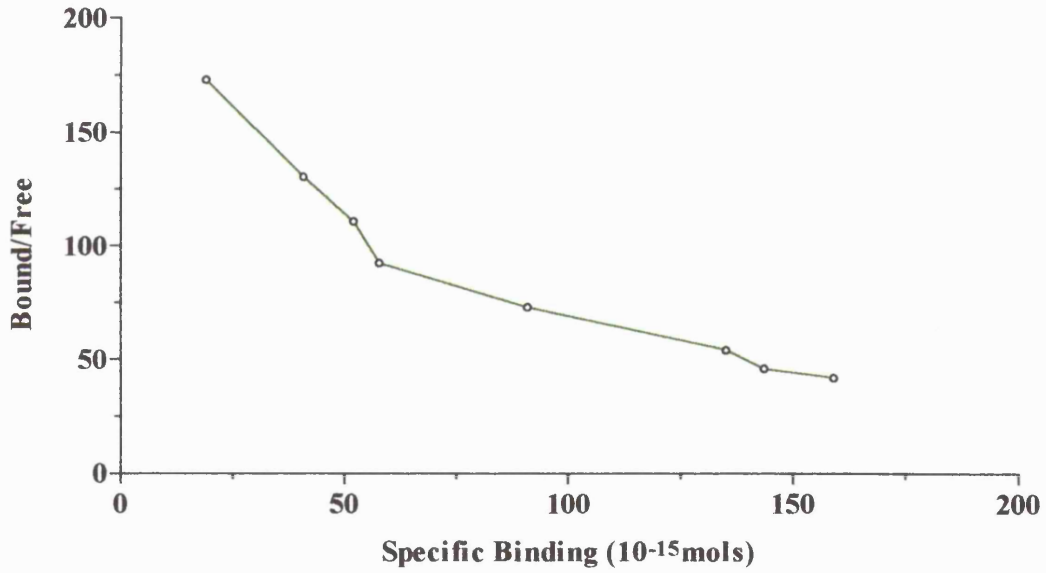

Figure 4.2 Scatchard transformation.
Scatchard transformation of the binding data. At least three experiments were carried out in triplicate and the S.E.M. was never greater than $\pm$ 5%.

4.3 Binding Studies with [^{125}I]-fnLLFnLYK

[^{125}I]-fnLLFnLYK has been shown to have a ten fold greater affinity than [^{3}H]-fMLF for human cells so that ligand concentrations can be reduced, assuming that murine FPR has a higher affinity for the hexapeptide, lowering the nonspecific binding from 25-30% to 5-10% (Niedel *et al.*, 1979). The specific activity of iodinated peptides is one to two orders of magnitude greater than tritium so that less cells can be used reducing cell lysis, and ligand proteolysis, and cell agglutination.

Total binding was measured using [^{125}I]-fnLLFnLYK and non-specific binding was determined in the presence of 1000-fold excess of unlabelled fnLLFnLYK. To determine the concentration of the iodinated peptide synthesised a competitive inhibition experiment was carried out as shown in Figure 4.3. By increasing the concentration of unlabelled peptide in buffer containing a known concentration of labelled peptide the 50% inhibition point can be calculated. This is the point were the two peptides are at equal concentration; by knowing one the other can be calculated assuming that iodination does not affect binding. Using this method the iodination was calculated on average to produce 70% of labelled peptide with a specific activity of approximately 1500-1700 Ci.mmol^{-1}.

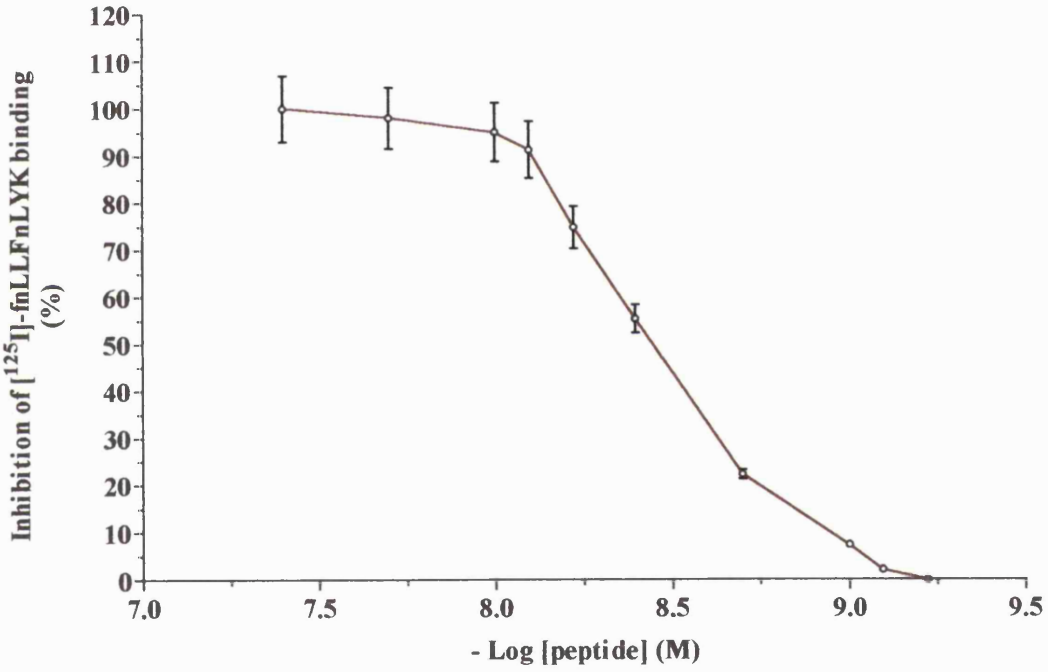

Figure 4.3 Calculation of the concentration of iodinated peptide.
By increasing the concentration of unlabelled peptide in buffer containing a known concentration of labelled peptide, the 50% inhibition point can be found. This can be used to give the concentration of the labelled peptide. Each data point on the graph represents the mean ± S.E.M. of at least three experiments carried out in triplicate.

4.4 Establishing the Concentration of G-CSF

Initial experimental results with the differentiated FDCP cells and [^{125}I]-fnLLFnLYK binding showed an unacceptable amount of variation. This was found to be due to the cytokine G-CSF (1 000Uml^{-1}) from Sigma. Figure 4.4 shows the effect of different concentrations and the commercial source of the G-CSF. Both G-CSF from Sigma and Genzyme gave comparable binding, but Genzyme G-CSF gave lower nonspecific binding (Figure. 4.5) and so this G-CSF was used in further experiments.

4.5 Time Course of [^{125}I]-fnLLFnLYK Binding

A time course with the iodinated peptide and differentiating FDCP cells was carried out to identify the point of maximal binding. A shown in Figure 4.6 this was six days after differentiation was initiated. This agrees with the appearance of the respiratory burst and cell adhesion response (see Section 3.4.2, Figure 3.6 and Section 3.4.4, Figure 3.9). All subsequent experiments were therefore carried out on six day FDCP differentiated cells.

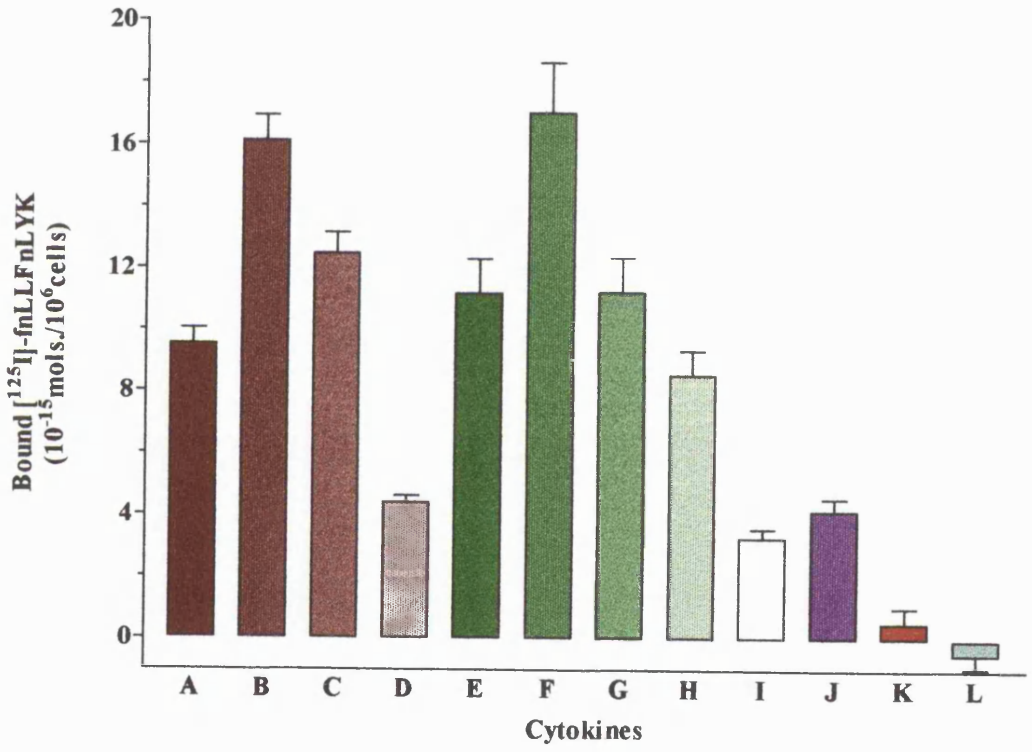

Figure 4.4 Effect of cytokines on binding of [^{125}I]-fnLLFnLYK.
FDCP cells were differentiated under standard conditions but the concentration and origin of G-CSF was varied. After six days the cells were assayed for [^{125}I]-fnLLFnLYK binding. All the preparations (except J,K, and L) contained 1U.ml^{-1} of IL-3 and 50U.ml^{-1} GM-CSF. The G-CSF concentrations were A = 4 000U.ml^{-1} GEN, B = 2 000U.ml^{-1} GEN, C = 400U.ml^{-1} GEN, D = 100U.ml^{-1} GEN, E = 4000U.ml^{-1} S, F = 2 000U.ml^{-1} S, G = 1 500U.ml^{-1} S, H = 1 000U.ml^{-1} S, I = 200U.ml^{-1} S. The G-CSFs used were either from Genzyme (GEN) or Sigma (S). J, K and L were all controls. J = 1U.ml^{-1} of IL-3 and 50U.ml^{-1} GM-CSF, K = 1U.ml^{-1} of IL-3 and L = no cytokines. Each data point on the graph represents the mean $\pm$ S.E.M. of at least three experiments carried out in triplicate.

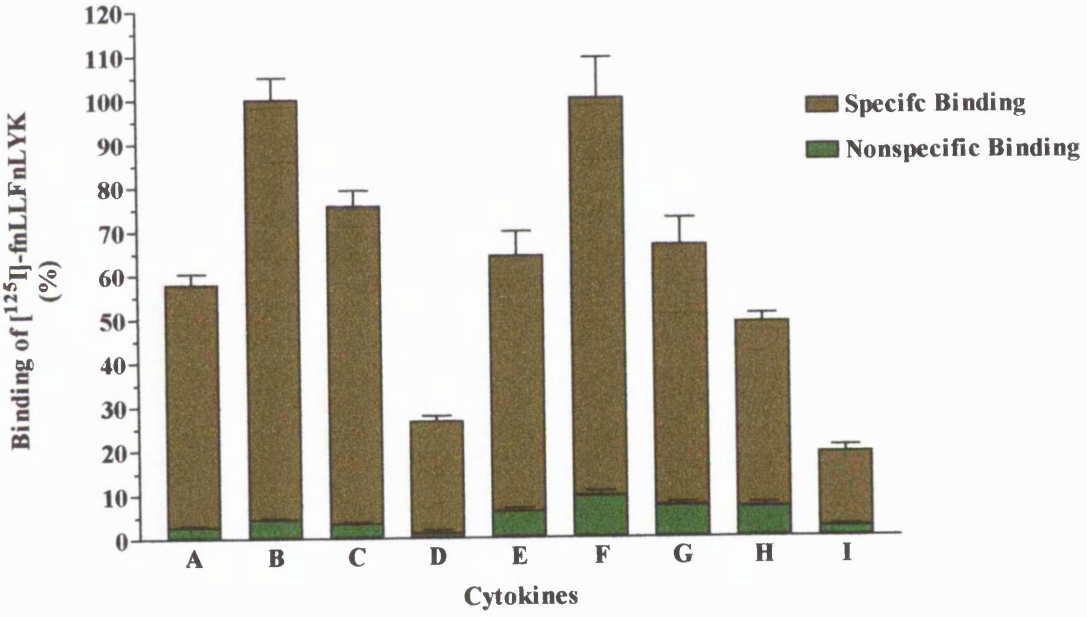

Figure 4.5 The degree of nonspecific binding caused by different preparations of G-CSF.
FDCP cells were differentiated under standard conditions but the concentration and origin of G-CSF was varied. After six days the cells were assayed for [^{125}I]-fnLLFnLYK binding. All the preparations contained 1U.ml^{-1} of IL-3 and 50U.ml^{-1} GM-CSF. The G-CSF concentraions were A = 4 000U.ml^{-1} GEN, B = 2 000U.ml^{-1} GEN, C = 400U.ml^{-1} GEN, D = 100U.ml^{-1} GEN, E = 4000U.ml^{-1} S, F = 2 000U.ml^{-1} S, G = 1 500U.ml^{-1} S, H = 1 000U.ml^{-1} S, I = 200U.ml^{-1} S. The G-CSFs used were either from Genzyme (GEN) or Sigma (S). Each data point on the graph represents the mean $\pm$ S.E.M. of at least three experiments carried out in triplicate. SB = specific binding and NSB = nonspecific binding.

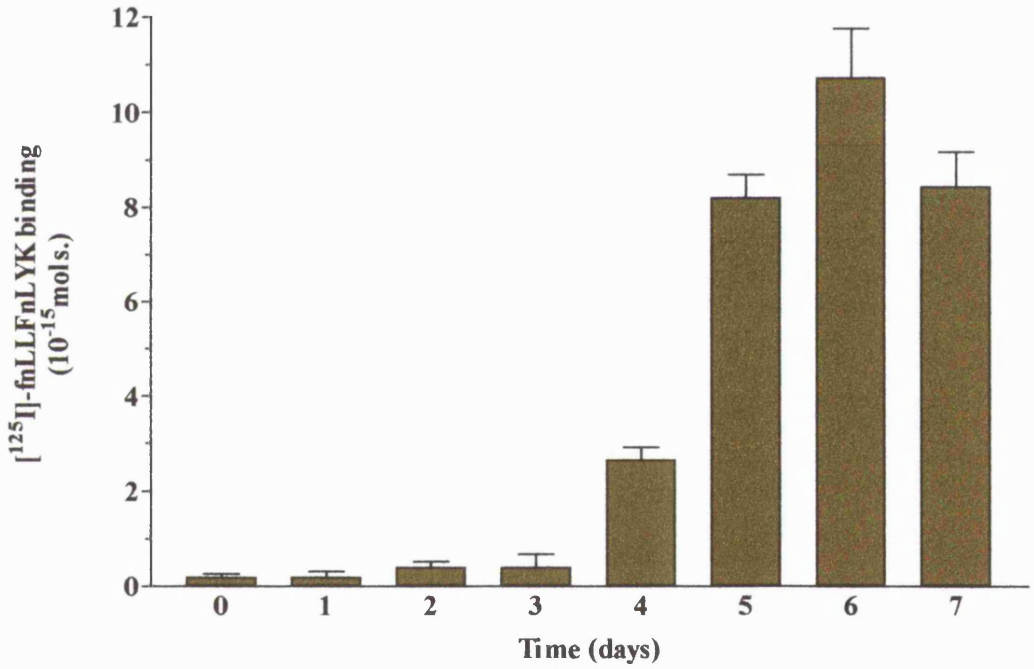

Figure 4.6 Time course of [^{125}I]-fnLLFnLYK binding to differentiating FDCP. Using standard conditions cells were assayed for [^{125}I]-fnLLFnLYK binding at time intervals of 24 hours. The data were then converted to bound [^{125}I]-fnLLFnLYK (fmols.). Each data point on the graph represents the mean ± S.E.M. of at least three experiments carried out in triplicate.

4.6 Kinetic Analysis of [^{125}I]-fnLLFnLYK Binding

Six day differentiated FDCP cells displayed specific and saturable binding of the [^{125}I]-fnLLFnLYK (Figure 4.7). Scatchard transformation of the binding data indicated that the specific binding data could be best fitted into a two-site model ($p<0.01$) with K_ds of 3.7 x 10^{-9} and 22.6 x 10^{-9} M (Figure 4.8). B_{max} was calculated to be 16 000 high affinity receptors and 47 000 low affinity receptors per cell. As approximately 80% of the cells were found to be neutrophils the actual number of receptors per cell would be 79 000, with 20 000 high affinity and 59 000 low affinity. The nonspecific binding was approximately 7 to 10 %.

4.7 Relative Affinities of Various N-formylated peptides

Figure 4.9 shows the relative potencies of various formyl peptides to displace [^{125}I]-fnLLFnLYK from the muFPR. The order of formyl peptide potencies was: fnLLFnLYK (EC_{50} 4nM) > fMLF (EC_{50} 112nM) > fMLFK (EC_{50} 501nM) > fMLFF (EC_{50} >10^{-4} M) > fMF (EC_{50} >10^{-2} M). EC_{50}s were not obtained for fMLFF and fMF because of the difficulty in solubilising these hydrophobic molecules at the high concentrations required.

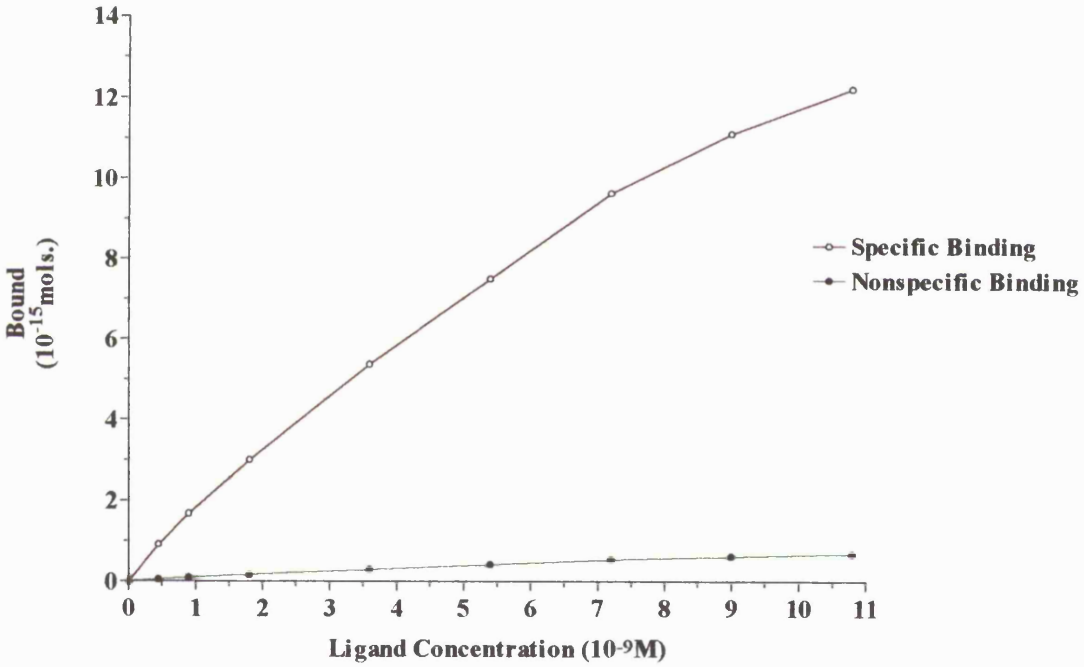

Figure 4.7 Specific ligand binding.
Standard assay conditions were used at the [^{125}I]-fnLLFnLYK concentrations indicated. At least three experiments were carried out in triplicate and the S.E.M. was never greater than $\pm$ 5%.

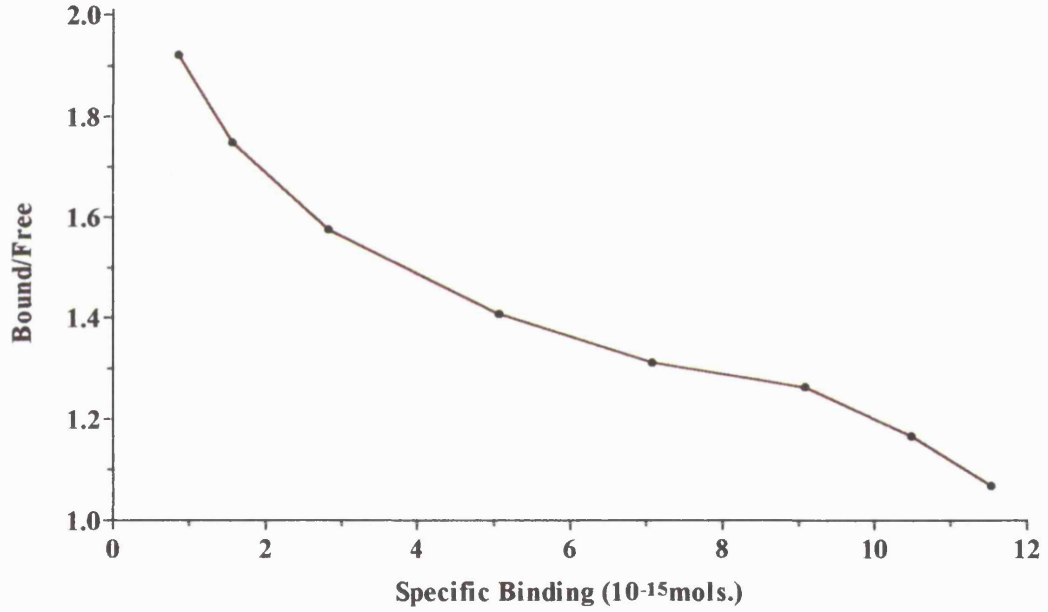

Figure 4.8 Scatchard transformation.
Scatchard transformation of the binding data. At least three experiments were carried out in triplicate and the S.E.M. was never greater than $\pm$ 5%.

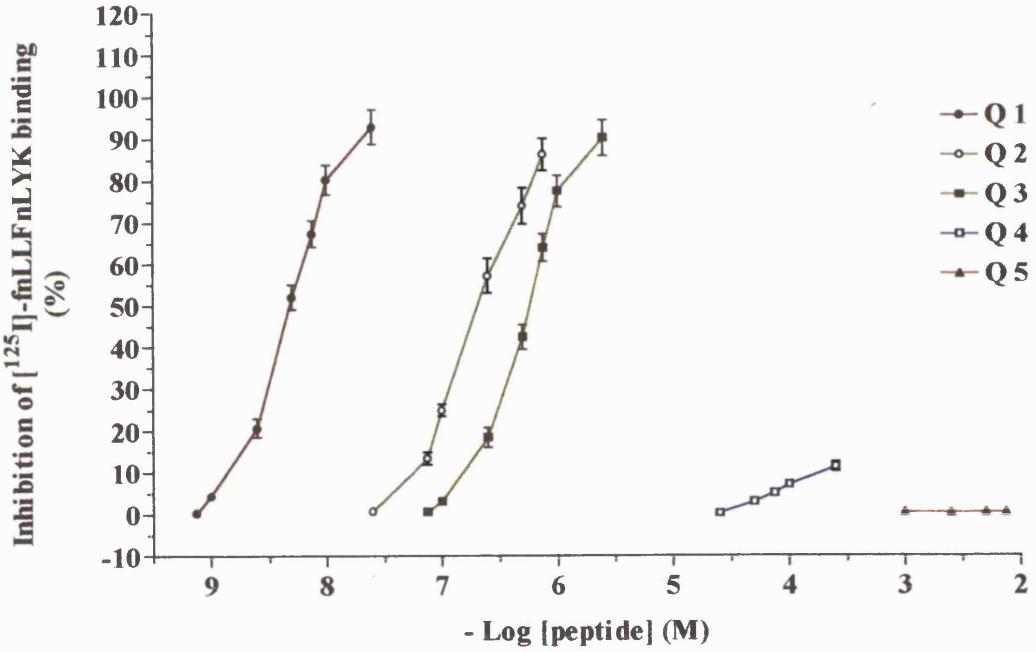

Figure 4.9 Comparison of receptor affinities for a series of formyl peptides. Inhibition of [^{125}I]-fnLLFnLYK binding by the various peptides was determined under standard binding assay conditions. fnLLFnLYK (Q1), fMLFK (Q2), fMLF (Q3), fMLFF (Q4), fMF (Q5). Each data point on the graph represents the mean ± S.E.M. of at least three experiments carried out in triplicate.

4.8 [^{125}I]-fnLLFnLYK binding to various cell lines

Figure 4.10 shows the results obtained when using WEHI-3b cells as negative controls. It can be clearly seen that the WEHI-3b cells express a formyl peptide receptor although the amount of binding was much less than that to the FDCP cells. WEHI-3b cells have two growth stages in their life cycle. Initially the cells adhere, spreading out to form a monolayer. But when confluence has been reached the cells start to bud, producing cells that are rounded and in suspension. Cells taken from a monolayer, from a suspension culture and a mixed culture (where confluency had been reached and cells had started to bud) were assayed for [^{125}I]-fnLLFnLYK binding. Figure 4.11 shows that it is the cells from the monolayer that bind the iodinated peptide.

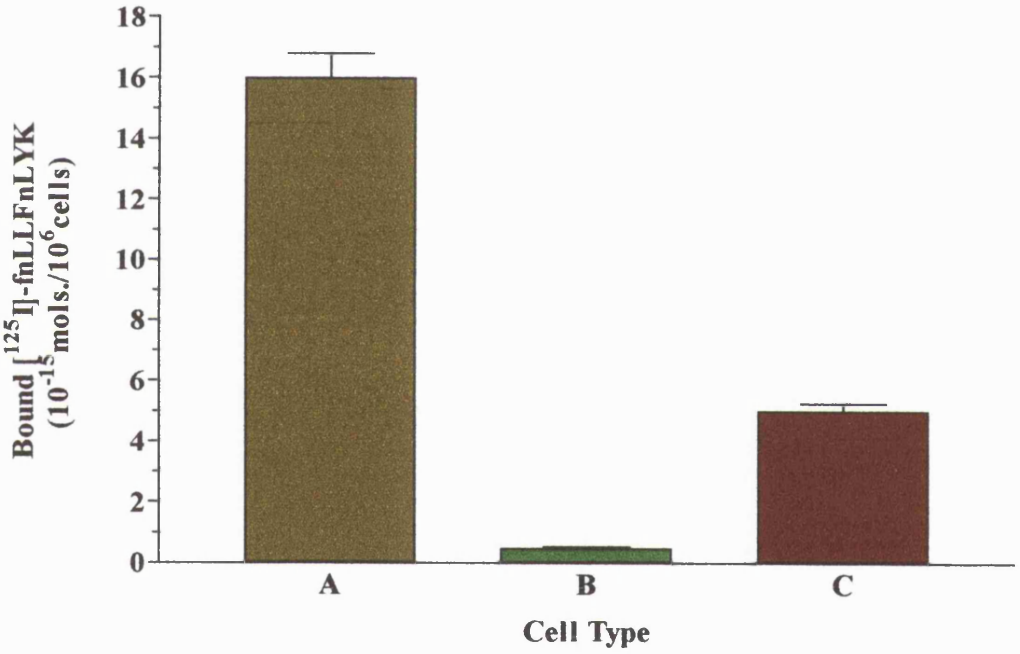

Figure 4.10 Comparison of [^{125}I]-fnLLFnLYK binding in different cell lines. FDCP differentiated (A) and undifferentiated (B) were compared to WEHI-3b cells (C) under standard conditions for their ability to bind [^{125}I]-fnLLFnLYK. Each data point on the graph represents the mean ± S.E.M. of at least three experiments carried out in triplicate.

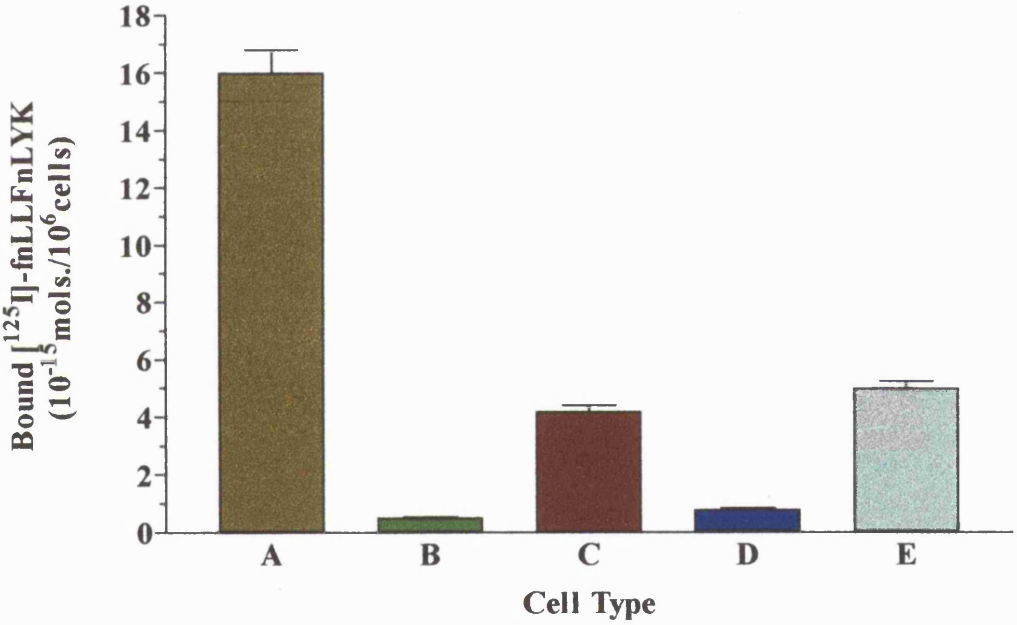

Figure 4.11 Comparison of [^{125}I]-fnLLFnLYK binding to WEHI-3b cells at various stages of growth.
FDCP differentiated (A) and undifferentiated (B) were compared to WEHI-3b cells (C, D and E) under standard conditions for their ability to bind [^{125}I]-fnLLFnLYK. Sample C contains adherent cells, sample D contains cells in suspension, and sample E contains a mixture (i.e. cells from a flask containing adherent and budding cells). Each data point on the graph represents the mean $\pm$ S.E.M. of at least three experiments carried out in triplicate.

4.9 Discussion

In this study we optimised the G-CSF concentration and time required to differentiate FDCP cells into neutrophils which bind the maximum amount of [^{125}I]-fnLLFnLYK. The increase in binding of the iodinated peptide could be due to the cells either expressing more receptors as they differentiate, or that the G protein coupled to murine FPR is differentially expressed.

The muFPR showed high and low affinity binding sites for [^{3}H]-fMLF with K_d values of 2.0 and 0.71 μM, respectively. The B_{max} value of 132 000 receptors per cell, with 32% high affinity demonstrated in this study is in good agreement with other studies on isolated neutrophils (Kermode *et al.*, 1991; Sklar *et al.*, 1984; Koo *et al.*, 1982).

Using [^{125}I]-fnLLFnLYK muFPR showed high and low affinity binding with K_d values of 3.7 and 22.6 nM, respectively. The B_{max} value of 79 000 receptors per cell, with 25% high affinity I report in this study, agrees well with other studies on isolated neutrophils (Kermode *et al.*, 1991; Sklar *et al.*, 1984; Koo *et al.*, 1982).

The kinetics of the receptor for the two peptides do not agree but are comparable. This is because of the different conditions and the different affinities of the two peptides. In addition, [^{3}H]-fMLF gave a higher, but inconsistent, estimation of receptor numbers than [^{125}I]-fnLLFnLYK. This may be due to possible proteolysis and cell agglutination, since 2 x 10^6 cells were used for [^{3}H]-fMLF and 4 x 10^5 with [^{125}I]-fnLLFnLYK.

To date, two other groups have studied the murine FPR. Gao and Murphy (Gao and Murphy, 1993) have cloned and expressed one muFPR isoform in *Xenopus* oocytes, and Sasagawa and co-workers (Sasagawa *et al.*, 1992) have studied the chemotactic response of blood-isolated neutrophils to fMLF. The DNA sequence of the most homologous muFPR to the huFPR is 76% identical and is published, while the other five isoforms have between 54% to 67% homology. To characterise the expression product of the muFPR Gao and Murphy (Gao and Murphy, 1993) co-injected oocytes with the muFPR transcript plus total RNA from undifferentiated HL-60 cells, and assayed Ca^{2+} efflux in response to fMLF, obtaining an EC_{50} of 100nM. As a control they repeated the experiment with the huFPR mRNA transcript and obtained an EC_{50} of 0.5nM. The EC_{50} of the expressed muFPR (100nM) agrees with the [^{3}H]-fMLF binding studies (K_d 10^{-6} - 10^{-7} M, see Figure 4.1), (Mitrophanous and Charalambous, 1993)), and an EC_{50} of 112nM for the competitive binding of fMLF in the presence of [^{125}]-fnLLFnLYK. Furthermore, Gao and Murphy (Gao and Murphy, 1993) found a greater response when mRNA from undifferentiated HL-60 cells was co-injected, suggesting that additional co-factors were required that are not present in oocytes. However, fMLF-stimulated chemotaxis of murine polymorphonuclear cells determined in a Boyden chamber indicated an EC_{50} in the micromolar range (calculated from Sasagawa *et al*'s data (Sasagawa *et al.*, 1992)).

A comparison of the FPR binding affinities to fMLF, determined by the direct binding of radiolabelled peptide to the receptor, reveals that the huFPR has a high affinity site (K_d 2.2nM) and a low affinity site (K_d 23nM) (Williams *et al.*, 1977; Koo *et al.*, 1982). The lagomorph rabFPR has fMLF binding affinities of 0.4nM (high affinity) and 5.8nM (low affinity) (Kermode *et al.*, 1991; Ye *et al.*, 1993), which are approximately ten fold greater than the huFPR. Other workers have used the

hexapeptide fnLLFnLYK to characterise huFPRs because it has an approximately 10-fold greater binding affinity (1.3nM with fnLLFnLYK - (Niedel *et al.*, 1979); 13nM with fMLF binding - (Williams *et al.*, 1977)). This means that lower ligand concentrations can be used in the binding assay, reducing the nonsaturable binding from 25 to 30% to 5 to 10%. In addition, this hexapeptide can be iodinated which results in specific activities 1 to 2 orders of magnitude greater than tritiated peptides. This means that lower numbers of cells can be used, resulting in decreased ligand proteolysis and cell agglutination during the assay. Neidel and co-workers (Niedel *et al.*, 1979) reports an EC_{50} of 1.3nM for the saturable binding of fnLLFnLYK, 10-fold greater than Williams *et al.* (Williams *et al.*, 1977). This value does not take into account the presence of high and low affinity receptors. The approximated EC_{50}s for binding would be about 0.2 to 0.4nM for the high affinity and 2 to 4nm for the low affinity.

The relative potencies for other oligopeptides were established (Figure 4.9) and found to be similar to that reported for the huFPR (Niedel *et al.*, 1979), but different from that reported for the rabFPR (Kermode *et al.*, 1991). The relative potencies of the peptides are as follows for muFPR: fnLLFnLYK > fMLF > fMLFK > fMLFF > fMF. For huFRP they are: huFPR: fnLLFnLYK > fMLF > fMLFK (Freer *et al.*, 1980). For rabFPR they are; fMLFF > fMLF (Freer *et al.*, 1982; Kermode *et al.*, 1991).

Cytokine-differentiating FDCP cells, as indicated from the NBT assay of the respiratory burst, the glass adherence assay, and the radiolabelled peptide binding assays, begin to respond physiologically to N-formyl peptide stimulation after three days, with a maximum response after six days, at which point the response decreases, and may be indicative of apoptosis (Crompton, 1991).

Although WEHI-3b cells are a monocyte derived cell line they expressed an FPR (Kajigaya *et al.*, 1990). The binding was lower than in the FDCP cells and this may be due either to a different isoform of the receptor being expressed or that the cells are only minimally expressing it.

CHAPTER 5

HIGH STRINGENCY SOUTHERN BLOT HYBRIDIZATION WITH huFPR

5.1 Introduction

At the time this particular aspect of the project was begun little information was available on murine FPR. Heyworth and co-workers had shown that FDCP cells differrentiated to neutrophils expressed and a N-formyl peptide receptor (Heyworth *et al.*, 1990a). Probing the murine genome with the human huFPR probe revealed one strongly hybridizing band *Eco* RI and with *Hind* III (Bao *et al.*, 1992). The kinetic analysis of muFPR discussed in section 4 showed that, unlike the human (huFPR) and the rabbit receptors (rabFPR) it had a low affinity for fMLF. By cloning and sequencing muFPR a comparison between the different species may provide a way to further characterize peptide binding. Studies using chimeras have shown that there is no definitive domain for N-formyl peptide binding. Dramatic differences are seen between huFPR and FPRL1 in fMLF binding, even though they are 69% identical at the amino acid level. By using the kinetic data produced in this study in conjunction with sequence comparisons the critical regions within the receptor for peptide binding may be pinpointed and used in structure and function analysis.

Most of the chemoattractant receptors have been cloned by expression cloning. This involves making cDNA out of mRNA isolated from a cell line expressing the gene of interest. The cDNA is then ligated into an expression vector and appropriate cells transfected with the constructs. These cells are then screened for the binding of the labelled ligand of interest. This technique is not feasible for the cloning of murine FPR because sufficient mRNA cannot be obtained from murine blood neutrophils.

In order to clone the murine FPR gene a restriction map was first constructed. This provides information on the number of potential genes and their degree of homology

to the probe being used. The mapping was done by Southern blot analysis with the appropriate probe. The banding pattern obtained was also analyzed for the restriction enzymes which would be suitable for cloning the gene. The gene can be cloned either by screening a complete phage or cosmid library, or the band or bands which give the strongest hybridization signal can be purified and subcloned into appropriate vectors (plasmid or phage) to make a partial library. Positive clones can then be sequenced to identify the gene.

As described earlier, the majority of chemoattractant receptor genes lack introns within the open reading frame (ORF) but have at least one large intron between the points of transcription and translation (Gao *et al.*, 1993; Murphy *et al.*, 1993; Gerard *et al.*, 1993; Mutoh *et al.*, 1993; Libert *et al.*, 1989). The few exceptions to this are the tachykinin receptors which have multiple introns (Gerard *et al.*, 1991b; Gerard *et al.*, 1991a). This information is useful for cloning the receptor gene since a strongly hybridizing band is more likely to contain the whole ORF than a gene containing a number of large introns. Therefore, a partial library could be constructed with a high probability of obtaining the entire coding region. By using a number of restriction enzymes with different restriction sites, an appropriate band or bands could be isolated and made into a partial library. Multiple digests could be carried out to further characterize the gene.

5.2 Southern blot analysis of murine genomic DNA

Murine genomic DNA was prepared from non-differentiated FDCP, WEHI-3b cells, and murine brain samples. Human genomic DNA was prepared from HL-60 cells to be used as a positive control. Non-differentiated FDCP, HL-60, and WEHI-3b cells

were used for genomic DNA preparations as these are easy to obtain in large numbers. In addition cell lines give purer DNA as they contain less extracellular protein as in the case of tissue samples. The genomic DNA from murine brain samples was used to validate the DNA isolated from the murine cell lines FDCP and WEHI-3b (data not shown).

FDCP genomic DNA was restricted with a variety of endonucleases. These were size fractionated on a 0.7% w/v agarose gel and transferred by capillary action onto nylon membrane. DNA probes were labelled with [α-^{32}P] dCTP by random priming (see Section 2.5.7). Two probes were used. The first, P1, was a full length cDNA clone of huFPR (a kind gift from P. M. Murphy) which includes upstream and down stream untranslated DNA as well as the coding region (Murphy and McDermott, 1991),. The second, P2, was an *Nco* I/*Pst* I fragment (770bp) of the huFPR cDNA coding region. High stringency washes were employed to identify the most homologous sequences. Figure 5.1a shows a typical genomic digest size-fractionated on an agarose gel (Figure 5.1a). The gel contains DNA from the size range of 3.0 to 30 kb. Larger sized DNA will not enter the agarose matrix. The DNA was restricted by various enzymes to give a large number of fragments, which appear as a smear of DNA. *Xho* I did not cut the DNA frequently, thus generating large fragments which do not readily enter the gel (lane 5). The DNA was transferred to a nylon membrane, probed with P2, and autoradiographed (Figure 5.1b). The human genomic DNA (positive control) when restricted with *Eco* RI and probed, gave three fragments with the expected sizes of 5.7, 3.8 and 2.8 kb (lane 13). The strongest hybridization band was the 2.8kb, which is the huFPR gene, *FPR1*. The *Hind* III digest of murine DNA gives six large bands from 11.0 to 3.0 kb of which the 7.8kb band gave the strongest murine signal (lane 3). No hybridization to the λ

markers was seen, indicating that the binding was specific. The hybridization pattern seen with *Eco* RI and *Hind* III restricted murine DNA digests matches that published by other groups (Bao *et al.*, 1992). To further characterize the murine genome with respect to FPR different enzymes were used. Figure 5.2a shows another set of DNA digests. The DNA was DNA transferred to a nylon membrane, probed with P1, and autoradiographed (Figure 5.2b). Tables 5.1 and 5.2 give a summary of the hybridization patterns obtained with single and double digests, respectively. The figures in bold indicate the bands which gave the strongest signals and are thus more homologous to huFPR. The different enzymes generate many bands which add up to a gene greater than 1kb (the size of the expected ORF) indicating that there may be more than one copy of the murine FPR gene; multiple copies of a single gene; or a number of isoforms. There is also the possibility of large introns.

Figure 5.1 Genomic mapping using P2
(**A**). Size fractionation of genomic DNA restricted with a variety of endonucleases. Lane 1, λ/*Hind* III markers, lane 2, *Eco* RI, lane 3, *Hind* III, lane 4, *Eco* RI/*Hind* III, lane 5, *Xho* I, lane 6, λ/*Hind* III markers, lane 7, λ/*Hind* III/*Eco* RI markers, lane 8, *Eco* RI/*Xho* I, lane 9, *Pst* I, lane 10, *Pst* I/*Xho* I, lane 11, λ/*Hind* III markers, lane 12, *Pst* I/*Hind* III, lane 13, *Hind* III/*Eco* RI, lane 14, human/*Eco* RI and lane 15, λ/*Hind* III markers. All the digests were of FDCP genomic DNA except lane 13 which was HL-60 genomic DNA. 15μg of genomic DNA was used.

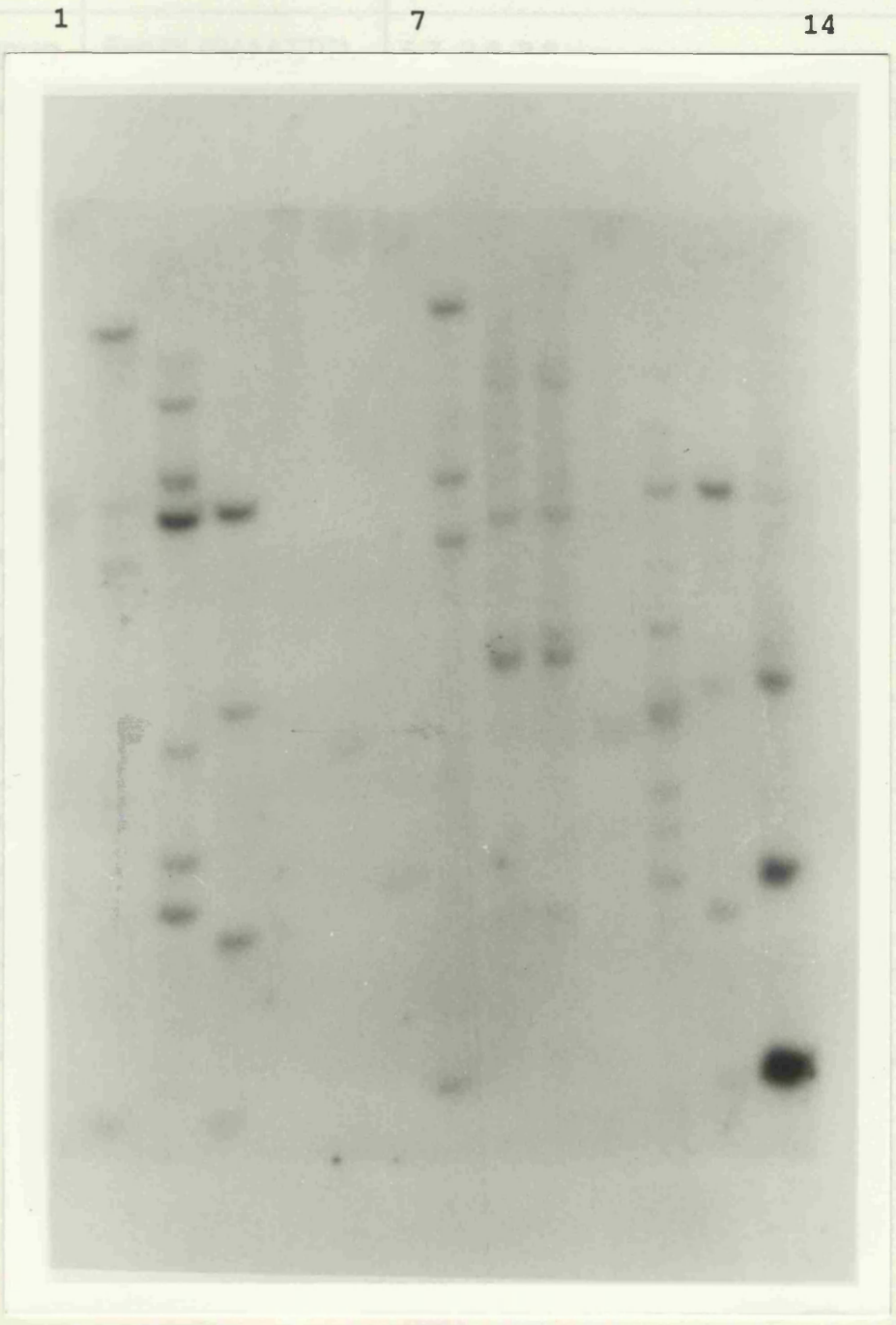

Figure 5.1 Genomic mapping using P2.
(**B**). Autoradiograph of sSuthern blot probed with P2. The lanes contents are as described in Figure 5.1a.

DNA	ENDONUCLEASE	SIZE (kb)
Human	*Eco* RI (G^AATTC)	5.7, 3.8, **2.8.**
Murine	*Bam* HI (G^GATCC)	19.0, 17.0, 15.0, 7.5, 6.0, 2.6, 1.8, 1.0.
Murine	*Eco* RI (G^AATTC)	**17.0**, 8.0, 7.6, 7.3, **2.6**.
Murine	*Hind* III (A^AGCTT)	12.0, 8.7, **7.8**, 4.5, 4.0, 3.6
Murine	*Hpa* II (C^CGG)	DNA ~ 30-8kb.
Murine	*Pst* I (CTGCA^G)	12.0, 8.5, 7.6, 7.4, **5.7**, 1.5, 1.0.
Murine	*Sau* 3AI (^GATC)	1.5, 1.4, 0.9, **0.5**.
Murine	*Sca* I (AGT^ACT)	11.0, **7.9**, 6.0, 4.8, 0.9.
Murine	*Stu* I (AGG^CCT)	11.0, **6.0**, 4.2, 2.6.
Murine	*Taq* I (T^CGA)	20.0, **9.5**, 7.5, 5.5, 2.7.
Murine	*Xba* I (T^CTAGA)	15.0, 9.5, **8.0**, 7.0, 4.5, 3.2, 3.0, 2.2.
Murine	*Xho* I (C^TCGAG)	Above 30kb.

Table 5.1 Restriction patterns obtained with single digests of murine DNA. Genomic DNA was restricted with a variety of endonucleases and size fractionated on 1.0 to 0.7% w/v agarose gels. The bands were sized using the hybridization pattern generated by *Eco* RI restricted human genomic DNA as markers (5.7, 3.8 and 2.8 kb). The figures in bold indicate the bands which gave the strongest signals and are thus more homologous to huFPR.

DNA	ENDONUCLEASE	SIZE (kb)
Murine	*Bam* HI/*Hind* III	**7.9**, 3.2, 2.6, 2.3.
Murine	*Bam* HI/*Eco* RI	**16.0**, 7.5, 7.0.
Murine	*Bam* HI/*Pst* I	11.0, 8.0, 7.6, 6.2, 5.9, 5.4, 4.5, 3.6, 3.4, 1.5, **1.1**.
Murine	*Eco* RI/*Hind* III	**7.8**, 5.6, 3.4, 2.2.
Murine	*Eco* RI/*Sca* I	15.0, 7.6, 6.2, 6.0, 3.8, 1.7, 1.4, 1.2, 1.1.
Murine	*Eco* RI/*Pst* I	12.0, 7.8, **7.2**, 6.2, 6.0, 5.9, 2.6, **1.0**.
Murine	*Eco* RI/*Xho* I	**19.0**, 8.5, 7.4, 2.6.
Murine	*Hind* III/*Eco* RV	**9.0**, 8.0, **4.5**, 4.2, 3.6.
Murine	*Hind* III/*Nco* I	**9.0**, 8.0, **4.5**, 4.2, 3.6.
Murine	*Hind* III/*Pst* I	6.0, 5.6, 4.0, 2.4, 1.2, **1.1**.
Murine	*Hind* III/*Spe* I	**6.2**, 4.5, 3.5, 2.5, 2.3.
Murine	*Hind* III/*Stu* I	6.2, **4.4**, 3.8, 2.8, 2.7, 2.5.
Murine	*Hind* III/*Xba* I	8.0, **4.5**, 3.7, 2.6, 2.4.
Murine	*Pst* I/*Sca* I	3.8, 1.4, **0.9**.
Murine	*Pst* I/*Xho* I	12.0, 7.6, 5.9, **5.7**, 1.5, 1.0.

Table 5.2 Restriction patterns obtained with double digests of murine DNA. Genomic DNA was restricted with a variety of endonucleases and size fractionated on 1.0 to 0.7% w/v agarose gels. The bands were sized using the hybridization pattern generated by *Eco* RI restricted human genomic DNA as markers (5.7, 3.8 and 2.8 kb). The figures in bold indicate the bands which gave the strongest signals and are thus more homologous to huFPR.

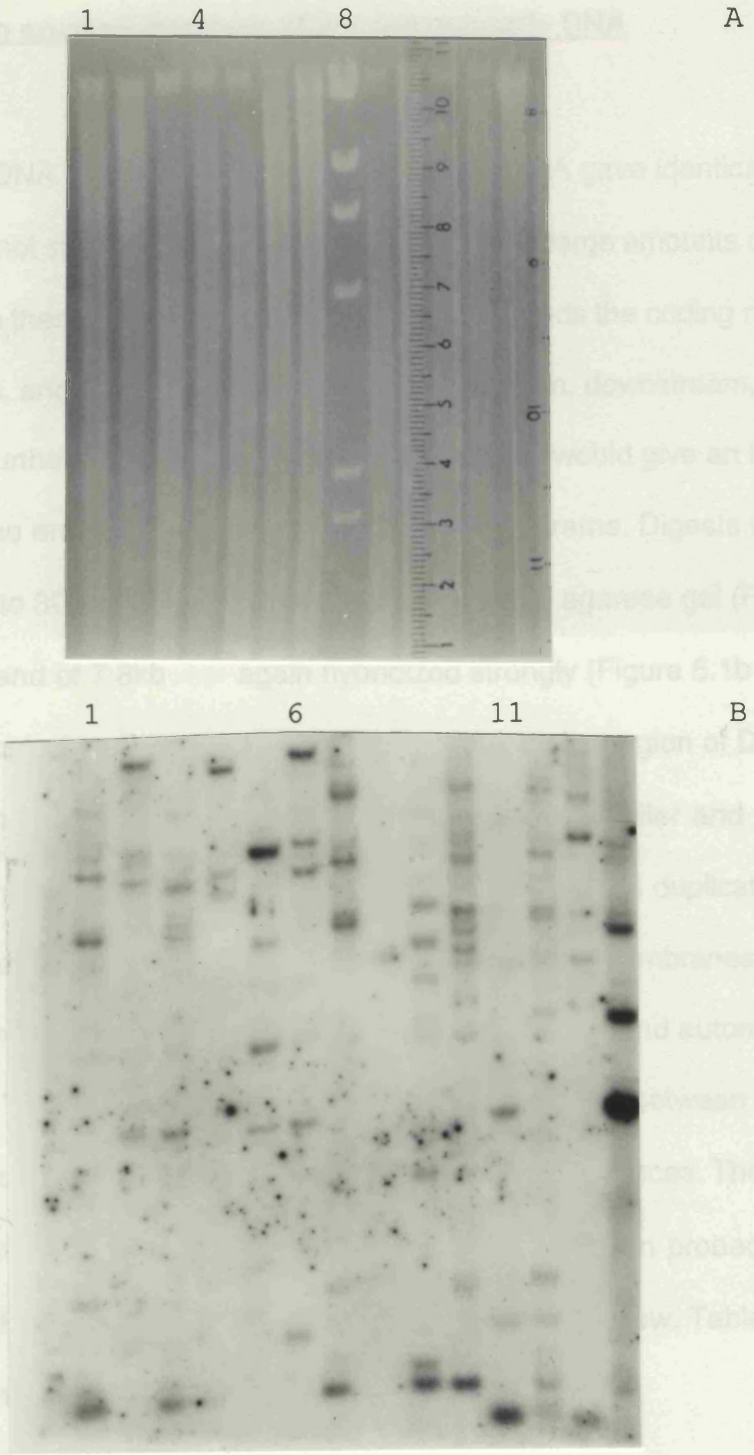

Figure 5.2 Genomic mapping using P1
(**A**). Size fractionation of genomic DNA restricted with a variety of endonucleases. Lane 1, *Pst* I, lane 2, *Eco* RI, lane 3, *Eco* RI/*Pst* I, lane 4, *Eco* RI/*Bam* HI, lane 5, *Eco* RI/*Hind* III, lane 6,*Eco* RI/*Xho* I, lane 7, *Pst* I/*Xho* I, lane 8, λ/*Hind* III markers, lane 9, *Pst* I/*Hind* III, lane 10, *Pst* I/*Bam* HI, lane 11, *Pst* I/*Sca* I, lane 12, *Eco* RI/*Sca* I, lane 13, *Sca* I, lane 14, human/*Eco* RI and lane 15, λ/*Hind* III markers. All the digests were of FDCP genomic DNA except lane 14 which was HL-60 genomic DNA. 15µg of genomic DNA was used.
(**B**). Autoradiograph of southern blot probed with P2. The lanes contents are as described in Figure 5.2a.

5.3 Restriction enzyme mapping of murine genomic DNA

Since murine DNA from FDCP, WEHI-3b and brain DNA gave identical restriction patterns (data not shown), and as it was easier to obtain large amounts of DNA from WEHI-3b, cells these were used. To establish which bands the coding region probe (P2) hybridizes, and which hybridize to both the upstream, downstream, and coding regions (P1), further experiments were carried out. This would give an indication of the length of the entire gene not just the open reading frame. Digests were scaled up from 15µg to 30µg and the samples loaded onto an agarose gel (Figure 5.3a). The *Hind* III band of 7.8kb again hybridized strongly (Figure 5.1b lane 3) and I therefore decided to construct a partial library of this size region of DNA. *Hind* III digests were carried out with other enzymes to give a smaller and more easily clonable fragment. The restricted DNA was size-fractionated in duplicate on a 0.7% w/v agarose gel and transferred by capillary action to nylon membranes and cut into two. The two membranes were then probed with P1 and P2 and autoradiographed (Figure 5.3b). The agarose gel shows the same DNA pattern between the two sets of samples. However, the autoradiograph shows some differences. The *Hind* III/*Stu* I gave two extra hybridization bands, a 3.8 and 2.5 kb when probed with P1 as compared to P2. In general though the differences are very few. Table 5.3 gives a summary of the differences between P1 and P2.

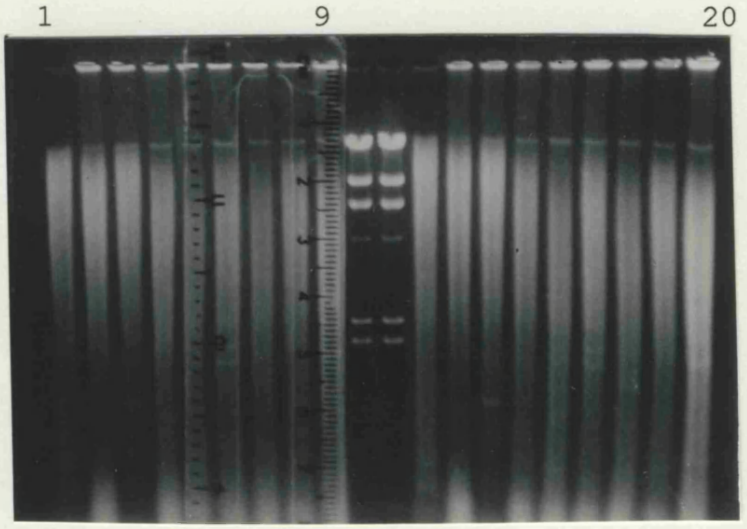

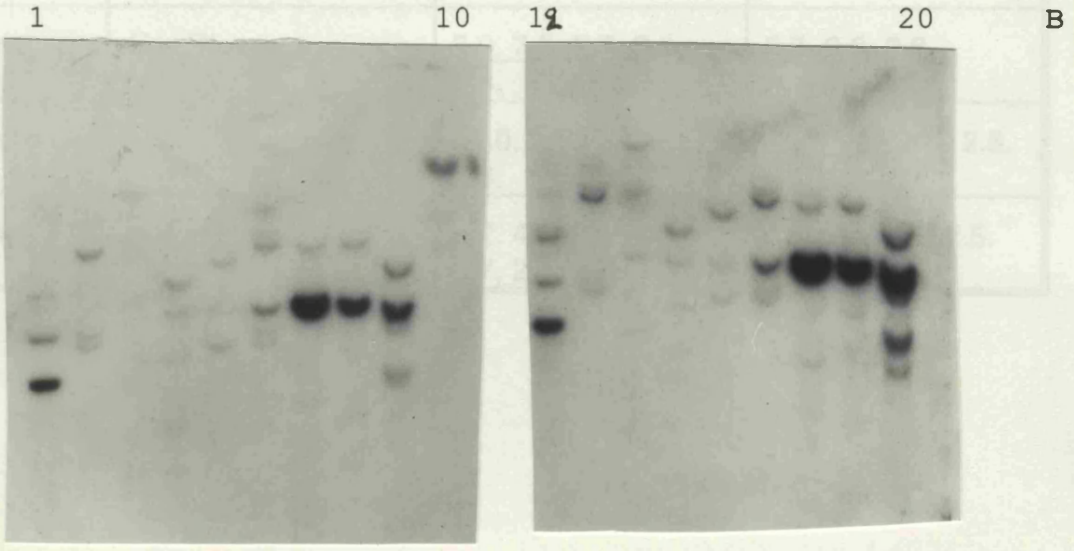

Figure 5.3 Genomic mapping using P1 and P2.
(**A**). Size fractionation of genomic DNA restricted with a variety of endonucleases. Lane 1, human/*Eco* RI, lane 2, *Hind* III, lane 3, *Eco* RI, lane 4, Hind III/*Spe I*, lane 5, *Hind* III/*Nco* I, lane 6, Hind III/*Eco* RV, lane 7, *Hind* III/*Xba* I, lane 8, *Hind* III/*Bam* HI, lane 9, *Hind* III/*Stu* I, lane 10, λ/*Hind* III markers, lane 11, λ/*Hind* III markers, lane 12, human/*Eco* RI, lane 13, *Hind* III, lane 14, *Eco* RI, lane 15, Hind III/*Spe I*, lane 16, *Hind* III/*Nco* I, lane 17, Hind III/*Eco* RV, lane 18, *Hind* III/*Xba* I, lane 19, *Hind* III/*Bam* HI, lane 20, *Hind* III/*Stu* I, 15µg of Wehi-3b DNA was used.
(**B**). Autoradiograph of southern blot. The lanes contents are as described in Figure 5.3a. The left blot was probed with P2 and the right with P1.

DNA	ENDONUCLEASE	PROBE 1 (P1)	PROBE 2 (P2)
Human	*Eco* RI	8.0, 7.5, 5.7, 3.8, **2.8.**	5.7, 3.8, **2.8.**
Murine	*Eco* RI	**17.0**, 8.0, 7.6, 7.3, **2.6.**	**17.0**, 7.6, 7.3, **2.6.**
Murine	*Hind* III/*Stu* I	6.2, **4.4**, 3.8, 2.8, 2.7, 2.5.	6.2, **4.4**, 2.7, 2.5.

Table 5.3 Comparison of P1 and P2 banding patterns. The figures in bold indicate the bands which gave the strongest signals and are thus more homologous to huFPR.

The digests with *Hind* III/*Xba* I, *Hind* III/*Bam* HI and *Hind* III/*Stu* I (Figure 5.3, lanes: 7, 8 , 9 and 18, 19, 20) with both probes gave an unusually strong hybridization signal in the size range of 3.4 - 4.0 kb. During the purification of genomic DNA, no RNA usually co-purifies. However, in this case some RNA may have done so leading to the unusually strong hybridization bands. Normally an RNAse step is not necessary and so is not done. To produce long and intact genomic DNA the less manipulation of it the better. To determine whether it was an mRNA contamination, the DNA was RNAse treated and an identical set of digests were carried out and probed with P1. Figure 5.4a shows the agarose gel and Figure 5.4b shows the autoradiograph. The strongly hybridizing band found in Figure 5.3 is absent, indicating that the band was due to mRNA and not to murine genomic DNA. The band may have been a contaminant from some of the plasmid containing the huFPR probe, but this seems unlikely since the DNA in all the lanes came from the same DNA preparation and the hybridized band was absent in the single digests of the same enzymes.

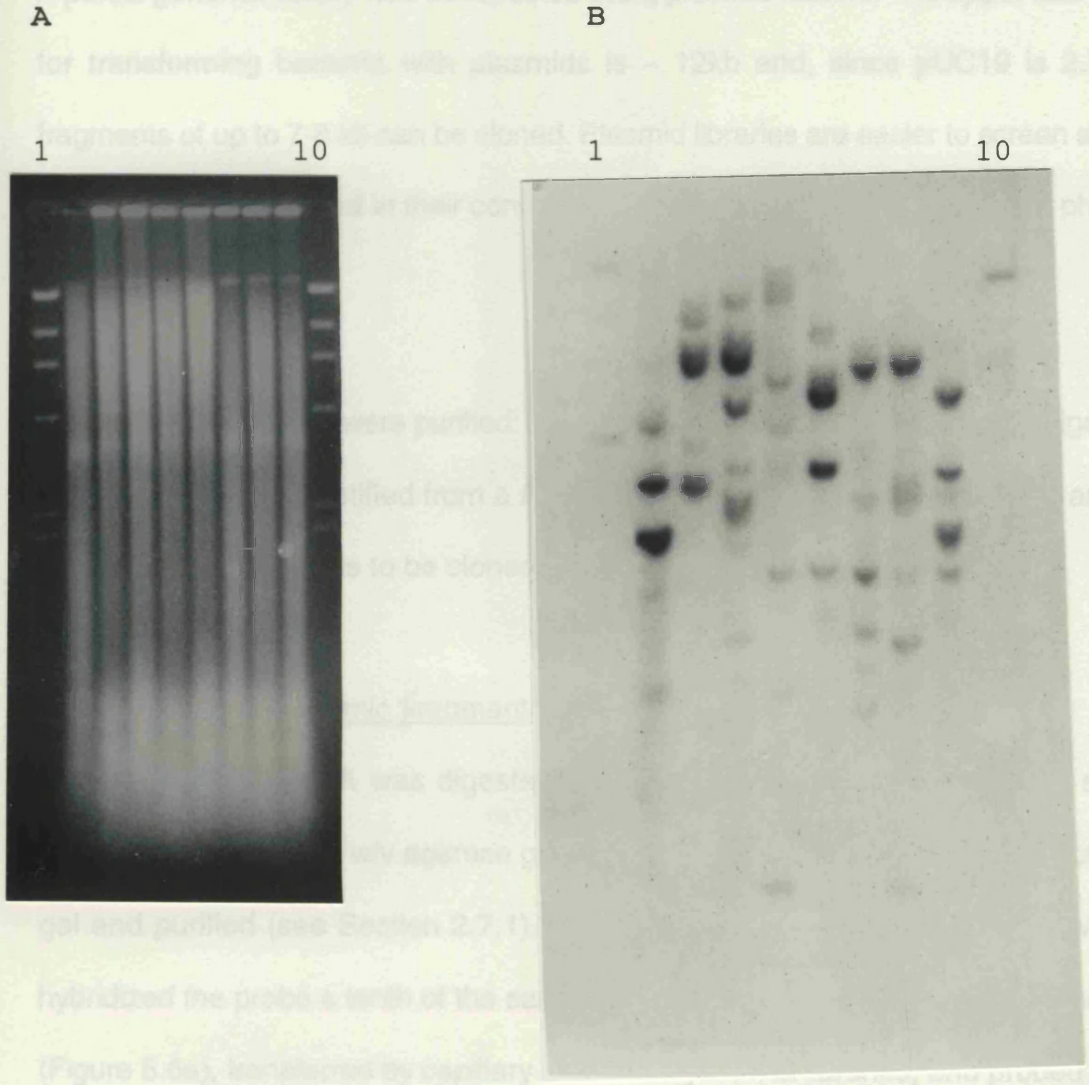

Figure 5.4 Genomic mapping of WEHI-3b DNA after an RNAase step.
(**A**). Size fractionation of genomic DNA restricted with a variety of endonucleases. Lane 1, λ/*Hind* III markers, lane 2, human/*Eco* RI, lane 3, *Hind* III, lane 4, *Xba* I, lane 5, *Bam* HI, lane 6, *Stu* I, lane 7, *Hind* III/*Xba* I, lane 8, *Hind* III/*Bam* HI, lane 9, *Hind* III/*Stu* I and lane 10, λ/*Hind* III markers. The blot was probed P1.
(**B**). Autoradiograph of southern blot. The lane contents are as described in Figure 5.4a. The blot was probed with P1.

5.4 Construction of a Partial Murine Genomic DNA Library

A partial genomic library was constructed using plasmid vectors. The upper size limit for transforming bacteria with plasmids is ~ 12kb and, since pUC19 is 2.7kb, fragments of up to 7-8 kb can be cloned. Plasmid libraries are easier to screen since fewer steps are required in their construction and screening as compared to phage or cosmid libraries.

Four hybridized bands were purified: 8.7 and 7.8 kb identified from a *Hind* III digests, and 7.6 and 5.7kb identified from a *Pst* I digest. Figure 5.1 lanes 3 (*Hind* III) and 9 (*Pst* I) shows the bands to be cloned.

5.4.1 Isolation of genomic fragments

30µg of genomic DNA was digested with each of *Hind* III and *Pst* I, and size-fractionated on a 0.7% w/v agarose gel (Figure 5.5). The bands were cut out of the gel and purified (see Section 2.7.1). To confirm the presence of the band which hybridized the probe a tenth of the sample was loaded onto a gel size-fractionated (Figure 5.6a), transferred by capillary action to nylon membranes, and probed with P2 (Figure 5.6b). To increase the chances of isolating the coding regions, P2 was used instead of P1. Lanes 2 and 3 contain the *Pst* I 5.7 and 7.6 kb bands, respectively. Lanes 4 and 5 contain the *Hind* III 7.8 and 8.7 kb, respectively. The *Pst* I purification was the more successful as there is a slight cross contamination of the two *Hind* III bands with each other.

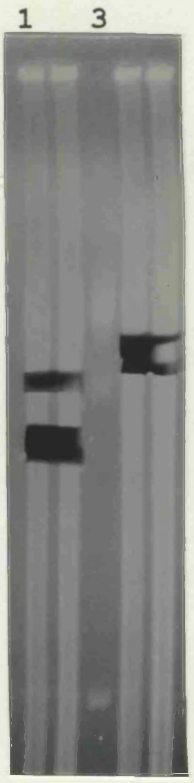

Figure 5.5 Purification of DNA for library construction.
Lanes 1 and 2 contain *Pst* I digested DNA, lane 3 contains λ/*Hind* III markers, and lanes 4 and 5 contain *Hind* III digested DNA.

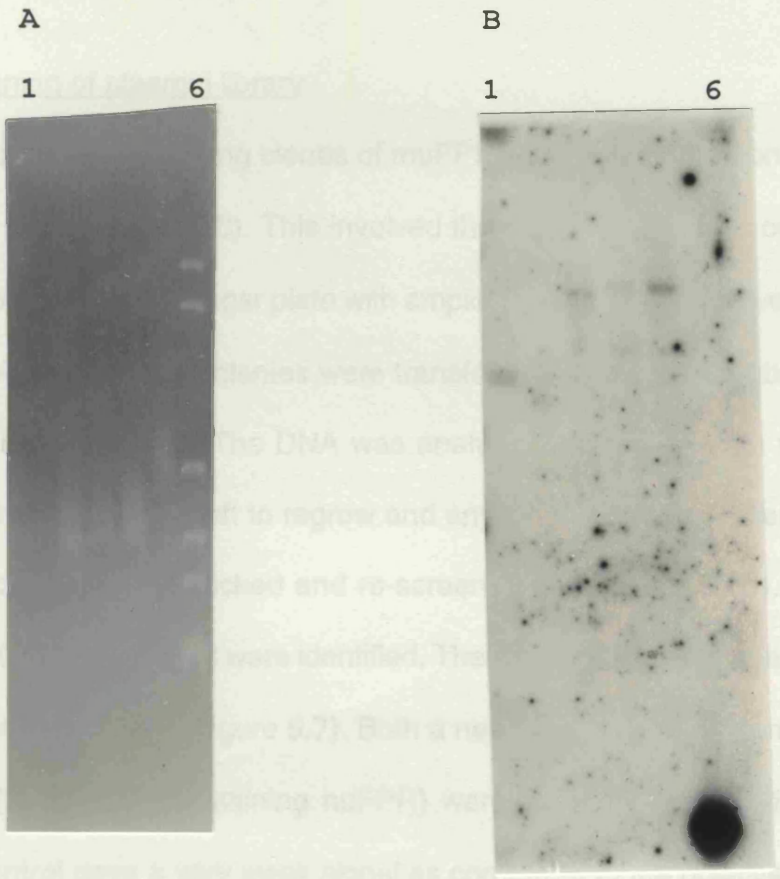

Figure 5.6 Characterizing purified DNA.
(A). Size fractionation of purified genomic DNA. Lane 1, λ/*Hind* III markers, lane 2, *Pst* I 5.7kb, lane 3, *Pst* I 7.6 kb, lane 4, *Hind* III 7.8kb, lane 5, *Hind* III 8.7kb, lane 6, huFPR (positive control).
(B). Autoradiograph of Southern blot. Lanes areas in Figure 5.6a. Probed with P2.

5.4.2 Subcloning into plasmid

The purified DNA restriction fragments were cloned into pUC19 which had been cut with either *Hind* III or *Pst* I and the 5' ends and dephosphorylated to prevent self-ligation (see Section 2.7.4.).

5.4.3 Screening of plasmid library

To identify colonies containing clones of muFPR, colony hybridization with P2 was carried out (see Section 2.8). This involved the plating of bacteria containing the pUC19 recombinant on an agar plate with ampicillin and incubating overnight to give bacterial colonies. These colonies were transferred to a nylon membrane and the DNA fixed after cell lysis. The DNA was analyzed by hybridization with P2. The original culture plate was left to regrow and any positive colonies identified by the screening could then be picked and re-screened (see Section 2.8). From 3 000 colonies 200 positive clones were identified. These were re-screened after streaking onto a nylon membrane (Figure 5.7). Both a negative (plasmid with no insert) and a positive (pBluescript containing huFPR) were also placed onto the filter. The negative control gave a very weak signal as compared to the positive.

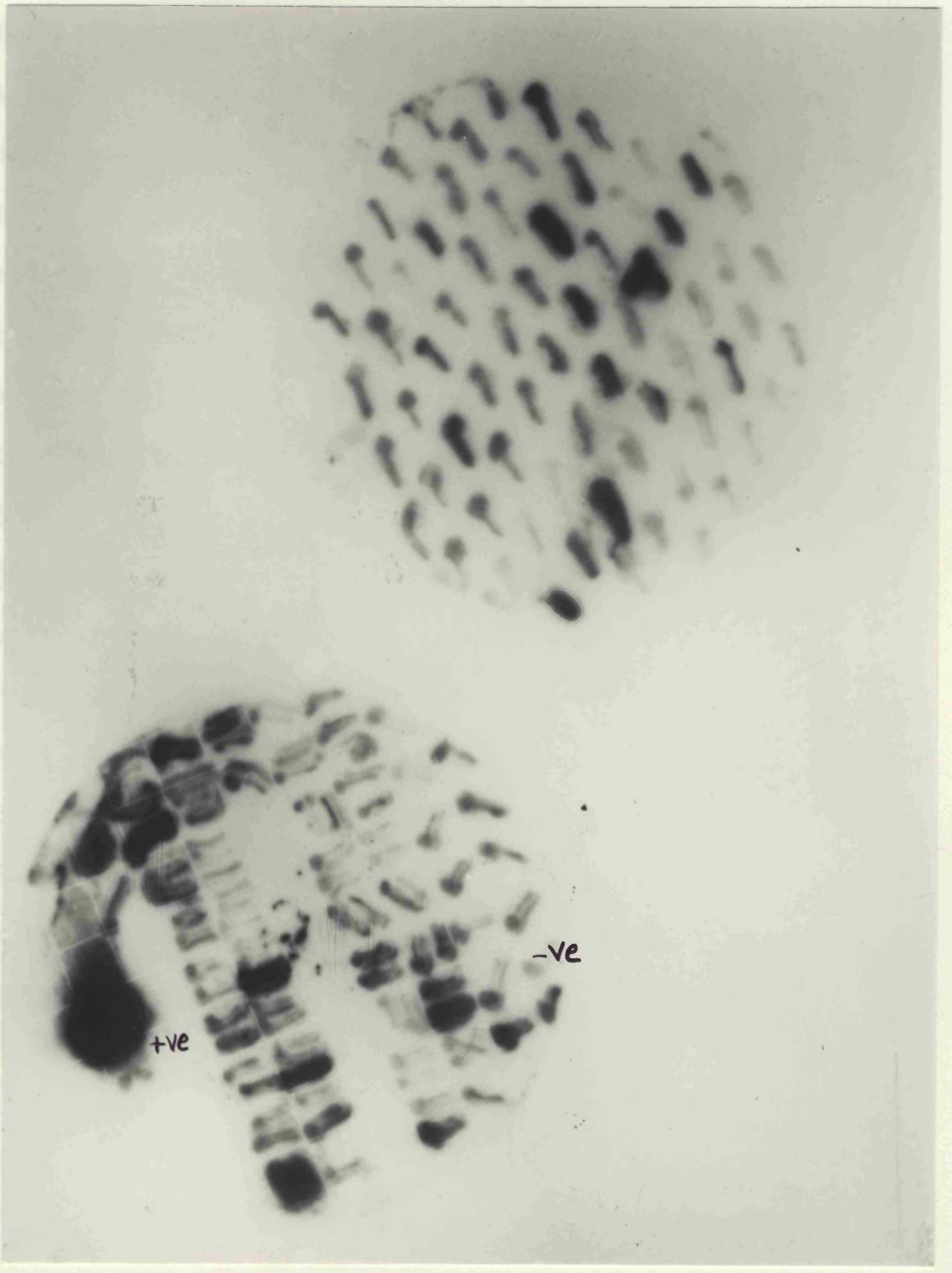

Figure 5.7 Screening of Plasmid Library.
Two filters containing colonies from four ligations (Figure 5.6). Positive and Negative colonies are marked.

The final screening involved preparing plasmid DNA from the strongly hybridizing clones and digesting it with *Hind* III/*Eco* RI in order to excise the insert. These were then size-fractionated on a 0.7% w/v agarose gel (Figure 5.8a). Lanes 2 to 6 and lanes 8 to 10 are digests of plasmid containing the *Hind* III 7.8kb band. Lanes 11, 12 and 14 to 18 are digests of plasmid containing the *Hind* III 8.7kb band. Lanes 21 to 24 are digests of plasmid containing the *Pst* I 7.6kb band. Lanes 26, 27 and 29 to 31 and 32 to 34 and 35 to 36 are digests of plasmid containing the *Pst* I 5.6kb band. Only inserts of up to 5kb have been cloned with the majority being 3 to 4 kb in length. This was probably due to the low transformation efficiency of large plasmid constructs. The DNA was transferred by capillary action and probed with P2 (Figure 5.8b). Several strongly hybridizing bands are visible in addition to the vector DNA (2.7kb). The vector hybridized because a slight contamination of the probe with vector DNA occured even though the probe was size-fractionated and purified. No hybridization to the λ phage DNA markers was visible. In contrast the probe hybridized to the plasmid. This is probably due to a contaminant, in the probe, present from the probe purification from its plasmid. Both plasmids contain the *lac* Z gene sequences. The non-plasmid bands which gave strong hybridization signals were partially sequenced (data not shown). None of these bands had any homology to any FPRs known or to any other sequences in the EMBL database.

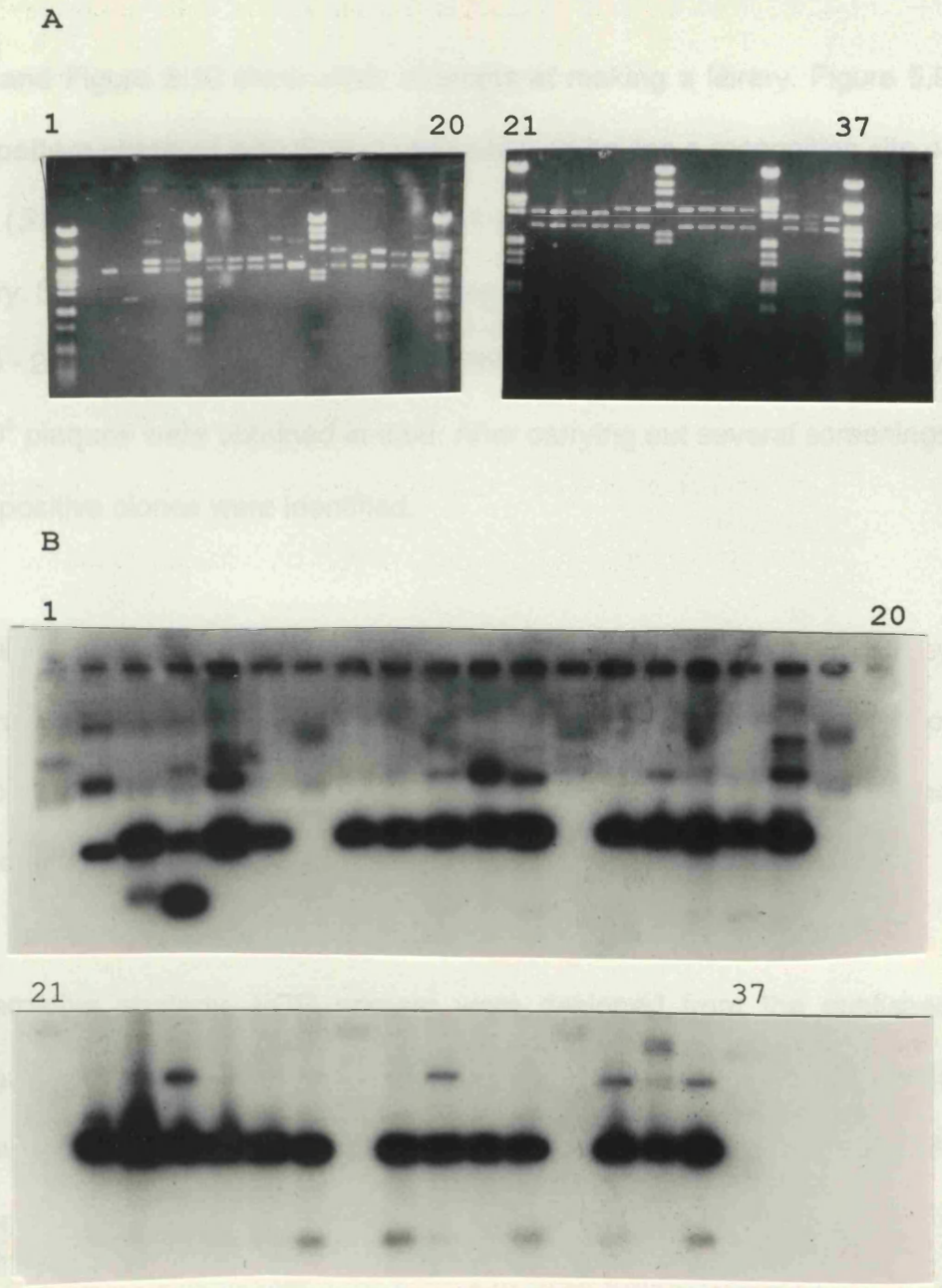

Figure 5.8 Screening recombinant plasmids.
(**A**). Size-fractionation of plasmid DNA restricted with *Hind* III/*Eco* RI.
Lanes 2 to 6 and lanes 8 to 10 are digests of plasmid containing the *Hind* III 7.8kb band. Lanes 11, 12 and 14 to 18 digests of plasmid containing the *Hind* III 8.7kb band. Lanes 21 to 24 are digests of plasmid containing the *Pst* I 7.6kb band. Lanes 26, 27, 29 to 31, 32 to 34 and 35 to 36 are digests of plasmid containing the *Pst* I 5.k band. Lanes 1 and 37 are λ/*Pst* I markers. Lanes 7, 20, 21 and 33 are λ/*Hind* III/*Eco* RI markers. Lanes 14 and 28 are λ/*Hind* III markers.
(**B**). Autoradiograph of Southern blot. The lane contents are as described in Figure 5.8a. The blot was probed with P2.

5.5 Construction of other murine genomic libraries

Figure 5.9 and Figure 5.10 show other attempts at making a library. Figure 5.9 shows the pattern obtained with three endonucleases having a recognition site of four bases (*Sau* 3AI, *Taq* I and *Hpa* II). These enzymes were used to produce a phage library. Sau 3AI partially cut DNA was size fractionated on a sucrose gradient to obtain 10 - 20kb fragments (Figure 5.10) for the construction of a λ phage library. Only 1 x 10^5 plaques were obtained in total. After carrying out several screenings with P2 no positive clones were identified.

Additional libraries were constructed in phage vectors, using DNA purified by sucrose gradients and electroporation, but these also led to the cloning of unidentifiable DNA. Finally, a murine cosmid library was screened but at this time the sequence of murine FPR was published (Gao and Murphy, 1993).

As an alternative strategy, PCR primers were designed from the published sequence and used to attempt the amplification of the gene from murine genomic DNA. This would then be used in the characterization of the FDCP expressed FPR (see Section 6.3).

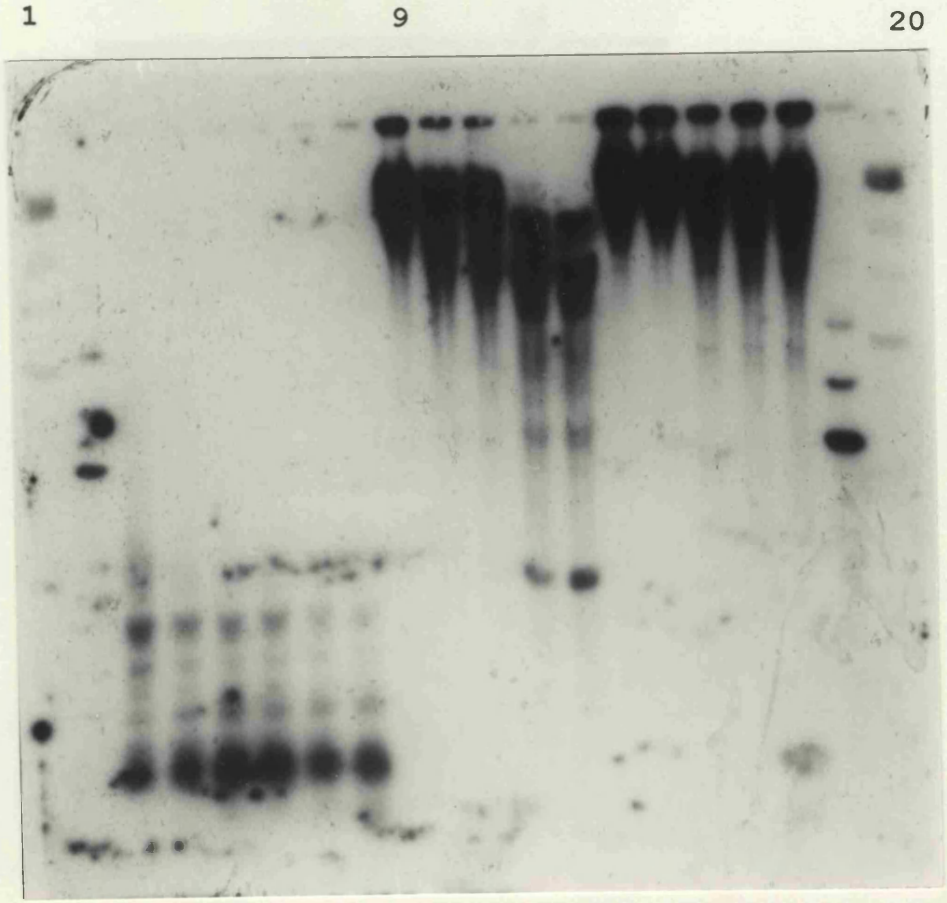

Figure 5.9 Genomic mapping with frequent cutting endonucleases. Autoradiograph of Southern blot. Lane 1, λ/*Hind* III markers, lane 2, human/*Eco* RI, lane 3 to lane 8, *Sau* 3AI (0.4, 1.2, 3.0, 8.0, 10.0 and 12.0 units), lane 9 to 13, *Taq* I (0.4, 1.2, 3.0, 8.0 and 12.0 units), lane 14 to lane 18 *Hpa* II (0.4, 1.2, 3.0, 8.0 and 12.0 units) and lane 19 λ/*Hind* III markers. 15μg of FDCP DNA was used. The digests were carried out for one hour and then the reaction was stopped. The blot was probed with P1.

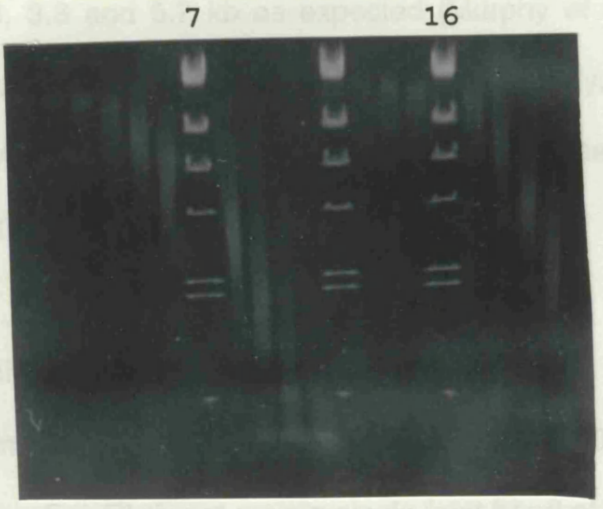

Figure 5.10 Size-fractionation of genomic DNA on a sucrose gradient. Lanes 7, 12 and 16 are *λHind* III markers. Lanes 1 to 6, 13 to 15 and 17 to 20 contains fractions from the sucrose gradient on which genomic DNA partially cut with *Sau* 3AI was fractionated.

5.6 Discussion

To characterize and enable the cloning of the murine FPR gene, genomic DNA was restricted with a variety of endonucleases, Southern blotted, and analyzed with the two probes P1 and P2. Human genomic DNA digested with *Eco* RI gave three bands of 2.8, 3.8 and 5.7 kb as expected (Murphy *et al.*, 1992). These three correspond to *huFPR, FPRL1, and FPRL2*, respectively. The hybridized human genomic DNA provided a positive control and the λ phage markers acted as a negative control.

There has only been a single publication on the analysis of murine genomic DNA with the enzymes *Eco* RI, *Pst* I and *Hind* III (Bao *et al.*, 1992) and this data was not very clear. The *Eco* RI digest gave a single faint band of approximately 12kb, the *Hind* III two faint bands of 7 and 6 kb, and the *Pst* I digest gave no hybridization.

Endonucleases cut DNA with a frequency dependent on their recognition site. The DNA is infrequently cut with endonucleases, having a recognition site containing a cytosine/guanosine (CpG) doublet (*Hpa* II and *Xho* I) (Maniatis *et al.*, 1982). This is because mammalian DNA contains methylated cytosine (^{m5}C) residues. These are mainly found at the 5' end of guanosine residues. This methylation is highly cell-type specific. The hybridization pattern obtained with *Hpa* II and *Xho* I indicates that the DNA used is highly methylated at these doublets as these enzymes have a GC recognition sequence and they restricted the DNA infrequently.

When these enzymes are used in double digests they enhance the bands that would be obtained from singe enzyme digests. This is because they cut the DNA

into large pieces (greater than 30kb) and so grant other endonuclease better access to the DNA.

The two probes generated very similar hybridization patterns. This is probably due to the method used: random primed labelling. This method involves the synthesis of probe DNA with a radiolabelled nucleotide. But, because DNA polymerase only acts in a 5' to 3' direction, the amount of probe made from the 3' end would be under represented. Also the 5' untranslated region is ~60bp and the 3' is ~200bp, as compared to the 1050bp coding region. The coding region would therefore generate more probe.

At least six putative murine FPR genes were identified with the *Hind* III digests by high stringency hybridization analysis. This was because of the large band sizes detected. However, this could also be due to the presence of large introns. The PCR results (see Section 6.3.3) would indicate that no introns are present in *muFPR*, but that they may be present in the other five putative genes. After sequencing the muFPR genes, Murphy and co-workers analyzed them for introns and exons (Gao and Murphy, 1993). They found that the entire reading frame is in one exon, as is the case for the human FPR genes (Bao *et al.*, 1992). Figure 5.1b shows that *Hind* III generates six bands of 11.0, 9.5, 6.7, 4.4, 3.8 and 3.0. Since the coding region of *muFPR* is only 1.0kb and due to the fact that six genes have been found to have a high homology to huFPR (54% to 76%), it is highly probable that the six *Hind* III bands correspond to the six genes. Since the 7.8kb gave the strongest hybridization signal when compared to the other bands it is probably *muFPR* (76%) (Gao and Murphy, 1993). Because high stringency conditions were used, signal strength correlates with the degree of homology between the probe and the target DNA.

The construction of a cDNA library was ruled out because of the difficulty in isolating enough messenger RNA. For a cDNA library at least 10µg of cDNA is required. Assuming 100% efficiency in the reverse transcriptase this means 10µg of mRNA. A typical cell has 10^{-7}µg of mRNA. Therefore 10^8 cells are required. This is too difficult to isolate from mice and it was too prohibitive to produce them by the *in vitro* system used in these studies. In the *in vitro* system typically 5 x 10^5 cells.ml^{-1} can be obtained (see section 3.2, Figure 3.3). To obtain 10µg of mRNA, 200mls of these cells would be needed. Since only approximately 80% of cells are neutrophils (see Section 3.4.2, Figure 3.6), and more than 10µg of mRNA would realistically be needed, the amount of cytokines required to differentiated enough cells would be prohibitive.

The library construction using plasmid was not successful because bacteria can only be transformed with a high efficiency by small plasmids. This biased the transformed colonies to recombinant plasmids with small inserts. Only a few of the plasmids contained inserts above 4kb. A phage vector should overcome this problem, so the construction of a partial phage library was also attempted using *Hind* III restricted DNA fragments.

However, this too was unsuccessful in isolating the 6.7kb *Hind* III band from a gel. This method would only give a twenty times increase in purification over a total genomic library. The *Hind* III restricted genomic DNA was size-fractionated over 10cm of an agarose gel. 0.5cm of this contained the 6.7kb *Hind* III fragment. For a genome size of 3 x 10^9bp, 3 x 10^6 clones have to be screened if the gene is 1.0kb in size. Because of the additional inefficiency in cloning DNA purified from agarose gels (due to damaged DNA termini) the number of clones to be screened would still

be in the order of 10^6. So although there is a theoretical advantage in screening a partial library in practise there is not a great deal of difference to that of screening a complete genome library. This is because because there were six genes and assuming 1kb in length only 5×10^5 clones would need to be screened to obtain a clone. In fact it was this method which was used to clone the murine FPR genes (Gao and Murphy, 1993).

In hindsight, the construction of a partial library should not have been attempted. The gene which was cloned by a group headed by Murphy (Gao and Murphy, 1993), was isolated by screening 1×10^7 plaques. Nineteen positive clones containing six putative genes (of which only one has been published) were isolated. It was therefore consistent with this that the phage library constructed, which contained only 10^4plaques, was unsuccessful.

CHAPTER 6

PCR CLONING OF huFPR AND muFPR

6.1. Introduction

The aim of this aspect of the project was to determine the primary structure of the murine FPR by cloning and sequencing the gene. Work had been carried out to characterize the receptor at the protein level, but because of the two different affinities demonstrated by FPR it, was not known whether it was a single receptor or two and whether it was a single polypeptide or multiple polypeptides. HL-60 differentiated to neutrophil-like cells were to be used to isolate the human FPR and N-terminal sequence it. The human FPR cDNA could then be cloned by screening a cDNA library made from differentiated HL-60 cells. This sequence information could be used to PCR amplify the FPR gene from murine genomic DNA or screen a murine genomic library.

The human FPR gene was cloned by another group just before the work was begun (Boulay *et, al.,* 1990a). The sequence information was therefore used to design PCR primers in order to clone the human FPR gene. This could be used to screen a murine genomic library (see Section 5) and attempt to isolate the murine FPR gene.

6.1.1 Cloning of the human FPR (huFPR)

The human leukemic cell lines, HL-60 and U937, have been used to study the receptors which bind chemotactic factors (Collins *et al.*, 1977; Harris and Ralph, 1985). They can be differentiated to neutrophil-like cells with dibutyryl-cAMP.

In 1990 two huFPR cDNA clones (fMLP-R98 and fMLP-R26) were isolated from a cDNA library constructed from HL-60 neutrophil mRNA (Boulay *et al.*, 1990a). fMLP-R26 differed from fMLP-R98 in the following respects: the 5' untranslated region of

fMLP-R98 showed a 16bp deletion at position -39 as compared to fMLP-R26; the sequence also diverged in the 3' untranslated region, at position 1175 and 1219-1220 (see Appendix 2). In addition, the 3' untranslated sequence of fMLP-R98 was extended by 661bp. In the coding region there were two base substitutions C to G at position 301 and C to A at position 1037, resulting in the replacement of Val^{101} and Glu^{346} in fMLP-R26 by Leu^{101} and Ala^{346} in fMLP-R98.

In 1993 another cDNA clone of huFPR was isolated from U937 cells, differentiated to neutrophils, and designated UF1 (Haviland *et al.*, 1993). UF1 had an extra 16bp on the 5' untranslated sequence as compared to fMLP-R98 and fMLP-R26. In addition it had a combination of the variations found in fMLP-R98 and fMLP-R26. UF1 was identical to fMLP-R26 in the 5' untranslated sequence, the nucleotide 301 (non-silent variation) and was polyadenylated at the same nucleotide position. UF1 was identical to fMLP-R98 at the nucleotide position 1037 (non-silent variation) and at position 1175 (base pair deletion). All the cDNAs encoded for a 350 amino acid polypeptide. The differences between fMLP-R26, fMLP-R98 and UF1 are assumed to be due to allelic variations and that the only non-allelic difference, the additional 3' untranslated sequence of fMLP-R98, is due to different polyadenylation of the primary transcript (Haviland *et al.*, 1993; Murphy *et al.*, 1993). The differences are thought to be allelic variations as genomic and Southern mapping data demonstrate a single-copy gene with no evidence for multiple coding exons. In addition I have established, through PCR, that there are no introns within the coding region of the FPR gene. In 1992 De Nardin and co-workers published the same observation (De Nardin *et al.*, 1992).

The gene for FPR was designated *FPR1* and its gene product huFPR (Murphy *et al.*, 1992). The structural organization of the huFPR gene was established by two groups; Haviland and co-workers, and by Murphy and co-workers. Haviland and co-workers showed that the gene is approximately 7.5kb in length with two exons separated by a 5.0kb intron. Exon one encodes 66bp of the 5' untranslated sequence and exon two encodes 11bp of the 5' untranslated sequence, the coding region and the 3' untranslated sequences (Haviland *et al.*, 1993). Murphy and co-workers showed that the gene is organized over 6kb with three exons and two introns. The coding region was found to be 4909bp form the transcription start point and consisted of three exons and two large introns (Murphy *et al.*, 1993). Thus, the 5kb intron found by Haviland and co-workers was shown by Murphy and co-workers to contain another exon.

6.1.2 The cloning of human FPR homologues

In 1992 a homologue to huFPR was identified from a cDNA library constructed from HL-60 neutrophil mRNA by two groups. Ye and co-workers isolated a 1.65kb transcript having a 69% homology, in the ORF, to huFPR encoding a polypeptide of 351 amino acids (Ye *et al.*, 1992). Murphy and co-workers isolated a 2.6kb transcript having a 69% homology, in the ORF, to huFPR encoding a polypeptide of 351 amino acids (Murphy *et al.*, 1992). The only differences between the clones from the two groups was an extra 733bp in the 5' untranslated sequence and 256bp in the 3' untranslated sequences. The coding region was identical. This clone was designated FPRL1 and its gene *FPRL1* (FPRL1 - human formyl peptide receptor like-1).

Through screening of genomic DNA with huFPR and FPRL1 another putative gene, designated *FPRL2*, was identified. Ye and co-workers also found a third transcript expressed by neutrophil HL-60 cells possibly FPRL2. Murphy and co-workers did not identify any transcripts that could be FPRL2 even though they followed the same basic procedure. In the same year Bao and co-workers isolated three clones using a human genomic library (Bao *et al.*, 1992). They isolated and sequenced these clones which they designated *FPRH1* and *FPRH2* with homology to *huFPR* of 69% and 56%, respectively. *FPRH1* has 98% homology with *FPRL1*. There is an amino acid change in *FPRL1* from Ser^{19} to Thr^{19} and Thr^{265} to an Ala^{265}, as compared to *FPRH1*. In addition, *FPRL1* has an extra Gly at position 264. This would indicate that *FPRL1* and *FPRH1* are allelic variants and that *FPRH2* is probably the *FPRL2* identified by Ye and co-workers and by Murphy and co-workers. The FPR genes cluster at chromosome 19q13.3 (Gerard *et al.*, 1993).

6.2 Cloning of Human FPR (huFPR)

The method chosen to clone the human huFPR gene was a polymerase chain reaction (PCR) procedure using degenerate primers (Saiki *et al.*, 1985). PCR is an *in vitro* method of generating sufficient quantities of DNA for cloning. It allows for the physical separation of any particular sequence of interest from its context, and then provides for an *in vitro* amplification of this sequence which is virtually without limit. It can provide enrichment of a specific DNA fragment by a factor of 10^6-10^8 fold (Saiki *et al.*, 1986). The ability of oligodeoxynucleotides to bind tightly and specifically to their complementary nucleic acid sequences, discriminating between hundreds of thousands of sites, accounts for the success of PCR. The process involves replicating a specific segment of DNA by repetitive cycles of melting the

DNA, annealing a set of primers that flank the DNA fragment to be amplified, and DNA synthesis/extension from these primers with a DNA polymerase. The primers anneal to opposite strands of the target DNA, and are orientated so that DNA synthesis proceeds across the region between the primers. Each cycle of amplification doubles the amount of target DNA synthesised, since the extension products are complementary and capable of annealing to the primers. This results in an exponential production of DNA, (approximately 2^n, where n is the number of cycles). Further, the use of a thermostable polymerase has allowed the process to be automatically cycled without additions of fresh polymerase after each thermal denaturation step (Saiki *et al.*, 1988).

Although PCR is a very powerful and rapid procedure circumventing the need to construct a library, screen it and then identify and clone the gene into a suitable vector, it is prone to two main disadvantages. The first is the infidelity and error rate of the *Taq* polymerase, which is about 1 in 400 bases after 30 cycles. The second is the possibility of DNA contamination in the reaction mixture, particularly if similar sequences of target DNA are used. Due to the possible presence of intron sequences in eukaryotic genomic DNA, another difficulty in PCR cloning may be the length of DNA to be amplified. Reliable PCR can only occur over a length of approximately 3kb.

The success of PCR is dependent on the production of a specific band. Multiple bands due to non-specific priming can effect the subsequent PCR cycles, DNA analysis of the bands, and subcloning of the correct fragment. To reduce this problem, the specificity of the primers to their target sequences should be optimized. Of particular importance is the concentration of both the magnesium ions and the

primers. Decreasing the magnesium ion concentration increases the specificity of annealing. Magnesium ion concentrations at around 1 to 5 mM are normally used. In addition, the primer and nucleotide concentration can be lowered but these tend to reduce the yield. The temperature of annealing provides a cruder method of increasing specificity.

To prevent any primer/DNA complexes which form at low temperatures, and are thus non-specific, from being extended 'hot start' PCR can be used (D'Aquila *et al.*, 1991) (see Section 2.6.7). All primer sets were optimised with respect to primer concentration and especially magnesium ion concentration as this was found to be the most important factor in specificity. Figure 6.1 shows the approximate positions of the primers chosen in relation to the coding region of huFPR.

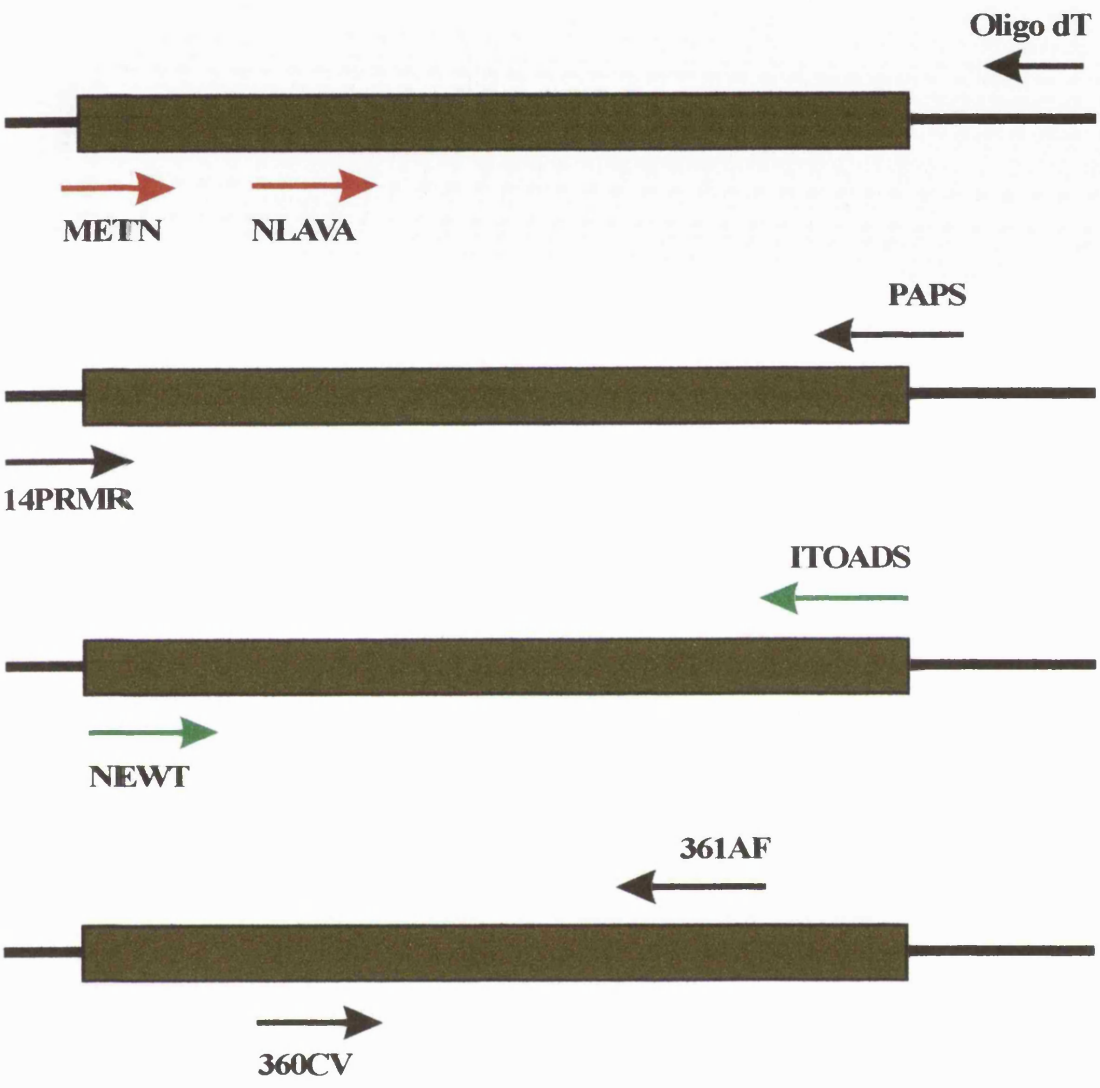

Figure 6.1 The positions of primers used in this study.
The arrows in red represent primers with degeneracies. The arrows in green represent primers with inosine. The arrows in black represent primers with no degeneracies or inosine.

With the availability of the DNA sequence of human FPR it was possible to amplify the gene by PCR. The strategy employed was to make cDNA from differentiated HL-60 messenger RNA using a fifteen base thymidine oligonucleotide (Oligo dT) primer. This was subsequently used as target for a PCR reaction using a primer specific to the 5' end of the huFPR gene *FPR1* and the Oligo dT primer. The final step would be to clone the amplimer obtained and to confirm its identity by DNA sequencing.

6.2.1 cDNA Synthesis

As described in section 3, HL-60 cells express FPR when differentiated to neutrophil-like cells. Total RNA was isolated from both differentiated and non-differentiated HL-60 cells. The non-differentiated RNA was used as a negative control. The total RNA (200ng) was reverse transcribed using Oligo dT. The resultant cDNA was labelled by adding 10% of the total dATP as ^{32}P-dATP. Following the reverse transcriptase step, a sample of the reaction was size-fractionated on a 1.0% w/v agarose gel (Figure 6.2a). Only the samples in lanes 3 and 7 contained reverse transcriptase. Lanes 2 and 6 acted as negative controls. From the agarose gel it is clear that the reverse transcriptase step generated DNA spanning sizes of 0.1 to 4 kb as compared to the negative controls (reverse transcriptase). The ribosomal RNA is clearly visible and indicates that no RNAses were present in the reaction. When this agarose gel was autoradiographed, the incorporation of ^{32}P-dATP, and hence the synthesis of cDNA, could be seen in lanes 3 and 7 (Figure 6.2b). There were equal amounts of total RNA in the reverse transcriptase reactions, but the autoradiograph indicates that much more cDNA has been synthesised from the differentiated RNA than the non-differentiated RNA. This means that a smaller percentage of the total RNA is present as mRNA in non-differentiated cells. Since the transcripts for FPR are known to be 1.6-1.7, 2.3 and

3.1 kb in length (Boulay *et al.*, 1990a) the cDNA produced was of the required length.

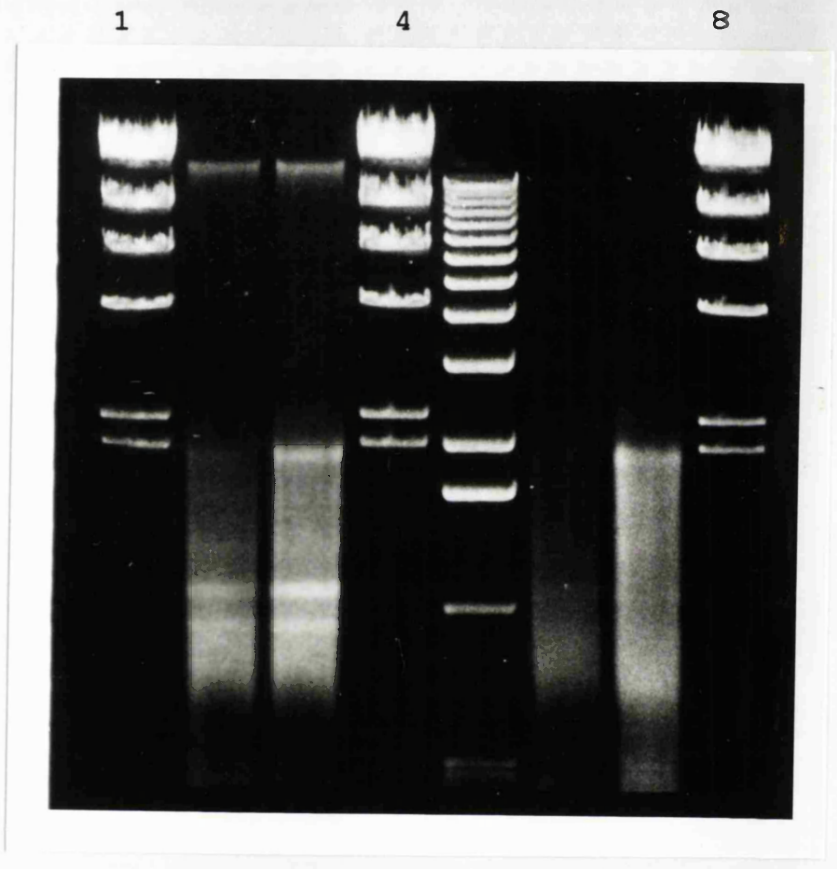

Figure. 6.2 (**A**). cDNA synthesis of non-differentiated and differentiated HL-60 total RNA.
Lane 1, 4, 8 contains λ *Hind* III markers; lane 5 contains λ *Bgl* II. Lanes 2 and 3 contain total RNA from non-differentiated HL-60 cells. Lanes 6 and 7 contain total RNA from differentiated HL-60 cells. Lanes 3 and 7 contain material with reverse transcriptase. All the samples had ^{32}P-dATP. Only lanes 3 and 7 contained reverse transcriptase.

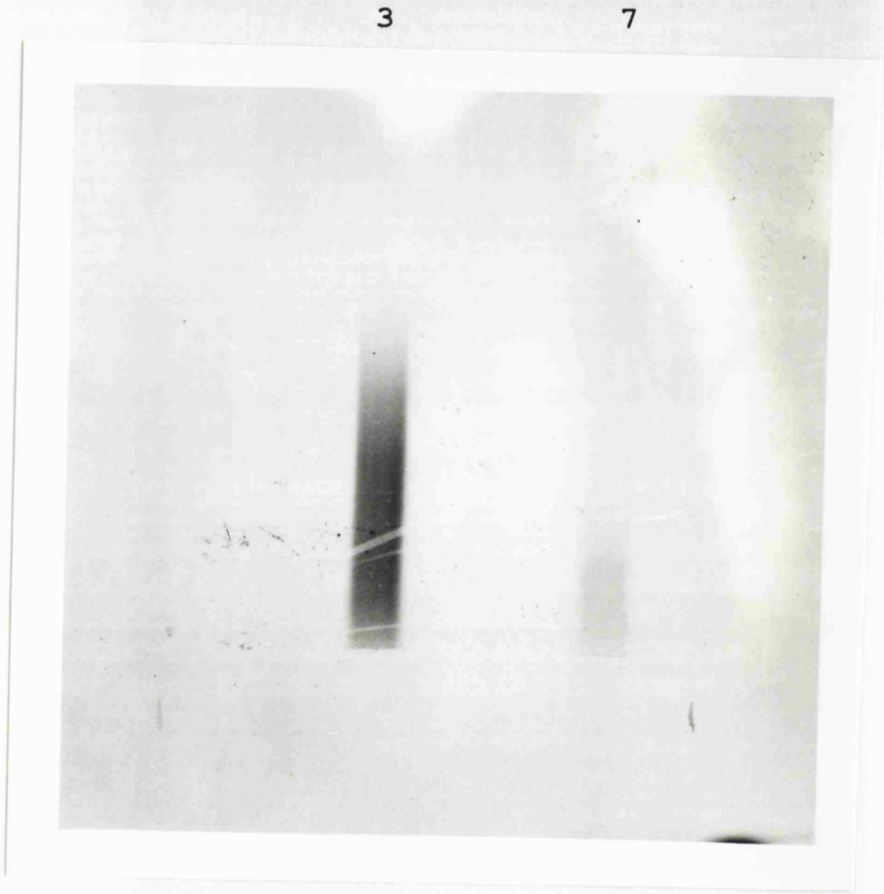

Figure 6.2 (**B**). Autoradiograph of cDNA synthesis of non-differentiated and differentiated HL-60 total RNA. Lanes as in Figure 6.2a: lane 1, 4, 8 contains λ *Hind* III markers; lane 5 contains λ *Bgl* II. Lanes 2 and 3 contain total RNA from non-differentiated HL-60 cells. Lanes 6 and 7 contain total RNA from differentiated HL-60 cells. Lanes 3 and 7 contain material with reverse transcriptase. All the samples had ^{32}P-dATP. Only lanes 3 and 7 contained reverse transcriptase. Film exposed for 48 hours.

6.2.2 Amplification of cDNA with degenerate primers

Primers were designed for the 5' and 3' ends of the coding region. The primer corresponding to the 5' end was designated METN and should anneal to position 1 to 12. Certain degeneracies were added to the oligonucleotide thus allowing for the possibility of using this primer to clone the gene from other species which might have similar DNA sequences as does FPR at their 5' ends. This is based on the fact that the β_2-adrenergic receptor family shows homologous 5' and 3' termini (see Appendix 3). In addition to the METN primer, another primer NLAVA, was designed, which corresponded to the conserved region 210 to 195 (based on sequence alignments between the chemotactic complement C5a receptor and FPR). The NLAVA primer also contained degeneracies as it was to be used for the cloning of other chemotactic receptor genes such as the PAF and LTB_4 receptors. The fifteen base oligonucleotide, Oligo dT was chosen for the 3' primer. This corresponds to the 3' end of all mRNA transcripts having a polyadenylated tail and would also anneal at position 1205 to 1220 of huFPR. Like METN and NLAVA,this could also be used to clone FPRs from other species.

The primer sequences are shown below. The numbers on the right hand-side refer to the position of the nucleotides with respect to the open reading frame. The sense sequence of the Oligo dT primer is shown.

```
huFPR              5' ATG GAG ACA AAT  3'          12
METN (dg = 16)     5' ATG GAR ACN AAY  3'

huFPR              5' AAC CTG GCC GTG GCT  3'     210
NLAVA (dg = 2048)  5' AAY YTN RCN GTN GCN  3'

huFPR              5' AAA AAA AAA AAA AAG  3'     1250
Oligo dT              AAA AAA AAA AAA AAA
```

N = A, C, G or T, R = A or G, Y = C or T. dg = degeneracy.

The cDNA was used as the target material in a PCR amplification using the METN/Oligo dT primer set. Figure 6.3a the shows optimization of the concentration of the METN primer. This was found to be 7.5μM, a higher concentration (approximately 8.3 times) as compared to that of the Oligo dT (0.9μM) primer. This was because of the METN primers degeneracy for, theoretically, only one in sixteen of the species in the METN primer mix would anneal. Two amplicons of 1.0kb and 1.4kb were obtained. The expected amplicon size would be either 1.2kb, if Oligo dT annealed to position 1220, or greater if Oligo dT annealed to any part of the polyadenylated 3' end (Figure 6.16). Therefore, the 1.4kb amplicon was the most promising candidate for huFPR. This amplicon was cut out of the gel, purified (see Section 2.7.1), and reamplified (Figure 6.3b). However, the purified 1.4kb amplicon as target gave two extra amplicons, of 1.0kb and 1.3kb. This indicates that the purified 1.4kb amplicon gives rise to the 1.0 and the 1.3kb amplicons. To identify these amplicons suitable restriction enzymes were chosen based on the analyses of the published huFPR DNA sequence (Figure 6.4a), and a secondary, nested PCR reaction with the NLAVA/Oligo dT primer set was performed (Figure 6.4b). Figure 6.4a shows fragments generated by the restriction enzymes used to digest the DNA. Three endonucleases were selected to map the amplicons: *Rsa* I, *Pvu* II and *Bcl* I. *Rsa* I should give three fragments of 224, 276 and 550 bp. *Pvu* II should give two fragments of 260 and 881 bp. *Bcl* I should give two fragments of 424 and 650 bp. It is clear that the 1.0kb amplicon has not been cut. The 1.3 kb amplicon has been cut to give fragments of 1.0kb with *Pvu* II, and at least four fragments with *Bcl* I. *Rsa* I did not cut any of the amplicons. *Bcl* I was the only enzyme to cut the 1.4kb amplicon, giving a doublet of 750 and 650bp.

To further confirm the identity of both the 1.4 and 1.0kb amplicons from the METN/Oligo dT primer set a nested PCR with the NLAVA/Oligo dT primer set was carried out (Figure 6.4b). As can be seen in lane 1 the NLAVA/Oligo dT secondary PCR produced a number of amplicons. The amplicons of around 900bp (with the 1.4kb as the target DNA) would be expected if the Oligo dT was annealing to different parts of the polyadenylated tail. If the Oligo dT annealed at position 1220 then an 870bp amplicon would be produced. This is clearly seen in lane 1. Extra bands are visible, of around 300bp, which may be due to non-specific annealing of the primers. As a control the 1.4kb amplicon was reamplified with the original METN/Oligo dT primer set (lane 3). This reaction resulted in two bands (1.4 and 1.0kb) instead of the expected, original 1.4kb amplicon. This indicates that there may be internal 'METN' and Oligo dT priming sites on the 1.4kb amplicon. The 1.3kb amplicon (see Figure 6.3b: lane 1) does not appear when reamplified with the METN/Oligo dT primers, or with NLAVA/Oligo dT. This indicates that it was not a true amplicon but an artifact of PCR, possibly a single-strand molecule of the 1.4kb amplicon. Various modifications to the PCR protocol were carried out to increase the specificity (such as lowering the magnesium, primer and dNTP concentration, raising annealing temperatures, and lowering cycle times). However, none of these could overcome the inherent problem of the degeneracy and insufficient length of the primers. To summarise, the restriction digests produced ambiguous results, which may be due to partial cutting or that the amplicon was not huFPR. Although the nested PCR with the NLAVA/Oligo dT primers gave a main amplicon of 870bp (which was the expected size if the 1.4kb amplicons was the FPR), it also gave several minor amplicons.

To detect and clone other chemoattractant receptors, a PCR amplification was carried out with NLAVA/Oligo dT using differentiated HL-60 cDNA as target (Figure 6.5). The main amplicon obtained (1.7kb) was cloned and sequenced. A search of the EMBL database failed to identify any homologuess.

Since both the DNA endonuclease digests, and the nested PCR reactions were inconclusive, I proceeded to subclone, and sequence the 1.4 and 1.0 kb amplicons. Neither the 1.0, nor the 1.4 kb amplicon matched the FPR sequence. In fact a search of the EMBL DNA database failed to find any homologies to known sequences.

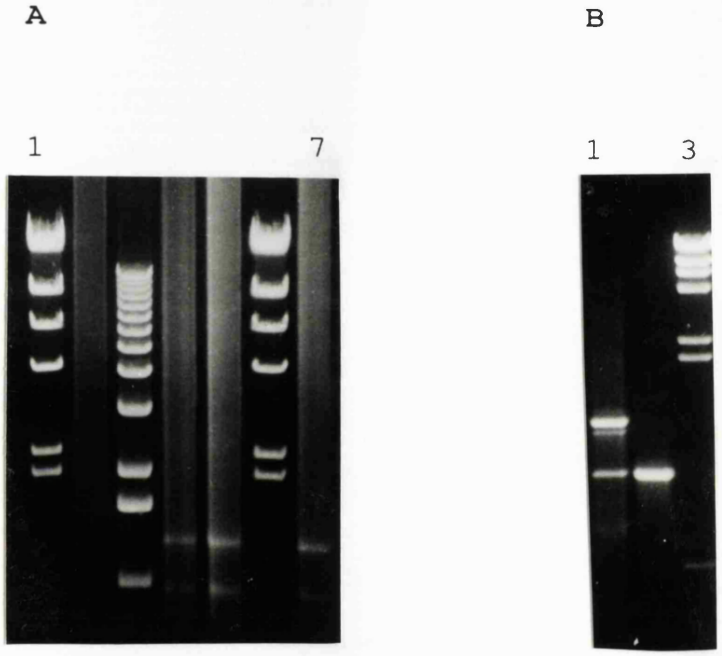

Figure 6.3 PCR amplification of HL-60 cDNA.
(**A**). Lanes 1 and 6 contains λ *Hind* III markers; lane 3 contains λ *Bgl* II. Lanes 2, 4, 5, 6, contain cDNA which has been PCR amplified using METN/Oligo dT (the concentration of Oligo dT was 0.9μM while METN was 0.9, 1.2, 7.5 and 14.0 μM). Lane 8 contains no cDNA. The bands were purified and reamplified.
(**B**). Lane 3 contains λ *Hind* III markers. Lanes 1 and 2 contain the reamplified products from the 1.4 and 1.0 kb products and lane 1 contains no DNA.

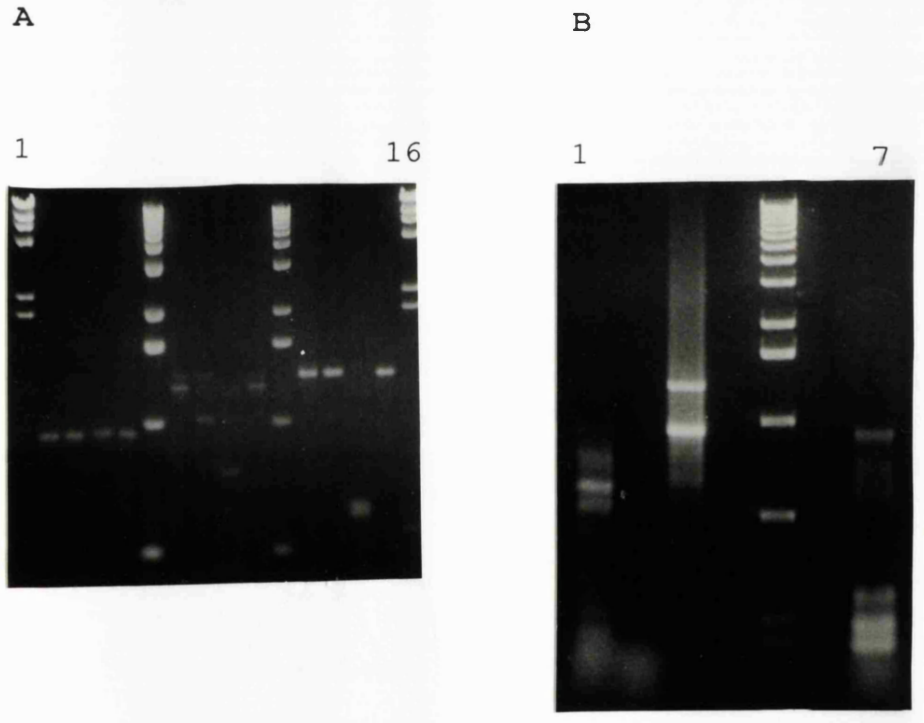

Figure 6.4 Verification of amplicon identity; restriction mapping and secondary PCR.
(**A**). The purified material from Figure 6.3b was cut with a variety of endonucleases. Lanes 1 and 16 contain λ *Hind* III markers; lane 6 and 11 contain λ *Bgl* II. Lanes 2-5 contain the 1.0kb fragment (order of digests: *Rsa* I, *Pvu* II, Bcl I, Control). Lanes 7-10 contain the 1.3kb fragment (order of digests: *Rsa* I, *Pvu* II, Bcl I, Control). Lanes 12-15 contain the 1.4kb fragment (order of digests: *Rsa* I, *Pvu* II, Bcl I, Control).
(**B**). Nested PCR with NLAVA using METN produced DNA as template. Lane 5 contains λ *Hind* III markers. Lanes 1 and 3 contain the 1.4kb fragment as template with NLAVA/Oligo dT and METN/Oligo dT primers respectively. Lanes 2 and 4 contain NLAVA/Oligo dT and METN/Oligo dT respectively but no target. Lanes 6 and 7 contain the 1.0kb fragment as template with NLAVA/Oligo dT and METN/Oligo dT primers respectively. 9μM NLAVA, 7.5μM METN and 0.9μM Oligo dT were used.

Figure 6.5 PCR of HL-60 cDNA with the internal primer NLAVA.
Lane 2 contains λ *Hind* III markers. Lanes 1 and 3 contains NLAVA/Oligo dT (the concentration of Oligo dT was 0.9μM and NLAVA 9.0 μM). Lane 3 contains cDNA from differentiated HL-60 cells. Lane 1 contains no cDNA.

In conclusion the probable reasons that human FPR (huFPR) was not succesfully cloned were the length and the high degeneracy of the primers. No specificity was conferred by the Oligo dT primer, and the METN primer was only twelve bases long of which the first codon is ATG, the most common of the two start codons. Out of the rest of the nine bases two were degenerate for two bases while a third was degenerate for all four bases. Because of the degeneracy, higher primer concentrations were needed as only one in sixteen of the primer species could anneal. However, this also increases the potential for non-specific binding, and fifteen of the primer species could anneal to other sequences.

Because the METN primer is only twelve bases long, conditions of low specificity were needed to obtain a product. For example, since there was only a degeneracy of two in the first six bases, half the species in the primer mix could anneal to the first six bases of the target site. Thus, these primers could act as competitive inhibitors to the correct primer species. In summary, the degenerate primers because of their high concentration, would produce more non-specific bands and would inhibit the production of the correct amplicon by blocking access to it by the 'correct' primers. This problem of degeneracy would also apply for the NLAVA primer.

The problems caused by degeneracy and insufficient primer length were not known at the time the primers were made. The degeneracies were designed into the primer to allow the cloning of other FPRs (METN) and other chemotactic receptors (NLAVA). It would have been better to use inosine at points of degeneracy as this can anneal to all the nucleotides found in DNA. This would mean that all the species in the primer mix could anneal to the target sequence.

6.2.3 Amplification of huFPR with specific primers

Two new sets of primers were designed, with no degeneracies, that corresponded to the published human FPR sequence. The aim was to use these primers to amplify the coding region of FPR and then to use this clone to screen a genomic library. It also offered the possibility of directly amplifying the murine gene if the primers corresponded to conserved regions within this gene. The primers were designed to anneal to positions -14 to 9 (14PRMR) and to 1121 to 1065 (PAPS) (see Figure 6.16). This data is shown below. The numbers on the right hand-side refer to the position of the nucleotides with respect to the open reading frame. The sense sequence of the PAPS primer is shown.

```
huFPR          5' CCA GGA GCA GAC AAG ATG GAG ACA 3'      9
14PRMR         5' CCA GGA GCA GAC AAG ATG GAG ACA 3'      9

huFPR          5' CAG GCA AAG TGA GGA GGG AGC TGG 3'   1065
PAPS              CAG GCA AAG TGA GGA GGG AGC TGG
```

The PCR was carried out with human genomic DNA as target at various magnesium concentrations (Figure 6.6). This resulted in a 1.0kb amplicon which, when subcloned and sequenced, matched the coding region of the 1.35kb transcript fMLP-R26, as published by Boulay and co-workers (Boulay *et al.*, 1990a). The entire clone was sequenced and shown to contain no introns. This was as expected for a G protein coupled receptor (GPCR).

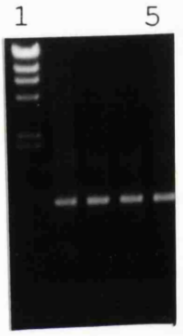

Figure 6.6 Optimization of PCR with 14PRMR/PAPS using human genomic DNA as target.
Lane 1 contains λ *Hind* III markers. Lanes 2-5 contain human genomic DNA. PCR was carried out using 14PRMR/PAPS. Lane 1 contains no genomic DNA.

6.3 Cloning of muFPR

In sections 3 and 4 I have shown that the murine model of FPR (murine pluripotent stem cells - FDCP) expressed a formyl peptide receptor. To further characterise the receptor at the structural level, it was necessary to clone and sequence the gene for this receptor. This would also allow the study of gene expression during cell differentiation. A structural analysis of the translated sequence could be made by alignment to the human and rabbit FPRs. This would highlight conserved regions that may be important in structure and/or function.

PCR and the screening of a genomic library (see section 5) was used to attempt to clone the muFPR gene. The primers used to succesfully clone the huFPR were used to PCR murine genomic DNA. The putative G protein coupled receptors are reported to have no introns, or if they do, they would be relatively small and outside the coding region (Libert *et al.*, 1989). It should therefore be possible to PCR amplify the whole open reading frame of muFPR from genomic DNA.

6.3.1. PCR with a variety of Primers - 14PRMR, NLAVA, PAPS and Oligo dT

Using murine genomic DNA as target, the PCR protocol was optimized in various magnesium concentrations (Figure 6.7). This resulted in a 1.0kb amplicon which, when analysed by sequencing, was shown to have no homology to huFPR or rabFPR. In fact, a comparison with the EMBL DNA database found no sequences of significant homology.

Figure 6.7 Optimization of $MgCl_2$ in PCR with 14PRMR/PAPS using murine genomic DNA as target.
Lane 1 contains λ *Hind* III markers. Lanes 2-5 contain murine genomic DNA. PCR was carried out using 14PRMR/PAPS. Lane 6 contains no genomic DNA.

The possibility existed that one of the primers used was annealing to the correct sequence. Therefore a different combination of the primers available (NLAVA, 14PRMR, Oligo dT and PAPS) was used in the PCR. Amplification was carried out using different sets of primers in the following combinations; NLAVA/Oligo dT, NLAVA/PAPS, NLAVA/PAPS and 14PRMR/PAPS. This strategy was used with murine genomic DNA and with huFPR acting as a positive control (Figure 6.8). Lanes 1 through to 4 contain murine genomic DNA as target. No bands were produced with these primers. The smear in lanes 1 and 2 is in the correct size range expected when using NLAVA as the 5' end primer (i.e 750bp with NLAVA/PAPS and 870bp for NLAVA/Oligo dT). With NLAVA/PAPS and 14PRMR/PAPS the DNA smear was spread over a larger size range. The PCR, with huFPR as target, gave amplicons only with NLAVA/PAPS and 14PRMR/PAPS. Since in the presence of a high concentration of huFPR the Oligo dT failed to give the correct amplicon, the possibility of it doing so from genomic DNA, where it is at a relative abundance of one part in a million, is negligible. Therefore, using Oligo dT for the amplification of muFPR was abandoned. The PCR was also optimised with respect to NLAVA/PAPS and 14PRMR/PAPS but no amplicon could be obtained (data not shown).

In conclusion, from the absence of a PCR product the sequence of murine FPR must be different to that of huFPR at the primer sites chosen (the 5' and the 3' ends of the ORF). There is also the possiblity that cloning failed because of the presence of introns within the coding region, but this is unlikely (Libert *et al.*, 1989).

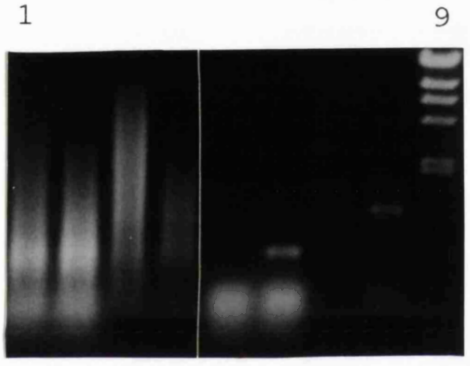

Figure 6.8 PCR with a variety of primers with the human and murine genomic DNA as target.
Lane 9 contains λ *Hind* III markers. Lanes 1 and 5 contain primer NLAVA/Oligo dT, lanes 2 and 6 contain NLAVA/PAPS, lanes 3 and 7 contain 14PRMR/Oligo dT and lanes 4 and 8 contain 14PRMR and PAPS. Lanes 11, 12, 13 and 14 contain NLAVA/Oligo dT, NLAVA/PAPS, 14PRMR/Oligo dT and 14PRMR and PAPS respectively but no DNA. Lanes 1-4 and 5-8 contain murine genomic DNA and *huFPR* respectively.

6.3.2 PCR withNEWT/ITOADS

New primers were designed taking into account the data from previous PCR experiments with METN and NLAVA (see Section 6.2.2). That is, they were designed with inosine at positions of redundancy and their lengths increased. The primers corresponded to the 5' and 3' ends of the coding region, to positions 1 to 26 (NEWT) and to 1053 to 1020 (ITOADS).

This data is shown below. The numbers on the right hand-side refer to the position of the nucleotides with respect to the open reading frame. The sense sequence of the ITOADS primer is shown.

```
huFPR 5' ATG GAG ACA AAT TCC TCT CTC CCC AC 3'              26
NEWT  5' ATG GAI ACI AAI TCI TCI CTI ACI AC 3'

huFPR 5' CCT TCT GCA GAG GTG GCG TTA CAG GCA AAG TGA 3'   1053
ITOADS   CCI TCI GCI GAI GTI GII TTI CAI GCI AAI TGA
```

These primers were used in conjunction with 14PRMR and PAPS. Figure 6.9 shows the optimization of these primers using human genomic DNA as target. Lanes 1 to 4 contain 14PRMR/PAPS, lanes 5-8 contain 14PRMR/ITOADS, lanes 10-13 contain NEWT/ITOADS and lanes 15-17 contain NEWT/PAPS. Each set of primers was titrated with 4, 3, 2 and 1 mM magnesium. As the 1mM magnesium gave minimal non-specific products it was used for further PCR as it. Lanes 18, 19 and 20 contain 14PRMR/PAPS, 14PRMR/ITOADS, NEWT/ITOADS, respectively but no DNA. The PCRs containing the new primers gave less non-specific bands, despite the presence of inosine, indicating that longer primers are better. All four 1.0kb amplicons obtained with each primer set were cloned and sequenced (data not shown). All the amplicons were identified as huFPR (fMLP-R26). Therefore, these

primers (NEWT and ITOADS) specifically amplify huFPR and if the murine gene is conserved at the same region encompassed by the primers, it should also be amplified.

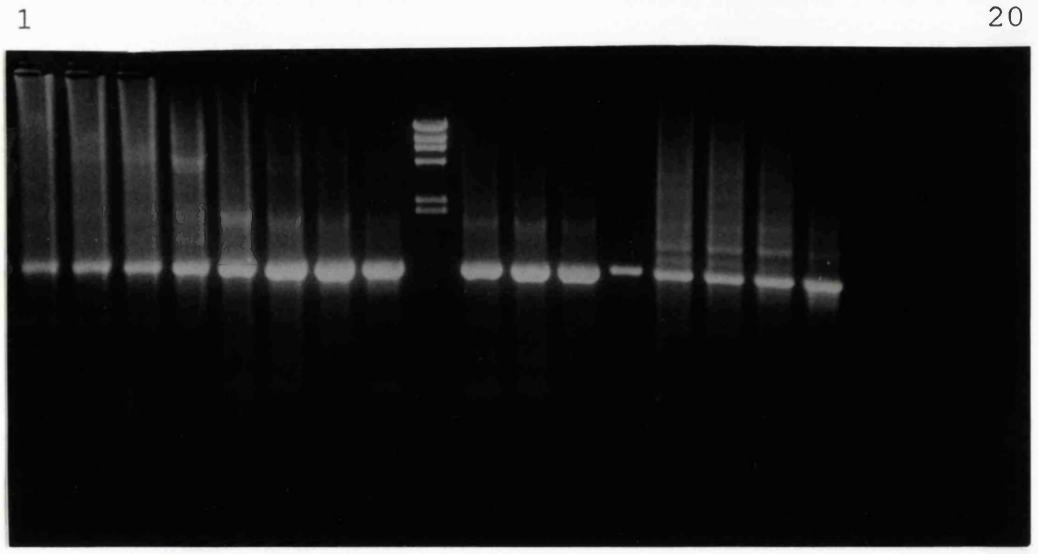

Figure 6.9 Optimization of PCR with a variety of primers using human genomic DNA as target.
Lane 9 contain λ *Hind* III markers. Lanes 1-4 contain 14PRMR/PAPS, lanes 5-8 contain 14PRMR/ITOADS, Lanes 10-13 contain NEWT/ITOADS and lanes 15-17 contain NEWT/PAPS. Each set of primers was titrated with 4, 3, 2 and 1 mM $MgCl_2$. The target was human genomic DNA. Lanes 18, 19 and 20 contain 14PRMR/PAPS, 14PRMR/ITOADS, NEWT/ITOADS respectively but no DNA.

Using murine genomic DNA and the sets of primers described in Figure 6.9, a PCR reaction was carried out (Figure 6.10). PCR with the primer 14PRMR in the primer set produced many non-specific bands even with human genomic DNA. NEWT/ITOADS gave a single band of 1.0kb with human DNA (lane 15). NEWT/PAPS produced many non-specific bands with human DNA (lane 16). NEWT/ITOADS produced a weak band only with the higher concentration of murine DNA (lane 3). NEWT/PAPS produced a main band of 1.0kb with murine DNA as well as several longer but weaker bands (lane 4 and 10). Figure 6.11 shows the optimization of PCR with NEWT/ITOADS (lanes 1, 2, 3 and 5) and NEWT/PAPS (lanes 6, 7, 8 and 10). Each set of primers was titrated with 500, 400, 300 and 200ng of murine genomic DNA. Lanes 11 and 12 contained NEWT/ITOADS and NEWT/PAPS, respectively but no DNA. PCR with 14PRMR in the primer set are not shown as these did not generate any specific bands with murine DNA as target. The main bands (0.6, 1.1, and 1.9 kb) with NEWT/PAPS were cloned and sequenced, but did not match any of the known FPRs. Also, bands 0.8, 1.1 and 1.4 kb from NEWT/ITOADS were purified and cloned (Figure 6.12). Figure 6.12 shows the clones obtained after ligation into pUC 19 and digestion with *Eco* RI and *Hind* III (which would drop out the ligated fragment). Lanes 1-4 and 6-7 are clones from the NEWT/PAPS PCR productligation and two types of clones can be seen (lanes 1 and 2 of 1.1 and 0.2 kb respectively). Lanes 8-9 and 11-14 were clones from the NEWT/ITOADS PCR products ligation and two types of clones can be seen (lanes 9 and 13 of 1.1 and 1.4 kb respectively). These clones were sequenced (data not shown) and found not to match any known sequences in the EMBL database.

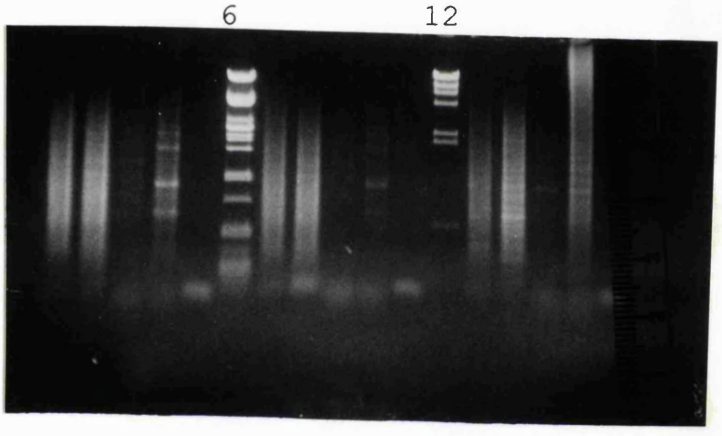

Figure 6.10 PCR with a variety of primers using human and murine genomic DNA as target.
Lanes 6 and 12 contain λ *Hind* III/*Eco* RI and λ *Hind* III markers, respectively. Lanes 1, 7 and 13 contained 14PRMR/PAPS. Lanes 2, 8 and 14 contained 14PRMR/ITOADS. Lanes 3, 9 and 15 contain NEWT/ITOADS. Lanes 4, 10 and 16 contain NEWT/PAPS. Lanes 5, 11 and 17 contain 14PRMR/PAPS. Lanes 1-5 contain 500ng murine genomic DNA as template. Lanes 7-11 contain 500ng murine genomic DNA as template. Lanes 17 contain 100ng human genomic DNA as template. Lanes 18, 19 and 20 contain 14PRMR/PAPS, 14PRMR/ITOADS, NEWT/ITOADS, respectively but no DNA.

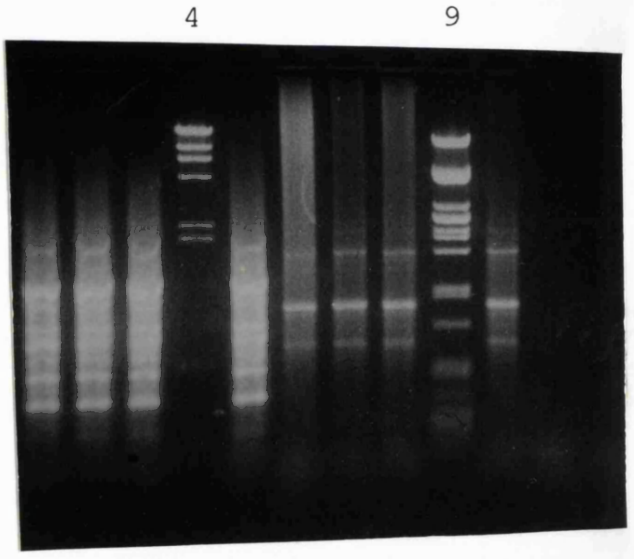

Figure 6.11 PCR with a variety of primers using murine genomic DNA as target.
Lanes 4 and 9 contain λ *Hind* III and λ *Hind* III/*Eco* RI markers, respectovely. Lanes 1, 2, 3 and 5 NEWT/ITOADS, lanes 6, 7, 8 and 10 contain NEWT/PAPS. Each set of primers was titrated with 500, 400, 300 and 200ng of murine genomic DNA. Lanes 11 and 12 contain NEWT/ITOADS and NEWT/PAPS respectively but no DNA.

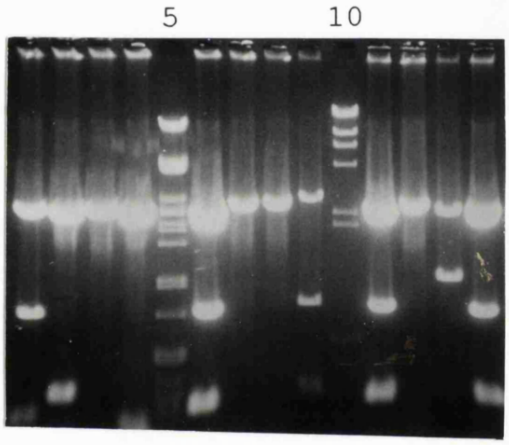

Figure 6.12 Cloning of the NEWT/ITOADS and NEWT/PAPS amplicons. Lanes 5 and 10 contain λ *Hind* III/*Eco* RI markers and λ *Hind* III, respectively. Lanes 1-4 are plasmid digests of the ligation with the 0.8kb amplicon from NEWT/ITOADS. Lanes 6-9 are plasmid digests of the ligation with the 0.8kb amplicon from NEWT/PAPS. Lanes 11-14 are plasmid digests of the ligation with the 1.0kb amplicon from NEWT/ITOADS. The plasmids were endonucleased with *Eco* RI and *Hind* III.

6.3.3 PCR amplification of muFPR with 360CV and 361AF Primers

At this point in the project the sequence of muFPR became available. Six genes had been identified from screening a genomic library. Of these six only one was published (Gao and Murphy, 1993). This had 76% homology with huFPR in the open reading frame and was designated muFPR. Of the other five the homology was from 54% to 67%. An alignment of the known FPR (huFPR, FPRL1, FPRH1, FPRH2, rabFPR and muFPR) sequences was carried out and two conserved regions were used to design new primers: 360CV and 361AF. These primers were designed to amplify all six of the putative murine FPR genes identified by Murphy and co-workers (Gao and Murphy, 1993). This would allow us to assay the RNA from our model system (Sections 3 and 4) and thus identify the gene which was transcribed and probably expressed by murine neutrophils. The amplicon expected of 500bp could be easily cloned and sequenced. The primers corresponded to the following positions within the coding region of muFPR; 372 to 396 (360CV) and to 893 to 869 (361AF). The 3' end of the 360CV primer corresponds to a highly conserved amino acid, tryptophan, which is encoded by a single codon.

The less conserved (as compared to the area around the primers) regions following the 360CV primer and the 361AF primer are boxed. These regions would be easily distinguishable after PCR amplification, cloning and sequencing. By PCR amplifying murine genomic DNA the five murine genes not yet published would be easy to identify (by a comparison of the boxed areas), if they shared the same conserved regions as the other FPRs. This data is shown below. The numbers on the right hand-side refer to the position of the amino acids or to the position of the nucleotides with respect to the open reading frame. The underlined amino acids

correspond to the primer sequence. The sense sequence of the 361AF primer is shown. The boxed regions indicate sequences that are poorly conserved.

Primer 360CV

```
                                                    ┌──────────────────────┐
huFPR  VFLIALIALDRCVCVLHPVWTQNHRTVSLAKKVIIGPW VMALLLTLPVIIRVTTVPGK   168
FPRL1  VFLIGFIALDRCICVLHPVWAQNHRTVSLAMKVIVGPW ILALVLTLPVFLFLTTVTIP   168
FPRH1  VFLIGFIALDRCICVLHPVWAQNHRTVSLAMKVIVGPW ILALVLTLPVFLFLTTVTIP   168
FPRH2  VYLITIIALDRCICVLHPAWAQNHRTMSLAKRVMTGLW IFTIVLTLPNFIFWTTISTT   168
rabFPR VFLIALIALDRCICVLHPVWAQNHRNVSLAKKVIVGPW ICALLLTLPVIIRVTTLSHP   168
muFPR  VFLIALIALDRCICVLHPVWAQNHRTVSLAKKVIIVPW ICAFLLTLPVIIRLTTVPNS   176


huFPR              5' GTT TGC GTC CTG CAT CCA GTC TGG 3'   396
fPR2A              5' ATT TGT GTC CTG CAT CCA GTC TGG 3'   396
rabFPR             5' ATC TGT GTC CTG CAC CCA GTC TGG 3'   396
muFPR              5' ATT TGT GTT CTG CAT CCA GTC TGG 3'   420
360CV              5' ATT TGT GTC CTG CAT CCA GTC TGG 3'

                       I   C   V   L   H   P   V   W
          Amino Acid Sequence
```

Primer 361AF

```
                ┌──────────────────────────────────┐
huFPR  AAAFFLCW SPYQVVALIATVRIRELLQGMYKE-IGIAVDV TSALAFFNSCLNPMLYVFM 304
FPRL1  VASFFICW FPFQLVALLGTVWLKEMLFYGKYKIIDILVNP TSSLAFFNSCLNPMLYVFV 305
FPRH1  VASFFICW FPFQLVALL-AVWLKEMLFYGKYKIIDILVNP TSSLAFFNSCLNPMLYVFV 304
FPRH2  VASFFICW FPYELIGILMAVWLKEMLLNGKYKIILVLINP TSSLAFFNSCLNPILYVFM 305
rabFPR VASFLLCW SPYQIAALIATVRIRELLLGMGKDLRI-VLDV TSFVAFFNSCLNPMLYVFM 306
muFPR  VAAFFLCW CPFQVVALISTIQVRERLKNMTPGIVT-ALKI TSPLAFFNSCLNPMLYVFM 315


huFPR              5' TTC TTC AAC AGC TGC CTC AAC CCC 3'   893
fPR2A              5' TTC TTC AAC AGC TGC CTC AAC CCC 3'   896
rabFPR             5' TTC TTC AAC AGC TGC CTC AAC CCC 3'   902
muFPR              5' TTC TTC AAC AGC TGC CTC AAT CCA 3'   926
361AF                 TTC TTC AAC AGC TGC CTC AAC CC

                       F   F   N   S   C   L   N   P
Amino Acid Sequence
```

Murine genomic DNA was used as target in PCR amplification with the primers 360CV and 361AF. Figure 6.13 shows the optimization of the magnesium concentration using murine genomic DNA. Lanes 1, 2, 3, 4 and 6 contain magnesium of 5, 4, 3, 2 and 1 mM, respectively. The size of the amplicon (500bp) was as expected indicating that no introns are present within this part of the gene and if present are very short less than 50bp. To identify the other genes, the

products of three PCR reactions were subcloned and ten recombinant clones were sequenced. The pooling of three PCR reactions prevents the biasing of the amplicon mix which can take place in some PCR reactions. Figure 6.14 shows an example of the isolation of clones containing the 500bp amplicon. The amplicons were ligated into pUC19 and the insert was characterized by *Eco* RI and *Hind* III endonuclease cleavage. Ten clones were sequenced to determine the population of sequences amplified by PCR. All ten clones sequenced were identical and were identified as the published muFPR (Gao and Murphy, 1993) which has 78% homology to huFPR.

In conclusion, the fact that the PCR did not amplify the other five isoforms of muFPR indicates that they have different sequences in the primer regions chosen. There is also the possibility that the other five may contain introns within the amplification region which would prevent PCR amplification under the conditions used in this study.

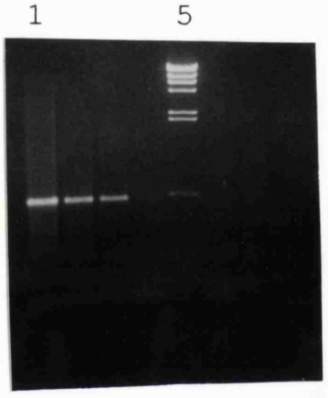

Figure 6.13 Optimization of the $MgCl_2$ concentration with 361CV and 360AF primers.
Lane 5 contains λ *Hind* III markers. Lanes 1-4 and 6 contain a titration of magnesium of 5, 4, 3, 2 and 1 mM. The target was murine genomic DNA. Lanes 7 and 8 contain magnesium of 5 and 3 mM but no DNA.

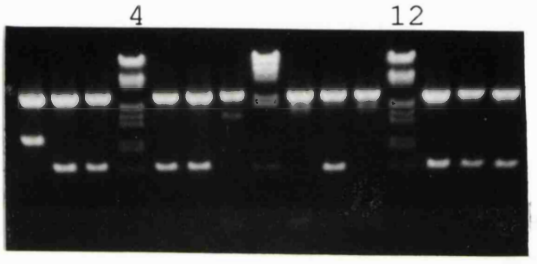

Figure 6.14 Cloning of the 361CV and 360AF amplicons.
Lanes 4 and 12 contain λ *Hind* III/*Eco* RI markers and lane 8 contains λ *Hind* III markers. The products of three PCR reactions were subcloned and ten positive clones were sequenced. The plasmids were endonucleased with *Eco* RI and *Hind* III.

6.4 Transcription studies of muFPR

In sections 3 and 4 I demonstrated through ligand binding assays that murine pluripotent stem cells (FDCP) differentiated to neutrophils express a receptor which mediates cell responses to N-formyl peptides. By determining which of the six putative genes is expressed I can relate any kinetic differences with other FPRs to sequence differences. This may indicate the regions responsible for different activities of the receptor. In addition determining when the gene is transcribed and then translated tells us which RNA transcript is used in FDCP cells. It also allows us to design new experiments to understand other aspects of the action of FPRs upon stimulation with N-formyl peptides, such as identifying which G protein the receptor is coupled to and which other proteins may be expressed at the same time and are involved in the functioning of a neutrophil as regards to FPR.

To determine which one of the six putative isoforms of murine FPR were transcribed, I undertook RNA studies using primers 360CV and 361AF. Even though the other murine FPRs were not amplified by these primers when genomic DNA was used as target (Section 6.3) it should still be possible to determine if the putative *muFPR* gene is transcribed. Reverse transcriptase PCR was carried out on total RNA isolated from differentiating FDCP cells at various times (Figure 6.15). Lanes 1-7 and 9 contain the amplicon obtained from murine total RNA (200ng) which has been reverse transcribed and then PCR amplified from day 0 to day 7 cells; lanes 10 and 15 from 200ng of total RNA from undifferentiated FDCP cells and WEHI-3b cells, respectively. Lane 16 (positive control) was the PCR product of genomic DNA from undifferentiated FDCP cells. A PCR product was visualised after 2 days of differentiation with maximum levels between 3 and 6 days. On the 7th day no PCR

product was visualised (Figure 6.15). This data shows that after 48 hours of cytokine-stimulated differentiation the cells are beginning to transcribe the muFPR gene. No PCR product from the undifferentiated FDCP and WEHI-3b cells was seen.

WEHI-3b cells did not yield a PCR product although they are a monocyte derived cell line and may express an FPR. However, In section 4 I showed that WEHI-3b cells expressed a receptor with either a lower affinity or lower receptor numbers than that found in differentiated FDCP cells. As shown in section 6, when using WEHI-3b genomic DNA for southern blots and screening with the whole huFPR gene, a strongly hybridizing band was seen which was probably due to RNA. Therefore, two separate pieces of evidence indicate that WEHI-3b cells express FPR at the early part of their life cycle (see Section 4). The fact that RT-PCR did not give an amplicon indicates that the gene expressed in these cells is probably another isoform of muFPR not yet published.

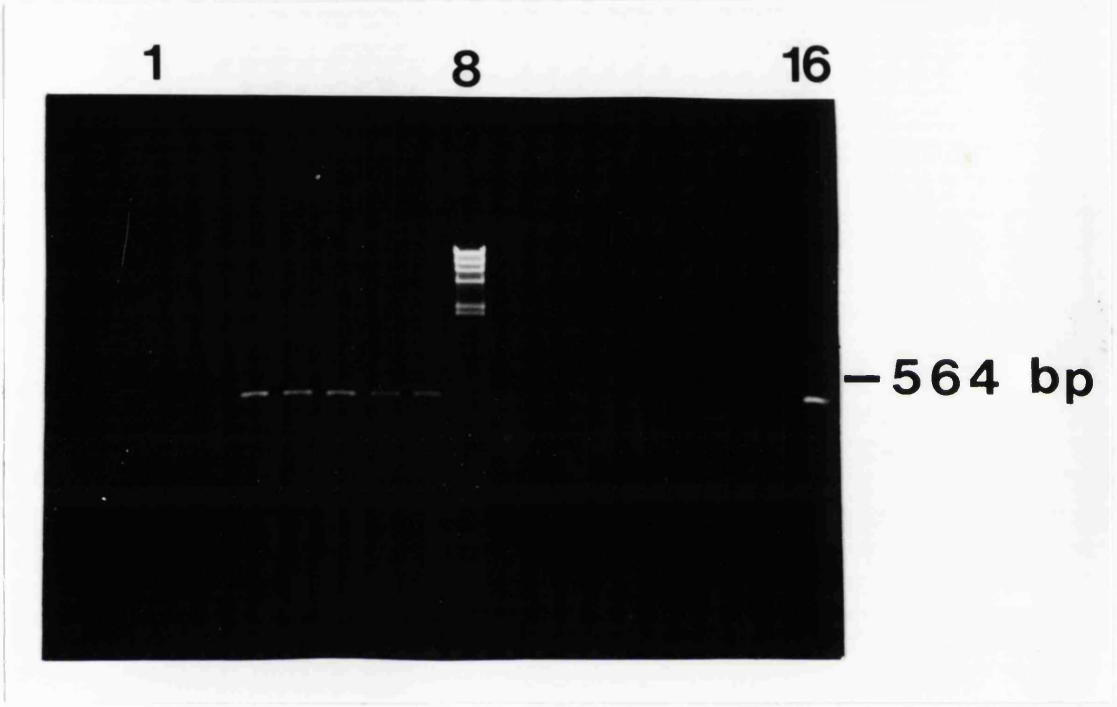

Figure 6.15 Detection of the *muFPR* transcript by RT-PCR.
Lane8 contains λ *Hind* III markers. All lanes contain 1/10th of the PCR reaction. Lanes 1-7 and 9 contain the reaction products of 50ng total RNA isolated from differentiating FDCP cells from day 0 to day 7; lanes 10 and 15 from 200ng of total RNA from undifferentiated FDCP cells and WEHI-3b cells, respectively. Lane 11 had only amplimer 361CV, lane 12 had only amplimer 360AF, and lane 14 had neither amplimer with 200ng of day 5 total RNA. Lane 16 (positive control) is the PCR product of genomic DNA from FDCP cells. Lane 8 contains λ *Hind* III markers.

```
huFPR  5' CCA GGA GCA GAC AAG ATG GAG ACA AAT TCC TCT CTC CCC AC 3'26
FPRL1  5' CAG GTG CTG GCA AAG ATG GAA ACC AAC TTC TCC ACT CCT CT 3'26
rabFPR 5' CCA GGT GCG GGC AAG ATG GAC AGC AAT GCC TCT CTT CCC CT 3'26
muFPR  5' CTA GGA GTC TAC AAG ATG GAC ACC AAC ATG TCT CTC CTC AT 3'26

METN                          5'ATG GAR ACN AAY 3'
14PRMR  5'CCA GGA GCA GAC AAG ATG GAG ACA 3'
NEWT                          5'ATG GAI ACI AAI TCI TCI CTI ACI AC 3'


huFPR  5' AAC CTG GCC GTG GCT GAC TTC 3'    216
FPRL1  5' AAC CTG GCC CTG GCT GAC TTT 3'    216
rabFPR 5' AAC CTG GCC TTG GCC GAT TTC 3'    216
muFPR  5' AAC TTG GCC ATT GCT GAC TTT 3'    240

NLAVA  5' AAY YTN RCN GTN GCN 3'


huFPR  5' TTA CCT TCT GCA GAG GTG GAG TTA CAG GCA AAG TGA GGA 3' 1056
FPRL1  5' TCA CCT CCT GCA GAG ACT GAG TTA CAG GCA ATG TGA GGA 3' 1059
rabFPR 5' TCA GCG CCA GCA GAG GCT GAG TTG CAG GCG ATA TGA GCA 3' 1062
muFPR  5' ACT TCC CTT TCT GAA AAC ACT TTA AAT GCA ATG TAA AGA 3' 1098

PAPS                        CAG GCA AAG TGA GGA GGG AGC TGG
ITOADS     TTI CCI TCI GCI GAI GII GII TTI CAI GCI AAI TGA


huFPR              5' GTT TGC GTC CTG CAT CCA GTC TGG 3'    396
FPRL1              5' ATT TGT GTC CTG CAT CCA GTC TGG 3'    396
rabFPR             5' ATC TGT GTC CTG CAC CCA GTC TGG 3'    396
muFPR              5' ATT TGT GTT CTG CAT CCA GTC TGG 3'    420

360CV               5'ATT TGT GTC CTG CAT CCA GTC TGG 3'


huFPR              5' TTC TTC AAC AGC TGC CTC AAC CCC 3'    893
FPRL1              5' TTC TTC AAC AGC TGC CTC AAC CCC 3'    896
rabFPR             5' TTC TTC AAC AGC TGC CTC AAC CCC 3'    902
muFPR              5' TTC TTC AAC AGC TGC CTC AAT CCA 3'    926

361AF              5'TTC TTC AAC AGC TGC CTC AAC CC 3'
```

N = A, C, G or T, R = A or G, Y = C or T.

Figure 6.16 A comparison of the primers used and their annealing sites. The numbers on the right hand side refer to the sequence relative to the open reading frame. fMLP-R98 and fMLP-R26 are very close isoforms with fMLP-R26 appearing to be the most abundant transcript of huFPR (Boulay *et al.*, 1990). FPRL1 codes for another human FPR which is 69% identical to huFPR (Murphy *et al.*, 1992). rabFPR is the only rabbit FPR to be sequenced (Ye *et al.*, 1992). It has a homology of 78% to huFPR. *muFPR* is the murine FPR which has 78% homology to huFPR. The sequences are shown from 5' (left

6.5 Discussion

The cloning of human FPR (huFPR), using the polymerase chain reaction, proved to be a difficult project. At the onset of this work (1990) little was known about the PCR technique or the gene under investigation. Within three years it had been sequenced and homologues identified within the human, rabbit and murine genome. PCR was only just begininng to be understood. PCR amplification using the degenerate primers METN, NLAVA and Oligo dT failed to amplify the correct sequence. This was probably due to the degeneracies (16) and the length of these primers. These primers were chosen so that they could be used to isolate not only human FPR but also FPRs from other species. The Oligo dT primer used to produce cDNA further increased the non-specificity by reverse transcribing all polyadenylated mRNA molecules. This strategy would have been more successful if a primer specific to the 3' end had been used. This was the probable reason why the NLAVA primer (15b, degeneracy = 2048) also did not work, the advantage of extra length was outweighed by its higher degeneracy. Only when amplifying the actual cDNA inserted into a plasmid (i.e in the presence of large amounts of huFPR) did this primer, in conjunction with a specific 3' end primer (PAPS), give the correct amplicon (Figure 6.7). Even though the secondary PCR with NLAVA/Oligo dT gave an amplicon of the expected size, sequencing showed this to be unidentifiable DNA. Because of the high degeneracy these primers could not amplify huFPR and were thus unable to amplify other FPRs or other chemotactic receptors.

When these problems became evident new primers were designed, 14PRMR and PAPS, which were longer and did amplify huFPR. The amplicon with produced with these primers was sequenced and identified to be fMLP-R26. It is interesting to note

that the other isoform of huFPR that is fMLP-R98 was not amplified. This only differs by two bases within the opening reading frame from fMLP-R26.

For the subsequent cloning of muFPR a variety of primers were used (Figure 6.16). From the alignment of METN primer to the subsequently published muFPR sequence, it is clear that METN would have worked if its 5' end had been longer and if inosine had been substituted for degeneracies. 14PRMR did not amplify the murine FPR as in the most critical regions for PCR, the 3' end, 14PRMR was not complementary to the murine sequence. Because of the single incompatible base at the 3' end, a C not a T, NEWT failed to amplify muFPR. PAPS and ITOADS did not amplify the correct sequence for the same reason. It is apparent that the 5' and 3' ends of muFPR are highly different to that expected. Appendix 3 shows the amino acid sequence of β_2 adrenergic receptors (hamster, human, rat and mouse) and the FPRs known (human isoforms, rabbit and murine FPR). The FPRs vary greatly with each other when compared with other classes of G protein coupled receptors.

The outcome of the PCR experiments showed that even though conserved regions were present in human and rabbit at the 5' and 3' ends, this was not the case in the mouse. Published data indicates that the six putative genes of muFPR vary by 54% to 76%. Despite alignments to determine highly conserved areas of the three huFPR isoforms, the rabFPR, and the muFPR, and the use of inosine in positions of degeneracy, the other five putative murine FPR genes could still not be detected by PCR. This could be because these genes do not have the same conserved regions or that there are multiple copies of muFPR biasing the PCR products. There is also the possibility that they contain introns within the coding regions, although this is unusual for G protein coupled receptors (Libert *et al.*, 1989).

Cytokine-differentiating FDCP cells, as indicated from the NBT, glass adherence and the binding assays (Sections 3 and 4), begin to respond to formyl peptide stimulation after 3 days, with a maximum response after six days at which point the response decreases, possibly due of apoptosis (Crompton, 1991). Reverse transcriptase PCR and sequencing of the PCR products revealed that only one muFPR transcript appears after 2 days of differentiation. It is possible that other FPRs are transcribed but that the primers used could not anneal to them. However, since the muFPR transcript is present 24 hours before the receptor-mediated responses, and mRNA is usually transcribed 12 to 24 hours before protein is expressed this indicates that this muFPR isoform is the likely transcript for the functional chemotactic receptor expressed in the FDCP model system.

Although WEHI-3b cells showed a functional FPR with differences to that found on differentiated FDCP cells as observed by N-formyl peptide binding (Sections 3 and 4), it was interesting to note that the murine FPR mRNA transcript identified in differentiated FDCP by RT-PCR cells was absent. WEHI-3b are a monocyte derived cell line and may express a different muFPR isoform with a different phenotype (Kajigaya *et al.*, 1990). This tissue specific expression has been describe in human cells; the human isoform FPRL2 is expressed only in monocytes and not in neutrophils while huFPR and the isoform FPRL1 is expressed in both cell types (Durstin *et al.*, 1994).

CHAPTER 7

GENERAL DISCUSSION

7.1 Overview

When this work began the *in vitro* model system available for the study of neutrophils was the human leukaemic cell line HL-60. The aim of this project was to extend the work on elucidating the mechanism of action of FPR, by first developing a good physiological model and secondly studying the receptor expressed by murine neutrophils at both the protein and gene levels and comparing it with the human and rabbit FPRs. The murine pluripotent stem cell line, FDCP, which could be differentiated with physiological cytokines, was assessed for its suitability for the study FPR.

The optimal seeding conditions for maintaining FDCP and HL-60 cells in an undifferentiated state were established. This allowes the culture to proliferate before the nutrients denature and waste products accumulate preventing the irreversible differentiation of the cells. At low seeding densities the FDCP cells failed to proliferate. This is probably due to too few pluripotential cells preventing logarithmic growth to occur before the cytokines denature.

The effect of cytokines on cell proliferation and differentiation was studied. Consistent with previously published observations (Spooncer *et al.*, 1986) in the absence of any cytokines cells failed to proliferate and apoptose (Crompton, 1991). G-CSF alone failed to cause cell proliferation or differentiation. High concentrations of IL-3 ($100U.ml^{-1}$) showed the greatest proliferation and the lowest spontaneous differentiation. Low levels of IL-3 ($1U.ml^{-1}$) gave very little proliferation but a doubling in the percentage of neutrophils. GM-CSF ($50U.ml^{-1}$) gave the highest percentage of neutrophils but virtually no cell increase. The combination of low IL-3 and GM-

CSF gave a lower percentage of neutrophils, than GM-CSF alone, but there was an increase in cell numbers. A combination of low IL-3, GM-CSF and G-CSF resulted in a large percentage of neutrophils with high cell numbers. This combination of cytokines was therefore chosen as the optimal cytokine mixture for the differentiation of FDCP cells to neutrophils. It was also found that the commercial source of G-CSF, as well as its concentration, had an effect on the percentage of promyelocytes going on to form mature neutrophils. A specific stain was used in order to determine the number of promyelocytes differenting to neutrophils. The NBT assay was used to confirm that these were funtional neutophils. Approximately 80% of cells were found to be neutrophils after six of the initiation of differentiation. The onset of expression of cell adhesion molecules in the presence of fMLF occured three days after cytokine-mediated differentiation. Maximal cell adherence occured after six days, after which this decreased as the cells apoptosed (Crompton, 1991). The cells also showed pseudpod formation, indicating stimulation of actin polymerization. The respiratory burst in response to N-formyl peptide mirrored this activity.

The mature neutrophil characteristics of differentiated FDCP and HL-60 cells were compared. Mature neutrophils respond to N-formyl peptides in a number of ways. N-formyl peptides activate cell adhesion molecules and actin polymerization as a first step in neutrophil migration. Glass adherence assays were carried out to measure this effect. Similar responses were observed in both the human and the murine cell lines. In response to the high concentrations of N-formyl peptides differentiated neutrophils produce a respiratory burst which generates cytotoxic superoxide radicals. To assay this response an NBT assay was used. A similar increase in the level of NBT reduction was observed when differentiated cells were

compared to their undifferentiated counterparts. However, when the levels of NBT reduction were compared between differentiated human and murine cells a hundred fold greater NBT reduction was observed in murine FDCP cells. Other groups have demonstrated that HL-60 neutrophils are deficient in the myeloperoxidase/peroxide/halide system (Pullen and Hosking, 1985).

These findings indicate that physiologically, FDCP cells were further differentiated than HL-60 cells, making them a more accurate system for the study of cellular events such as FPR mediated chemotaxis. In addition to providing a more physiologically accurate model of neutrophils, the kinetics of N-formyl peptide binding to murine FPR, in the FDCP system, and how these compared to the human and rabbit FPRs are of great interest.

Therefore, the kinetics of murine FPR were studied first, with [^{3}H]-fMLF and secondly with [^{125}I]-fnLLFnLYK. The differentiated FDCP cells demonstrated low affinity for [^{3}H]-fMLF. The number of receptors was found to be 132 000 per cell, with 32% being of high affinity. The receptor numbers obtained agree well with other studies on isolated neutrophils (Niedel *et al.*, 1979; Koo *et al.*, 1982). Human and rabbit FPRs (Ye *et al.*,1992; Koo *et al.*, 1982) have a higher affinity for fMLF than murine cells.

The hexapeptide fnLLFnLYK has been used to characterise huFPRs (Williams *et al.*, 1977) because it has greater binding affinity than fMLF. In addition, the iodination of this peptide results in much higher specific activities than that of tritiated peptides. A greater affinity and higher specific activity allows lower peptide concentration and a lower number of cells to be used. This results in decreased

ligand proteolysis and cell agglutination during the assay. The nonspecific binding is also lowered. Kinetic analysis of murine FPR with [^{125}I]-fnLLFnLYK gave high and low affinity binding with K_d values of 3.7 and 22.6 nM, respectively. The number of receptors was found to be 79 000 cell, with 25% being of high affinity. This was 1.6 times lower than the numbers obtained with [^{3}H]-fMLF (132 000). Isolated neutrophils have between 55 000 to 120 000 receptors for N-formyl peptides (Niedel *et al.*, 1979; Koo *et al.*, 1982). Cytokine-differentiated FDCP cells showed reproducible expression of receptor numbers (79 000) when assayed by the [^{125}I]-fnLLFnLYK. In contrast, [^{3}H]-fMLF gave a higher but inconsistent estimation of receptor numbers. This is consistent with proteolysis and cell agglutination, which would trap the [^{3}H]-fMLF.

The competitive displacement of the [^{125}I]-fnLLFnLYK with fMLF and the direct estimation of the affinity of [^{3}H]-fMLF for murine FPR gave comparable results. That is, fMLF binds to murine FPR with a low affinity.

To date two other groups have studied the murine FPR. Murphy and co-workers (Gao and Murphy, 1993) have cloned and expressed one muFPR isoform in *Xenopus* oocytes, and Sasagawa and co-workers. (Sasagawa *et al.*, 1992) have studied the chemotactic response of blood-isolated neutrophils to fMLF. In agreement with the present study, these groups found that the murine FPR has a low affinity for fMLF.

To further characterize the specificity of murine FPR, competition assays were carried out. The relative potencies of a variety of formyl peptides for murine FPR was as follows: fnLLFnLYK > fMLF > fMLFK > fMLFF > fMF. The relative potencies

for the human FPR: fnLLFnLYK > fMLF > fMLFK (Freer *et al.*, 1980), and for the rabbit FPR; fMLFF > fMLF (Freer *et al.*, 1982; Kermode *et al.*, 1991). The relative potencies of the murine FPR are similar to the huFPR (Niedel *et al.*, 1979), but different to the rabFPR (Kermode *et al.*, 1991).

Phenotypic characterisation of the murine FPR had shown significant differences in N-formyl peptide binding. In order to understand how the differences in function related to structure, the cloning of first, the human and secondly the murine FPR genes was undertaken.

Experiments using covalent linking of N-formyl peptides to human FPR were planned with the aim of obtaining partial protein sequence data to be used in PCR cloning the human FPR gene. However, the sequence of the human FPR was published before this work was begun (Boulay *et. al.,* 1990a). Primers were designed based on this published sequence to clone the human FPR and use it for the screening of a murine genomic library. Initially, short and degenerate primers were designed to PCR amplify the human and the murine FPR. However, these primers were too degenerate and failed to amplify the any FPRs. Longer and specific primers were designed and used to successfully clone the human FPR. To clone the murine FPR primers were designed to the 5' and 3' end of the coding region, and at positions of degeneracy inosine was used. These proved unsuccessful as the 5' and 3' end of murine FPR was not as conserved as expected from the data on the β_2-adrenergic receptors.

In addition to the PCR strategy, the construction and screening of libraries was carried out. A restriction map was first constructed in order to clone the murine FPR

gene. This provided information on the number of potential genes and their degree of homology to the huFPR probe being used. At least six genes were identified by high stringency hybridization analysis in the murine genome, from restriction mapping with the *Hind* III digests. However, attempts to clone these genes failed, before the murine FPR gene, was cloned and sequenced by Murphy and co-workers (Gao and Murphy, 1993). This group confirmed that there were six FPR genes and went on to sequence them. However, they only published the sequence of the putative murine FPR designated *muFPR*. This has 76% homology to huFPR. From the restriction map analysis it is likely that the 7.8kb *Hind* III band, the most strongly hybridizing, is the muFPR isoform published. The other five genes may correspond to the rest of the *Hind* III bands. Of the six genes identified by Murphy and co-workers the muFPRs vary by 54% to 76% with one gene probably being a pseudogene (Murphy, 1994).

Sequence alignments were used to determine highly conserved areas between the three huFPR isoforms, the rabFPR and the muFPR. Using inosine in positions of degeneracy, primers to conserved regions were designed. PCR of murine genomic DNA with these primers failed to clone the other five genes. This could be because these genes do not have the same conserved regions or that there are multiple copies of muFPR biasing the PCR products.

Reverse transcriptase PCR and sequencing of the PCR products revealed that only one muFPR transcript appears after two days of differentiation. It is possible that other FPRs are transcribed but the primers used could not anneal to them. However, since the muFPR transcript is present 24 hours before the receptor-mediated responses, and mRNA is usually transcribed 12 to 24 hours before protein

is expressed it indicates that this muFPR isoform is the likely transcript for the functional chemotactic receptor expressed in the model system I describe in this project.

WEHI-3b cells are a monocyte derived cell line (Kajigaya *et al.*, 1990), and when these cells were assayed for N-formyl peptide binding it was found that the adherent stage showed FPR expression. This was lower than in the FDCP cells. This may be due to a different isoform of the receptor, or that the cells are expressing lower receptor numbers. Reverse transcriptase PCR failed to amplify the muFPR transcript from these cells. This may also indicate that they are expressing another isoform. When WEHI-3b cells were used in genomic mapping of murine FPR a strongly hybridizing band was detected. This was probably an RNA contaminant. This would indicate that WEHI-3b cells transcribe a muFPR gene or genes and as the RT-PCR failed to identidy the muFPR, it is probable that WEHI-3b cells are expressing another isoform. In the human genome there are three genes. huFPR and FPRL1 are both expressed in neutrophils and monocytes. FPRL2 is only expressed in monocytes. Tissue-specific expression of FPR may also occur in the murine system.

7.2 Future Investigations

This study has demonstrated that the murine pluripotent cell line, FDCP, is a powerful model for the study of promyelocyte differentiation, neutrophils, and their receptors. Further, this study has identified which of the six putative genes of the murine FPR gene is expressed in neutrophils. There are many avenues for future investigations.

FDCP cells can be used to characterise the differentiation process. For instance by constructing differential cDNA libraries one can isolate cytokine-mediated gene expression to study differentiation. The possibility of the differential expression of FPR and G protein giving rise to the apparent increase in ligand binding seen during differentiation can be found by studying the transcription and expression of these genes.

The murine genome has six putative genes for FPR while the human has three and the rabbit only one. This may be due to the need for murine cells to detect a more variable group of N-formyl peptides, or that there is tissue specific difference in expression. The potential of FDCP cells to produce fully differentiated myeloid cells, in response to various cytokines, can be used to address the tissue-specificity of the FPR genes. The monocyte derived WEHI-3b cell line appears to express a different FPR isoform than FDCP cells differentiated to neutrophils. The FPR of macrophages, monocytes, and eosinophils can be characterised. When the sequence data on the five unpublished murine FPR isoforms becomes available, a comparison of the binding data and the expression of FPR genes by the various cell types could be carried out. The human genome contains three FPR genes which appear to have differential expression (Durstin *et al.*, 1994). This may also be the case in murine cells. In addition, the binding characteristics of these other isoforms can be studied.

Structural and functional relationships can be studied by directed mutagenesis of FPR genes. Using the six murine genes and by isolating genes from other species, the model of N-formyl peptide activation of FPR can be refined.

The murine model may be used to study other mature neutrophil characteristics such as the expression of cell surface molecules for example cell adhesion molecules.

The heterogeneity of circulating neutrophils may be investigated. For example, are circulating neutrophils hetegenous because they have been derived form different stem cells, or is it due to variability in differentiation ?

REFERENCES

Ahuja, S.K., Ozcelik, T., Milatovitch, A., Francke, U., and Murphy, P.M. (1992). Molecular evolution of the human interleukin-8 receptor gene cluster. Nature Genetics *2*, 31-36.

Ahuja, S.K. and Murphy, P.M. (1993). Molecular piracy of mammalian interleukin-8 receptor type B by herpesvirus saimiri. Journal of Biological Chemistry *268*, 20691-20694.

Ali, H., Richardson, R.M., Tomhave, E.D., Didsbury, J.R., and Snyderman, R. (1993). Differences in phosphorylation of formylpeptide and C5a chemoattractant receptors correlate with differences in desensitization. Journal of Biological Chemistry *268*, 24247-24254.

Alon, R., Kassner, P.D., Carr, M.W., Finger, E.B., Hemler, M.E., and Springer, T.A. (1995). The integrin VLA-4 supports tethering and rolling in flow on VCAM-1. Journal of Cell Biology *128*, 1243-1253.

Aswanikumar, S., Corcoran, B., Schiffmann, E., Day, A.R., Freer, R.J., Showell, H.J., and Becker, E.L. (1977). Demonstration of a receptor on rabbit neutrophils for chemotactic peptides. Biochemical & Biophysical Research Communications *74*, 810-817.

Baggiolini, M., Dewald, B., and Moser, B. (1994). Interleukin-8 and related chemotactic cytokines--CXC and CC chemokines. Advances in Immunology *55*, 97-179.

Baldwin, J.M. (1993). The probable arrangement of the helices in G protein-coupled receptors. EMBO Journal *12*, 1693-1703.

Bao, L., Gerard, N.P., Eddy, R.L., Jr., Shows, T.B., and Gerard, C. (1992). Mapping of genes for the human C5a receptor (C5AR), human FMLP receptor (FPR), and two FMLP receptor homologue orphan receptors (FPRH1, FPRH2) to chromosome 19. Genomics *13*, 437-440.

Benyunes, M.C. and Snyderman, R. (1984). Characterization of an oligopeptide chemoattractant receptor on human blood monocytes using a new radioligand. Blood *63*, 588-592.

Berman, M.E. and Muller, W.A. (1995). Ligation of platelet/endothelial cell adhesion molecule 1 (PECAM-1/CD31) on monocytes and neutrophils increases binding capacity of leukocyte CR3 (CD11b/CD18). Journal of Immunology *154*, 299-307.

Bogen, S., Pak, J., Garifallou, M., Deng, X., and Muller, W.A. (1994). Monoclonal antibody to murine PECAM-1 (CD31) blocks acute inflammation in vivo. Journal of Experimental Medicine *179*, 1059-1064.

Bokoch, G.M. and Gilman, A.G. (1984). Inhibition of receptor-mediated release of arachidonic acid by pertussis toxin. Cell *39*, 301-308.

Bommakanti, R.K., Klotz, K.N., Dratz, E.A., and Jesaitis, A.J. (1993). A carboxyl-terminal tail peptide of neutrophil chemotactic receptor disrupts its physical complex with G protein. Journal of Leukocyte Biology *54*, 572-577.

Borregaard, N., Schwartz, J.H., and Tauber, A.I. (1984). Proton secretion by stimulated neutrophils. Significance of hexose monophosphate shunt activity as source of electrons and protons for the respiratory burst. Journal of Clinical Investigation *74*, 455-459.

Borregaard, N., Miller, L.J., and Springer, T.A. (1987). Chemoattractant-regulated mobilization of a novel intracellular compartment in human neutrophils. Science *237*, 1204-1206.

Borregaard, N. (1988). Subcellular localization and dynamics of components of the respiratory burst oxidase. Journal of Bioenergetics & Biomembranes *20*, 637-651.

Borregaard, N., Christensen, L., Bejerrum, O.W., Birgens, H.S., and Clemmensen, I. (1990). Identification of a highly mobilizable subset of human neutrophil intracellular vesicles that contains tetranectin and latent alkaline phosphatase. Journal of Clinical Investigation *85*, 408-416.

Borregaard, N., Kjeldsen, L., Rygaard, K., Bastholm, L., Nielsen, M.H., SengelovH., Bjerrum, O.W., and Johnsen, A.H. (1992). Stimulus-dependent secretion of plasma proteins from human neutrophils. Journal of Clinical Investigation *90*, 86-96.

Borregaard, N., Lollike, K., Kjeldsen, L., Sengelov, H., Bastholm, L., NielsenMH., and Bainton, D.F. (1993). Human neutrophil granules and secretory vesicles. European Journal of Haematology *51*, 187-198.

Borregaard, N., Kjeldsen, L., Sengelov, H., Diamond, M.S., Springer, T.A., Kishimoto, T.K., and Bainton, D.F. (1994). Changes in subcellular localization and surface expression of L-selectin, alkaline phosphatase, and Mac-1 in human neutrophils during stimulation with inflammatory mediators. Journal of Leukocyte Biology *56*, 80-87.

Borregaard, N., Sehested, M., Nielsen, B.S., Sengelov, H., and Kjeldsen, L. (1995). Biosynthesis of granule proteins in normal human bone marrow cells. Gelatinase is a marker of terminal neutrophil differentiation. Blood *85*, 812-817.

Boulay, F., Tardif, M., Brouchon, L., and Vignais, P. (1990a). The human N-formylpeptide receptor. Characterization of two cDNA isolates and evidence for a new subfamily of G-protein-coupled receptors. Biochemistry *29*, 11123-11133.

Boulay, F., Tardif, M., Brouchon, L., and Vignais, P. (1990b). Synthesis and use of a novel N-formyl peptide derivative to isolate a human N-formyl peptide receptor cDNA. Biochemical & Biophysical Research Communications *168*, 1103-1109.

Boulay, F., Mery, L., Tardif, M., Brouchon, L., and Vignais, P. (1991). Expression cloning of a receptor for C5a anaphylatoxin on differentiated HL-60 cells. Biochemistry *30*, 2993-2999.

Boyden, S.E., Jr. (1962). The chemotactic effects of mixtures of antibody and antigen on polymorphonuclear leukocytes. Journal of Experimental Medicine *115*, 453-466.

Breitman, T.R., Collins, S.J., and Keene, B.R. (1980). Replacement of serum by insulin and transferrin supports growth and differentiation of the human promyelocytic cell line, HL-60. Experimental Cell Research *126*, 494-498.

Brennan, J.K., Abboud, C.N., DiPersio, J.F., Barlow, G.H., and Lichtman, M.A. (1981). Autostimulation of growth by human myelogenous leukemia cells (HL-60). Blood *58*, 803-812.

Butcher, E.C. (1991). Leukocyte-endothelial cell recognition: three (or more) steps to specificity and diversity. Cell *67*, 1033-1036.

Carlos, T.M. and Harlan, J.M. (1994). Leukocyte-endothelial adhesion molecules. Blood *84*, 2068-2101.

Cassatella, M.A., Bazzoni, F., Ceska, M., Ferro, I., Baggiolini, M., and Berton, G. (1992). IL-8 production by human polymorphonuclear leukocytes. The chemoattractant formyl-methionyl-leucyl-phenylalanine induces the gene expression and release of IL-8 through a pertussis toxin-sensitive pathway. Journal of Immunology *148*, 3216-3220.

Chanock, S.J., el Benna, J., Smith, R.M., and Babior, B.M. (1994). The respiratory burst oxidase. Journal of Biological Chemistry *269*, 24519-24522.

Chaplinski, T.J., Bennett, T.E., and Caro, J.F. (1986). Alteration in insulin receptor expression accompanying differentiation of HL-60 leukemia cells. Cancer Research *46*, 1203-1207.

Chaplinski, T.J. and Niedel, J.E. (1982). Cyclic nucleotide-induced maturation of human promyelocytic leukemia cells. Journal of Clinical Investigation *70*, 953-964.

Chase, P.B., Halonen, M., and Regan, J.W. (1993). Cloning of a human platelet-activating factor receptor gene: evidence for an intron in the 5'-untranslated region. American Journal of Respiratory Cell & Molecular Biology *8*, 240-244.

Chenoweth, D.E. and Hugli, T.E. (1978). Demonstration of specific C5a receptor on intact human polymorphonuclear leukocytes. Proceedings of the National Academy of Sciences of the United States of America *75*, 3943-3947.

Collins, S.J., Gallo, R.C., and Gallagher, R.E. (1977). Continuous growth and differentiation of human myeloid leukaemic cells in suspension culture. Nature *270*, 347-349.

Collins, S.J., Ruscetti, F.W., Gallagher, R.E., and Gallo, R.C. (1978). Terminal differentiation of human promyelocytic leukemia cells induced by dimethyl sulfoxide and other polar compounds. Proceedings of the National Academy of Sciences of the United States of America *75*, 2458-2462.

Collins, S.J., Ruscetti, F.W., Gallagher, R.E., and Gallo, R.C. (1979). Normal functional characteristics of cultured human promyelocytic leukemia cells (HL-60) after induction of differentiation by dimethylsulfoxide. Journal of Experimental Medicine *149*, 969-974.

Collins, S.J. (1987). The HL-60 promyelocytic leukemia cell line: proliferation, differentiation, and cellular oncogene expression. Blood *70*, 1233-1244.

Cotecchia, S., Exum, S., Caron, M.G., and Lefkowitz, R.J. (1990). Regions of the alpha 1-adrenergic receptor involved in coupling to phosphatidylinositol hydrolysis and enhanced sensitivity of biological function. Proceedings of the National Academy of Sciences of the United States of America *87*, 2896-2900.

Crompton, T. (1991). IL3-dependent cells die by apoptosis on removal of their growth factor. Growth Factors *4*, 109-116.

D'Aquila, R.T., Bechtel, L.J., Videler, J.A., Eron, J.J., Gorczyca, P., and Kaplan, J.C. (1991). Maximizing sensitivity and specificity of PCR by pre-amplification heating. Nucleic Acids Research *19*, 3749

De Nardin, E., Radel, S.J., Lewis, N., Genco, R.J., and Hammarskjold, M. (1992). Identification of a gene encoding for the human formyl peptide receptor. Biochemistry International *26*, 381-387.

Dewald, B., Bretz, U., and Baggiolini, M. (1982). Release of gelatinase from a novel secretory compartment of human neutrophils. Journal of Clinical Investigation *70*, 518-525.

Dickenson, J.M., Camps, M., Gierschik, P., and Hill, S.J. (1995). Activation of phospholipase C by G-protein beta gamma subunits in DDT1MF-2 cells. European Journal of Pharmacology *288*, 393-398.

Didsbury, J.R., Uhing, R.J., Tomhave, E., Gerard, C., Gerard, N., and Snyderman, R. (1992). Functional high efficiency expression of cloned leukocyte chemoattractant receptor cDNAs. Febs Letters *297*, 275-279.

Dittmann, K.H. and Petrides, P.E. (1991). A 41 kDa transferrin related molecule acts as an autocrine growth factor for HL-60 cells. Biochemical & Biophysical Research Communications *176*, 473-478.

Durstin, M., Gao, J.L., Tiffany, H.L., McDermott, D., and Murphy, P.M. (1994). Differential expression of members of the N-formylpeptide receptor gene cluster in human phagocytes. Biochemical & Biophysical Research Communications *201*, 174-179.

Eberle, M., Traynor-Kaplan, A.E., Sklar, L.A., and Norgauer, J. (1990). Is there a relationship between phosphatidylinositol trisphosphate and F-actin polymerization in human neutrophils?. Journal of Biological Chemistry *265*, 16725-16728.

Engelman, D.M., Henderson, R., McLachlan, A.D., and Wallace, B.A. (1980). Path of the polypeptide in bacteriorhodopsin. Proceedings of the National Academy of Sciences of the United States of America *77*, 2023-2027.

Farago, A. and Nishizuka, Y. (1990). Protein kinase C in transmembrane signalling. Febs Letters *268*, 350-354.

Fay, S.P., Posner, R.G., Swann, W.N., and Sklar, L.A. (1991). Real-time analysis of the assembly of ligand, receptor, and G protein by quantitative fluorescence flow cytometry. Biochemistry *30*, 5066-5075.

Fay, S.P., Domalewski, M.D., and Sklar, L.A. (1993). Evidence for protonation in the human neutrophil formyl peptide receptor binding pocket. Biochemistry *32*, 1627-1631.

Freer, R.J., Day, A.R., Radding, J.A., Schiffmann, E., Aswanikumar, S., Showell, H.J., and Becker, E.L. (1980). Further studies on the structural requirements for synthetic peptide chemoattractants. Biochemistry *19*, 2404-2410.

Freer, R.J., Day, A.R., Muthukumaraswamy, N., Pinon, D., Wu, A., and Showell, H.J. (1982). Formyl peptide chemoattractants: a model of the receptor on rabbit neutrophils. Biochemistry *21*, 257-263.

Gallagher, R., Collins, S., Trujillo, J., McCredie, K., Ahearn, M., Tsai, S., Aulakh, G., Ting, R., Ruscetti, F., and Gallo, R. (1979). Characterization of the continuous, differentiating myeloid cell line (HL-60) from a patient with acute promyelocytic leukemia. Blood *54*, 713-733.

Gao, J.L., Kuhns, D.B., Tiffany, H.L., McDermott, D., Li, X., Francke, U., and Murphy, P.M. (1993). Structure and functional expression of the human macrophage inflammatory protein 1 alpha/RANTES receptor. Journal of Experimental Medicine *177*, 1421-1427.

Gao, J.L. and Murphy, P.M. (1993). Species and subtype variants of the N-formyl peptide chemotactic receptor reveal multiple important functional domains. Journal of Biological Chemistry *268*, 25395-25401.

Gearing, A.J. and Newman, W. (1993). Circulating adhesion molecules in disease [see comments]. Immunology Today *14*, 506-512.

Gerard, C., Bao, L., Orozco, O., Pearson, M., Kunz, D., and Gerard, N.P. (1992). Structural diversity in the extracellular faces of peptidergic G-protein-coupled receptors. Molecular cloning of the mouse C5a anaphylatoxin receptor. Journal of Immunology *149*, 2600-2606.

Gerard, C. and Gerard, N.P. (1994). C5A anaphylatoxin and its seven transmembrane-segment receptor. Annual Review of Immunology *12*, 775-808.

Gerard, N.P., Eddy, R.L., Jr., Shows, T.B., and Gerard, C. (1991a). The human neurokinin A (substance K) receptor. Molecular cloning of the gene, chromosome

localization, and isolation of the cDNA from tracheal and gastric tissues. Journal of Biological Chemistry *266*, 1354

Gerard, N.P., Garraway, L.A., Eddy, R.L., Jr., Shows, T.B., Iijima, H., and Paquet, J.L. (1991b). Human substance P receptor (NK-1): organization of the gene, chromosome localization, and functional expression of cDNA clones. Biochemistry *30*, 10640-10646.

Gerard, N.P., Bao, L., Xiao-Ping, H., Eddy, R.L., Jr., Shows, T.B., and Gerard, C. (1993). Human chemotaxis receptor genes cluster at 19q13.3-13.4. Characterization of the human C5a receptor gene. Biochemistry *32*, 1243-1250.

Gerard, N.P. and Gerard, C. (1991). The chemotactic receptor for human C5a anaphylatoxin. Nature *349*, 614-617.

Goetzl, E.J., Shames, R.S., Yang, J., Birke, F.W., Liu, Y.F., Albert, P.R., and An, S. (1994). Inhibition of human HL-60 cell responses to chemotactic factors by antisense messenger RNA depletion of G proteins. Journal of Biological Chemistry *269*, 809-812.

Goldman, D.W. and Goetzl, E.J. (1982). Specific binding of leukotriene B4 to receptors on human polymorphonuclear leukocytes. Journal of Immunology *129*, 1600-1604.

Harris, P. and Ralph, P. (1985). Human leukemic models of myelomonocytic development: a review of the HL-60 and U937 cell lines. Journal of Leukocyte Biology *37*, 407-422.

Haviland, D.L., Borel, A.C., Fleischer, D.T., Haviland, J.C., and Wetsel, R.A. (1993). Structure, 5'-flanking sequence, and chromosome location of the human N-formyl peptide receptor gene. A single-copy gene comprised of two exons on chromosome 19q.13.3 that yields two distinct transcripts by alternative polyadenylation. Biochemistry *32*, 4168-4174.

Heyworth, C.M., Dexter, T.M., Kan, O., and Whetton, A.D. (1990a). The role of hemopoietic growth factors in self-renewal and differentiation of IL-3-dependent multipotential stem cells. Growth Factors *2*, 197-211.

Heyworth, C.M., Vallance, S.J., Whetton, A.D., and Dexter, T.M. (1990b). The biochemistry and biology of the myeloid haemopoietic cell growth factors. Journal of Cell Science - Supplement *13*, 57-74.

Holmes, W.E., Lee, J., Kuang, W.J., Rice, G.C., and Wood, W.I. (1991). Structure and functional expression of a human interleukin-8 receptor. Science *253*, 1278-1280.

Honda, Z., Nakamura, M., Miki, I., Minami, M., Watanabe, T., Seyama, Y., Okado, H., Toh, H., Ito, K., Miyamoto, T., and *et al.* (1991). Cloning by functional expression of platelet-activating factor receptor from guinea-pig lung. Nature *349*, 342-346.

Hourihan, H., Allen, T.D., and Ager, A. (1993). Lymphocyte migration across high endothelium is associated with increases in alpha 4 beta 1 integrin (VLA-4) affinity. Journal of Cell Science *104*, 1049-1059.

Huey, R. and Hugli, T.E. (1985). Characterization of a C5a receptor on human polymorphonuclear leukocytes (PMN). Journal of Immunology *135*, 2063-2068.

Hwang, S.B. (1990). Specific receptors of platelet-activating factor, receptor heterogeneity, and signal transduction mechanisms. Journal of Lipid Mediators *2*, 123-158.

Jacobs, A.A., Huber, J.L., Ward, R.A., Klein, J.B., and McLeish, K.R. (1995). Chemoattractant receptor-specific differences in G protein activation rates regulate effector enzyme and functional responses. Journal of Leukocyte Biology *57*, 679-686.

Kajigaya, Y., Ikuta, K., Sasaki, H., and Matsuyama, S. (1990). Growth and differentiation of a murine interleukin-3-producing myelomonocytic leukemia cell line in a protein-free chemically medium. Leukemia *4*, 712-716.

Kaziro, Y., Itoh, H., Kozasa, T., Nakafuku, M., and Satoh, T. (1991). Structure and function of signal-transducing GTP-binding proteins. Annual Review of Biochemistry *60*, 349-400.

Keller, H.U. and Sorkin, E. (1967). Studies on chemotaxis. VI. Specific chemotaxis in rabbit polymorphonuclear leucocytes and mononuclear cells. International Archives of Allergy & Applied Immunology *31*, 575-586.

Kelvin, D.J., Michiel, D.F., Johnston, J.A., Lloyd, A.R., Sprenger, H., Oppenheim, J.J., and Wang, J.M. (1993). Chemokines and serpentines: the molecular biology of chemokine receptors. Journal of Leukocyte Biology *54*, 604-612.

Kermode, J.C., Freer, R.J., and Becker, E.L. (1991). The significance of functional receptor heterogeneity in the biological responses of the rabbit neutrophil to stimulation by chemotactic formyl peptides. Biochemical Journal *276*, 715-723.

Kishimoto, T.K., Jutila, M.A., Berg, E.L., and Butcher, E.C. (1989). Neutrophil Mac-1 and MEL-14 adhesion proteins inversely regulated by chemotactic factors. Science *245*, 1238-1241.

Kishimoto, T.K. and Rothlein, R. (1994). Integrins, ICAMs, and selectins: role and regulation of adhesion molecules in neutrophil recruitment to inflammatory sites. Advances in Pharmacology *25*, 117-169.

Kjeldsen, L., Bainton, D.F., Sengelov, H., and Borregaard, N. (1993). Structural and functional heterogeneity among peroxidase-negative granules in human neutrophils: identification of a distinct gelatinase-containing granule subset by combined immunocytochemistry and subcellular fractionation. Blood *82*, 3183-3191.

Kjeldsen, L., Bainton, D.F., Sengelov, H., and Borregaard, N. (1994a). Identification of neutrophil gelatinase-associated lipocalin as a novel matrix protein of specific granules in human neutrophils. Blood *83*, 799-807.

Kjeldsen, L., Sengelov, H., Lollike, K., Nielsen, M.H., and Borregaard, N. (1994b). Isolation and characterization of gelatinase granules from human neutrophils. Blood *83*, 1640-1649.

Koo, C., Lefkowitz, R.J., and Snyderman, R. (1982). The oligopeptide chemotactic factor receptor on human polymorphonuclear leukocyte membranes exists in two affinity states. Biochemical & Biophysical Research Communications *106*, 442-449.

Kunz, D., Gerard, N.P., and Gerard, C. (1992). The human leukocyte platelet-activating factor receptor. cDNA cloning, cell surface expression, and construction of a novel epitope-bearing analog. Journal of Biological Chemistry *267*, 9101-9106.

Kupper, R.W., Dewald, B., Jakobs, K.H., Baggiolini, M., and Gierschik, P. (1992). G-protein activation by interleukin 8 and related cytokines in human neutrophil plasma membranes. Biochemical Journal *282*, 429-434.

Lawrence, M.B., Bainton, D.F., and Springer, T.A. (1994). Neutrophil tethering to and rolling on E-selectin are separable by requirement for L-selectin. Immunity *1*, 137-145.

Lehrer, R.I., Lichtenstein, A.K., and Ganz, T. (1993). Defensins: antimicrobial and cytotoxic peptides of mammalian cells. Annual Review of Immunology *11*, 105-128.

Libert, F., Parmentier, M., Lefort, A., Dinsart, C., Van Sande, J., Maenhaut, C., Dumont, J.E., and Vassart, G. (1989). Selective amplification and cloning of four new members of the G protein-coupled receptor family. Science *244*, 569-572.

Lubbert, M., Herrmann, F., and Koeffler, H.P. (1991). Expression and regulation of myeloid-specific genes in normal and leukemic myeloid cells. Blood *77*, 909-924.

Malech, H.L., Gardner, J.P., Heiman, D.F., and Rosenzweig, S.A. (1985). Asparagine-linked oligosaccharides on formyl peptide chemotactic receptors of human phagocytic cells. Journal of Biological Chemistry *260*, 2509-2514.

Maniatis, T., Fritsch, E.F., and Sambrook, J. (1982). Molecular Clonin: A Laboratory Manual (NY: Cold Spring Harbor).

Martin, S.J., Bradley, J.G., and Cotter, T.G. (1990). HL-60 cells induced to differentiate towards neutrophils subsequently die via apoptosis. Clinical & Experimental Immunology *79*, 448-453.

Matsuoka, M., Kaziro, Y., Asano, S., and Ogata, E. (1993). Analysis of the expression of seven G protein alpha subunit genes in hematopoietic cells. American Journal of the Medical Sciences *306*, 89-93.

Mitrophanous, K. and Charalambous, B.M. (1993). Molecular studies on chemotactic receptors. Biochemical Society Transactions *21*, 297-299.

Moser, B., Barella, L., Mattei, S., Schumacher, C., Boulay, F., and Colombo, M.P. (1993). Expression of transcripts for two interleukin 8 receptors in human phagocytes, lymphocytes and melanoma cells. Biochemical Journal *294*, 285-292.

Mueller, H., Weingarten, R., Ransnas, L.A., Bokoch, G.M., and Sklar, L.A. (1991). Differential amplification of antagonistic receptor pathways in neutrophils. Journal of Biological Chemistry *266*, 12939-12943.

Muller, W.A., Weigl, S.A., Deng, X., and Phillips, D.M. (1993). PECAM-1 is required for transendothelial migration of leukocytes. Journal of Experimental Medicine *178*, 449-460.

Murphy, G., Reynolds, J.J., Bretz, U., and Baggiolini, M. (1982). Partial purification of collagenase and gelatinase from human polymorphonuclear leucocytes. Analysis of their actions on soluble and insoluble collagens. Biochemical Journal *203*, 209-221.

Murphy, P.M., Eide, B., Goldsmith, P., Brann, M., Gierschik, P., and Spiegel, A. (1987). Detection of multiple forms of Gi alpha in HL60 cells. Febs Letters *221*, 81-86.

Murphy, P.M., Ozcelik, T., Kenney, R.T., Tiffany, H.L., McDermott, D., and Francke, U. (1992). A structural homologue of the N-formyl peptide receptor. Characterization and chromosome mapping of a peptide chemoattractant receptor family. Journal of Biological Chemistry *267*, 7637-7643.

Murphy, P.M., Tiffany, H.L., McDermott, D., and Ahuja, S.K. (1993). Sequence and organization of the human N-formyl peptide receptor-encoding gene. Gene *133*, 285-290.

Murphy, P.M. (1994). The molecular biology of leukocyte chemoattractant receptors. Annual Review of Immunology *12*, 593-633.

Murphy, P.M. and McDermott, D. (1991). Functional expression of the human formyl peptide receptor in Xenopus oocytes requires a complementary human factor. Journal of Biological Chemistry *266*, 12560-12567.

Murphy, P.M. and Tiffany, H.L. (1991). Cloning of complementary DNA encoding a functional human interleukin-8 receptor. Science *253*, 1280-1283.

Mutoh, H., Bito, H., Minami, M., Nakamura, M., Honda, Z., Izumi, T., Nakata, R., Terano, A., and Shimizu, T. (1993). Two different promoters direct expression of two distinct forms of mRNAs of human platelet-activating factor receptor. Febs Letters *322*, 129-134.

Nakamura, M., Honda, Z., Izumi, T., Sakanaka, C., Mutoh, H., Minami, M., Bito, H., Matsumoto, T., Noma, M., and *et al.* (1991). Molecular cloning and expression of

platelet-activating factor receptor from human leukocytes. Journal of Biological Chemistry *266*, 20400-20405.

Neubig, R.R. and Sklar, L.A. (1993). Subsecond modulation of formyl peptide-linked guanine nucleotide-binding proteins by guanosine 5'-O-(3-thio)triphosphate in permeabilized neutrophils. Molecular Pharmacology *43*, 734-740.

Niedel, J.E., Wilkinson, S., and Cuatrecasas, P. (1979). Receptor-mediated Uptake and Degradation of ^{125}I-Chemotactic peptide by Human Neutrophils.. Journal of Biological Chemistry *254*, 10700-10706.

Norgauer, J., Eberle, M., Fay, S.P., Lemke, H.D., and Sklar, L.A. (1991). Kinetics of N-formyl peptide receptor up-regulation during stimulation in human neutrophils. Journal of Immunology *146*, 975-980.

Omann, G.M. and Sklar, L.A. (1988). Response of neutrophils to stimulus infusion: differential sensitivity of cytoskeletal activation and oxidant production. Journal of Cell Biology *107*, 951-958.

Oppenheim, J.J., Zachariae, C.O., Mukaida, N., and Matsushima, K. (1991). Properties of the novel proinflammatory supergene "intercrine" cytokine family. Annual Review of Immunology *9*, 617-648.

Owen, W.F., Jr., Petersen, J., and Austen, K.F. (1991). Eosinophils altered phenotypically and primed by culture with granulocyte/macrophage colony-stimulating factor and 3T3 fibroblasts generate leukotriene C4 in response to FMLP. Journal of Clinical Investigation *87*, 1958-1963.

Pantazis, P., Lazarou, S.A., and Papadopoulos, N.M. (1981). Isoenzymes of lactate dehydrogenase in human leukemic cells in culture treated with inducers of differentiation. Journal of Cell Biology *90*, 396-401.

Perez, H.D., Kelly, E., and Holmes, R. (1992). Regulation of formyl peptide receptor expression and its mRNA levels during differentiation of HL-60 cells. Journal of Biological Chemistry *267*, 358-363.

Perez, H.D., Holmes, R., Vilander, L.R., Adams, R.R., Manzana, W., and Jolley, D. (1993). Formyl peptide receptor chimeras define domains involved in ligand binding. Journal of Biological Chemistry *268*, 2292-2295.

Perez, H.D., Vilander, L., Andrews, W.H., and Holmes, R. (1994). Human formyl peptide receptor ligand binding domain(s). Studies using an improved mutagenesis/expression vector reveal a novel mechanism for the regulation of receptor occupancy. Journal of Biological Chemistry *269*, 22485-22487.

Pittet, D., Krause, K.H., and Lew, D.P. (1992). Inositol phosphates. Metabolism and site of action in neutrophil granulocytes. Advances in Second Messenger & Phosphoprotein Research *26*, 369-398.

Pizcueta, P. and Luscinskas, F.W. (1994). Monoclonal antibody blockade of L-selectin inhibits mononuclear leukocyte recruitment to inflammatory sites in vivo. American Journal of Pathology *145*, 461-469.

Plesner, T., Ploug, M., Ellis, V., Ronne, E., Hoyer-Hansen, G., Wittrup, M., Tscherning, T., Dano, K., and Hansen, N.E. (1994). The receptor for urokinase-type plasminogen activator and urokinase is translocated from two distinct intracellular compartments to the plasma membrane on stimulation of human neutrophils. Blood *83*, 808-815.

Polakis, P.G., Uhing, R.J., and Snyderman, R. (1988). The formylpeptide chemoattractant receptor copurifies with a GTP-binding protein containing a distinct 40-kDa pertussis toxin substrate. Journal of Biological Chemistry *263*, 4969-4976.

Posner, R.G., Fay, S.P., Domalewski, M.D., and Sklar, L.A. (1994). Continuous spectrofluorometric analysis of formyl peptide receptor ternary complex interactions. Molecular Pharmacology *45*, 65-73.

Probst, W.C., Snyder, L.A., Schuster, D.I., Brosius, J., and Sealfon, S.C. (1992). Sequence alignment of the G-protein coupled receptor superfamily. DNA & Cell Biology *11*, 1-20.

Prossnitz, E.R., Quehenberger, O., Cochrane, C.G., and Ye, R.D. (1993). The role of the third intracellular loop of the neutrophil N-formyl peptide receptor in G protein coupling. Biochemical Journal *294*, 581-587.

Prossnitz, E.R., Schreiber, R.E., Bokoch, G.M., and Ye, R.D. (1995). Binding of low affinity N-formyl peptide receptors to G protein. Characterization of a novel inactive receptor intermediate. Journal of Biological Chemistry *270*, 10686-10694.

Pullen, G.R. and Hosking, C.S. (1985). Differentiated HL60 promyelocytic leukaemia cells have a deficient myeloperoxidase/halide killing system. Clinical & Experimental Immunology *62*, 304-309.

Quehenberger, O., Prossnitz, E.R., Cochrane, C.G., and Ye, R.D. (1992). Absence of G(i) proteins in the Sf9 insect cell. Characterization of the uncoupled recombinant N-formyl peptide receptor. Journal of Biological Chemistry *267*, 19757-19760.

Quehenberger, O., Prossnitz, E.R., Cavanagh, S.L., Cochrane, C.G., and Ye, R.D. (1993). Multiple domains of the N-formyl peptide receptor are required for high-affinity ligand binding. Construction and analysis of chimeric N-formyl peptide receptors. Journal of Biological Chemistry *268*, 18167-18175.

Saiki, R.K., Scharf, S., Faloona, F., Mullis, K.B., Horn, G.T., and Erlich, H.A. (1985). Enzymatic amplification of beta-globin genomic sequences and restriction site analysis for diagnosis of sickle cell anemia. Science *230*, 1350-1354.

Saiki, R.K., Bugawan, T.L., Horn, G.T., Mullis, K.B., and Erlich, H.A. (1986). Analysis of enzymatically amplified beta-globin and HLA-DQ alpha DNA with allele-specific oligonucleotide probes. Nature *324*, 163-166.

Saiki, R.K., Gelfand, D.H., Stoffel, S., Scharf, S.J., Higuchi, R., Horn, G.T., and Erlich, H.A. (1988). Primer-directed enzymatic amplification of DNA with a thermostable DNA polymerase. Science *239*, 487-491.

Samama, P., Cotecchia, S., Costa, T., and Lefkowitz, R.J. (1993). A mutation-induced activated state of the beta 2-adrenergic receptor. Extending the ternary complex model. Journal of Biological Chemistry *268*, 4625-4636.

Maniatis, T., Fritsch, E.F., and Sambrook, J. (1982). Molecular Clonin: A Laboratory Manual (NY: Cold Spring Harbor).

Sasagawa, S., Satow, Y., Suzuki, K., and Hosokawa, T. (1992). Chemotactic activities of peripheral blood polymorphonuclear leukocytes and peritoneal exudate polymorphonuclear leukocytes in MRL mice. Immunopharmacology & Immunotoxicology *14*, 625-635.

Savarese, T.M. and Fraser, C.M. (1992). In vitro mutagenesis and the search for structure-function relationships among G protein-coupled receptors. Biochemical Journal *283*, 1-19.

Schepers, T.M., Brier, M.E., and McLeish, K.R. (1992). Quantitative and qualitative differences in guanine nucleotide binding protein activation by formyl peptide and leukotriene B4 receptors. Journal of Biological Chemistry *267*, 159-165.

Schiffmann, E., Corcoran, B.A., and Wahl, S.M. (1975). N-formylmethionyl peptides as chemoattractants for leucocytes. Proceedings of the National Academy of Sciences of the United States of America *72*, 1059-1062.

Schleiffenbaum, B., Spertini, O., and Tedder, T.F. (1992). Soluble L-selectin is present in human plasma at high levels and retains functional activity. Journal of Cell Biology *119*, 229-238.

Schreiber, R.E., Prossnitz, E.R., Ye, R.D., Cochrane, C.G., Jesaitis, A.J., and Bokoch, G.M. (1993). Reconstitution of recombinant N-formyl chemotactic peptide receptor with G protein. Journal of Leukocyte Biology *53*, 470-474.

Schreiber, R.E., Prossnitz, E.R., Ye, R.D., Cochrane, C.G., and Bokoch, G.M. (1994). Domains of the human neutrophil N-formyl peptide receptor involved in G protein coupling. Mapping with receptor-derived peptides. Journal of Biological Chemistry *269*, 326-331.

Sengelov, H., Kjeldsen, L., and Borregaard, N. (1993). Control of exocytosis in early neutrophil activation. Journal of Immunology *150*, 1535-1543.

Sengelov, H., Boulay, F., Kjeldsen, L., and Borregaard, N. (1994). Subcellular localization and translocation of the receptor for N-formylmethionyl-leucyl-phenylalanine in human neutrophils. Biochemical Journal *299*, 473-479.

Sham, R.L., Phatak, P.D., Belanger, K.A., and Packman, C.H. (1995). Functional properties of HL60 cells matured with all-trans-retinoic acid and DMSO: differences in response to interleukin-8 and fMLP. Leukemia Research *19*, 1-6.

Shimizu, Y., Newman, W., Tanaka, Y., and Shaw, S. (1992). Lymphocyte interactions with endothelial cells. Immunology Today *13*, 106-112.

Showell, H.J., Freer, R.J., Zigmond, S.H., Schiffmann, E., Aswanikumar, S., and Becker, E.L. (1976). The structure-activity relations of synthetic peptides as chemotactic factors and inducers of lysosomal secretion for neutrophils. Journal of Experimental Medicine *143*, 1154-1169.

Sklar, L.A., Finney, D.A., Oades, Z.G., Jesaitis, A.J., Painter, R.G., and Cochrane, C.G. (1984). The dynamics of ligand-receptor interactions. Real-time analyses of association, dissociation, and internalization of an N-formyl peptide and its receptors on the human neutrophil. Journal of Biological Chemistry *259*, 5661-5669.

Sklar, L.A., Hyslop, P.A., Oades, Z.G., Omann, G.M., Jesaitis, A.J., and Painter, R.G. (1985a). Signal transduction and ligand-receptor dynamics in the human neutrophil. Transient responses and occupancy-response relations at the formyl peptide receptor. Journal of Biological Chemistry *260*, 11461-11467.

Sklar, L.A., Omann, G.M., and Painter, R.G. (1985b). Relationship of actin polymerization and depolymerization to light scattering in human neutrophils: dependence on receptor occupancy and intracellular Ca++. Journal of Cell Biology *101*, 1161-1166.

Sklar, L.A. (1986). Ligand-receptor dynamics and signal amplification in the neutrophil. Advances in Immunology *39*, 95-143.

Sklar, L.A., Bokoch, G.M., Button, D., and Smolen, J.E. (1987). Regulation of ligand-receptor dynamics by guanine nucleotides. Real-time analysis of interconverting states for the neutrophil formyl peptide receptor. Journal of Biological Chemistry *262*, 135-139.

Sklar, L.A., Mueller, H., Omann, G., and Oades, Z. (1989). Three states for the formyl peptide receptor on intact cells. Journal of Biological Chemistry *264*, 8483-8486.

Snyderman, R., Pike, M.C., Edge, S., and Lane, B. (1984). A chemoattractant receptor on macrophages exists in two affinity states regulated by guanine nucleotides. Journal of Cell Biology *98*, 444-448.

Spooncer, E., Heyworth, C.M., Dunn, A., and Dexter, T.M. (1986). Self-renewal and differentiation of interleukin-3-dependent multipotent stem cells are modulated by stromal cells and serum factors. Differentiation *31*, 111-118.

Springer, T.A. (1994). Traffic signals for lymphocyte recirculation and leukocyte emigration: the multistep paradigm. Cell *76*, 301-314.

Sutherland, R., Delia, D., Schneider, C., Newman, R., Kemshead, J., and Greaves, M. (1981). Ubiquitous cell-surface glycoprotein on tumor cells is proliferation-associated receptor for transferrin. Proceedings of the National Academy of Sciences of the United States of America *78*, 4515-4519.

Tanaka, Y., Adams, D.H., and Shaw, S. (1993). Proteoglycans on endothelial cells present adhesion-inducing cytokines to leukocytes. Immunology Today *14*, 111-115.

Truett, A.P., Verghese, M.W., Dillon, S.B., and Snyderman, R. (1988). Calcium influx stimulates a second pathway for sustained diacylglycerol production in leukocytes activated by chemoattractants. Proceedings of the National Academy of Sciences of the United States of America *85*, 1549-1553.

Weinberg, J.B., Muscato, J.J., and Niedel, J.E. (1981). Monocyte chemotactic peptide receptor. Functional characteristics and ligand-induced regulation. Journal of Clinical Investigation *68*, 621-630.

Weissman, I.L. and Cooper, M.D. (1993). How the immune system develops [published erratum appears in Sci Am 1993 Dec;269(6):10]. Scientific American *269*, 64-71.

Williams, L.T., Snyderman, R., Pike, M.C., and Lefkowitz, R.J. (1977). Specific receptor sites for chemotactic peptides on human polymorphonuclear leukocytes. Proceedings of the National Academy of Sciences of the United States of America *74*, 1204-1208.

Ye, R.D., Cavanagh, S.L., Quehenberger, O., Prossnitz, E.R., and Cochrane, C.G. (1992). Isolation of a cDNA that encodes a novel granulocyte N-formyl peptide receptor. Biochemical & Biophysical Research Communications *184*, 582-589.

Ye, R.D., Quehenberger, O., Thomas, K.M., Navarro, J., Cavanagh, S.L., Prossnitz, E.R., and Cochrane, C.G. (1993). The rabbit neutrophil N-formyl peptide receptor. cDNA cloning, expression, and structure/function implications. Journal of Immunology *150*, 1383-1394.

APPENDICES

Appendix 1

```
huFPR          METNSSLPTNISGGTPAVSAGYLFLDIITYLVFAVTFVLGVLGNGLVIWVAG 52
FPRL1          METNFSTPLNEYEEVSYESAGYTVLRILPLVVLGVTFVLGVLGNGLVIWVAG 52
FPRL2          METNFSIPLNETEEVLPEPAGHTVLWIFSLLVHGVTFVFGVLGNGLVIWVAG 52
rabFPR         MDTNASLPLNVSGGTQATPAGLVVLDVFSYLILVVTFVLGVLGNGLVIWVTG 52
muFPR MDTNMSLLMNKSAVNLMNVSGSTQSVSAGYIVLDVFSYLIFAVTFVLGVLGNGLVIWVAG 60

huFPR FRMTHTVTTISYLNLAVADFCFTSTLPFFMVRKAMGGHWPFGWFLCKFLFTIVDINLFGS 112
FPRL1 FRMTRTVTTICYLNLALADFSFTATLPFLIVSMAMGEKWPFGWFLCKLIHIVVDINLFGS 112
FPRL2 FRMTRTVNTICYLNLALADFSFSAILPFRMVSVAMREKWPFASFLCKLVHVMIDINLFVS 112
rabFPRFRMTHTVTTISYLNLALADFSFTSTLPFFIVTKALGGHWPFGWFLCKFVFTIVDINLFGS 112
muFPR FRMKHTVTTISYLNLAIADFCFTSTLPFYIASMVMGGHWPFGWFMCKFIYTVIDINLFGS 120

huFPR VFLIALIALDRCVCVLHPVWTQNHRTVSLAKKVIIGPWVMALLLTLPVIIRVTTVPGK-- 170
FPRL1 VFLIGFIALDRCICVLHPVWAQNHRTVSLAMKVIVGPWILALVLTLPVFLFLTTVTIP-- 170
FPRL2 VYLITIIALDRCICVLHPAWAQNHRTMSLAKRVMTGLWIFTIVLTLPNFIFWTTISTT-- 170
rabFPRVFLIALIALDRCICVLHPVWAQNHRNVSLAKKVIVGPWICALLLTLPVIIRVTTLSHP-- 170
muFPR VFLIALIALDRCICVLHPVWAQNHRTVSLAKKVIIVPWICAFLLTLPVIIRLTTVPNS-- 178

huFPR ----TGTVACTFNFSPWTNDPKERINVAVAMLTVRGIIRFIIGFSAPMSIVAVSYGLIAT 226
FPRL1 ----NGDTYCTFNFASWGGTPEERLKVAITMLTARGIIRFVIGFSLPMSIVAICYGLIAA 226
FPRL2 ----NGDTYCIFNFAFWGDTAVERLNVFITMAKVFLILHFIIGFTVPMSIITVCYGIIAA 226
rabFPR--RAPGKMACTFDWSPWTEDPAEKLKVAISMFMVRGIIRFIIGFSTPMSIVAVCYGLIAT 228
muFPR -RLGPGKTACTFDFSPWTKDPVEKRKVAVTMLTVRGIIRFIIGFSTPMSIVAICYGLITT 237

huFPR KIHKQGLIKSSRPLRVLSFVAAAFFLCWSPYQVVALIATVRIRELLQGMYKE-IGIAVDV 285
FPRL1 KIHKKGMIKSSRPLRVLTAVVASFFICWFPFQLVALLGTVWLKEMLFYGKYKIIDILVNP 286
FPRL2 KIHRNHMIKSSRPLRVFAAVVASFFICWFPYELIGILMAVWLKEMLLNGKYKIILVLINP 286
rabFPR KIHRQGLIKSSRPLRVLSFVVASFLLCWSPYQIAALIATVRIRELLLGMGKDLRI-VLDV 287
muFPR KIHRQGLIKSSRPLRVLSFVVAAFFLCWCPFQVVALISTIQVRERLKNMTPGIVT-ALKI 296

huFPR TSALAFFNSCLNPMLYVFMGQDFRERLIHALPASLERALTE--DSTQTSDTATNSTLPSA 343
FPRL1 TSSLAFFNSCLNPMLYVFVGQDFRERLIHSLPTSLERALSE--DSAPTNDTAANSASPPA 344
FPRL2 TSSLAFFNSCLNPILYVFMGRNFQERLIRSLPTSLERALTEVPDSAQTSNTHTTSASPPE 346
rabFPRTSFVAFFNSCLNPMLYVFMGQDFRERLIHSLPASLERALSE--DSAQTSDTGTNSTSAPA 345
muFPR TSPLAFFNSCLNPMLYVFMGQDFRERLIHSLPASLERALTE--DSAQTSDTGTNLGTNST 354

huFPR ---EVALQAK                                                  350
FPRL1 ---ETELQAM                                                  351
FPRL2 ---ETELQAM                                                  353
rabFPR---EAELQAI                                                  352
muFPR SLSENTLNAM                                                  364
```

Alignment of Formyl Peptide Receptor amino acid sequences. huFPR, FPRL1, and FPRL2 were human derived sequences from cDNA libraries. rabFPR was derived form a rabbit cDNA library and muFPR from a murine genomic library.

Appendix 2

```
R98    ----------------CCCAGAGCAAGACCACAGCTGGTGAACAGTCCAGGAGCAGACAA    44
R26    cccagacctagaactaCCCAGAGCAAGACCACAGCTGGTGAACAGTCCAGGAGCAGACAA    60

R98    GATGGAGACAAATTCCTCTCTCCCCACGAACATCTCTGGAGGGACACCTGCTGTATCTGC    104
R26    GATGGAGACAAATTCCTCTCTCCCCACGAACATCTCTGGAGGGACACCTGCTGTATCTGC    120

R98    TGGCTATCTCTTCCTGGATATCATCACTTATCTGGTATTTGCAGTCACCTTTGTCCTCGG    164
R26    TGGCTATCTCTTCCTGGATATCATCACTTATCTGGTATTTGCAGTCACCTTTGTCCTCGG    180

R98    GGTCCTGGGCAACGGGCTTGTGATCTGGGTGGCTGGATTCCGGATGACACACACAGTCAC    224
R26    GGTCCTGGGCAACGGGCTTGTGATCTGGGTGGCTGGATTCCGGATGACACACACAGTCAC    240

R98    CACCATCAGTTACCTGAACCTGGCCGTGGCTGACTTCTGTTTCACCTCCACTTTGCCATT    284
R26    CACCATCAGTTACCTGAACCTGGCCGTGGCTGACTTCTGTTTCACCTCCACTTTGCCATT    300

R98    CTTCATGGTCAGGAAGGCCATGGGAGGACATTGGCCTTTCGGCTGGTTCCTGTGCAAATT    344
R26    CTTCATGGTCAGGAAGGCCATGGGAGGACATTGGCCTTTCGGCTGGTTCCTGTGCAAATT    360

R98    CCTCTTTACCATAGTGGACATCAACTTGTTCGGAAGTGTCTTCCTGATCGCCCTCATTGC    404
R26    CGTCTTTACCATAGTGGACATCAACTTGTTCGGAAGTGTCTTCCTGATCGCCCTCATTGC    420

R98    TCTGGACCGCTGTGTTTGCGTCCTGCATCCAGTCTGGACCCAGAACCACCGCACCGTGAG    464
R26    TCTGGACCGCTGTGTTTGCGTCCTGCATCCAGTCTGGACCCAGAACCACCGCACCGTGAG    480

R98    CCTGGCCAAGAAGGTGATCATTGGGCCCTGGGTGATGGCTCTGCTCCTCACATTGCCAGT    524
R26    CCTGGCCAAGAAGGTGATCATTGGGCCCTGGGTGATGGCTCTGCTCCTCACATTGCCAGT    540

R98    TATCATTCGTGTGACTACAGTACCTGGTAAAACGGGGACAGTAGCCTGCACTTTTAACTT    584
R26    TATCATTCGTGTGACTACAGTACCTGGTAAAACGGGGACAGTAGCCTGCACTTTTAACTT    600

R98    TTCGCCCTGGACCAACGACCCTAAAGAGAGGATAAATGTGGCCGTTGCCATGTTGACGGT    644
R26    TTCGCCCTGGACCAACGACCCTAAAGAGAGGATAAATGTGGCCGTTGCCATGTTGACGGT    660

R98    GAGAGGCATCATCCGGTTCATCATTGGCTTCAGCGCACCCATGTCCATCGTTGCTGTCAG    704
R26    GAGAGGCATCATCCGGTTCATCATTGGCTTCAGCGCACCCATGTCCATCGTTGCTGTCAG    720

R98    TTATGGGCTTATTGCCACCAAGATCCACAAGCAAGGCTTGATTAAGTCCAGTCGTCCCTT    764
R26    TTATGGGCTTATTGCCACCAAGATCCACAAGCAAGGCTTGATTAAGTCCAGTCGTCCCTT    780

R98    ACGGGTCCTCTCCTTTGTCGCAGCAGCCTTTTTTCTCTGCTGGTCCCCATATCAGGTGGT    824
R26    ACGGGTCCTCTCCTTTGTCGCAGCAGCCTTTTTTCTCTGCTGGTCCCCATATCAGGTGGT    840

R98    GGCCCTTATAGCCACAGTCAGAATCCGTGAGTTATTGCAAGGCATGTACAAAGAAATTGG·   884
R26    GGCCCTTATAGCCACAGTCAGAATCCGTGAGTTATTGCAAGGCATGTACAAAGAAATTGG    900

R98    TATTGCAGTGGATGTGACAAGTGCCCTGGCCTTCTTCAACAGCTGCCTCAACCCCATGCT    944
R26    TATTGCAGTGGATGTGACAAGTGCCCTGGCCTTCTTCAACAGCTGCCTCAACCCCATGCT    960

R98    CTATGTCTTCATGGGCCAGGACTTCCGGGAGAGGCTGATCCACGCCCTTCCCGCCAGTCT   1004
R26    CTATGTCTTCATGGGCCAGGACTTCCGGGAGAGGCTGATCCACGCCCTTCCCGCCAGTCT   1020

R98    GGAGAGGGCCCTGACCGAGGACTCAACCCAAACCAGTGACACAGCTACCAATTCTACTTT   1064
R26    GGAGAGGGCCCTGACCGAGGACTCAACCCAAACCAGTGACACAGCTACCAATTCTACTTT   1080

R98    ACCTTCTGCAGAGGTGGCGTTACAGGCAAAGTGAGGAGGGAGCTGGGGGACACTTTCGAG   1124
R26    ACCTTCTGCAGAGGTGGAGTTACAGGCAAAGTGAGGAGGGAGCTGGGGGACACTTTCGAG   1140

R98    CTCCCAGCTCCAGCTTCGTCTCACCTTGAGTTAGGCTGAGCACAGGCATTTCCTGCTTAT   1184
R26    CTCCCAGCTCCAGCTTCGTCTCACCTTGAGTTAGGCTGAGCACAGGCATTTCCTGCTTAT   1200

R98    TTTAGGATTACCCACTCATCAGAAAAAAAAAAAAAA-GCCTTTGTGTCCCCTGATTTGGGG  1243
R26    TTTAGGATTACCCACTCATCAGAAAAAAAAAAAAAaGCCTTTGTGTCCCCTGATTTGGGG   1260

R98    AGAATAAACAGATATGAGTTTattattgacttctttttgattttggacctcagcctcgg    1303
R26    AGAATAAACAGATATGAGTTT-----------------------------------------  1281

R98    gtggtcagggtgggaaatgataggaagaagctgtcatctgcatcctagtttgcctgaaat    1363
R98    gaacccaaataatacccattattattagtcctgaattatgagtagtgaatgatacccatc    1423
```

```
R98    attctggcatcatgatgagtagtgtccacttccattctgaaaagtgccctgctgtgaaaa  1483
R98    ataaattatatagtcatcctaggtaaatgaaggaggagggagaagtgtgaaagagtatgg  1543
R98    cttaaatcagacaagatatacaagaagatactttatatagggcaggagcggtggctcatg  1603
R98    cctgtaatcccagcactttgggaggccgaggcaggcggatcaccagaggtcaggaattcg  1663
R98    agaacagcctggccaacatggtgaaaccctgtctctactaaaaatacaaaaattagctgg  1723
R98    gcgtagtggcaggctcccgtaatcccagctactcaggagaccgaggcaggagaatcgctt  1783
R98    ggacctggaaggcggaggttgtagtgagccaagaaaacgccactacactccagcctgggt  1843
R98    gacagagagagactccggctcag                                       1866
```

A comparison of two human FPR allelic and splice varients of the human FPR gene *FPR1*. R-98 represents fMLP-R98 and R26 fMLP-R26 (Boulay *et al.*, 1990a). The letters in upper case indicate identical identity of bases, those in lower case indicate differrences between the two varients.

Appendix 3

```
Mur   MGPHGNDSDFLLAPNGSRAPHHDVTQERDEAWVVGMAILMSVIVLAIVFGNVLVITAIAK   60
Ham   MGPPGNDSDFLLTTNGSHVPDHDVTEERDEAWVVG-AILMSVIVLAIVFGNVLVITAIAK   59
Rat   MEPHGNDSDFLLAPNGSRAPGHDITQERDEAWVVGMAILMSVIVLAIVFGNVLVITAIAK   60
Hum   MGQPGNGSAFLLAPNRSHAPDHDVTQQRDEVWVVGMGIVMSLIVLAIVFGNVLVITAIAK   60

Mur   FERLQTVTNYFIISLACADLVMGLAVVPFGASHTSMKMWNFGNFWCEFWTSIDVLCVTAS   120
Ham   FERLQTVTNYFITSLACADLVMGLAVVPFGASHILMKMWNFGNFWCEFWTSIDVLCVTAS   119
Rat   FERLQTVTNYFITSLACADLVMGLAVVPFGASHILMKMWNFGNFWCEFWTSIDVLCVTAS   120
Hum   FERLQTVTNYFITSLACADLVMGLAVVPFGAAHILMKMWTFGNFWCEFWTSIDVLCVTAS   120

Mur   IETLCVIAVDRYVAITSPFKYQSLLTKNKARVVILMVWIVSGLTSFLPIQMHWYRATHKK   180
Ham   IETLCVIAVDRYIAITSPFKYQSLLTKNKARMVILMVWIVSGLTSFLPIQMHWYRATHQK   179
Rat   IETLCVIAVDRYVAITSPFKYQSLLTKNKARVVILMVWIVSGLTSFLPIQMHWYRATHKQ   180
Hum   IETLCVIAVDRYFAITSPFKYQSLLTKNKARVIILMVWIVSGLTSFLPIQMHWYRATHQE   180

Mur   AIDCYTEETCCDFFTNQAYAIASSIVSFYVPLVVMVFVYSRVFQVAKRQLQKIDKSEGRF   240
Ham   AIDCYHKETCCDFFTNQAYAIASSIVSFYVPLVVMVFVYSRVFQVAKRQLQKIDKSEGRF   239
Rat   AIDCYAKETCCDFFTNQAYAIASSIVSFYVPLVVMVFVYSRVFQVAKRQLQKIDKSEGRF   240
Hum   AINCYANETCCDFFTNQAYAIASSIVSFYVPLVIMVFVYSRVFQEAKRQLQKIDKSEGRF   240

Mur   HAQNLSQVEQDGRTGHGLRRSSKFCLKEHKALKTLGIIMGTFTLCWLPFFIVNIVHVIRD   300
Ham   HSPNLGQVEQDGRSGHGLRRSSKFCLKEHKALKTLGIIMGTFTLCWLPFFIVNIVHVIQD   299
Rat   HAQNLSQVEQDGRSGHGLRSSSKFCLKEHKALKTLGIIMGTFTLCWLPFFIVNIVHVIRA   300
Hum   HVQNLSQVEQDGRTGHGLRRSSKFCLKEHKALKTLGIIMGTFTLCWLPFFIVNIVHVIQD   300

Mur   NLIPKEVYILLNWLGYVNSAFNPLIYCRSPDFRIAFQELLCLRRSSFETYGNGYSSNSNG   360
Ham   NLIPKEVYILLNWLGYVNSAFNPLIYCRSPDFRIAFQELLCLRRSSSKAYGNGYSSNSNg   359
Rat   NLIPKEVYILLNWLGYVNSAFNPLIYCRSPDFRIAFQELLCLRRSSSKTYGNGYSSNSNG   360
Hum   NLIRKEVYILLNWIGYVNSGFNPLIYCRSPDFRIAFQELLCLRRSSLKAYGNGYSSNGN-   359

Mur   RTDYTGEPNTCQLGQEREQELLCEDPPGMEGFVNCQGTVPSLSVDSQGRNCSTNDSPL     418
Ham   ktdyMGEASGCQLGQEKESERLCEDPPGTESFVNCQGTVPSLSLDSQGRNCSTNDSPL     417
Rat   RTDYTGEQSAYQLGQEKENELLCEEAPGMEGFVNCQGTVPSLSIDSQGRNCNTNDSPL     418
Hum   ----TGEQSGYHVEQEKENKLLCEDLPGTEDFVGHQGTVPSDNIDSQGRNCSTNDSLL     413
```

Amino Acid Alignment of β_2 Adrenergic Receptors.
Mur = Murine, Ham = Hamster, Rat = Rat, Hum = Human.
The letters in upper case indicate identical identity of bases, those in lower case indicate differrences between the two varients.

A 4.1 G Protein Coupled Receptors

A large number of intracellular signals are received at the cell surface by specific receptors. These signals include neurotransmitters, peptide hormones, autocrine and paracrine factors. These receptors are coupled to intracellular effectors by guanine-nucleotide-binding regulatory proteins (G proteins). For each type of signal there may be more than one type of receptor. For example, there are five types of muscarinic acetylcholine receptors (m_1-m_5).

Stimulation of these G protein coupled receptors (GPCRs) activates the G proteins that regulate a variety of enzymes or ion channels. Changes in the ionic composition of the cell, or the level of second messengers such as inositol phosphates, regulate cellular responses. A cell's response to a signal depends on the presence of the receptor and the specificity with which it interacts with G proteins. This interaction defines the range of responses a cell can make. If the receptor can only interact with one subtype of G protein, which in turn can interact with only a single effector pathway, then the response of the cell will be very specific. If the receptor interacts with many types of G protein many effector pathways will be effected leading to a broad cellular response.

A 4.1.1 General Features of G Protein Coupled Receptors

The GPCRs are all single polypeptide chains ranging in length from 324 amino acids (*mas* oncogene) to 744 amino acids (human thyroid stimulating hormone receptor). All GPCRs have seven stretches of 20 - 26 hydrophobic amino acids which are predicted to form membrane spanning α-helices (Strader et al., 1994). This prediction has been supported by electron diffraction studies on

bacteriorhodopsin and proteolytic cleavage studies of rhodopsin (Hargrave et al., 1982, Henderson et al., 1990). The areas of greatest similarity within the GPCRs are the transmembrane regions. The similarity varies between 85-95%, for receptor subtypes, to 20-25% for unrelated GPCRs. The extracellular and intracellular domains of GPCRs display more divergent amino acid sequences. For both rhodopsin and β_2 adrenergic receptor the N terminus is located on the extracellular surface and the C terminus is on the intracellular side (Wang et al., 1989; Applebury and Hargrave, 1986). Sequence comparisons of GPCRs reveal that there are common amino acids and common domains (Attwood et al., 1991). It is thought that the most conserved amino acids are essential for protein folding.

Prolines are found within transmembrane domains (TM) 4, 5, 6, and 7. These are thought to be important to the formation of the binding pocket as they introduce kinks in the α-helices (Findlay and Eliopoulos, 1990). Cysteines are conserved in extracellular loops 1 and 2. They form a disulphide bridge which imposes a constraint in the conformation of the extracellular domain. This is probably a common structural feature as these cysteines are invariant in most GPCRs. The C terminus of the biogenic amine receptors (β adrenergic) contains an invariant cysteine which can be palmitylated. This is thought to anchor part of the C terminus to the plasma membrane, thus controlling the tertiary structure of this region (O'Dowd et al., 1989).

There are also other well conserved residues. These include a glycine, an asparigine and a valine in TM1; a leucine, two alanines, and an aspartate in TM2; an isoleucine in TM3; a tryptophan in TM4; a phenylalanine and a tryptophan in TM6; and an asparigine and a tyrosine in TM7.

The triplet Asp-Arg-Tyr is the most highly conserved intracellular sequence adjacent to TM3 and has been implicated in signal transduction. The arginine is invariant but the aspartate and asparagine can be conservatively replaced in several GPCRs. The N terminal varies from seven to three hundred amino acids in length. There is little sequence similarity in the first extracellular domain. GPCRs usually contain at least one N-linked glycosylation consensus sequence (Asn-X-Ser/Thr). Glycosylation is thought to be important for expression (Rands et al., 1990). There are potential phosphorylation sites in the third cytoplasmic loop and the C terminus. Protein kinase A and specific receptor kinases mediate receptor desensitisation by phosphorylation of serine and threonine residues in this region (Section A 4.4).

Three dimensional models of the structure of GPCRs have been proposed (Baldwin, 1993). The helices pack with their lipid surfaces on the outside and the polar groups on the inside. The helices are at small positive angles, relative to each other, except for helix 3 and 4 which has a small negative angle. This means that the intracellular surface has a compact structure for interaction with the G protein and that the extracellular surface has an open structure to accommodate the ligand.

Primary sequence alignments has led to the identification of four subfamilies within the GPCRs. These are receptors that bind biogenic amines (dopamine and acetylcholine), glycoproteins hormones (thyroid stimulating hormone), neurokinins (substance P) and calcitonin (parathyroid hormones).

A 4.2 Ligand Binding Domains

Within GPCRs, two types of binding have been identified. Small ligand GPCRs have a binding pocket which is within the transmembrane helices. The peptide hormone receptors have a large ligand which binds to the extracellular part of the receptor.

A 4.2.1 Ligand Binding Domain for Small Ligands

The structure of the binding pocket in small ligand GPCRs is based on the structure of bacteriorhodopsin which has been resolved to high resolution (Henderson et al., 1990; Strader et al., 1989b). Large regions of the intracellular and extracellular hydrophillic domains of β_2 adrenergic receptors can be deleted without affecting the binding of agonists or antagonists. This indicates that the determinants of ligand binding lie within the transmembrane domains (Dixon et al., 1987). Site-directed mutagenesis studies of the β_2 adrenergic receptors have identified three residues important in ligand binding among receptors that bind catecholamine agonists but not in other GPCRs (Strader et al., 1989a). These residues are two serines at positions 204 and 207 in TM5 and a phenylalanine at position 290 in TM6. The serines hydrogen bond to the hydroxyls of the catechol moiety of the catecholamine agonists giving rise to higher affinity binding. The phenylalanine is thought to be important in stabilizing the interaction of the catechol with the receptor. In addition, the aspartate residue at position 113 in TM3 of β_2 adrenergic receptors interacts with the amine group of the ligand.

In the muscarinic, α adrenergic and dopaminergic receptors, the ligand binds to a pocket comparable to that of the β_2 adrenergic receptors.

A 4.2.2 Ligand Binding Domain for Large Ligands

The GPCRs which bind large ligands can be subdivided into two families: the glycoprotein hormone receptors and the tachykinin receptors. The ligands for these receptors are very large compared to the other GPCR ligands.

A 4.2.3 Ligand Binding Domain of the Glycoprotein Hormone Receptors

The extracellular domains of the glycoprotein receptors are involved in ligand binding. This became apparent when deletion studies showed that removal of these domains leads to loss of high affinity binding (Keinanen and Rajaniemi, 1986). Further studies pinpointed the high affinity binding site for the glycoprotein hormone receptors to be within the first cytoplasmic domain. This domain is glycosylated and is rich in cysteines that can form disulphide bridges. The large N terminus contains 20 amino acid repeats which are rich in leucines. The leucine-rich repeats are known to interact with both hydrophillic and hydrophobic surfaces.

In addition to the extracellular binding pocket, the glycoprotein hormone receptors have also been found to have a similar binding pocket to that of the small ligand GPCRs. However, this site is of low affinity. It is thought that the extracellular high affinity binding site may act to capture the hormone and present it to the intramembranous low affinity site for signal transduction (Ji and Ji, 1991).

A 4.2.4 Ligand Binding Domain of The Tachykinin Receptors

The three tachykinins (substance P, substance K and neuromedin K) share a common C terminus sequence, Phe-X-Gly-Leu-Met-NH_2. It has been proposed that the three receptors for these ligands, designated neurokinin 1, neurokinin 2 and neurokinin 3 (NK1, 2 and 3), recognise the common C terminus and that the specificity is determined by the divergent N terminus (Buck et al., 1988). Chimeric studies with the NK1/NK2 have located the binding site from TM2 to the second extracellular loop together with the N terminus (Yokota et al., 1992). Further work with NK1/NK2 and NK1/NK3 chimeric receptors has shown that the tachykinins do not interact with the same functional groups on each receptor (Fong et al., 1992). However, residues have been identified which interact with all the tachykinins, but to varying degrees. These are in position 23, 24, 25 (N terminus), 96, and 108 (first extracellular loop) (Watling and Krause, 1993).

A 4.3 Activation of G Protein Coupled Receptors

Recent data suggest that the receptor exists in several dynamic states. The receptor has a low affinity for both the ligand and the G protein. When the ligand binds to the receptor an inactive complex forms which leads to the activation of the receptor. Recent mutagenesis experiments with β adrenergic and formyl peptide receptors have led to the production of receptors that are constitutively active (Samama et al., 1993; Prossnitz et al., 1995). Substitution of Ala293 in α_1 adrenergic receptor by any other amino acid creates a constitutively active receptor (Cotecchia et al., 1990). In addition, the receptor has a higher affinity for the ligand although its affinity for antagonists is unchanged. The receptor is

thought to exist in equilibrium between two interconvertible states, the active and the inactive. The conversion between the active and the inactive state can occur spontaneously but in the absence of a ligand the equilibrium is such that the receptor is inactive. When the ligand binds, it shifts the equilibrium towards the active receptor causing cellular activation. Therefore, the constitutively active mutants are due to the equilibrium favouring the active state of the receptor. The current model of activation is as follows. The ligand binds to the receptor, activating it through a conformational change. The receptor can only activate the G protein when it is in this state. The G protein binding site of the receptor is thought to be buried inside the receptor structure. When the ligand binds to the receptor, activating it by a conformational change, this site is exposed and can interact specifically with its G protein. This activates the G protein by allowing it to exchange GDP for GTP. The Ala293 in the α_1 adrenergic receptor is thought to be important in shielding the G protein binding site from the G protein.

A 4.3.1 Heterotrimeric G Proteins

Currently, twenty distinct G_α subunits have been identified. These have been divided into four classes based on their amino acid similarities (Rens Domiano and Hamm, 1995). The $G_{\alpha s}$ family mediates the hormonal stimulation of adenylyl cyclase and the closing of Ca^{2+} channels. The $G_{\alpha i}$ family is generally involved in the inhibition of adenylyl cyclase and opening K^+ channels. The $G_{\alpha z}$ and $G_{\alpha gust}$ families have not been well characterized and the effector systems they activate are unknown.

Five G_β subunits and twelve G_γ subunits have been identified (Roth et al., 1991). The $G_{\beta\gamma}$ can act as regulators of many effectors such as K^+ channels, adenylyl cyclase, PI3-kinase and via *ras* on MAP kinase pathways (Clapham and Neer, 1993; Faure et al., 1994). The G protein subunits G_α and G_γ contain lipid molecules. This is important in localizing these subunits to the membrane. G_α may be myristoylated and palmitoylated. G_γ can be farnesylated or geranylgeranylated.

Recent crystallographic studies have revealed the structure of the G protein heterotrimer (Sondek et al., 1996; Lambright et al., 1996; Wall et al., 1995). The G_β is shaped like a seven-bladed propeller with a tapering, water filled shaft. The G_γ subunit makes contact with one side and over the face of the G_β subunit. On the other side of G_β, the G_α subunit is tethered close to the G_γ subunit. The G_α subunit has two major contacts with G_β subunit. The first is the myristoylated or palmitoylated N terminus. The second is between the two switch regions of G_α and one of the electronegative faces of G_β. This shields the switch domains until the activation of the receptor. The receptor acts as a cationic lever when activated, flipping the switch domain and triggering the conformational change in G_α. As the intracellular GTP level is much higher than the GDP level, GDP is rapidly replaced with GTP once the G_α helical/G_α GTPase domain cleft is open. The switch domain then closes and the free G_α and $G_{\beta\gamma}$ subunits can interact with effectors.

A 4.3.2 G Protein Binding Domain

Proteolysis and mutagenesis studies indicate that the third intracellular loop is the most important domain in the coupling of α, β and muscarinic receptors to

G proteins (Strader et al., 1989b; Lefkowitz and Caron, 1988; Campbell et al., 1991). The third intracellular loop is predicted to form amphipathic α helices (Lefkowitz and Caron, 1988). In α_1 adrenergic receptors, the C terminal region of the third intracellular loop is important for the activation of phospholipase C. Substitution of Ala293 to Leu and Lys 290 to His increases the potency of agonists, stimulating phospholipase C by two orders of magnitude (Cotecchia et al., 1990). In muscarinic receptors, m_1, m_3 and m_5 are coupled to phospholipase C and all contain a highly conserved N terminal in the third intracellular loop. m_2 and m_4 are negatively coupled to adenylate cyclase and do not have this conserved sequence (Wess et al., 1989). Chimeras of the third intracellular loop of m_2 and m_3 have confirmed the importance of this region for G protein coupling (Wess et al., 1990a; Wess et al., 1990b).

A 4.4 Down Regulation of the Receptor

Prolonged exposure to agonist results in desensitization of receptor responsiveness. This is a biphasic response with an initial short term component followed by a long-term response (Hausdorff et al., 1990). Short term desensitization occurs over a time period of seconds to minutes followed by a rapid recovery which does not require protein synthesis. Long term desensitization leads to a loss in total receptor numbers and recovery requires *de novo* protein synthesis. Three main methods of desensitization have been identified in β adrenergic receptors: phosphorylation, sequestration and degradation. The short term desensitization is thought to be mediated by phosphorylation of the receptor by G protein coupled receptor kinases (GRKs)

such as rhodopsin kinase or β-adrenergic receptor kinase (βARK) (Freedman et al., 1995) and by sequestration of the receptor away from the plasma membrane and into vesicles that lack $G_{\alpha s}$ (Barak et al., 1994). Down regulation is thought to involve the degradation of the receptor via a lysosomal pathway leading to a prolonged loss in receptor numbers from the plasma membrane. When the ligand binds to its receptor it undergoes a conformational change. The ligand bound receptor can either activate the G protein or it can become desensitized. If the receptor interacts with G protein it will activate it. This causes the dissociation of the G protein in to G_{α} and $G_{\beta\gamma}$ subunits which can then activate cellular pathways. If the activated receptor interacts with other proteins, such as receptor kinases or the arrestin proteins the activity of the receptor is shut down. Once the receptor has been activated by ligand binding, it becomes a substrate for the cytoplasmic GRKs. There are six known members of these. They act by binding to the conformationally active receptor and phosphorylating multiple serines and threonines at the C terminal of the receptor. This leads to an increase of the binding affinity of the receptor for β arrestins. These proteins act to down regulate the receptor by sterically preventing it from interacting with G proteins so that the pathway leading to cellular responses cannot be activated (Premont et al., 1995; Inglese et al., 1993). The cytoplasmic GRKs are rapidly recruited to the membrane. Both rhodopsin kinase and βARK can very rapidly translocate to the membrane. In the case of rhodopsin kinase, this is achieved by its CAAX box which can become farnesylated, thus allowing it to reach the plasma membrane and interact with the receptor (Inglese et al., 1992). In the case of βARK, there is a pleckstrin homology domain at its C terminus which can bind to $G_{\beta\gamma}$ (Touhara

et al., 1994). The pleckstrin domain can also bind the lipid PIP_2 (Harlan et al., 1994). Therefore, when the receptor becomes activated, the $G_{\beta\gamma}$ subunit and PIP_2 are available to bind to βARK. This causes βARK to translocate to the membrane, enabling it to phosphorylate the receptor and thus to down regulate it (Pitcher et al., 1995b). The receptor is then thought to be sequestered into endosomal vesicles. β arrestin is thought to mediate this process (Ferguson et al., 1996). The receptor can then either be recycled or degraded. Recycling involves the action of phosphatase on the receptor and the fusion of the vesicle with the plasma membrane (Pitcher et al., 1995a; Yu et al., 1993). Degradation involves the lysosomal pathway. This leads to a long term down regulation of receptor numbers, requiring *de novo* protein synthesis to restore receptor numbers.

The level of mRNA can also be controlled to regulate the number of receptors. Following ligand stimulation there is an initial rise in β adrenergic mRNA levels. However, if ligand stimulation occurs over hours there is a down regulation in the level of mRNA (Hadcock et al., 1989).

A 4.5 References

Applebury, M.L. and Hargrave, P.A. (1986). Molecular biology of the visual pigments. Vision Res. *26*, 1881-1895.

Attwood, T.K., Eliopoulos, E.E., and Findlay, J.B. (1991). Multiple sequence alignment of protein families showing low sequence homology: a methodological approach using database pattern-matching discriminators for G-protein-linked receptors. Gene *98*, 153-159.

Baldwin, J.M. (1993). The probable arrangement of the helices in G protein-coupled receptors. EMBO J. *12*, 1693-1703.

Barak, L.S., Tiberi, M., Freedman, N.J., Kwatra, M.M., Lefkowitz, R.J., and Caron, M.G. (1994). A highly conserved tyrosine residue in G protein-coupled receptors is required for agonist-mediated beta 2-adrenergic receptor sequestration. J. Biol. Chem. *269*, 2790-2795.

Buck, S.H., Pruss, R.M., Krstenansky, J.L., Robinson, P.J., and Stauderman, K.A. (1988). A tachykinin peptide receptor joins an elite club. Trends. Pharmacol. Sci. *9*, 3-5.

Campbell, P.T., Hnatowich, M., O'Dowd, B.F., Caron, M.G., Lefkowitz, R.J., and Hausdorff, W.P. (1991). Mutations of the human beta 2-adrenergic receptor that impair coupling to Gs interfere with receptor down-regulation but not sequestration. Mol. Pharmacol. *39*, 192-198.

Clapham, D.E. and Neer, E.J. (1993). New roles for G-protein beta gamma-dimers in transmembrane signalling. Nature *365*, 403-406.

Cotecchia, S., Exum, S., Caron, M.G., and Lefkowitz, R.J. (1990). Regions of the alpha 1-adrenergic receptor involved in coupling to phosphatidylinositol hydrolysis and enhanced sensitivity of biological function. Proc. Natl. Acad. Sci. U. S. A. *87*, 2896-2900.

Dixon, R.A., Sigal, I.S., Rands, E., Register, R.B., Candelore, M.R., Blake, A.D., and Strader, C.D. (1987). Ligand binding to the beta-adrenergic receptor involves its rhodopsin-like core. Nature *326*, 73-77.

Faure, M., Voyno Yasenetskaya, T.A., and Bourne, H.R. (1994). cAMP and beta gamma subunits of heterotrimeric G proteins stimulate the mitogen-activated protein kinase pathway in COS-7 cells. J. Biol. Chem. *269*, 7851-7854.

Ferguson, S.S., Downey, W.E., Colapietro, A.M., Barak, L.S., Menard, L., and Caron, M.G. (1996). Role of beta-arrestin in mediating agonist-promoted G protein-coupled receptor internalization. Science *271*, 363-366.

Findlay, J. and Eliopoulos, E. (1990). Three-dimensional modelling of G protein-linked receptors [published erratum appears in Trends Pharmacol Sci 1991 Mar;12(3): 81]. Trends. Pharmacol. Sci. *11*, 492-499.

Fong, T.M., Huang, R.R., and Strader, C.D. (1992). Localization of agonist and antagonist binding domains of the human neurokinin-1 receptor. J. Biol. Chem. *267*, 25664-25667.

Freedman, N.J., Liggett, S.B., Drachman, D.E., Pei, G., Caron, M.G., and Lefkowitz, R.J. (1995). Phosphorylation and desensitization of the human beta 1-adrenergic receptor. Involvement of G protein-coupled receptor kinases and cAMP-dependent protein kinase. J. Biol. Chem. *270*, 17953-17961.

Hadcock, J.R., Ros, M., and Malbon, C.C. (1989). Agonist regulation of beta-adrenergic receptor mRNA. Analysis in S49 mouse lymphoma mutants. J. Biol. Chem. *264*, 13956-13961.

Hargrave, P.A., McDowell, J.H., Siemiatkowski Juszczak, E.C., Fong, S.L., Kuhn, H., Wang, J.K., Curtis, D.R., Mohana Rao, J.K., Argos, P., and Feldmann, R.J. (1982). The carboxyl-terminal one-third of bovine rhodopsin: its structure and function.Vision Res. *22*, 1429-1438.

Harlan, J.E., Hajduk, P.J., Yoon, H.S., and Fesik, S.W. (1994). Pleckstrin homology domains bind to phosphatidylinositol-4,5-bisphosphate. Nature *371*, 168-170.

Hausdorff, W.P., Caron, M.G., and Lefkowitz, R.J. (1990). Turning off the signal: desensitization of beta-adrenergic receptor function [published erratum appears in FASEB J 1990 Sep; 4(12):3049]. FASEB J. *4*, 2881-2889.

Henderson, R., Baldwin, J.M., Ceska, T.A., Zemlin, F., Beckmann, E., and Downing, K.H. (1990). Model for the structure of bacteriorhodopsin based on high-resolution electron cryo-microscopy. J. Mol. Biol. *213*, 899-929.

Inglese, J., Glickman, J.F., Lorenz, W., Caron, M.G., and Lefkowitz, R.J. (1992). Isoprenylation of a protein kinase. Requirement of farnesylation/alpha-carboxyl methylation for full enzymatic activity of rhodopsin kinase. J. Biol. Chem. *267*, 1422-1425.

Inglese, J., Freedman, N.J., Koch, W.J., and Lefkowitz, R.J. (1993). Structure and mechanism of the G protein-coupled receptor kinases. J. Biol. Chem. *268*, 23735-23738.

Ji, I.H. and Ji, T.H. (1991). Human choriogonadotropin binds to a lutropin receptor with essentially no N-terminal extension and stimulates cAMP synthesis. J. Biol. Chem. *266*, 13076-13079.

Keinanen, K.P. and Rajaniemi, H.J. (1986). Rat ovarian lutropin receptor is a transmembrane protein. Evidence for an Mr-20,000 cytoplasmic domain. Biochem. J. *239*, 83-87.

Lambright, D.G., Sondek, J., Bohm, A., Skiba, N.P., Hamm, H.E., and Sigler, P.B. (1996). The 2.0 A crystal structure of a heterotrimeric G protein [see comments]. Nature *379*, 311-319.

Lefkowitz, R.J. and Caron, M.G. (1988). Adrenergic receptors. Models for the study of receptors coupled to guanine nucleotide regulatory proteins. J. Biol. Chem. *263*, 4993-4996.

O'Dowd, B.F., Hnatowich, M., Caron, M.G., Lefkowitz, R.J., and Bouvier, M. (1989). Palmitoylation of the human beta 2-adrenergic receptor. Mutation of Cys341 in the carboxyl tail leads to an uncoupled nonpalmitoylated form of the receptor. J. Biol. Chem. *264*, 7564-7569.

Pitcher, J.A., Payne, E.S., Csortos, C., DePaoli Roach, A.A., and Lefkowitz, R.J. (1995a). The G-protein-coupled receptor phosphatase: a protein phosphatase type 2A with a distinct subcellular distribution and substrate specificity. Proc. Natl. Acad. Sci. U. S. A. *92*, 8343-8347.

Pitcher, J.A., Touhara, K., Payne, E.S., and Lefkowitz, R.J. (1995b). Pleckstrin homology domain-mediated membrane association and activation of the beta-adrenergic receptor kinase requires coordinate interaction with G beta gamma subunits and lipid. J. Biol. Chem. *270*, 11707-11710.

Premont, R.T., Inglese, J., and Lefkowitz, R.J. (1995). Protein kinases that phosphorylate activated G protein-coupled receptors. FASEB J. *9*, 175-182.

Prossnitz, E.R., Schreiber, R.E., Bokoch, G.M., and Ye, R.D. (1995). Binding of low affinity N-formyl peptide receptors to G protein. Characterization of a novel inactive receptor intermediate. J. Biol. Chem. *270*, 10686-10694.

Rands, E., Candelore, M.R., Cheung, A.H., Hill, W.S., Strader, C.D., and Dixon, R.A. (1990). Mutational analysis of beta-adrenergic receptor glycosylation. J. Biol. Chem. *265*, 10759-10764.

Rens Domiano, S. and Hamm, H.E. (1995). Structural and functional relationships of heterotrimeric G-proteins. FASEB J. *9*, 1059-1066.

Roth, N.S., Campbell, P.T., Caron, M.G., Lefkowitz, R.J., and Lohse, M.J. (1991). Comparative rates of desensitization of beta-adrenergic receptors by the beta-adrenergic receptor kinase and the cyclic AMP-dependent protein kinase. Proc. Natl. Acad. Sci. U. S. A. *88*, 6201-6204.

Samama, P., Cotecchia, S., Costa, T., and Lefkowitz, R.J. (1993). A mutation-induced activated state of the beta 2-adrenergic receptor. Extending the ternary complex model. J. Biol. Chem. *268*, 4625-4636.

Sondek, J., Bohm, A., Lambright, D.G., Hamm, H.E., and Sigler, P.B. (1996). Crystal structure of a GA protein beta gamma dimer at 2.1A resolution [see comments]. Nature *379*, 369-374.

Strader, C.D., Candelore, M.R., Hill, W.S., Sigal, I.S., and Dixon, R.A. (1989a). Identification of two serine residues involved in agonist activation of the beta-adrenergic receptor. J. Biol. Chem. *264*, 13572-13578.

Strader, C.D., Sigal, I.S., and Dixon, R.A. (1989b). Structural basis of beta-adrenergic receptor function. FASEB J. *3*, 1825-1832.

Strader, C.D., Fong, T.M., Tota, M.R., Underwood, D., and Dixon, R.A. (1994). Structure and function of G protein-coupled receptors. Annu. Rev. Biochem. *63*, 101-132.

Touhara, K., Inglese, J., Pitcher, J.A., Shaw, G., and Lefkowitz, R.J. (1994). Binding of G protein beta gamma-subunits to pleckstrin homology domains. J. Biol. Chem. *269*, 10217-10220.

Wall, M.A., Coleman, D.E., Lee, E., Iniguez Lluhi, J.A., Posner, B.A., Gilman, A.G., and Sprang, S.R. (1995). The structure of the G protein heterotrimer Gi alpha 1 beta 1 gamma 2. Cell *83*, 1047-1058.

Wang, H., Lipfert, L., Malbon, C.C., and Bahouth, S. (1989). Site-directed anti-peptide antibodies define the topography of the beta-adrenergic receptor. J. Biol. Chem. *264*, 14424-14431.

Watling, K.J. and Krause, J.E. (1993). The rising sun shines on substance P and related peptides. Trends. Pharmacol. Sci. *14*, 81-84.

Wess, J., Brann, M.R., and Bonner, T.I. (1989). Identification of a small intracellular region of the muscarinic m3 receptor as a determinant of selective coupling to PI turnover. FEBS Lett. *258*, 133-136.

Wess, J., Bonner, T.I., and Brann, M.R. (1990a). Chimeric m2/m3 muscarinic receptors: role of carboxyl terminal receptor domains in selectivity of ligand binding and coupling to phosphoinositide hydrolysis. Mol. Pharmacol. *38*, 872-877.

Wess, J., Bonner, T.I., Dorje, F., and Brann, M.R. (1990b). Delineation of muscarinic receptor domains conferring selectivity of coupling to guanine nucleotide-binding proteins and second messengers. Mol. Pharmacol. *38*, 517-523.

Yokota, Y., Akazawa, C., Ohkubo, H., and Nakanishi, S. (1992). Delineation of structural domains involved in the subtype specificity of tachykinin receptors through chimeric formation of substance P/substance K receptors. EMBO J. *11*, 3585-3591.

Yu, S.S., Lefkowitz, R.J., and Hausdorff, W.P. (1993). Beta-adrenergic receptor sequestration. A potential mechanism of receptor resensitization. J. Biol. Chem. *268*, 337-341.